The Dissertation Committee for Franklin Thomas Heitmuller certifies that this is the approved version of the following dissertation:

Downstream Trends of Alluvial Sediment Composition and Channel Adjustment in the Llano River Watershed, Central Texas, USA: The Roles of a Highly Variable Flow Regime and a Complex Lithology

Committee:

_____

Paul F. Hudson, Supervisor

_____

William H. Asquith

_____

Karl W. Butzer

_____

Francisco L. Pérez

_____

John M. Sharp

_____

Kenneth R. Young

Downstream Trends of Alluvial Sediment Composition and Channel Adjustment in the Llano River Watershed, Central Texas, USA: The Roles of a Highly Variable Flow Regime and a Complex Lithology

by

Franklin Thomas Heitmuller, B.S., M.A.

Dissertation

Presented to the Faculty of the Graduate School of

The University of Texas at Austin

in Partial Fulfillment

of the Requirements

for the Degree of

Doctor of Philosophy

The University of Texas at Austin

May 2009

Dedication

This dissertation is dedicated to my tremendously supportive wife, Amanda, who tirelessly raised our lovely daughter, Olivia, during her incipient months while I prepared the majority of this document. It is further dedicated to my parents, who have endured, along with myself, too many years of inadequate visitation because of all my work. Finally, I dedicate this to Texas, a wonderful place to work and live and full of remarkable people, and the Llano River, a utopian natural corridor emblematic of the best Texas has to offer.

Acknowledgments

The following people deserve notable mention for their assistance and support of this project: Dr. Paul Hudson for his initial inquiry about the geomorphology of the Llano River and for serving as primary advisor during the course of this project; Dr. William H. Asquith for spending considerable time and energy during technical guidance sessions and for invoking a strong sense of professionalism in my career; and Clay Spivey for his assistance in the field and efforts in the sediment laboratory. Others who have helped along the way are the other committee members, including Dr. Karl Butzer, Dr. Francisco Pérez, Dr. Jack Sharp, and Dr. Ken Young; field assistants, including Erin Atkinson, Joe Beauchamp, Lance Christian, Ben Connor, Delbert Humberson, Meghan Roussel, and Karl Winters; collaborators on the bed-material entrainment project, including Dr. Ted Cleveland, Dr. Xing Fang, George R. Herrmann, Walter McCullough, Lewis Nowlin, Dr. Dave Thompson, and Dr. Keh-Han Wang; my U.S. Geological Survey (USGS) supervisors for patience and support, including Ann Ardis and Bob Joseph; Peter Bush (USGS) for enhancing my writing skills; and the numerous private landowners who permitted access to the river. Gratitude is further expressed to the following sources of funding for this project: the National Science Foundation (Doctoral Dissertation Improvement Award 0623230), the Braun & Associates Grant for Research on Private Lands and The University of Texas at Austin (UT) Environmental Science Institute, the Robert E. Veselka Endowed Fellowship for Graduate Research Travel—and in memory of Stephen T. Moore (UT Department of Geography and the Environment), the David Bruton, Jr., Graduate Fellowship (UT Graduate School), the Texas Department of Transportation, and the USGS.

Downstream Trends of Alluvial Sediment Composition and Channel Adjustment in the Llano River Watershed, Central Texas, USA: The Roles of a Highly Variable Flow Regime and a Complex Lithology

Franklin Thomas Heitmuller, Ph.D.

The University of Texas at Austin, 2009

Supervisor: Paul F. Hudson

This study investigates the downstream controls of alluvial sediment composition and river channel adjustment in the Llano River watershed, Central Texas, USA. The Llano River watershed is characterized by a highly variable, flood-prone flow regime and a complex lithology of Cretaceous carbonate rock, Paleozoic sedimentary rock, and Precambrian igneous and metamorphic rock. Sedimentary variables for this study include particle size, sorting, carbonate content, and magnetic susceptibility. Channel adjustment includes the planform dimension and cross-sectional dimensions of bankfull- and macro-channels. Nineteen sites along the Llano River and selected tributaries were visited to measure cross-sectional channel geometry and sample bed, bank, and overbank sediment. Laboratory analyses of sediment and hydraulic analyses of cross sections were accompanied by analyses of partial-duration flood frequency, flow resistance, hydrography, digital elevation models, and statistical

correlation. Findings include: (1) channel-bed material reduces in size with downstream distance, despite increasing valley confinement and bedrock exposure; (2) the downstream decrease in particle size is more evident for channel-bar deposits than for low-flow-channel (thalweg) deposits; (3) an abrupt gravel-to-sand transition occurs about 20 kilometers downstream of the Paleozoic-Precambrian contact; (4) an abrupt coarse- to fine-gravel transition occurs between 75 and 90 kilometers downstream the North Llano and South Llano Rivers; (5) channel-bank material increases downstream, contrasting with decreases in bed material; (6) carbonate content and magnetic susceptibility of alluvial sediment are inversely related, with carbonate content peaking near Junction; (7) four general categories to classify reaches of the North Llano, South Llano, and Llano Rivers are based on hydrology, planform morphology, lithology, and valley confinement; (8) mean depth increasingly compensates for bankfull discharge in a downstream direction; (9) mean depth compensates more than width for macro-channels; and (10) the return periods for bankfull and macro-channels are about 1 to 2 years and greater than 10 years, respectively. The results of this study will contribute to fluvial geomorphic theory of downstream trends in sediment composition and channel adjustment; as well as inform applied efforts related to aquatic biology, flood hazards, infrastructure design, and riparian and water-resource management in the region.

Table of Contents

List of Tables

List of Figures

Chapter 1. Introduction

River channel adjustment has long been a fundamental topic of fluvial geomorphology. Two primary dimensions of channel adjustment are pattern (planform geometry) and shape (cross-sectional geometry). Discharge and sediment commonly are referenced as the controls on alluvial channel adjustment for timescales ranging from decades to centuries. The most common index of discharge (cubic meters per second) is bankfull discharge, which is related to the scale of size of channel features. Indices of sediment commonly include bedload (tons per day), bed-material size (millimeters), or bank material (silt-clay percentage), all commonly related to the shape of a river channel (Schumm 1960, 1977; Knighton 1998). Much of our knowledge on the topic of channel adjustment derives from studies in humid settings. Recent studies, however, have shown that specific indices controlling channel morphology vary regionally, especially in settings dominated by highly variable flow regimes (e.g., Bourke and Pickup 1999; Gupta 1999; Heritage, Broadhurst, and Birkhead 2001; Kale and Hire 2007). This is particularly important when considering spatial variability in channel adjustment along transition zones in hydrology and lithology, commonly observed in drainage systems in Central Texas.

This study examines the downstream (headwaters to outlet) controls of alluvial sediment composition and mutual adjustment of channel pattern and shape in the Llano River watershed (11,568 square kilometers), which drains the Edwards Plateau and

Llano Uplift of Central Texas (Figure 1.1). The study area represents an opportunity to examine the controls of channel adjustment in a setting unique from the knowledge base on this topic (Baker 1977; Tinkler 2001), which mostly includes investigations in humid or snowmelt-dominated settings. The regional climate of the Llano River watershed is characterized by a transition from western semiarid to eastern subhumid conditions, and the hydrologic regime of the region is noted for low perennial flows punctuated by extreme flash floods. Channel reaches commonly alternate between bedrock-confined and alluvial, and a continuum of associated controls is evident throughout channels in the watershed. Additionally, river sediment abruptly varies as a result of three distinct lithologies, Cretaceous carbonate rocks associated with the Edwards Plateau, Paleozoic sedimentary rocks forming a transition zone, and Precambrian igneous and metamorphic rocks associated with the Llano Uplift. The flashy hydrologic regime has important implications to river channel adjustment in the region, particularly in examining the validity of bankfull discharge as a control on channel geometry. The ubiquitous presence of bedrock, especially that comprising the channel bed, exerts control on hydraulic and sediment transport processes, and thereby channel adjustment. Moreover, the sharply contrasting lithology provides an opportunity to observe how changes in sedimentary characteristics affect channel shape and pattern.

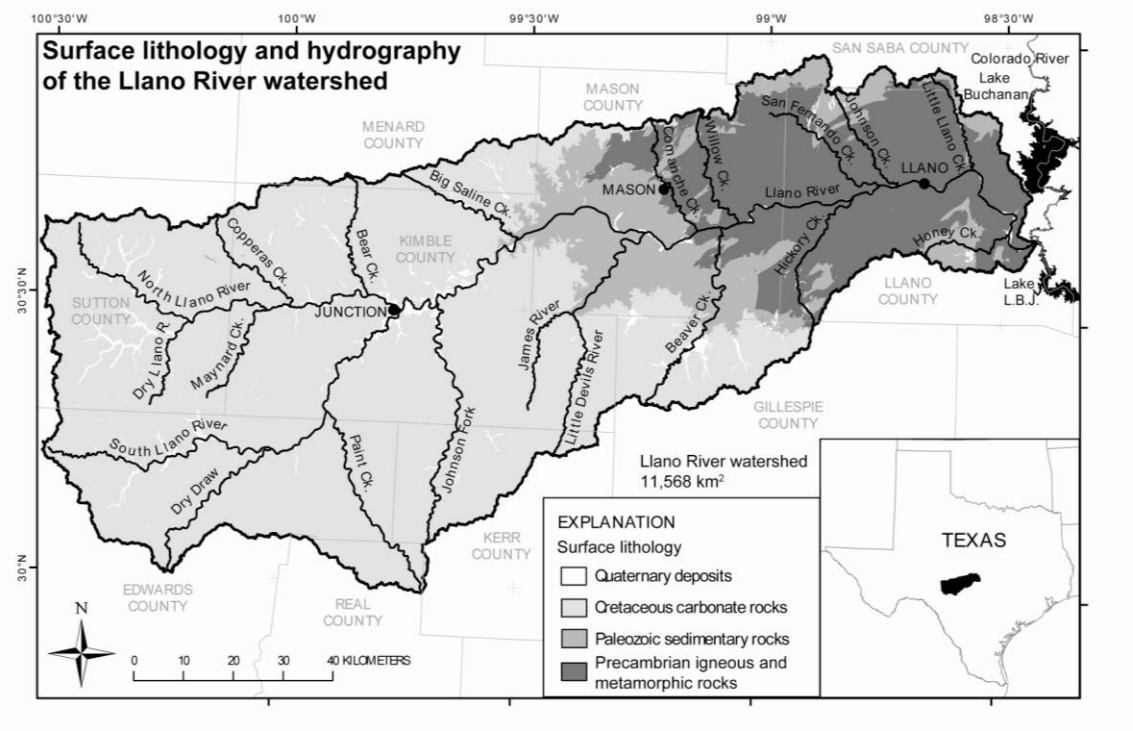

Figure 1.1. Surface lithology (Barnes 1981), hydrography, and county boundaries in the Llano River watershed, Central Texas, USA.

1.1 Current Model of Channel Adjustment

Channel geometry can be described in three modes of adjustment: (1) planform (pattern), (2) cross-section (shape), and (3) longitudinal (profile). Common indices used to describe channel pattern include radius of curvature (meters), channel width (meters), curvature (radius of curvature / width), meander wavelength (meters), sinuosity (channel length / valley-axis length), and various braiding measures. Channel shape is defined by the ratio of bankfull channel width (meters) to depth (meters), the presence of bars or islands, and the symmetry of these components. Channel profile is characterized by a bivariate plot of bed elevation (meters) and channel distance (kilometers) along a reach of interest. These three modes of channel adjustment typically are studied as distinct topics (e.g., Leopold and Maddock 1953; Leopold and Wolman 1957; Schumm 1963; Ferguson 1987; Rosgen 1994), precluding a comprehensive understanding of alluvial channel dynamics. Additionally, fluvial geomorphologists for decades have associated channel geometry either with energy or sediment characteristics, but neglected to integrate the two controls to understand mutual channel form adjustment. The classic work of Leopold and Maddock (1953) emphasized the importance of discharge on channel morphology through the concept of hydraulic geometry, and established that width, depth, and velocity (meters per second) are related to discharge by a power function. A hydraulic approach also was adapted to consideration of channel pattern by Leopold and Wolman (1957). Figure 1.2 shows the

relation proposed by Leopold and Wolman (1957), a threshold above which braiding occurs:

$S = 0.012Q^{-0.44}$, where

S is dimensionless channel slope and Q is bankfull discharge in cubic meters per second.

Most of the data used to generate the plot were derived from rivers in the humid eastern and mid-western United States and the northern Rocky Mountains. Few data points were from rivers with highly variable flow regimes.

The hydraulic threshold approach used by Leopold and Wolman (1957) was effective at discriminating broad categories of channel pattern (e.g., meandering, braided, straight). Other researchers (e.g., Schumm 1977) have employed a sedimentary approach to predict channel pattern adjustment. Although the channel patterns are not as distinct within the study area, such an approach holds promise because of abrupt changes in lithology and sediment size between the Edwards Plateau and Llano Uplift regions. For example, van den Berg (1995) used the Leopold and Wolman (1957) hydraulic approach integrated with an index of sediment size to effectively distinguish between single- and multi-thread channels.

Alternatively, Schumm (1960) has endorsed an approach to predict channel shape that primarily considers sediment. Schumm (1960) found that increased percentages of silt and clay in channel boundaries are associated with low width-depth ratios for rivers in the North American Great Plains (Figure 1.3) and that channel shape

is independent of discharge. However, the linear relation shown in Figure 1.3 violates the requirements of independence for regression-based analysis because the *M* factor is computed from width and depth, to which it is subsequently related in the plot. Schumm (1963) further advocates for sedimentary controls by showing a relation between silt-clay percentage and sinuosity, and Schumm and Khan (1972) argue that fine sediment is required before meandering develops in laboratory flume channels.

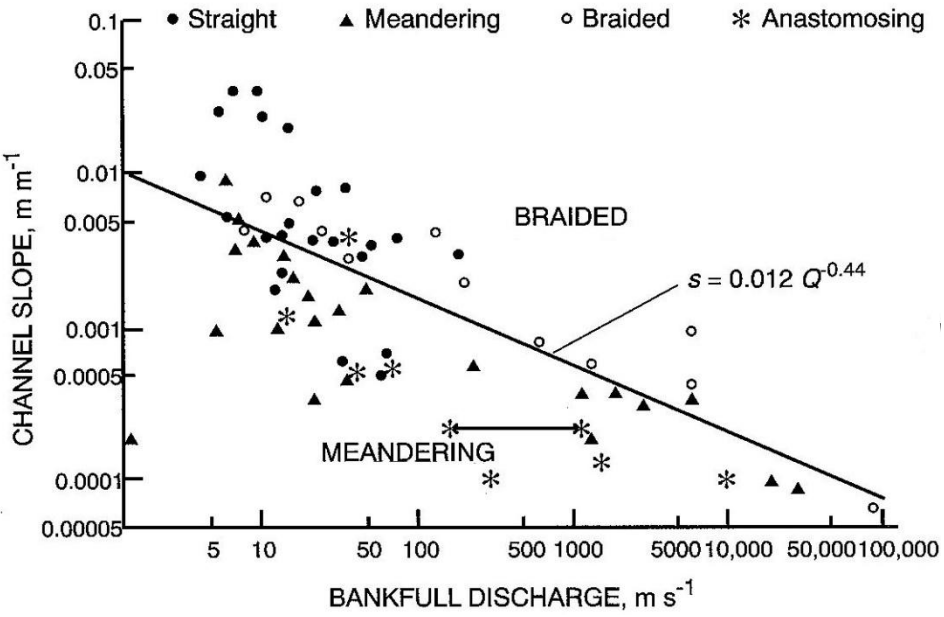

Figure 1.2. Leopold and Wolman (1957) transition between meandering and braided channels for a given channel slope and bankfull discharge (scanned from Knighton 1998).

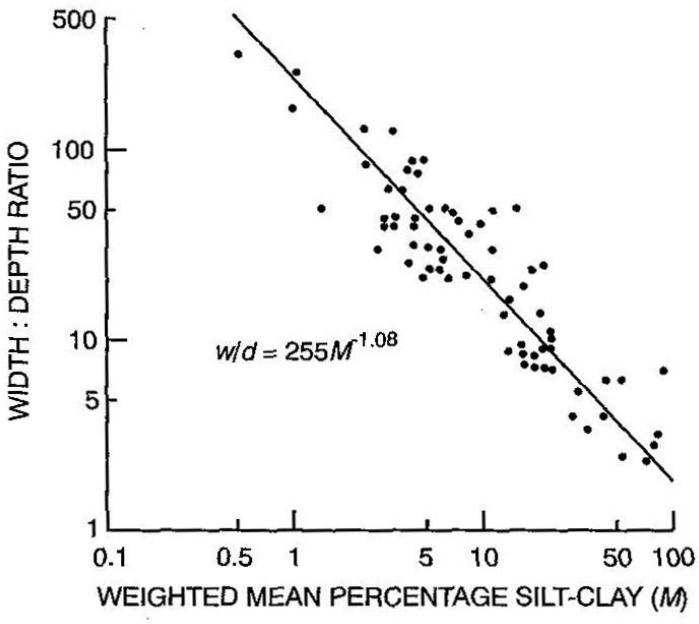

Figure 1.3. Relation between percentage silt-clay in channel boundaries and width-depth ratio (from Schumm 1960; scanned from Knighton 1998).

Further lack of understanding of channel adjustment is attributed to the diversity and contrast among quantitative indices for both discharge and sediment. For example, bankfull discharge commonly has been considered to be the flow responsible for observed channel morphology and often is approximated by the flow that occurs every one to two years (Leopold and Wolman 1957; Wolman and Miller 1960). However, the link between channel geometry, sediment transport, and bankfull discharge occurring every one to two years is problematic. First, bankfull stage is not always readily defined in field situations. Further, no consistent methods have been developed to determine bankfull stage (Williams 1978a). Another problem associated with bankfull discharge is that it does not always have a common frequency of occurrence (Williams 1978a), even within the same watershed (Pickup and Warner 1976; Andrews 1980). Bankfull discharge has been reported to occur at a variety of return periods, including 1.5 years (Leopold, Wolman, and Miller 1964; Dury 1973), the mean annual flood (Richards 1982), or 4 to 10 years (Pickup and Warner 1976). Further problems associated with bankfull discharge consider its lack of association to some aspects of channel form and sediment transport (Carlston 1965; Emmett and Wolman 2001).

The general concept of bankfull discharge might be problematic in the Llano River watershed because channel geometry and sediment transport are associated with infrequent extreme floods. Wolman and Gerson (1978) argue that channels in more arid climatic settings are likely to adjust to higher flows than those in humid settings. Validation of this idea is provided by Baker (1977), who discusses the climatic and

physiographic setting of the Texas Hill Country and concludes that extreme flood events control channel morphology. Others have shown that low-frequency, high-magnitude flows are responsible for observed channel morphology in arid to semi-arid regions (Huckleberry 1994; Heritage, Broadhurst, and Birkhead 2001; Tinkler 2001). However, the importance of flow variability has also been judged important in wetter climates. Gupta (1995), for example, found that rivers in the seasonal tropics of India display a channel-in-channel morphology, where a macro-channel has developed to accommodate large-magnitude floods and a low-water channel conveys moderate-magnitude floods and baseflow for the majority of time.

A number of scientists have used sedimentary indices to discriminate channel patterns, but there is no consensus as to which index is most appropriate. For example, Schumm (1960) advocates that silt-clay percentage in the channel banks controls cross-sectional shape. Alternatively, others have utilized bed-material parameters to differentiate planform and cross-sectional morphology (Howard 1987; van den Berg 1995; Xu 2004). Clearly, further research in unique settings is necessary to further elucidate the controls of river channel adjustment. Rivers that encounter abrupt downstream changes in lithology are good candidates to study the influence of sedimentary controls on channel morphology (Ferguson 1987).

1.2 Research Questions

The unique characteristics of the study area differ substantially from the studies comprising the base of knowledge on downstream trends in alluvial sediment composition and channel adjustment, illuminating several research questions:

1. What downstream trends emerge in the sediment composition (particle size, sorting, carbonate, and magnetic susceptibility) of instream and overbank deposits in watersheds with complex lithologic and flood-prone hydrologic conditions?
2. Because of problems associated with bankfull discharge, what discharge controls hydraulic geometry of rivers characterized by flashy, flood-dominated hydrologic regimes?
3. How does channel geometry adjust to the downstream continuum of bedrock exposures and alluvial surfaces?

1.3 Hypotheses

A summary of predicted controls and influences on mutual channel adjustment is presented in Table 1.1. The hypothesized controls and influences are based on previously published theories and qualitative observations. Further, a model of hypothesized downstream channel morphology is provided in Figure 1.4.

Table 1.1. Author-based hypotheses of downstream sedimentary and morphologic trends in the Llano River watershed, Central Texas, USA.

Control	Hypothesized influence
1. Flow regime	• Highly variable flow regime results in channel-in-channel morphology • Extreme flood magnitudes result in bankfull stage with return periods greater than 1 to 2 years
2. Lithology	• Cretaceous carbonate and Paleozoic sedimentary zones associated with high percentage of silt and clay in banks and gravel-sized bed material; Precambrian igneous and metamorphic zone associated with higher percentages of sand in both bed and bank material • Cretaceous carbonate and Paleozoic sedimentary zone with relatively high carbonate content; Precambrian igneous and metamorphic zone with relatively low carbonate content • Cretaceous carbonate and Paleozoic sedimentary zone with relatively low magnetic susceptibility; Precambrian igneous and metamorphic zone with relatively high magnetic susceptibility • Relatively resistant rocks associated with greater degree of valley confinement
3. Alluvial sediment composition	• Gravel-sized bed material results in relatively wide and shallow channels; sand-sized bed material with relatively deep and narrow channels • High percentage of silt-clay in channel banks result in relatively narrow channels; high percentage of sand in channel banks result in relatively wide channels
4. Locally steep channel slope	• Higher stream power per unit area • Coarse bed-material • Relatively wide channel • Braided channel pattern
5. Bedrock exposure (valley confinement)	• Greater proportion of bedrock exposure increases channel width • Highly variable bank morphology • More bedrock exposures associated with complexity in channel planform • Resistance of bedrock inversely related to alluvial channel development (i.e., weak bedrock promotes wider and deeper floodplains to develop) and meandering patterns • Bedrock joints control valley and channel position

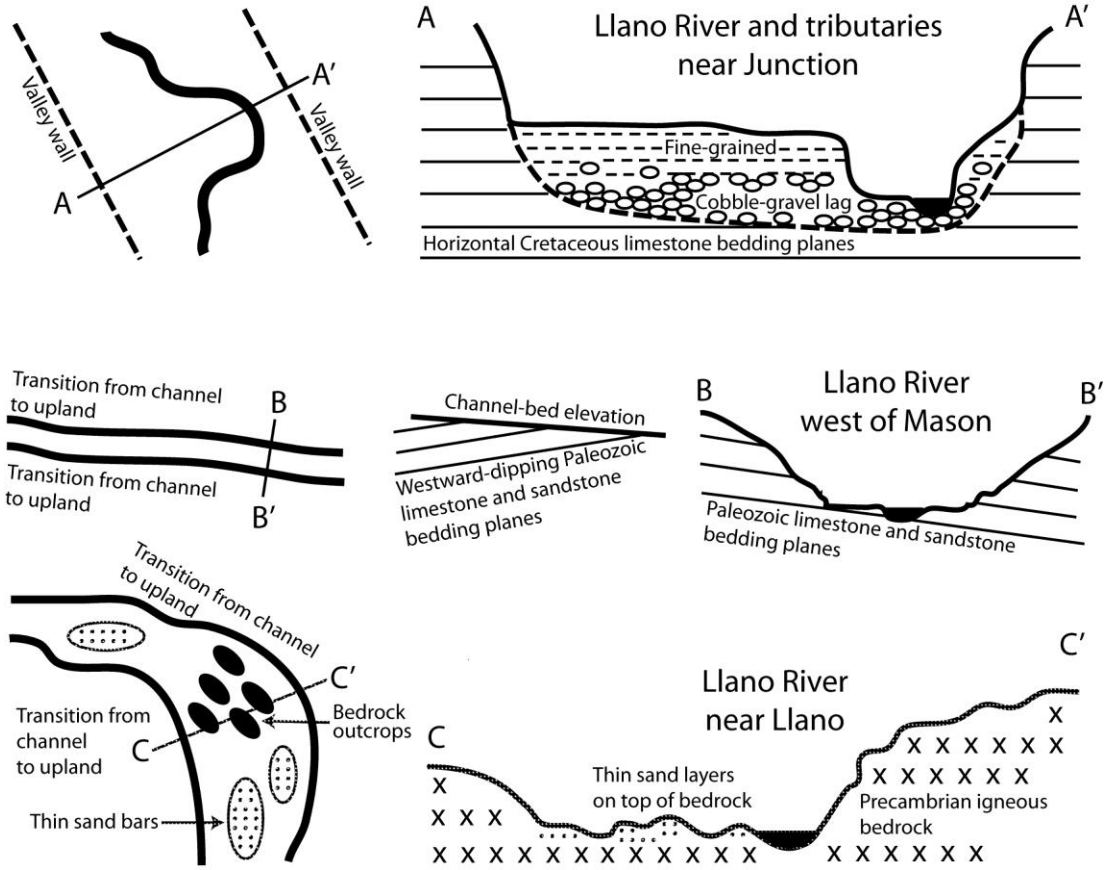

Figure 1.4. Author-based hypothesized model of downstream channel adjustment of the Llano River, Central Texas, USA.

1.4 Implications

The proposed study is expected to contribute to theoretical understanding in fluvial geomorphology by examining the controls of channel geometry for river systems that are underrepresented in the literature. The combination of the dynamic hydrologic regime, mixed alluvial and bedrock characteristics, and sharp lithologic transition between the carbonate and igneous rocks provides a unique setting to test concepts of dominant discharge and the influence of sediment type on channel adjustment. Further, this study will contribute to a broader understanding of equilibrium concepts pervasive in fluvial geomorphology.

The findings will also be of applied value to an audience of stream ecologists, engineers, and hydrologists. Stream ecologists in government agencies and other organizations are concerned with geomorphic-unit composition and channel stability as related to aquatic habitat within the study area because most models of channel adjustment originate from humid or snowmelt-dominated regions of the eastern United States, Rocky Mountains, Pacific Northwest, or the United Kingdom. An increased understanding of the geomorphic role of high-magnitude flows in hydrologically-variable rivers could enhance investigations of habitat availability and viability (Brierley and Fryirs 2005; Doyle et al. 2005). Additionally, state and county highway departments are concerned with the structural integrity of roads, bridges, low-water crossings, and culverts associated with rivers in Central Texas. High rates of channel adjustment or the episodic transport of gravel lobes can damage such infrastructure.

Further, river planning agencies (e.g., Lower Colorado River Authority) also have expressed concerns about channel adjustment, and are especially concerned with understanding sediment transport associated with reservoir sedimentation. Finally, the ability to predict changes in channel geometry for a given suite of hydraulic and sedimentary controls is important for riparian restoration efforts, which is a topic of increasing importance to Central Texas communities.

1.5 Dissertation Scope

This study utilizes field surveys and sediment samples, laboratory analyses of sediment, geographic-information-system (GIS) analyses, flood-frequency analyses, and statistical analyses to examine the combined roles of the hydrologic regime and channel bed and bank material characteristics in controlling mutual channel adjustment of the Llano River and selected tributaries in Central Texas. Between December 2004 and February 2008, various field-survey trips were made to the study area to collect data (Table 1.2). Field, laboratory, and statistical methods include established techniques and equipment common to geomorphologists and hydrologists. Field methods include cross-sectional surveys of channel morphology; surveys of high-water-mark elevations following high-magnitude flows in 2007; and sediment sampling of channel bed, bank, and floodplain material. Particle-size, carbonate-content, and magnetic susceptibility analyses of sediment were done at the Applied Geomorphology and Geoarchaeology Laboratory at the Department of Geography and the Environment,

The University of Texas at Austin. GIS analyses of 10-meter digital elevation models (DEMs), hydrography, and digital orthophoto quarter quadrangles (DOQQs) were done in ESRI ArcGIS 9. Statistics and flood frequency were analyzed using a combination of Microsoft Excel 2007 and R version 2.6.2 (R Development Core Team 2004).

Table 1.2. Field-survey trips to the study area by the author.

Approximate date of trips	Purpose
1. December 2004	Cross-sectional channel survey of North Llano River near Junction
2. June to August 2006	Cross-sectional channel surveys and sediment sampling of sites near Junction
3. November 2006	Cross-sectional channel surveys and sediment sampling of sites near Junction
4. April 2007	High-water marks along Llano River
5. May 2007	Cross-sectional channel surveys and sediment sampling of sites near Mason and Llano
6. June 2007	Cross-sectional channel surveys and sediment sampling of sites near Llano
7. July 2007	High-water-mark elevations established along Llano River
8. February 2008	High-water-mark elevations surveyed for Llano River

1.6 Dissertation Outline

The dissertation is organized into seven chapters, four of which have individual abstracts and conclusions and are meant to serve as stand-alone documents. Formatting, including citations, bibliography, and other details, of the document is based on the Annals of the Association of American Geographers. Some material is presented more than once in different chapters, but redundancy is kept to a minimum and used only when deemed necessary by the author. The chapters are described below:

1. INTRODUCTION—The introduction is this chapter, which describes the background, research questions, hypotheses, implications, and scope of the dissertation project.
2. LITERATURE REVIEW—The chapter reviews theory, techniques, and applications of at-a-station hydraulic geometry, downstream hydraulic geometry, and dominant and effective discharge. A primary objective of the literature review is to summarize contemporary trends and findings associated with the reviewed fluvial geomorphic concepts.
3. PHYSICAL SETTING AND PALEOENVIRONMENTAL HISTORY OF THE EDWARDS PLATEAU—The chapter provides details on the present-day climate, geology, physiography, and biota of the Edwards Plateau in Central Texas, but the majority of content is a review of the literature documenting environmental change in the plateau since the Last Glacial Maximum (20,000 years B.P.). The chronology of late-Quaternary environmental change serves as

important context for the present-day physical setting in the study area. A considerable portion of this chapter is devoted to changes in river-channel behavior and characteristics.

4. RESEARCH DESIGN—The chapter summarizes the research approaches used to elucidate the controls of alluvial sedimentology and channel adjustment in the Llano River watershed.
5. ALLUVIAL SEDIMENTOLOGY OF THE LLANO RIVER WATERSHED—The chapter presents and discusses results associated with alluvial sediment deposits in the Llano River watershed, including downstream trends in particle size, carbonate content, and magnetic susceptibility of channel-bed and bank deposits. Techniques include field sampling, laboratory sediment analyses, and statistical analyses. Various methods and characteristics of the physical setting are embedded in the chapter.
6. CHANNEL ADJUSTMENT IN THE LLANO RIVER WATERSHED—The chapter presents and discusses results associated with the downstream adjustment of channel pattern and shape related to hydrologic, lithologic, and sedimentary controls in the Llano River watershed. Techniques include GIS analyses, flood-frequency analyses, at-a-station hydraulic geometry, and downstream hydraulic geometry. Various methods and characteristics of the physical setting are embedded in the chapter.

7. SUMMARY AND CONCLUSIONS—The chapter summarizes the results of the dissertation, synthesizes the findings, narrows the findings down to a few conclusive statements, and poses further research questions to potentially guide future endeavors.

Chapter 2. A Review of Contemporary Applications that Use Hydraulic Geometry and Dominant or Effective Discharge: Implications for Environmental Assessments of Fluvial Systems

2.1 Abstract

Hydraulic geometry and fluvial geomorphic applications traditionally have relied on identification of a dominant or effective discharge. The increasing awareness that various flows are responsible for fluvial and ecological processes, operating within river channels and overbank, provides an alternative line of inquiry for these concepts to be utilized. Whereas many investigations have shown that channel geometry and cumulative sediment transport are associated with bankfull conditions and 1- to 2-year return periods, other studies in more dynamic systems have disassociated dominant or effective flows from those restrictions. In general, the traditional effective discharge concepts outlined by Wolman and Miller (1960) are most valid in humid or snowmelt-driven fluvial systems, have mixed results in seasonally-driven systems, and become less predictive for small watersheds, incised channels, or in systems with highly variable flow regimes. At-a-station and downstream hydraulic geometry analyses used to assess the environmental condition of fluvial and riparian ecosystems should not solely rely on identification of one formative discharge, but would benefit from an assessment of: (1) the discharges and stages at which certain sediment-transport processes initiate (e.g., critical shear stress) or operate (e.g., effective discharge) and (2)

the discharges and stages at which particular physical features occur (e.g., channel bars, succinct breaks in bank slope, perched flood channels, etc.). Further, accurate interpretations of sediment-transport processes and channel formation are likely if flows are analyzed with respect to antecedent conditions, timing, and typical durations of flow.

2.2 Introduction

The tenets of steady-state equilibrium and uniformitarianism are responsible for a number of concepts pervasive in applied fluvial geomorphology today, including hydraulic geometry and dominant, or effective, discharge. In many publications, hydraulic geometry and dominant discharge have been investigated or applied separately, but both concepts largely infer that flow energy controls channel morphology. This chapter introduces the concepts of hydraulic geometry and dominant discharge, discusses their strengths and limitations, and reviews the relevant literature prior to the mid-1990s. The findings of this review are expected to provide context and comparative examples useful for inquiries of cross-sectional channel adjustment and the relation of channel geometry to discharge.

2.2.1 Hydraulic Geometry

Hydraulic geometry, a largely empirical technique introduced by Leopold and Maddock (1953), quantifies the cross-sectional morphology of stream channels in relation to their flow regime. The three factors of discharge (width, depth, and velocity)

are plotted in log space with discharge on the abscissa axis, such that three slope-dependent exponents (*b*, *f*, and *m*) of the regression-fitted lines satisfy continuity by summing to the value "1" (Figure 2.1). The *b*, *f*, and *m* exponents represent the rate of change of width, depth, and velocity with discharge. The fundamental hydraulic geometry equations are:

$w = aQ^b$,

$d = cQ^f$,

$v = kQ^m$, where

w is water-surface width, in meters; d is mean depth, in meters; v is mean velocity, in meters per second; Q is discharge, in cubic meters per second; a, c, and k are empirically-derived coefficients; and b, f, and m are empirically-derived exponents.

Hydraulic geometry can be applied to the range of flows at one cross section, termed "at-a-station," or along a channel reach for a user-specified index of discharge at multiple cross sections, termed "downstream." At-a-station hydraulic geometry commonly has three phases in most river channels: (1) low-flow conditions that are incapable of entraining bed and bank material, (2) moderate-flow or active conditions associated with entrainment and transport of bed (and possibly bank) material, and (3) high-flow or overbank conditions (Knighton 1998). Breaks in line slope or inflections in the log-linear relations of width, mean depth, and mean velocity to discharge are associated with transitions between the three phases.

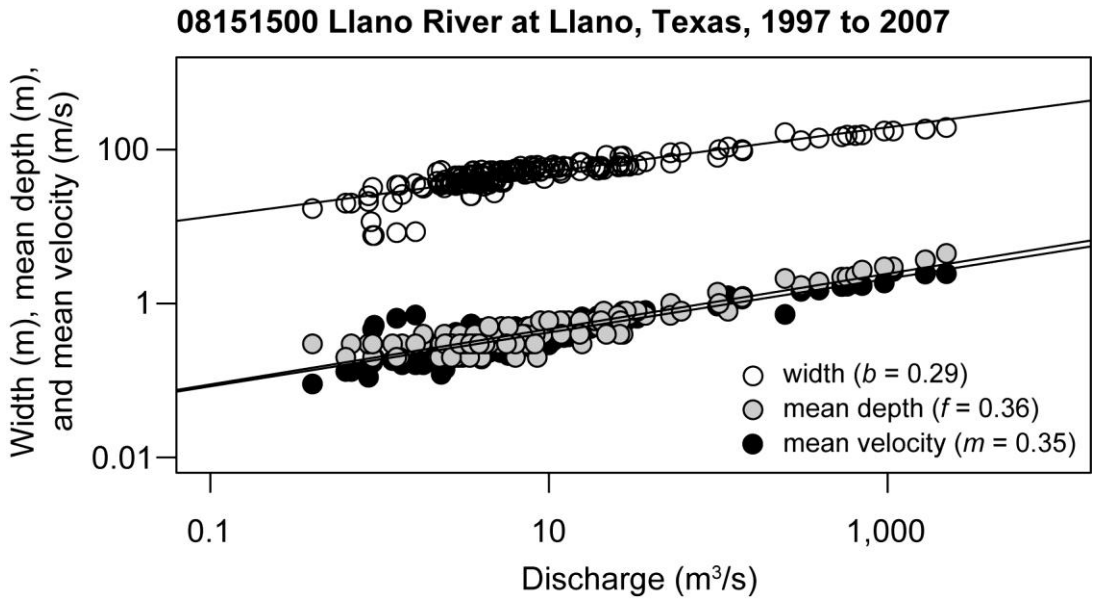

Figure 2.1. Example of at-a-station hydraulic geometry using discharge measurements at U.S. Geological Survey streamflow-gaging station 08151500 Llano River at Llano, Texas for hydrologic years 1997 to 2007.

For downstream hydraulic geometry, the choice of a discharge index is relegated to the practitioner. For downstream investigations specific to surface-water hydrology, mean annual discharge or another statistically-relevant flow is chosen, but investigations specific to channel geometry mostly use bankfull discharge (e.g., Xu 2004; Wohl and Wilcox 2005). Leopold and Maddock (1953), using data from a limited collection of rivers, computed average values of the b, f, and m exponents for downstream hydraulic geometry, which are 0.5, 0.4, and 0.1, respectively. The values, closely confirmed by Knighton (1987), indicate that: (1) channel width, mean depth, and mean velocity all increase with downstream distance, and (2) channel width increases at a greater rate than mean depth and mean velocity. In contrast, it was shown that mean depth increases at a greater rate than water-surface width for at-a-station analyses. In the time since the introduction of hydraulic geometry, other factors have been similarly related to discharge and its factor components, including channel slope, flow resistance, and suspended sediment load (e.g., Leopold and Maddock 1953; Rhodes 1977; Knighton 1998), and interpretive downstream applications often require simultaneous relations to be developed between these variables and cross-sectional geometry (Ferguson 1986).

Hydraulic geometry stems from equilibrium theory because it suggests that at-a-station cross-sectional form and downstream adjustment to channel shape are maintained by a definable hydrologic regime. A hydrologic regime can be defined by the unique relations of flow magnitude and frequency, and essentially represents flow

variability. For example, the oft-mentioned flashy-flow regime displays relatively low baseflow for the vast majority of time, punctuated by extreme events with peak discharges that are magnitudes larger than the mean annual flow. Quantifiable measures of a hydrologic regime are computed through various statistics, such as flow-duration curves, ratios of peak discharge to mean annual discharge (Lewin 1989), flood-frequency analyses (Stedinger, Vogel, and Foufoula-Georgiou 1993), and zero-flow days (Smakhtin 2001), among many others. In essence, a hydrologic regime is defined by flow statistics for the lumped period of record, and the definition, therefore, does not consider hydrologic change during that timeframe or the expected morphologic consequences (Knighton 1975; Knighton 1977). Only when hydraulic geometry is analyzed for subdivisions or "moving windows" of the period of record can variations in the flow regime be identified and subsequently used to investigate the tendency of a fluvial system to exhibit steady-state equilibrium. Hydraulic geometry applications are inseparable from equilibrium theory, and it is a circuitous argument to suggest that a stream channel exhibits steady-state equilibrium because of similarities in the hydraulic geometry relations to a known stable channel, especially when considering possibilities for multiple modes of adjustment (Phillips 1991).

Further, at-a-station exponents have large variation (Park 1977), which suggests to some that cross-sectional geometry is inherently unstable (Phillips 1990; Fonstad and Marcus 2003). Even more problematic is application of downstream hydraulic geometry because: (1) the choice of a discharge index is highly subjective, chosen to suit the

needs of a particular investigation; and (2) morphologic indices, such as bankfull, can be difficult to determine (Williams 1978a). In general, both at-a-station and downstream hydraulic geometry techniques are not particularly insightful for infrequent flow events above bankfull stage along rivers with extensive floodplains, because substantial changes in width, mean depth, and mean velocity no longer compare with flows below bankfull. For geomorphic investigations of alluvial channels, practitioners now recognize that a range of flows and their sequential order are responsible for maintenance of channel geometry (Pickup and Rieger 1979; Yu and Wolman 1987; Knighton 1998; National Research Council of the National Academies 2005), not just one dominant discharge.

Aside from complications that exist because of the dependence on equilibrium theory and variability, at-a-station hydraulic geometry can be a very useful technique to associate the hydrologic regime of a stream to its channel shape. If applied in conjunction with flood-frequency analysis, itself a problematic technique (Kidson and Richards 2005), much can be learned about the relation of various instream geomorphic surfaces to the magnitude and frequency of high-flow events (Gregory and Madew 1982). For example, at-a-station hydraulic geometry could identify a threshold mean velocity that occurs at a particular frequency, which effectively limits the vertical extent of channel bars at that location.

At-a-station hydraulic geometry analyses can be especially insightful for practitioners who operate streamflow-gaging stations, civil engineers who design

instream structures, and aquatic biologists who investigate habitat structure and function. Possibly more useful to fluvial geomorphologists, especially those operating at the watershed scale, is downstream hydraulic geometry, because channel morphology facilitates the choice of a morphologic-dependent index of discharge, usually the value at bankfull stage. In this manner, downstream trends in channel width and depth are identified, and inflections in the log-linear relations highlight the influence of other controls, possibly sedimentary, anthropogenic, or vegetation, among others. The variation in downstream hydraulic geometry data, as a proxy for the predictability of channel shape, could further indicate if other variables are influential (Wharton 1995), or that another discharge index would be more applicable. Finally, another widely utilized application of downstream hydraulic geometry is the development of regional at-a-station regression equations to predict channel shape (e.g., Betson 1979; Castro and Jackson 2001).

Previous investigations that targeted or utilized hydraulic geometry have highlighted the opportunities and disadvantages of the technique. Langbein (1964) and Langbein and Leopold (1964), in developing their theoretical explanation for probable energy distribution and channel equilibrium, deduced that minimization of the sum of squares of the b, f, and m exponents, termed the theory of minimum variance, is an internal goal of a river channel, in addition to the basic physical requirements of continuity, flow resistance, and sediment transport. Williams (1978b) used data from a variety of rivers in the United States to generally support the theory, finding that

predictions of width exponents are most predictive and velocity exponents are least predictive.

The theory of minimum variance has been refuted from a number of angles, including negligence of a physical explanation (Ferguson 1986), disregard for sediment transport (Knighton 1998), indeterminacy and equifinality (Thornes 1977), and reliance on log-linear relations of hydraulic geometry (Richards 1973), which should not be expected because of non-linear changes in roughness with discharge. Further, a number of researchers have noted that channel boundary composition (e.g., Parker 1979; Osterkamp and Hedman 1982; Knighton 1987; Huang and Warner 1995) and vegetation (e.g., Hey and Thorne 1986) substantially affect hydraulic geometry relations, especially where cohesive banks (Schumm 1960) and dense vegetation effectively reduce channel width, complicating the simple association with discharge. Other dimensions of stream channel geometry influence hydraulic geometry relations, including pool-riffle sequences (Figure 2.2) (Richards 1976) and channel pattern (Knighton 1974; Knighton 1982). Finally, others have either graphically reproduced hydraulic geometry relations, such as the triangular b, f, and m diagram (Figure 2.3) (Rhodes 1977; Rhodes 1987), or introduced new models of hydraulic geometry, including log-quadratic regression (Richards 1973), dimensionless relations (Parker 1979), piecewise linear regression (Bates 1990), compositional data analysis (Ridenour and Giardino 1991), among others (Rhoads 1992). For further detail about the advantages, disadvantages, and alternative uses of hydraulic geometry, excellent

reviews are given in Richards (1977), Ferguson (1986), and Knighton (1998); and an appreciable set of equations are provided in Wharton (1995).

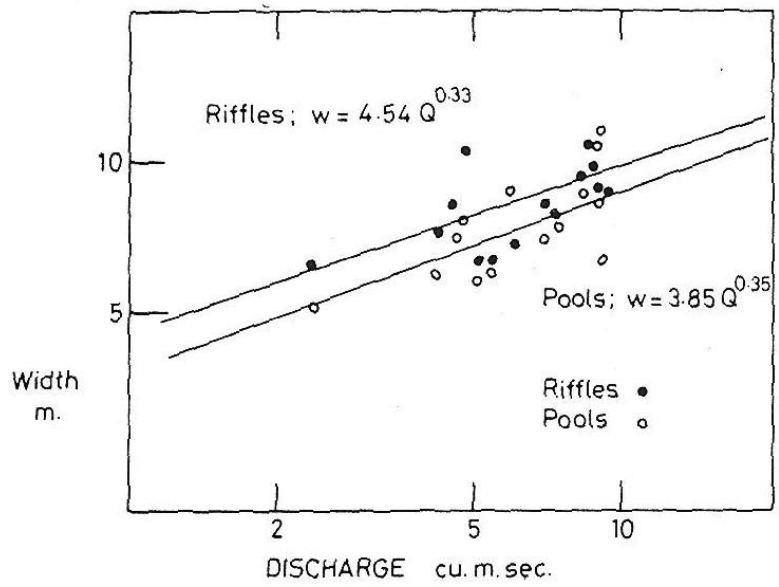

Figure 2.2. Example of downstream hydraulic geometry of channel width separately considered for reaches associated with pools and riffles (from Richards 1976).

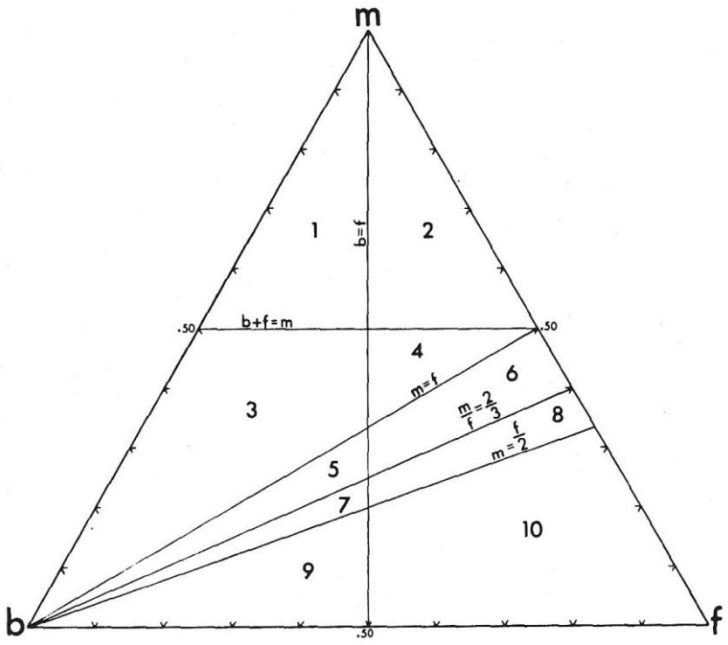

Figure 2.3. The b, f, and m diagram is used to distinguish ten different channel types based on observed relations of width, mean depth, and mean velocity (from Rhodes 1977).

2.2.2 Dominant Discharge

Hydraulic geometry and other techniques used to quantify channel morphology often are applied to stream channels with the assumption of a dominant, or channel-forming, discharge (Table 2.1). The concept of dominant discharge was originally proposed by Inglis (1941), who states that a single flow exists that, if continuous and constant through time, would generate the same channel geometry as the natural flow regime. Wolman and Miller (1960) expanded and popularized this idea in the landmark paper on effective discharge (Table 2.1), in which they conclude that moderate floods are responsible for the majority of sediment transport through time (Figure 2.4). According to their moderate-flood theory, the effective discharge is large enough to generate the power necessary to mobilize and transport sediment, and occurs frequently enough to cumulatively transport the largest volume of sediment. Collectively, the more extreme floods simply do not occur frequently enough to exceed the moderate floods in terms of cumulative sediment transport through time. Essentially, the relatively frequent moderate floods are those that maintain the geomorphic equilibrium of natural stream channels. It is interesting to note that Wolman and Miller (1960) acknowledged that relatively highly variable flow regimes are more likely to experience the effective discharge on a more infrequent basis, but this documented caveat was overshadowed by the moderate-flood theory and, therefore, has generally been neglected in geomorphic assessments.

Table 2.1. Definitions of dominant and effective discharge.

Term	Definition
Bankfull discharge	The discharge that fills the channel to the top of its banks[a]
Dominant discharge	The theoretical discharge that if maintained indefinitely would result in the same channel geometry as the existing channel subject to the natural range of flow events[a]
Channel-forming discharge	Equivalent to "dominant discharge"[a]
Effective discharge	The discharge responsible for the cumulative majority of sediment transport over time; the maximum product of the sediment transport rate and frequency of a given discharge for a range of flows at a channel cross section

[a] Definition from Biedenharn et al. (2000).

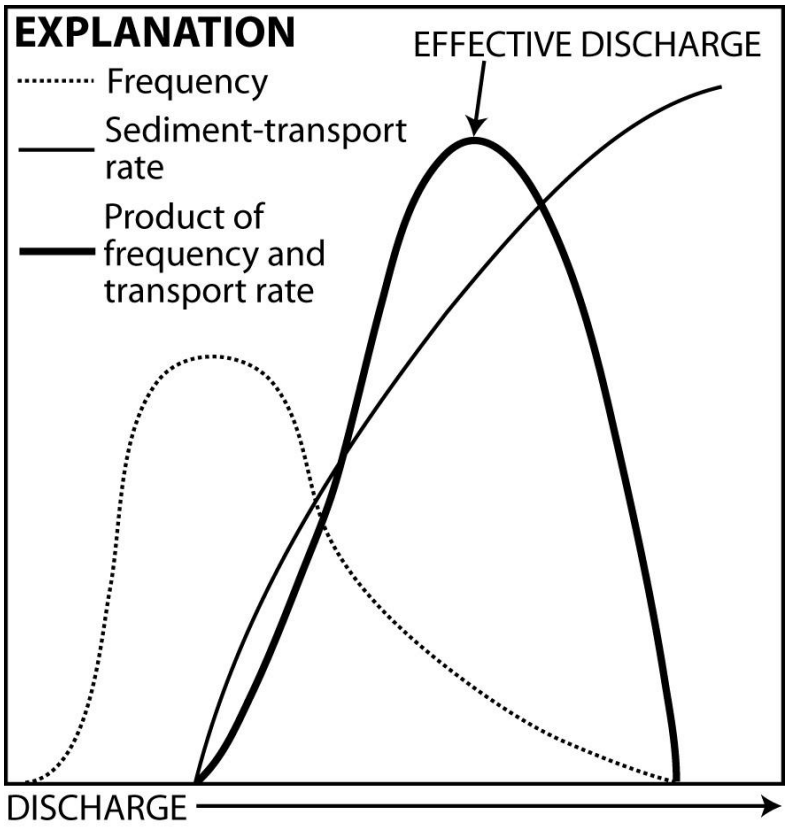

Figure 2.4. Conceptual diagram of effective discharge (modified from Wolman and Miller 1960), which is the maximum product of flow frequency and its associated sediment transport rate.

Using channel morphology as a guide, dominant discharge often is equated to bankfull discharge (e.g., Wolman and Leopold 1957; Leopold, Wolman, and Miller 1964). Theoretically, the channel dimensions have adjusted over time to fully accommodate the flow that cumulatively transports the most sediment over time. Using various rivers in the United States, Wolman and Miller (1960) documented that the frequency of bankfull discharge occurs, on average, between one and two years. However, other studies have shown that the bankfull (Pickup and Warner 1976) and effective discharges (Baker 1977) can be less frequent, especially in river systems characterized by highly variable flow regimes. Further, it has been proposed that bankfull and effective discharges have different return periods for some rivers (Pickup 1976; Pickup and Warner 1976) and for sites with different drainage areas in the same watershed (Wolman and Gerson 1978; Ashmore and Day 1988).

In the time since the general acceptance of Wolman and Miller (1960), various studies have explored the application of dominant or effective discharge, and the association with bankfull conditions. Invariably, those studies either confirmed or undermined the general claim that bankfull discharge is dominant and has a return period of 1 to 2 years. Whereas cross-sectional shape possibly is most indicative of dominant discharge, some researchers have shown that planform geometry also can be explained by the dominant-discharge concept (Carlston 1965; Ackers and Charlton 1970; Ackers 1982).

In an assessment of rivers in the USA from Barnes (1967), Dury (1973) computes that bankfull discharge has an average return period of 1.58 years, and further suggests that underfit rivers complicate the association of channel geometry with contemporary dominant discharge. Gupta and Fox (1974) document the reduction of channel width by small and moderate events following a series of large floods in the humid, eastern United States, but also acknowledge that more variable hydrologic regimes maintain relatively wide channels. Further support to Gupta and Fox (1974) is provided by Patton (1988b) and Pitlick and Thorne (1987), who document recovery of rivers following rare, extreme floods in the New England region and a mountain stream in Colorado, respectively. Combining measured suspended-sediment loads with bedload transport estimates in the Yampa River basin, Colorado and Wyoming, USA, Andrews (1980) finds that the effective discharge matches the bankfull discharge, confirmed by Leopold (1992), and has a return period between 1 and 1.5 years.

Some case studies have retained a more neutral sentiment regarding the 1- to 2-year bankfull association of dominant discharge. Only considering bedload transport, Pickup (1976) suggests return periods between 1.1 and 1.5 years for maximum cumulative bedload transport in selected streams of southeastern Australia, but also shows that bankfull discharge substantially exceeds the optimal discharge for bedload transport. To slightly modify previous conclusions and emphasize geomorphic form instead of sediment transport, Wolman and Gerson (1978) find that less frequent, high-magnitude events become more effective as aridity increases and drainage area

decreases. Pickup and Rieger (1979) propose an alternative model that associates the sequential nature and variability of flows to observed channel characteristics, avoiding acceptance of a singular dominant discharge. Baker (1977) submits that catastrophic response of stream channels to high-magnitude events are expected in small watersheds in highly variable flow regimes, but does not claim that the largest events transport the most sediment over time, essentially segregating a flow that controls channel geometry from one that cumulatively transports the most sediment. Similarly, Church (1988) suggests that relatively frequent events control cumulative suspended-sediment loads of rivers in cold climates, but more powerful and less frequent flows might control gravel transport and channel morphology.

Others have highlighted deviation of dominant discharge from the oft-cited 1- to 2-year return period. Schick (1974), in one of the first refinements of Wolman and Miller (1960), shows that arid-channel geometry reflects the work done by large, infrequent floods, because the lack of vegetation limits boundary resistance and moderate events rarely occur to restore previous conditions. Dury (1980) summarizes various pieces of evidence indicating that catastrophic fluvial events have operated in the past, and suggests that sudden shifts in global or regional climate increase the likelihood of highly-effective, but low-frequency, events. Walling and Webb (1987), focusing on suspended sediment, find that some fluvial systems can only access sources during extreme, high-magnitude events, such that 50 percent of the total load was transported only 0.2 percent of the time in one stream in England. Focusing on bedload,

Komar (1988) suggests that large floods can transport tremendous quantities of bed material, and also points out that the largest clasts, which can greatly influence long-term channel morphology (Harvey 1987), can only be transported by extreme velocities. Gupta (1988) explores the frequency and effectiveness of large floods in humid tropical environments, concluding that a suite of alluvial forms in the valley are maintained at stages above bankfull, and events with a return period greater than 10 years are responsible for more cumulative work than depicted in Wolman and Miller (1960). In a review of progress associated with the concept of dominant discharge, Kochel (1988) argues that some rivers displaying highly variable flow regimes, steep slopes, abundant bedload, erodible banks, or narrow bedrock cross sections only adjust during extreme events with return periods exceeding 50 years. Operating at larger spatial scales and temporal scales, Patton (1988a) suggests that drainage basin morphometry, including network extension, becomes increasingly controlled by high-magnitude, low-frequency events when recovery times are sufficiently long.

As a result of these often conflicting studies, the most controversial topic in fluvial geomorphology surrounds the role of the high-magnitude event in controlling sediment transport and channel form (Baker 1988), a situation not unheard of since the debates on the Channeled Scablands of the Pacific Northwest, USA (Bretz 1923). Some have even suggested that magnitude-frequency analysis is not as appropriate as other techniques, including distribution of stream power during floods (Magilligan 1992), in assessing the influence of floods on morphology.

In summary, much of the research prior to contemporary environmental assessments (circa 1995) show that rivers in humid mid-latitude environments or those that experience annual snowmelt events are likely to experience a dominant and effective discharge at bankfull stage occurring, on average, every 1 to 2 years. Rivers that experience more variable flow regimes in semi-arid to arid climates (Schick, Lekach, and Hassan 1987; Graf 1988), rivers that require extreme erosive power to modify their boundaries (e.g., bedrock channels) (Kochel 1988), or streams with relatively small drainage areas (Baker 1977; Wolman and Gerson 1978) are likely to experience a dominant or effective discharge less frequently. Further, others have suggested that sediment transport and channel form are more reliant on the chronologic sequence of events (Pickup and Rieger 1979; Yu and Wolman 1987) than a particular return period. Because downstream hydraulic geometry, and some interpretations of at-a-station hydraulic geometry, requires a geomorphically significant discharge to be established, it can be problematic if the practitioner does not adequately address the linkages between flow magnitude, frequency, duration, and observed channel geometry or rates of sediment transport.

Currently, a variety of environmental applications at widely variable spatial scales rely on fundamental geomorphic assessments of fluvial systems. Ubiquitous to many of these applications is the identification of a dominant discharge and the use of hydraulic geometry to quantify channel geometry, patterns of downstream adjustment, connectivity to overbank riparian environments, and comparison to other stream

channels. The original downstream hydraulic geometry plots in Leopold and Maddock (1953) used the mean annual discharge as the index flow, but numerous geomorphic investigations since Wolman and Miller (1960) specifically use bankfull discharge. The close association between dominant discharge and the quantification of channel geometry has influenced and saturated fluvial geomorphic literature for decades. It is not surprising to note that most fluvial geomorphic applications employ these theoretically-motivated, empirically-tested techniques. While many geomorphologists now acknowledge that a variety of flows occurring at various return periods are responsible for observed channel geometry and floodplain construction processes (Day and Hudson 2001; Brierley and Fryirs 2005; National Research Council of the National Academies 2005; Poff et al. 2006), very influential papers, handbooks, and applications are being published that fail to adequately address the limitations of both hydraulic geometry and dominant discharge (Rosgen 1994; U.S. Department of Agriculture Natural Resources Conservation Service 2007). From the broad spatial perspectives of instream flow programs to focused rehabilitation efforts along channel reaches, a review of contemporary hydraulic geometry applications and the reliance on dominant discharge is provided below with the goal of distinguishing the appropriate use and limitations of these fundamental geomorphic concepts.

2.3 Contemporary Hydraulic Geometry Applications

Hydraulic geometry remains a popular technique to quantify the association between channel form and the hydrologic regime, although its contemporary use deviates from more traditional applications. Some researchers have continued to focus on theoretical issues and mathematical derivation of hydraulic geometry techniques, and others have applied traditional techniques to innovative lines of questioning. The assortment of contemporary hydraulic geometry applications provided below represents research since the mid-1990s (Tables 2.2, 2.3).

Continuing with the log-linear critique of Richards (1973), Hickin (1995) highlights discontinuities in at-a-station hydraulic geometry relations when thresholds of scour are exceeded in the sandy gravel-bed Fraser River in British Columbia, Canada, showing that log transformation of hydraulic geometry obscures these process-driven discontinuities and suggests that data should not be transformed for investigations of instream geomorphic units and processes. Revisiting extremal hypotheses of optimal channel configuration for continuity, flow resistance, and sediment transport, Millar (2005) and Singh and Zhang (2008a, 2008b) derive theoretical solutions for hydraulic geometry. Assuming that maximum sediment transport efficiency defines the optimum state of channel geometry, Millar (2005) develops theoretical dimensionless equations for width, depth, slope, width-to-depth ratio, and the meandering-braiding transition of artificially-generated gravel-bed rivers. The equations require that: (1) a dominant (channel-forming) discharge is known

(assumed to be bankfull discharge), (2) a value for channel slope or sediment concentration is representative, and (3) a parameter that describes the comparative resistance of bed and bank material exists. Results show that exponents derived from the theoretical equations compare well with previously published empirical results. Singh and Zhang (2008a) emphasize temporal variation in stream power, channel form, and hydraulic variables with varying discharge; the distribution of stream power; and various extremal hypotheses (maximum entropy and minimum stream power) leading to a mathematical derivation of eleven at-a-station hydraulic geometry relations. The authors then calibrate and verify those equations using various data sets and a split sampling approach (Singh and Zhang 2008b), generally confirming their applicability.

Yet another modification of traditional hydraulic geometry formulae is provided by Stewardson (2005), which recognizes that a reach-based form of hydraulic geometry could minimize cross-sectional variability along the length of a given stream channel. Stewardson (2005) assesses reach-scale hydraulic geometry of streams in Victoria, Australia, through repeated surveys of multiple cross sections and straightforward computation of reach parameters for mean width, hydraulic depth, and the coefficients of variation of width, hydraulic depth, and cross-sectional velocity. Stewardson (2005) concludes that five cross sections are appropriate for reach-mean width, but ten or more are necessary for hydraulic depth. Ultimately, variation is reduced when compared with at-a-station exponents, but it is unknown how the application will perform in larger rivers or for high flows, because the streams used in this study are not large (all mean

discharges are less than 25 cubic meters per second) and flows used were less than bankfull stage.

Traditional forms of hydraulic geometry analysis have been used to discern channel pattern, infer historical adjustments of channel shape, quantify channels in diverse settings, and calibrate regional applications. In a traditional analysis of downstream hydraulic geometry using bankfull discharge for over 200 rivers, Xu (2004) quantitatively discriminates between combinations of meandering, braided, sand-bed, and gravel-bed rivers. Xu (2004) findings include: (1) sand-bed rivers are wider than gravel-bed rivers, (2) sand-bed rivers generally are deeper than gravel-bed rivers, (3) the difference in channel slope between sand- and gravel-bed rivers is greater than the difference in channel slope between meandering and braided rivers, and (4) the threshold between meandering and braided streams is better defined by comparing cross-sectional geometry as opposed to slope. Also focusing on channel pattern, Burge (2004) assesses at-a-station hydraulic geometry variables, including bankfull width and depth, to statistically distinguish differences between wandering, multi-thread channels and confined, single-thread channels in southeastern Canada, and shows little difference between the main channels for each pattern, but side channels in the multi-thread reaches are statistically different. Specifically focusing on at-a-station hydraulic geometry for large alluvial rivers, Latrubesse (2008) shows that the width exponent is generally low and the depth exponent is larger for sinuous single-thread channels than for low-sinuosity anabranching rivers.

Hydraulic geometry analyses of rivers in diverse settings are needed to adequately characterize the continuum of fluvial forms, and a number of researchers have recently responded to this gap in the literature. Deodhar and Kale (1999) technically investigate at-a-station hydraulic geometry at sites along monsoon-dominated rivers in India, but compare exponents in an analysis of downstream trends. The authors find that width-depth ratios decrease during large floods to compensate for discharge, thereby providing evidence that morphology is controlled by high-magnitude events. Further support of this is provided by Gupta (1999), which shows that at-a-station hydraulic geometry values of the annual peak discharge along the Narmada River of central India explain the box-shaped channel, associated with high-magnitude floods. Kale and Hire (2007) apply at-a-station hydraulic geometry on the monsoon-dominated Tapi River in central India, showing that a box-shaped channel results from the seasonal flow regime. Merritt and Wohl (2003) assess downstream hydraulic geometry of Yuma Wash, an arid, ephemeral channel in Arizona, USA, for a flood that increased in magnitude downstream, finding that a substantial increase in width was made possible by non-cohesive boundary materials and decreasing valley confinement.

Others have investigated the application of hydraulic geometry on non-fluvial channel systems. Based on a working hypothesis that trunk river stage and flow controls stage, flow direction, and sediment flux of small, tropical tributary mouths, Kennedy (1999) draws comparison between the at-a-station hydraulic geometry of those streams and mesotidal inlets along coastal shorelines. Only considering discharge of the

tributaries, Kennedy (1999) shows that no predictable relation exists between depth and flow and a negative relation exists between width and flow, enabling the comparison to tidal systems where peak flow occurs at mid-tide, rather than bankfull. Similarly, Williams, Orr, and Garrity (2002) use hydraulic geometry to predict cross-sectional characteristics of tidal channels from contributing marsh area and tidal prism along San Francisco Bay.

Finally, a large number of investigations utilizing hydraulic geometry have focused on mountain rivers. For example, Merigliano (1997) uses at-a-station hydraulic geometry to investigate the role of historical floods, dam construction, and scour-and-fill processes along the Snake River in Idaho, USA. Torizzo and Pitlick (2004), to accompany a study on effective bedload discharge, also examine downstream hydraulic geometry of mountain streams in Colorado, USA, and attribute the minimal increase in depth to inherited glacial coarse sediment. Wohl and Wilcox (2005), in another traditional downstream analysis, have well developed morphological relations to bankfull discharge, in spite of complexities introduced by colluvial inputs and discontinuous bedrock exposures. They conclude that relatively frequent hydraulic forces are sufficient to overcome the resisting framework of the channel boundary. In order to investigate the effects of inherited glacial morphology and lakes on stream geomorphology, Arp et al. (2007) apply at-a-station and downstream hydraulic geometry techniques to mountain rivers in Idaho. Their results show that weakly developed relations highlight the importance of sediment source and sink locations in

the region. Wohl (2004) clarifies the limitations of downstream hydraulic geometry by concluding that well-developed relations are associated with mountain rivers with a stream power (Ω) (W/m) to sediment size (d_{84}) (mm) ratio greater than 10,000 kilograms per cubic second, and poorly-developed relations are evident for mountain rivers less than 10,000 kilograms per cubic second. Finally, to develop more accurate regional hydraulic geometry models, Wilkerson (2008) concludes that the 2-year return period predicts bankfull geometry better than drainage area.

Table 2.2. Summary of contemporary publications utilizing at-a-station hydraulic geometry.

Publication	Main findings	Location or setting	Hydraulic geometry exponents
1. Hickin (1995)	Discontinuities in at-a-station relations as bed-scour threshold is exceeded; obscured by log-transformation of data	Fraser River, British Columbia, Canada; snowmelt-dominated	width = 0.07; depth = 0.47; velocity = 0.46
2. Merigliano (1997)	At-a-station hydraulic geometry *m*/*f* ratios provide insight to scour-and-fill processes and presence of pool-riffle sequences; historical assessment of post-impoundment conditions	Snake River, Idaho, USA; snowmelt-dominated	1950 to 1956 width = 0.08; depth = 0.54; velocity = 0.38 1957 to 1990 width = 0.08; depth = 0.55; velocity = 0.37
3. Deodhar and Kale (1999)	At-a-station hydraulic geometry shows decreasing width-depth ratios with increasing discharge; evidence for high-magnitude floods controlling geometry	Allochthonous (decreasing inputs of discharge with downstream distance) rivers, western India; monsoon-dominated	Twenty-one at-a-station values provided in publication; variable
4. Gupta (1999)	High-magnitude floods in a monsoon-dominated river generates a box-shaped geometry; at-a-station analysis of annual peak discharge	Narmada River, central India; monsoon-dominated system	width = 0.04; depth = 0.46; velocity = 0.50
5. Kennedy (1999)	Finds similarities between at-a-station geometry of small tributary mouths and mesotidal inlets	Small tributary mouths at confluences of a larger river in monsoon-dominated Sri Lanka	Relations graphically shown, but no exponents provided; no log-linear association between depth and discharge; negative association between width and tributary discharge
6. Burge (2004)	Statistical analysis of hydraulic geometry variables show that small side channels in multi-thread reaches are distinct, but main channels are similar to single-thread reaches	Humid rivers in continental glaciated terrain in southeastern Canada	Not included
7. Millar (2005)	Theoretical dimensionless regime equations developed	Artificial gravel-bed rivers	width = 0.5; depth= 0.37 (both modified by additional particle-size parameter)
8. Stewardson (2005)	Develops reach-based hydraulic geometry relations to reduce at-a-station variability	Mostly gravel-bed streams in southeastern Australia	width = 0.11; depth = 0.23; velocity = 0.52 (mean of all streams used)
9. Kale and Hire (2007)	At-a-station analyses show box-shaped channel of monsoon-dominated river	Seasonal monsoon river in central India	width = 0.21; depth = 0.46; velocity = 0.33
10. Latrubesse (2008)	At-a-station analyses for large rivers are characterized by low width exponents, and depth increases more for single-thread sinuous rivers than for anabranching rivers	Large alluvial rivers in South America	Various; width usually less than 0.1; depth and velocity relation associated with single-thread or anabranching channels
11. Singh and Zhang (2008a, b)	Derive eleven at-a-station hydraulic geometry equations, emphasizing temporal variation in stream power and extremal hypotheses	Theoretical	Various; compared to other data sets
12. Wilkerson (2008)	2-year return period predicts bankfull geometry better than drainage area for regional hydraulic geometry models	Various systems in the United States	Various; used numerous data sets

Table 2.3. Summary of contemporary publications utilizing downstream hydraulic geometry.

Publication	Main findings	Location or setting	Hydraulic geometry exponents
1. Williams, Orr, and Garrity (2002)	Uses a form of downstream hydraulic geometry (using increasing marsh area or tidal prism instead of discharge) to predict equilibrium morphology of tidal channels	Tidal channels along San Francisco Bay, California, USA	Contributing marsh area width = 0.55; depth = 0.20 Tidal prism width = 0.46; depth = 0.18
2. Merritt and Wohl (2003)	Downstream hydraulic geometry during a flood that increased in magnitude downstream; width increased as a result of non-cohesive boundary materials and decreasing valley confinement	Yuma Wash, Arizona, USA; arid, ephemeral channel	width = 0.78; depth = 0.15; velocity = 0.14
3. Torizzo and Pitlick (2004)	Downstream hydraulic geometry displays minimal increase in depth; attributed to glacial sources of coarse sediment	Steep, gravel-bed streams in Colorado, USA	width = 0.56; depth = 0.26
4. Wohl (2004)	Well-developed downstream hydraulic geometry relations for stream power (Ω) to particle size (d_{84}) ratio greater than 10,000 kg/s^3; poorly-developed relations less than 10,000 kg/s^3	Mountain rivers in USA, Panama, Nepal, and New Zealand	Various; used numerous data sets
5. Xu (2004)	Downstream hydraulic geometry used to discriminate between meandering/braiding and sand-bed/gravel-bed rivers worldwide	Various settings worldwide	width = 0.52; depth = 0.40 for braided-meandering transition
6. Wohl and Wilcox (2005)	Downstream hydraulic geometry shows well-developed relations at bankfull discharge for rivers with substantial colluvial inputs and bedrock outcrops	Steep, step-pool, gravel-bed rivers in New Zealand	Eastern stream: width = 0.50; depth = 0.33; velocity = 0.17 Western stream: width = 0.52; depth = 0.43; velocity = 0.07
7. Arp et al. (2007)	Weak downstream hydraulic geometry relations highlight importance of sediment sources and sinks, including lakes	Mountain rivers in formerly glaciated terrain in Idaho, USA	Downstream Warm Springs Creek: width = -0.47; depth = 0.45; velocity = 0.83 Sawtooth Mountain Lake District: width = 0.56; depth = 0.11; velocity = 0.24

2.4 Contemporary Dominant or Effective Discharge Applications

There are two distinct terms used to describe the flow driving the majority of fluvial work and the observed channel geometry. Biedenharn et al. (2000) distinguish the dominant discharge as the flow that is associated with channel geometry, and the effective discharge is associated with transport of bed-material load, but could be considered sediment transport in general (Table 2.1). Contemporary research and applications have thoroughly explored the concepts of dominant or effective discharge, indicating that debates surrounding magnitude and frequency are both applicable and lively (Tables 2.4, 2.5, and 2.6). A few researchers have investigated theory of dominant or effective discharge, but most have applied the theory in diverse settings either to confirm or refute the general concept of Wolman and Miller (1960). Discussed below are publications that have focused on the concepts and applications of dominant or effective discharge since the mid-1990s.

2.4.1 Contemporary Theoretical Applications

Assuming log-normal distributed discharge frequency and sediment transport as a power function of discharge to predict the frequency of effective discharge, Nash (1994) finds poor agreement between observed and predicted effective discharges of 55 streams in the United States. Nash (1994) also mathematically solves for the effective discharge as:

$Q_e = e^{b\beta^2+\alpha}$, where

Q_e is the effective discharge, in cubic meters per second; e approximately is 2.718; b is an empirically derived exponent of the relation between the sediment transport rate and discharge; and α and β are the mean and standard deviation of the logarithm of discharge, respectively. Additionally, Nash (1994) finds that the frequency of effective discharge greatly varies from place to place, underscoring the difficulty of predicting effective discharge using a universally applicable flow frequency or bankfull discharge.

In a review provided in Biedenharn et al. (2000), there are three approaches to establish the dominant discharge: (1) bankfull discharge, (2) flow of a given return period, and (3) effective discharge; it is recommended that all three are employed to ensure consistency and reduce uncertainty. Doyle et al. (2007), however, only supports the use of effective discharge for channel restoration applications. The methodology to determine effective discharge used by Biedenharn et al. (2000) uses a flow-duration curve and a sediment-discharge rating curve, both requiring considerable data collection through time. Recognizing that total load transported constitutes a complete analysis of effective discharge, Vogel, Stedinger, and Hooper (2003) propose a more valid half-load discharge index, which is defined as the flow at which half the total cumulative load is transported, and is identical to that of Nash (1994), although it was derived through alternative mathematics. Using the half-load discharge index, the authors find that flows responsible for most cumulative sediment transport are larger and less

frequent than previously shown by traditional effective discharge techniques. The return periods for half-load discharge often on the order of decades to centuries.

2.4.2 Contemporary Applications Supporting Frequent Dominant Discharge Events

Aside from deterministic evaluations of dominant discharge, a number of contemporary case studies support the original findings of Wolman and Miller (1960). Batalla and Sala (1995) claim that bedload transport in a humid Mediterranean, sandy gravel-bed river is dominated by frequent events of moderate magnitude that fill the channel to bankfull stage. However, empirical plots show considerable variation in the relation between bedload transport rates and discharge. Hudson and Mossa (1997) focus on the duration of effective flows responsible for suspended sediment transport in three large, impounded rivers in the USA Gulf Coastal Plain, and conclude that the majority of cumulative transport occurs during moderate events. Biedenharn, Little, and Thorne (1999) perform a magnitude-frequency analysis of sediment transport at three long-term streamflow-gaging stations along the lower Mississippi River, finding that the effective discharge has a return period slightly more frequent than one year and closely corresponds to bankfull geometry. Further, an extreme event was specifically addressed and the authors conclude that its geomorphic effects and long return period are offset by more frequently occurring moderate floods. Additionally, a few investigations of very large rivers show that effective discharge occurs at "bar-full" stages instead of bankfull stages (Thorne, Russell, and Alam 1993; Biedenharn and Thorne 1994; Latrubesse 2008), which occurs on a relatively frequent basis.

Notably, many investigations of dominant discharge are for mountain rivers or systems with floods contingent on annual snowmelt. For gravel-bed rivers in the Rocky Mountains of the United States, Andrews and Nankervis (1995) generally reinforce earlier findings from Andrews (1980) that effective discharge closely approximates bankfull discharge and occurs, on average, about 16 days per year. Whiting et al. (1999), working in snowmelt-dominated streams of Idaho, USA, find that the effective discharge of bedload has about a 1.4-year return period, and is about 80 percent of the bankfull discharge. Also working in the Pacific Northwest of the United States, Castro and Jackson (2001) show only minor differences in bankfull discharge between relatively humid (1.2-year return period) and dry areas (1.4- to 1.5-year return period). Torizzo and Pitlick (2004) investigate the relations between bedload transport, hydraulic geometry, and effective discharge in mountain streams in Colorado, USA. Those authors conclude that the effective flows occur about 4 days per year. Further, the effective discharge closely matches the bankfull discharge, and its flow duration does not tend to increase with drainage area.

2.4.3 Contemporary Applications Neutral on Frequent Dominant Discharge Events

A variety of investigations tend to have a neutral sentiment on Wolman and Miller (1960), either because magnitude-frequency is considered less important than flow duration or other hydraulic considerations, or because variation from the original model is not sufficient to refute the concept. Costa and O'Connor (1995), in an analysis of short-duration floods resulting from two dam failures, support show that flow

duration is more important for geomorphic effectiveness than magnitude, as evidenced by minimal adjustments to the downstream channels and floodplains. The authors also suggest that stream-power graphs have more explanatory power for geomorphic consequences of individual floods than simple magnitude-frequency analysis. Fuller (2007), constraining his analysis to one flood with a return period of about 150 years, contrasts the geomorphic responses of three streams in New Zealand and finds that some reaches exhibited catastrophic change whereas others were not greatly affected. In general agreement with Magilligan (1992), Fuller (2007) argues that altered reaches were more sensitive to extreme flows because of their local channel and valley floor configuration, especially at channel bends, where channel width was confined, or where bounding terraces limited flood extent.

Hey (1998), in commentary on management and restoration of gravel-bed rivers, advocates for the use of bankfull discharge as a design flow for rivers displaying steady-state equilibrium, but warns practitioners about the association of between dominant or effective and bankfull discharge. Further, Simon and Darby (1999) state that dominant and bankfull discharge should not be associated for recently incised river channels, because cross-sectional area has increased and allows greater flows without approaching bankfull conditions.

Linking concepts of effective discharge to ecological functions, Pitlick and Van Steeter (1998) investigate alluvial reaches of the Colorado River near Grand Junction, Colorado, and conclude that flows slightly below bankfull stage carry the majority of

cumulative sediment load. Further, the authors show that the dominant (channel-forming) discharge produces a shear stress about 1.5 times greater than that required for initial bed-material entrainment. Emmett and Wolman (2001) compute the effective discharges of five streams in the northern Rocky Mountains, USA, finding that armoring effects and a steep relation between bedload and discharge result in higher return periods for effective flows that occur at stages greater than bankfull.

Applying the concept of effective discharge, Heritage and Milan (2004) investigate the role of excess stream power in the maintenance of riffle-pool sequences in a small, gravel-bed stream in northern England. In their investigation, the sediment transport rate in the popular conceptual plot of Wolman and Miller (1960) is substituted with excess energy to distinguish the discharge at which a transfer of excess energy from riffles to pools occurs with increasing discharge. The results show a reversal in excess energy between about 20 and 50 percent of bankfull discharge, but challenge the idea that a reversal is required to maintain quasi-equilibrium of the riffle-pool sequence.

Using historical discharge and suspended-sediment data at over 2,900 sites across the United States to infer effective flows, Simon, Dickerson, and Heins (2004) argue that flows of a given recurrence interval (the 1.5-year return period in their study) are more appropriate to define the effective discharge than flows at bankfull stage. Further, the authors are able to produce regional curves for the 1.5-year flow and show that disturbed sites generally yield an order of magnitude more suspended-sediment than stable sites.

A variety of studies along seasonally-active fluvial systems have highlighted discrepancies associated with the assumption of a 1- to 2-year dominant discharge. Focusing on ephemeral channels with highly variable flow regimes in southeastern Spain, García (1995) defines three classes of effective flows and one ineffective flow. The first class of extreme events modifies the overall system, including the floodplain, and generally has return periods between 2 and 6 years. The second class controls channel geometry at bankfull stages, commonly occurring more than once per year to every 1.5 years. Finally, more frequently occurring flows are capable of bedload transport. García (1995) empirically shows that most sediment is transported by the extreme events, but offers that the streams still display equilibrium-like conditions.

Gupta (1999) explores the role of high-magnitude events in alternating bedrock-confined and alluvial reaches of the Narmada River in central India, and concludes that very extreme floods sculpt a macro-channel and transport vast quantities of sediment, whereas the inner channel is associated with moderate floods developed during the seasonal monsoon wet period. Kale and Hire (2007) point out that it is unknown if the cumulative effects of low-frequency extreme floods are more important than seasonal monsoon events. Further, the fact that an inner channel is maintained by seasonal monsoon flows indicates the effectiveness of the 1- to 2-year flow event. In seasonally-dominated highland South Africa, van Niekerk et al. (1999) investigate the morphology of the Sabie River, a bedrock anastomosing system (Figure 2.5). Results show that a large macro-channel is inundated on a very infrequent basis, without any flow

breaching its boundaries in approximately 50 years. However, individual low-flow channels easily transport the available sediment. Kemp (2004), in an investigation of a flood-prone river system in southeastern Australia, shows that floodplain morphology, including swirl pits and zones of stripping, is dominated by high-magnitude events with return periods greater than 1 to 2 years, but probably less than 10 years. However, the river channel within the floodplain is modified more frequently.

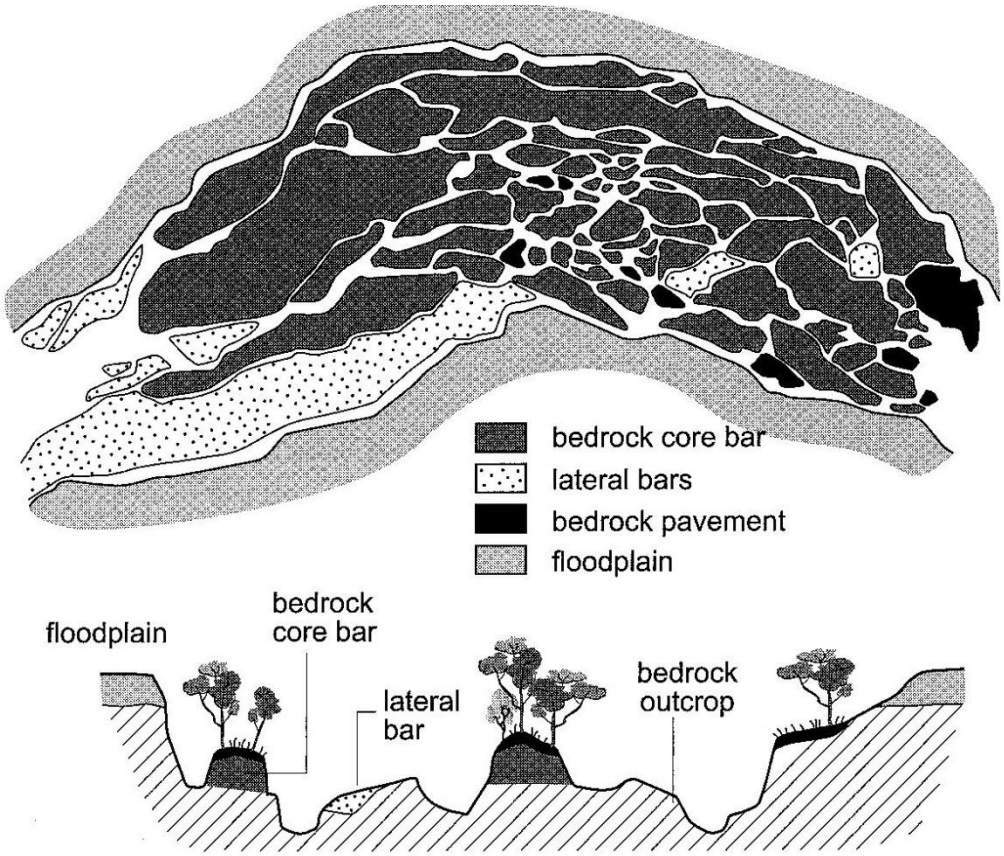

Figure 2.5. A bedrock-anastomosing river system is characterized by a series of bedrock core bars that are frequently inundated and a higher floodplain that is not frequently inundated (from van Niekerk et al. 1999; scanned from Brierley and Fryirs 2005).

In an application that might be the first of its kind, Doyle et al. (2005) make the step from effective discharge in geomorphology to flows that drive ecological processes in river systems, including organic matter transport, algal growth, nutrient retention, macroinvertebrate disturbance, and habitat availability. Using the effective discharge equation produced in Nash (1994) and Vogel, Stedinger, and Hooper (2003), Doyle et al. (2005) show that flow variability is most important for various processes. For example, nitrate loads in a Maryland stream and pool and riffle availability in an Arkansas stream are dominated by base flows, and cumulative organic matter loads are transported by moderate floods in a New Hampshire stream.

2.4.4 Contemporary Applications Refuting Frequent Dominant Discharge Events

Finally, a number of studies refute the general concept of Wolman and Miller (1960), mostly for rivers in dynamic environments or when associating the concept with processes other than sediment transport or channel-forming hydraulics. Similar to the investigations with a neutral sentiment on Wolman and Miller (1960) discussed above, seasonally-active fluvial systems offer an alternative model of dominant discharge not observed along humid or snowmelt-driven rivers. Gupta (1995) finds that river systems in seasonal tropical environments commonly have a channel-in-channel morphology (Figure 2.6), where the macro-channel conveys high-magnitude flows with return periods of ten or more years and the inset channel defined by seasonally high flows. Deodhar and Kale (1999) confirm that channel geometry of monsoon-dominated rivers in India is controlled by large, infrequent floods. Grams and Schmidt (1999), working

on the regulated Green River in the canyon country of Dinosaur National Monument in northwestern Colorado and northeastern Utah, USA, show that pre-regulation channel morphology was maintained by the 25-year discharge. Heritage, Broadhurst, and Birkhead (2001) specifically examine the role of discharge on different alluvial surfaces and features along the Sabie River, finding three distinct suites of discharge that affect channel adjustment at successively higher stages: (1) active channels, bars, and levees controlled by the 1- to 1.5-year discharge, (2) secondary channels and associated bars and levees controlled by the 2- to 10-year discharge, and (3) ephemeral channels and associated features controlled by extreme events greater than the 10-year return period. Focusing on ephemeral "ramblas" in the Mediterranean region of Spain, López-Bermúdez, Conesa-García, and Alonso-Sarría (2002) associate three types of events, including flash floods, single peak floods, and multiple peak floods, with morphologic impacts such as bank erosion, floodplain sedimentation, channel widening, among others. Bankfull discharge of Spanish ephemeral streams is estimated to have return periods ranging between 2 and 6 years.

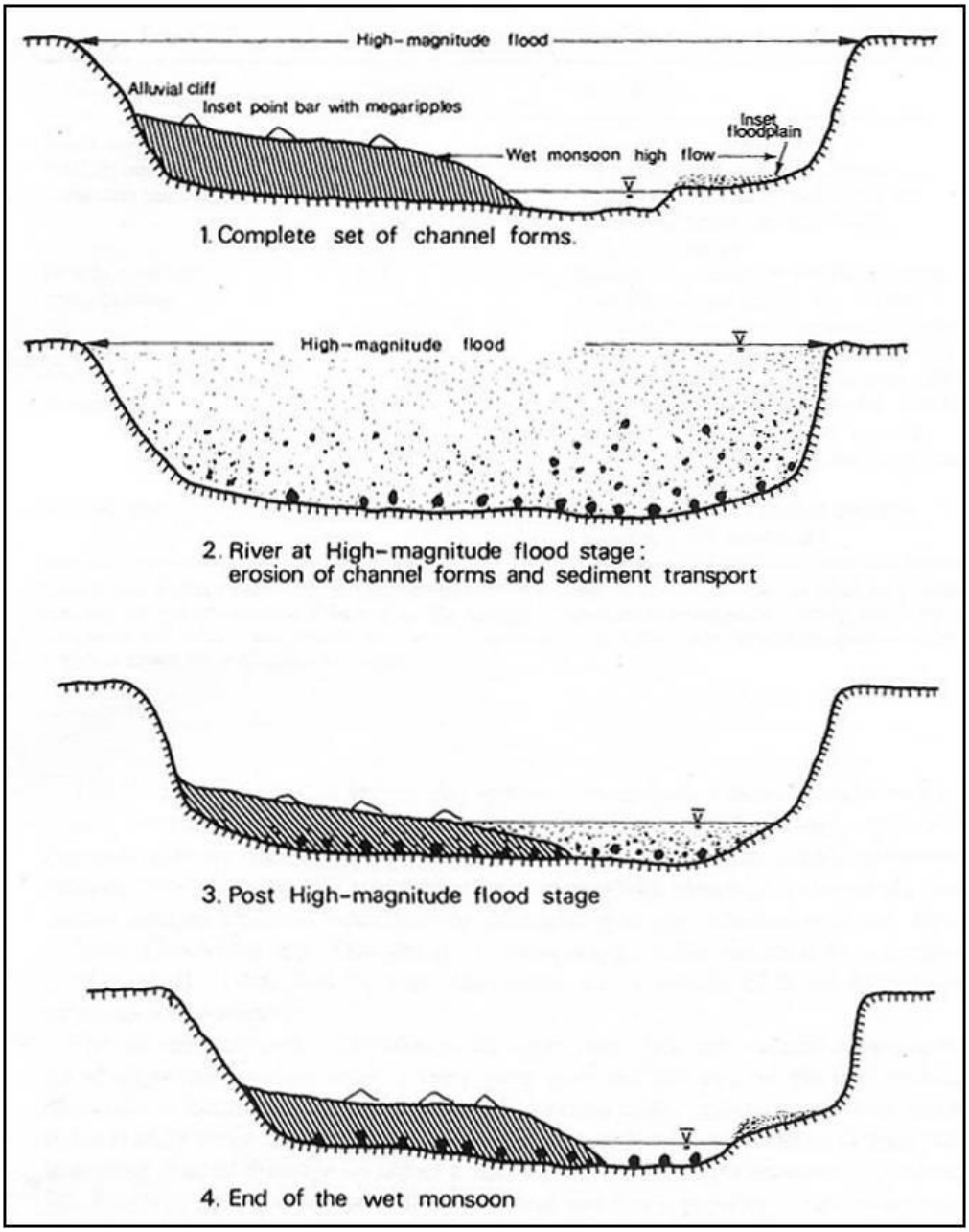

Figure 2.6. Sequence of flows that contribute to the formation of a channel-in-channel morphology (from Gupta 1999).

It is well established that arid rivers adjust during infrequent flash floods, and numerous contemporary studies are confirmatory. Huckleberry (1994) claims that large, infrequent floods greatly modify channels in arid environments but flood duration is of greater importance than magnitude, a finding supported by Costa and O'Connor (1995). Bourke and Pickup (1999), examining fluvial forms in arid central Australia, claim that large-scale geomorphic forms, including sand sheets, overflow channels, levee deposits, and avulsions, result from extreme floods that are estimated to occur about once in every 1,000 years. Smaller-scale forms and processes are engaged during moderate floods with more frequent return periods. Still, the 10-year return period is the lowest flow considered responsible for some localized instream erosion and deposition. Scheepers and Rust (1999) confirm that arid rivers are controlled by infrequent, high-magnitude floods, in their investigation of the Uniab River of Namibia, and highlight the role of dunefield barrier dams in releasing short-duration floods.

Additionally, fluvial processes and channel morphology of bedrock-confined rivers typically are associated with low-frequency, high-magnitude floods. Baker and Kale (1998) show examples of bedrock river channels that are sculpted by rare, extreme flood events, often finding that inner channels or gorges are inset within wide, shallow surfaces. Wende (1999) examines the role of rare, high-magnitude floods in the erosion of instream jointed-bedrock slabs and deposition of boulder clusters, which greatly contribute to the overall geometry of some river channels. Continuing with the focus on bedrock-dominated rivers with highly variable flow regimes, Erskine and Livingstone

(1999) associate depositional in-channel benches with diverse return periods. Although the lowest depositional bench is associated with flows occurring at the oft-cited 1.5- to 2-year return period, adjustment of higher benches required higher, less-frequent flows with return periods between about 4 and 10 years.

Table 2.4. Summary of contemporary dominant or effective discharge publications that generally agree with the concepts outlined in Wolman and Miller (1960).

Publication	Main findings	Location or setting	Basis for support
1. Batalla and Sala (1995)	Effective discharge of bedload transport is a frequent, bankfull event	Humid Mediterranean stream in northeast Spain	Effective discharge occurs relatively frequently at bankfull stage
2. Andrews and Nankervis (1995)	Effective discharge of gravel-bed rivers approximates bankfull discharge and occurs about 15.6 days per year	Gravel-bed rivers in mountainous western United States	Relatively frequent events transport the majority of sediment at bankfull stages
3. Hudson and Mossa (1997)	Moderate events cumulatively transport the majority of suspended sediment	Large, impounded rivers of the Gulf of Mexico Coastal Plain	Relatively frequent events of moderate magnitude constitute the effective discharge of suspended sediment transport
4. Biedenharn, Little, and Thorne (1999)	Effective discharge occurs, on average, about every year and closely corresponds to bankfull channel geometry	Lower Mississippi River, United States	Effective discharge associated with relatively frequent, moderate flow events and closely approximates bankfull conditions
5. Whiting et al. (1999)	Effective discharge of bedload transport has an approximate return period of 1.4 years, and is 80 percent of bankfull discharge	Snowmelt-dominated headwater streams in Idaho, USA	Effective flows have a 1.4-year return period and are only slightly less than bankfull
6. Castro and Jackson (2001)	Evaluate return periods of bankfull discharge for humid (1.2-year) and relatively dry (1.4- to 1.5-year) rivers in the Pacific Northwest	Humid and snowmelt-driven rivers in the Pacific Northwest, USA	Bankfull discharge between 1- and 1.5-year return period
7. Torizzo and Pitlick (2004)	Effective bedload discharge occurs during moderate flows for about 4 days/year and closely approximates bankfull; duration of effective discharge does not increase with drainage area	Gravel-bed mountain streams in Colorado, USA	Effective discharge occurs at bankfull conditions for about 4 days per year
8. Latrubesse (2008)	Effective discharge of large alluvial rivers often occurs at 'bar-full' conditions, a more frequent event than bankfull conditions	Mostly large rivers in South America; also Brahmaputra and lower Mississippi Rivers	Effective discharge occurs at stages less than bankfull and controls channel geometry

Table 2.5. Summary of contemporary dominant or effective discharge publications that generally are neutral about the concepts outlined in Wolman and Miller (1960).

Publication	Main findings	Location or setting	Basis for support
1. Costa and O'Connor (1995)	Flow duration more important than magnitude for channel adjustment	Humid Pacific Northwest United States	High-magnitude events not effective if short-lived; flow duration more important than magnitude
2. García (1995)	Defines three classes of effective flows; most extreme flows exert overall control on fluvial system	Semi-arid, ephemeral streams in southeast Spain	Return periods of effective flows are not much greater than 1 to 2 years; emphasize range of flows
3. Hey (1998)	Advocates for the use of bankfull discharge in design flows for rivers displaying steady-state equilibrium, but warns of the association between dominant and bankfull discharge	Gravel-bed rivers	Supports bankfull discharge as dominant or effective flow only for systems displaying steady-state equilibrium
4. Pitlick and Van Steeter (1998)	Effective discharge occurs slightly below bankfull stage; dominant discharge has a shear stress ~1.5 times greater than initial bed-material entrainment	Gravel-bed Colorado River in mountainous western United States	Effective discharge shown to have a return period ~1.5 years, but bankfull discharge has a return period between 4 and 6 years
5. Gupta (1999)	Large macro-channel and tremendous sediment transport loads associated with extreme floods; inner channel associated with seasonal monsoon	Narmada River, central India; seasonal, monsoon-dominated tropics	Macro-channel formed by low-frequency extreme events; inner channel maintained by seasonal monsoon development
6. Simon and Darby (1999)	Dominant discharge and bankfull discharge not an appropriate association for incised river channels	Incised river channels	Dominant discharge will not be bankfull discharge for non-equilibrium streams
7. van Niekerk et al. (1999)	Large macro-channel of bedrock anastomosing rive system rarely overtopped; low-flow channels easily transport sediment supply	Annually and seasonally variable flow regime of bedrock river in South Africa	Macro-channel formed by extreme, low-frequency events, but sediment transport easily transported through system by lower flows
8. Biedenharn et al. (2000)	Develop a practical technique to compute effective discharge using flow-duration curves and sediment-discharge rating curve	Theoretical; example applications in humid settings	Technique that is developed relies on fundamental principles, but authors acknowledge limitations
9. Emmett and Wolman (2001)	Effective discharge is slightly greater than bankfull conditions	Armored, gravel-bed rivers in snowmelt-dominated streams of the northern Rocky Mountains, USA	Effective discharge for bedload transport is only slightly greater than bankfull conditions; average return periods around 3 years
10. Heritage and Milan (2004)	Substitute excess energy for sediment transport rate in effective discharge analysis of pool-riffle sequences	Small, gravel-bed stream in humid, northern England	Authors apply effective discharge concept to investigate riffle-pool sequence, not full channel geometry
11. Kemp (2004)	Low-energy channel contrasts with floodplain morphology, including areas of stripping and swirl pits, that is controlled by extreme flows	Meandering river in southeastern Australia with highly variable flow regime	Although bankfull channel morphology is controlled by frequently occurring flows, floodplain morphology is dominated by less frequent extreme flows

Table 2.5 (continued). Summary of contemporary dominant or effective discharge publications that generally are neutral about the concepts outlined in Wolman and Miller (1960).

Publication	Main findings	Location or setting	Basis for support
12. Simon, Dickerson, and Heins (2004)	Effective discharge of suspended sediment should be based on flows of a given return period, not at bankfull conditions	Arid to humid systems across the United States	The 1.5-year return period is used to assess regional effective discharge, but authors disagree that bankfull conditions approximate effective discharge
13. Doyle et al. (2005)	Associate the effective discharge concept with ecological processes in streams	Mostly humid streams in North America	Various flows responsible for different ecological processes
14. Doyle et al. (2007)	Claim that effective discharge is the only index that should be associated with channel-forming discharge	Numerous rivers in diverse settings	Agreement of effective and bankfull discharge is best for snowmelt-driven, non-incised, gravel-bed rivers; agreement is poor for highly variable flow regimes
15. Fuller (2007)	Contrasts the geomorphic responses of streams to an extreme event; most geomorphic work accomplished along reaches characterized by meander bends, terrace confinement, or low channel width	Humid, alluvial rivers in New Zealand	Effectiveness of events controlled by reach-scale spatial configuration and event magnitude
16. Kale and Hire (2007)	Although substantial work is accomplished by extreme events; uncertainty remains about cumulative effects when compared with seasonal monsoon-generated events	Seasonal monsoon river in central India	Admitted uncertainty regarding cumulative effects of extreme and frequent floods

Table 2.6. Summary of contemporary dominant or effective discharge publications that generally disagree with the concepts outlined in Wolman and Miller (1960).

Publication	Main findings	Location or setting	Basis for support
1. Huckleberry (1994)	Flow duration of high-magnitude events important to modify channels in arid settings	Arid river in southwestern United States	High-magnitude floods control channel geometry, provided their duration is sufficient
2. Nash (1994)	Mathematically solves for effective discharge; recurrence interval of effective flow highly variable	Humid to arid streams in the United States	Failure of power function of discharge to predict sediment transport rate at high flows; highly variable return periods for effective flows
3. Gupta (1995)	Rivers in seasonal tropics dependent on high-magnitude, low-frequency floods to maintain a channel-in-channel geometry	Seasonal tropical rivers	High-magnitude, low-frequency floods important
4. Baker and Kale (1998)	Bedrock rivers in highly variable flow regimes only altered by rare, extreme floods; display inner channels or gorges within a broad, shallow surface	Bedrock channels with highly variable flow regimes	Only the rare, high-magnitude floods contribute to overall channel geometry
5. Bourke and Pickup (1999)	Large-scale alluvial features engaged about once in every 1,000 years; 10-year return period the minimal flow considered for minor instream erosion and deposition	Arid, central Australia	Arid river sediment transport and morphology controlled by very rare, extreme events
6. Erskine and Livingstone (1999)	Adjustment of lowest in-channel depositional bench requires flows with a 1.5- to 2-year return period; higher in-channel benches require flows with 4- to 10-year return periods or greater	Bedrock-confined rivers with highly variable flow regimes in southeastern Australia	Adjustment of in-channel depositional benches mostly requires flows with return periods greater than 2 years
7. Grams and Schmidt (1999)	Pre-regulation channel morphology was maintained by flows with a 25-year return period	Green River, canyon country; western USA; flow regulated by upstream reservoir	Pre-regulation dominant discharge with a return period of ~25 years
8. Scheepers and Rust (1999)	Hyper-arid channel morphology controlled by infrequent, high-magnitude floods; describe role of dunefield barriers acting as dams to floods	Uniab River, extreme arid conditions of Skeleton Coast, Namibia, Africa	Arid river systems dominated by infrequent, high-magnitude events
9. Wende (1999)	Instream jointed-bedrock slabs eroded and deposited as imbricated boulder clusters by rare, high-magnitude events; form considerable part of channel geometry	Bedrock channels in rivers with highly variable flow regimes in northwestern Australia	Considerable proportion of geomorphic work and channel geometry produced during rare, high-magnitude floods
10. Heritage, Broadhurst, and Birkhead (2001)	Three suites of dominant flows for features at successively higher stages: (1) active channel (1- to 1.5-year return period); (2) seasonal channel (2- to 10-year return period; (3) ephemeral channel (>10-year return period)	River with highly variable flow regime in South Africa	Range of flows important to successively higher in-channel geomorphic surfaces, some of which require extreme flows with return periods greater than 10 years
11. López-Bermúdez, Conesa-García, and Alonso-Sarría (2002)	Three events in ephemeral channels: (1) flash floods, (2) single peak floods, and (3) multiple peak floods. Morphologic impacts include bank erosion, floodplain sedimentation, and channel widening.	Ephemeral "ramblas" (channels) in Mediterranean Spain	Bankfull discharge occurs between 2 and 6 years, the upper limit being associated with highly variable flow regimes
12. Vogel, Stedinger, and Hooper (2003)	Develop rationale for half-load index as the effective discharge	Theoretical; one application on Susquehanna River in humid United States	High-magnitude, low-frequency flows responsible for most cumulative sediment transport

2.5 Implications

The number of environmental applications focused on river channels and riparian zones are increasing in both rural and urban settings, including rehabilitation projects, instream flow studies, and various engineering and ecological endeavors. Many practitioners, who generally are specialized in various disciplines, have finally come to rely on fundamental concepts introduced by geomorphologists, including hydraulic geometry and dominant or effective discharge. The utility of these concepts can provide further insight into the controls of channel shape and other physical features. However, a failure to realize conceptual limitations, especially the frequency of dominant, effective, or bankfull discharge, can mislead well-intended investigations.

Contemporary applications involving fluvial geomorphology are gradually acknowledging that a range of flows are required to maintain physical elements of stream channels on which structures are engineered and ecological processes are contingent. The acknowledgment of a "working flow regime" offers an opportunity to expand the applications of hydraulic geometry, both at-a-station and downstream, and dominant or effective discharge. Modern practitioners are no longer compelled or constrained by the literature to emphasize bankfull discharge or the flow occurring every 1 to 2 years to characterize fluvial or ecological processes that operate in diverse hydrologic and sedimentary settings, and at various spatial and temporal scales. In general, the concepts outlined by Wolman and Miller (1960) are most valid in humid or snowmelt-driven fluvial systems (Doyle et al. 2007), have mixed results in seasonally-

driven systems, and become less predictive for small watersheds, incised channels, or in systems with highly variable flow regimes.

Hydraulic geometry and other applications contingent on a dominant or effective discharge, as witnessed by contemporary research activity, provide merit to environmental management applications in rivers and riparian corridors. Accurate interpretations of hydraulic geometry require acknowledgment that: (1) a range of flows contributes to the maintenance of various fluvial processes and forms in most natural channels, (2) sediment transport processes can occur at stages above or below bankfull, and (3) observed channel characteristics and geomorphic units might not be associated with one dominant discharge, especially in fluvial systems with highly variable flow regimes.

In more specific terms, hydraulic geometry analyses, both at-a-station and downstream, would benefit from an assessment of cross-sectional data, in order to identify: (1) the discharges and stages at which certain sediment transport processes initiate (e.g., critical shear stress) or operate (e.g., effective discharge) and (2) the discharges and stages at which particular physical features occur (e.g., channel bars, succinct breaks in bank slope, perched flood channels, etc.). Further, accurate interpretations of sediment-transport processes and channel formation are likely if flows are analyzed with respect to antecedent conditions, timing, and typical durations of flow.

Chapter 3. Physical and Paleoenvironmental Setting of the Edwards Plateau, Central Texas, USA, since the Last Glacial Maximum

3.1 Abstract

The paleoenvironmental record of the Edwards Plateau, Texas, for the last 20,000 years has been established through evidence from fluvial deposits, pollen records, faunal remains, and isotopic dating techniques. Six distinct episodes based on a pre-existing scheme are used to conceptualize prevailing environmental conditions: (1) full glacial (about 20,000 to 14,000 years B.P.), (2) late glacial (about 14,000 to 10,500 years B.P.), (3) early to middle Holocene (about 10,500 to 5,000 years B.P.), (4) late Holocene I (about 5,000 to 2,500 years B.P.), (5) late Holocene II (about 2,500 to 1,000 years B.P.), and (6) modern (about 1,000 years B.P. to present).

The full-glacial episode is characterized by the coolest, wettest climatic regime in the past 20,000 years. Average summer temperatures may have been 5˚C cooler than present, indicating reduced seasonality. The presence of boreal genera and megafauna highlight biotic descriptions of the Last Glacial Maximum. A gradual increase in temperature and decrease in precipitation occurred during the late-glacial episode, as evidenced by channel incision, the disappearance of spruce and fir trees, increase in C_4 plant species, replacement of mesic microfauna with xeric forms, and reduced rates of speleothem growth. Megafauna become extinct during the late glacial episode. Expression of the Younger Dryas cooling episode (about 10,750 years B.P.) is absent in

the region, and minor fluctuations in overall climatic trends are related to glacial meltwater pulses into the Gulf of Mexico. Desiccation and warming continued through the early to middle Holocene, culminating with the Altithermal at about 5,500 years B.P. Fluvial systems slowly aggraded during this time, but later incised deeply after 5,000 years B.P. Grasslands steadily replaced woodlands, C_4 abundance increased, and xeric species dominated the faunal assemblage. By about 5,000 to 2,500 years B.P., the landscape consisted mostly of short grasses and desert scrub. A relatively wet cycle occurred between about 2,500 to 1,000 years B.P.; fluvial systems aggraded to levels above former terraces; and hickory trees and mesic faunal species increased in abundance. Finally, increasing warmth and aridity during the last 1,000 years have resulted in stream incision, open oak woodlands, and domination of xeric species.

3.2 Introduction

An increasing level of concern about patterns of extreme weather, climatic change, and associated spatial and temporal adjustments of the biosphere has generated much interest within the natural scientific community (Intergovernmental Panel on Climate Change 1990; Neilson and Marks 1994; Elsner, Liu, and Kocher 2000). The complexity of these problems is aggravated by the rapid rate at which humans are influencing atmospheric circulation processes and the hydrologic cycle. Further, direct human impact on the landscape through land-cover change has dramatically altered distributions and densities of life on Earth. As a context to discern natural and

anthropogenic controls, and the relative impact of present-day and previous conditions on the landscape, numerous efforts to describe environmental change over time have been published.

Investigations of environmental change during the Quaternary period provide Earth scientists with a history of natural adjustments to various conditions. Especially pertinent toward our understanding of current conditions and predictions of future adjustments are reviews of environmental change during the Late Pleistocene and Holocene, a period of time marked by frequent changes in climate (Butzer 1974; Knox 1995; Williams et al. 1998), and one which humankind rapidly developed and began to impact natural systems. Quaternary research uses different lines of evidence to reconstruct previous environmental conditions. Evidence derived from deep-sea sediment cores; ice cores; fluvial, lacustrine, glacial, and aeolian sediments; fossil pollen; fossils; anthropogenic artifacts; and isotopic dating techniques all contribute to understanding Quaternary environments, changes in climate, and the distribution of life on Earth.

Three goals seem to emerge from the extensive body of Quaternary research: (1) reconstructing environments of localities or regions, including biotic, geomorphic, and climatic characteristics; accompanied by inferences of the processes responsible for those conditions; (2) modeling of global atmospheric and oceanic circulation patterns; and (3) tracing the origins and dispersal of humans and determining their impact on the environment. Paleoenvironmental reconstructions of regions are commonly used to

make conclusions about global dynamics and, in turn, provide information about regional climatic regimes. Interrelationships are often developed between oceanic and atmospheric circulation dynamics, including El Niño-Southern Oscillation (ENSO), global dynamics and regional climatic characteristics, and among regions themselves.

This chapter explores the body of evidence used to reconstruct environments of the Edwards Plateau, Texas, USA, since the Last Glacial Maximum. A rather substantial volume of literature provides evidence for environmental conditions and change across the Edwards Plateau during the Late Pleistocene and Holocene. Evidence is derived from cave sediments, fluvial deposits, pollen, fossils, and isotopic signatures. These lines of evidence are organized to populate a definitive timeline of conditions since the Last Glacial Maximum. Additionally, it is useful to examine relations and discrepancies between the different lines of evidence.

Specifically, this review of paleoenvironmental conditions in the Edwards Plateau could serve as a platform for interpretation of alluvial deposits and contemporary channel morphology in the region. Sediment sampling strategies and the ability to distinguish inactive terrace deposits from late Holocene banks and floodplains should benefit from an understanding of landscape and channel evolution in the Edwards Plateau through time. Further, it is vitally important to correctly identify contemporary deposits if associating with the present-day hydrologic regime.

3.3 The Edwards Plateau

The Edwards Plateau of Central Texas, USA is located at the southern edge of the Great Plains physiographic province of North America (Osterkamp et al. 1987) and covers about 75,000 square kilometers (Figure 3.1). At the eastern edge, it is separated from the Texas Blackland Prairies of the Gulf Coastal Plain by the abrupt Balcones Escarpment, which also forms the southern border with the South Texas Brush Country. For most of the western edge, the Pecos River separates the Edwards Plateau from the arid Chihuahuan Desert ecoregion, more specifically the Stockton Plateau. The Edwards Plateau grades into the Southern High Plains in the northwest and the Rolling Plains to the north, although locally sharp demarcations occur, including low-relief escarpments. Although considered a separate natural subregion based on different surface geology, soils, and vegetation types (Lyndon B. Johnson School of Public Affairs 1978), the Llano Uplift will be included in the discussion based on its proximal location and similar responses to environmental change.

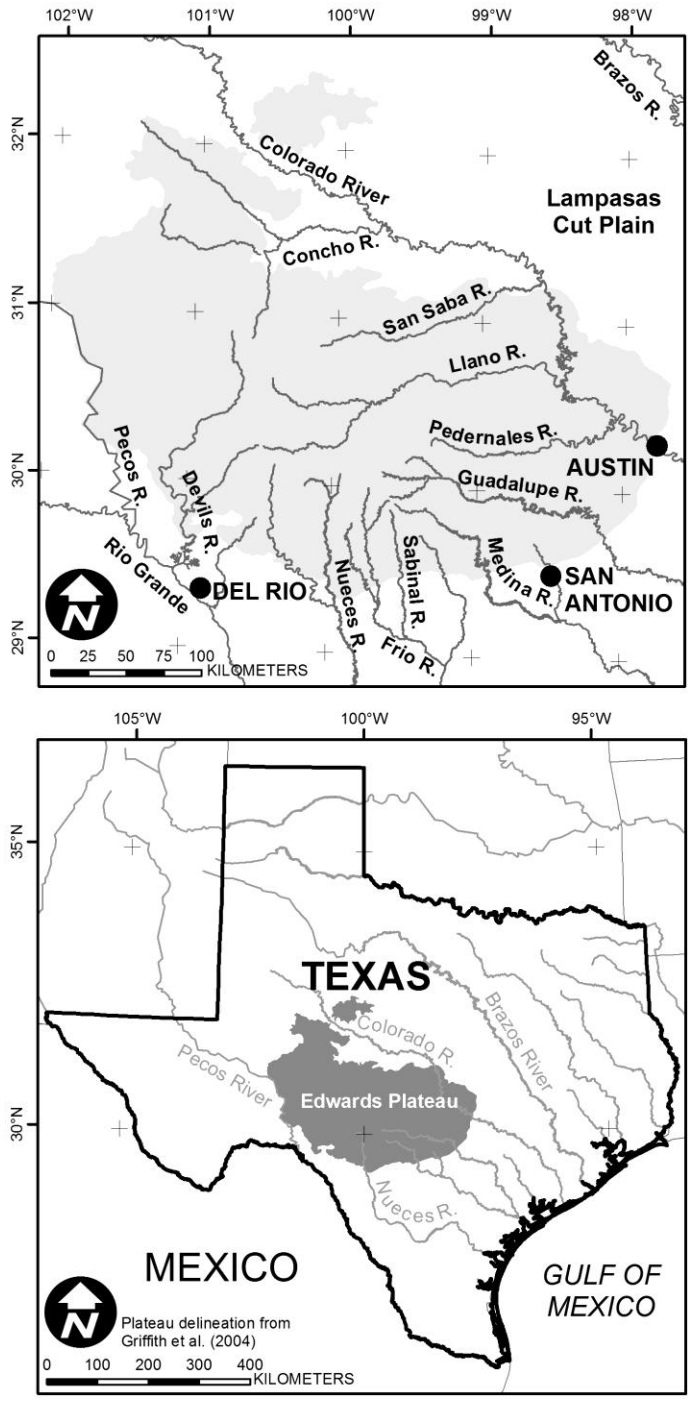

Figure 3.1. The Edwards Plateau in Central Texas, USA. The region is about 75,000 square kilometers, and occurs at a transition between semi-arid climatic conditions in the west to dry subtropical conditions in the east.

The Edwards Plateau is classified as dry subtropical in the east to semiarid in the west. Average annual precipitation decreases from east to west across the plateau, ranging from 35 to 85 centimeters per year, the western decrease attributed to the relaxation of available moisture from the Gulf of Mexico (Bomar 1983). Rainfall, however, is not uniform over space and time, and it is common for years of severe drought to rapidly transition into relatively wet conditions within a few months (Bomar 1983). Hydrologically, the region is noted for tremendous flash flooding (Beard 1975; Bomar 1983; Burnett 2008). A number of historic floods in the Edwards Plateau have peak flows exceeding 10,000 cubic meters per second (Burnett 2008).

Geologically, the Edwards Plateau is a tableland uplifted during the Cenozoic era (65.5 million years ago to present). Expressed at the surface, the northern and western sides of the Balcones Escarpment approximately range from 100 to 320 meters higher than the downthrown side. Lithologically, it is dominated by lower-Cretaceous limestones and dolomites deposited by a shallow, inland sea. Over time, rivers and streams have incised valleys into the Edwards Plateau, creating a well-dissected landscape. Additionally, dissolution of carbonate rock is responsible for the formation of cave systems, conduit-dominated aquifer systems, and numerous springs throughout the plateau.

Tertiary tectonic activity associated with the Llano Uplift was centered in the present-day eastern Llano River watershed. The uplift forced overlying Cretaceous strata upward, resulting in increased rates of erosion that exposed the underlying

Paleozoic sedimentary and Precambrian igneous and metamorphic formations. Expressed at the ground surface today, the exhumed "island" of older lithologic units is surrounded by an elevated Cretaceous rim.

The Edwards Plateau is divided into four subregions based on topography, surface geology and soils, and vegetation types (Lyndon B. Johnson School of Public Affairs 1978; Frye, Brown, and McMahan 1984): (1) the Balcones Canyonlands; (2) the central Plateau; (3) the Lampasas Cut Plain; and (4) the Llano Uplift. The Balcones Canyonlands are characterized by the deeply dissected southern and eastern margins of the plateau, creating a rugged landscape with numerous springs and streams. Scrub forests of Ashe juniper (*Juniperus ashei*), stunted live oak (*Quercus fusiformis*), Texas oak (*Quercus texana*), black cherry (*Prunus serotina*), Texas ash (*Fraxinus texensis*), and some endemic plants dominate on the shallow soils near the escarpment (Amos and Rowell 1988; Riskind and Diamond 1988). The central Plateau is characterized by rolling plains located on broad divides between river valleys. These uplands have slightly deeper soils covered by grassland and groves of oak, juniper, and honey mesquite (*Prosopis glandulosa*). The Lampasas Cut Plain, not included in the boundaries of the Edwards Plateau by Griffith et al. (2004) (Figure 3.1), is characterized by mature, broad river valleys and less relief than the Balcones Canyonlands. Grasslands occur in the alluvial valleys and woodlands of oak, juniper, and mesquite exist throughout the plain. Finally, the Llano Uplift displays rolling topography surrounded by an elevated rim of Cretaceous carbonate rocks. This region contains oak,

hickory (*Carya texana*), and mesquite trees within grassland, often described as a savanna. Ashe juniper is notably absent in the Llano Uplift, because of the lack of limestone-derived soils.

Biotically, the Edwards Plateau covers an area noted for its transition from mesic- to xeric-tolerant species and from temperate to subtropical species (Blair 1950; Riskind and Diamond 1988). A highly generalized vegetation description (Riskind and Diamond 1988) is that of deciduous forests or woodlands on floodplains and moist slopes, evergreen woods and grasslands on drier slopes and uplands, and evergreen and deciduous shrublands mixed with shortgrasses further west. Blair (1950) categorizes the Edwards Plateau as the Balconian biotic province, and concludes that out that of fifty-seven known species of mammals in the region, none are restricted to the province. All also are found in at least one of the bordering biotic provinces, which testifies to the transitional nature of the Edwards Plateau.

3.4 Environmental Conditions and Change since the Last Glacial Maximum

The Edwards Plateau, and the Great Plains in general, is noted for dramatic environmental responses to shifts in climate during the Late Quaternary (Osterkamp et al. 1987). Responses to shifts in climate across the plateau are associated with episodes of soil erosion, hydrologic change and associated fluvial activity, and fluctuation in the range limits and density of plant and animal species. A number of studies in the plateau

have used macrofossils, fossil pollen, cave sediments, fluvial deposits, and isotopic signatures and dating techniques to reconstruct environments for the last 20,000 years.

A comprehensive chronological framework since the Last Glacial Maximum for the Edwards Plateau has been developed by Toomey, Blum, and Valastro (1993), and is based on fossil vertebrates, cave fill sediments, and previously published Quaternary research. Their interpretations suggests six unique environmental conditions: (1) full glacial (about 20,000 to 14,000 years B.P.); (2) late glacial (about 14,000 to 10,500 years B.P.); (3) early to middle Holocene (about 10,500 to 5,000 years B.P.); (4) late Holocene I (about 5,000 to 2,500 years B.P.); (5) late Holocene II (about 2,500 to 1,000 years B.P.); and (6) modern (about 1,000 years B.P. to present). These timeframes will be used in this chapter to organize evidence for environmental conditions and climatic changes since the Last Glacial Maximum. Some evidence for environmental change in surrounding regions will also be included to provide a regional context.

3.4.1 Full-Glacial Environmental Conditions (about 20,000 to 14,000 years B.P.)

Fluvial geomorphic evidence of paleohydrological conditions in the Edwards Plateau during the Last Glacial Maximum are derived from Pleistocene river terrace deposits (Figure 3.2). Blum, Toomey, and Valastro (1994) conducted a detailed study of Quaternary terrace and fill deposits of the Pedernales River, which is a major tributary of the Colorado River (Figure 3.3). Radiocarbon ages of organic-rich sediments and soils and stratigraphic position of diagnostic archaeological artifacts were used to determine the chronology of the alluvial sequences. Of two identified Late Pleistocene

terraces, the younger was determined to have been deposited during the Last Glacial Maximum. This extensive terrace is composed of horizontally and cross-stratified gravel and sand overlain by interbedded sand and mud, which suggests a channel-related origin. These stratigraphic facies indicate a period of channel aggradation, lateral migration, and sediment storage. Such characteristics are indicative of a less flashy, more consistent flood regime and a large supply of sediment from tributary networks. Soils of the full-glacial terrace near the junction of the Colorado and Concho Rivers at the northern extent of the Edwards Plateau are similar to those of the Pedernales River with respect to morphologic structure and display extensive soil development during this time (Blum and Valastro 1992). Mature, argillic, calcic, silty soils are found in full-glacial terraces of the Sabinal River valley at the southern extent of the plateau, and some terraces have calcrete horizons in the upper 3 to 4 meters of the soil (Mear 1995). The thickness of full-glacial terraces in the Edwards Plateau ranges from 4.3 to 12.2 meters (Mear 1995).

Late Wisconsin terraces of the lower Colorado River just downstream of the Balcones Escarpment, called the Eagle Lake Alloformation, indicate that coarse sand and gravel aggradation was followed by the deposition of finer sediment by an enlarged, high sinuosity channel (Baker and Penteado-Orellana 1977). The terraces are composed of point bar and abandoned channel facies, suggesting floods were mostly contained in the channel banks (Blum and Valastro 1994). Waters and Nordt (1995) also describe thick cross-bedded gravel and sand deposits in full-glacial terraces along the Brazos

River in east-central Texas, presumably deposited as point bars of a laterally migrating river. Nordt et al. (1994) report the same stratigraphic unit in the Lampasas Cut Plain. In summary, full-glacial terraces indicate a less flashy, higher frequency flood regime associated with more humid conditions.

In addition to fluvial deposits, the presence of pluvial lakes in West Texas testifies to the relatively moist regional climate during the Last Glacial Maximum. Reeves (1973), in a study of a small playa lake, estimated a 34-percent runoff-to-precipitation rate in West Texas during the full-glacial episode, which is consistent with relatively wet conditions. Allen and Anderson (1993), however, determined that glacial advances in North America corresponded with high stands of pluvial lakes in the southwestern United States, which were maintained by high stream discharges that occurred only for a few decades. This is different from the model of persistent humid conditions throughout the full-glacial episode. An overall rise in the regional water table contributed to the emergence and continuous existence of pluvial lakes on the High Plains of West Texas (Holliday 1997) and Rolling Plains in northern Texas (Caran and Baumgardner 1990). It appears that areas west of the Edwards Plateau experienced moist conditions during the Last Glacial Maximum, but pulses of moisture were temporally erratic. Perennial lakes were sustained by gradual inputs of ground water.

Pollen records from Central Texas describe a mixed deciduous forest with some conifer species supported by cool, mesic conditions (Bryant and Holloway 1985). Potzger and Tharp (1947) and Potzger and Tharp (1954) first discovered boreal pollen

in Patschke Bog in Lee County, Gause Bog in Milam County, and Franklin Bog in Robertson County. All sites are located east of the Balcones Escarpment. Bog profiles, although not isotopically dated, reveal that spruce (*Picea*), fir (*Abies*), birch (*Betula*), and pine (*Pinus*) were present in the region, probably during the Last Glacial Maximum. Bryant (1977) also detects spruce, birch, and other northern species in nearby Boriack Bog in Lee County. The presence of these species indicates that summer temperatures were probably 5˚C lower than present (Toomey, Blum, and Valastro 1993). Analysis of pollen from Boriack Bog reveals high percentages of shrubby alder (*Alnus*), a current northern genus, surrounding bogs in Central Texas during the full-glacial episode (Bryant and Holloway 1985). Bousman (1998) describes an open grassland environment for most of the Last Glacial Maximum, interrupted by the increase of boreal tree species around 16,000 years B.P. Further, Hall and Valastro (1995) describe the Edwards Plateau as grassland with small clusters of pinyon pine and deciduous trees in riparian corridors and canyons. Holliday (1987) and Hall and Valastro (1995) criticize the support for a boreal forest located in the plateau and Southern High Plains based on problems of pollen preservation in regional soils. Based on $\delta^{13}C$ signatures extracted from alluvial deposits in central Texas, Nordt et al. (1994) determined that C_4 plants comprised only 45 to 50 percent of vegetative biomass during the full-glacial episode, implying the climate was cool and wet (Figure 3.4). Reduction in C_4 productivity around 15,000 years B.P. is associated with a pulse in glacial

meltwater from the Mississippi River and associated cooling of the Gulf of Mexico and the surrounding land areas (Nordt et al. 2002).

The fauna of the full-glacial episode also confirm the existence of a cooler and moister climate. Most assemblages of animal fossils are derived from caves scattered throughout the Edwards Plateau. The two distinguishing characteristics of fauna in the full-glacial episode are the presence of large mammals and other animals normally associated with cooler and moister climates living sympatrically with animals currently occupying the plateau (Lundelius 1967; Toomey, Blum, and Valastro 1993). Fossils of horses, camels, mammoths, peccaries, American mastodon, bison, and tapirs indicate species adapted to grassland and woodland environments in the plateau (Graham 1987). The remains of prairie dogs, pocket gophers, and moles found in red clay sediments in Hall's Cave in the central Edwards Plateau suggest the presence of deep upland soils during the Late Pleistocene (Toomey, Blum, and Valastro 1993) (Figure 3.5). Numerous faunal species identified by Lundelius (1967) in the Edwards Plateau are currently limited to northern and eastern ranges, and their coexistence with species currently found in the plateau may represent reduced seasonality, defined by cooler, moister summers and winters of the same magnitude as today (Toomey, Blum, and Valastro 1993).

Finally, chemical and isotopic evidence has been utilized to reconstruct full-glacial environments in the Edwards Plateau. Measurements of atmospheric noble gases in ground water of the Carrizo aquifer in south-central Texas show that the annual mean

temperature of the region during the Last Glacial Maximum was about 5˚C cooler than today (Stute et al. 1992). Isotopic dating of stalagmites from three caves in the Edwards Plateau identifies a period of rapid growth between 24,000 and 12,000 years B.P., which is consistent with a wetter climate (Musgrove et al. 2001) (Figure 3.6). Strontium isotope ratios of fossil hackberry seed coatings and tooth enamel of pocket gophers and voles in Hall's Cave identify steady, continuous soil erosion in the Edwards Plateau beginning during full-glacial conditions (Cooke et al. 2003). These strontium ratios are dependent the amount of carbonate in soils, where thicker soils contain less carbonate based on the greater depth to limestone bedrock.

3.4.2 Late-Glacial Environmental Conditions (about 14,000 to 10,500 years B.P.)

Fluvial systems in the Edwards Plateau deeply incised their bedrock valleys during the glacial decline at the end of the Pleistocene, leaving behind a noticeable unconformity (Blum, Toomey, and Valastro 1994; Mear 1995) (Figure 3.2). The Colorado and Concho Rivers incised more than 5 meters into Permian bedrock (Blum and Valastro 1992). Incision by the Colorado River in the Gulf Coastal Plain also is reported during this time (Baker and Penteado-Orellana 1977; Blum and Valastro 1994). Excavation of valleys is attributed to the near-complete removal of sediment from tributaries accompanied by upland slope stability that resulted in a decrease in available sediment. An initial decrease followed by an increase in effective moisture as well as a gradual rise in summer temperatures (greater seasonality) is postulated to be the cause for incision (Blum, Toomey, and Valastro 1994). Pluvial lakes in northern and

West Texas were still persistent during the late-glacial episode (Caran and Baumgardner 1990). Finally, carbon-isotope data of plants derived from lunette dunes on the Southern High Plains of Texas and New Mexico show considerable variation, suggesting alternating cool-warm cycles (Holliday 1997).

Palynological evidence accounts for the decline of deciduous woodlands and replacement by grasslands and oak savannas (Bryant and Holloway 1985), which implies a shift to warmer and drier conditions. Potzger and Tharp (1947) and Potzger and Tharp (1954) detected an increase in oak and grass pollen following the presence of boreal species. Other bog studies (Bryant 1977; Bryant and Holloway 1985) in the region have shown a gradual decrease of boreal trees during late-glacial times, and the complete loss of spruce pollen. Grassland dominance around 12,500 years B.P. in Central Texas is reported by Bousman (1998), which is consistent with the findings of Hall and Valastro (1995) who support the existence of prairie vegetation in the Southern High Plains. The percentage of C_4 plants in Central Texas increased to 50 to 60 percent during the late-glacial episode, alluding to the transition from moist to dry conditions (Nordt et al. 1994) (Figure 3.4). C_4 plant productivity was relatively low from 13,000 to 11,000 years B.P., however, and correlates with increased glacial meltwater into the Gulf of Mexico, whereas high C_4 productivity from 11,000 to 10,000 years B.P. suggests that the Younger Dryas cooling episode (about 10,750 years B.P.) did not impact the region around the Gulf of Mexico (Nordt et al. 2002).

Faunal assemblages from Hall's Cave in the Edwards Plateau indicate a rapid increase in summer temperatures from 15,000 to 13,000 years B.P. (Toomey, Blum, and Valastro 1993) (Figure 3.5). The masked shrew, a heat-intolerant species, disappeared from the region whereas the heat-tolerant cotton rat appeared. A decrease in available moisture forced the disappearance of the bog lemming, and the desert shrew replaced the least shrew. Pocket gophers in the western plateau required short-grasses, and prairie dog remains in the central plateau suggest mixed grasses. Burrowing animals at this time required sufficient soil thickness, however the absence of pocket gophers and the rarity of moles at 12,000 years B.P. indicate diminished soil. The end of the late-glacial episode witnessed the mass extinction of large mammals, arguably from a combination of climate change, especially increased seasonality (Lundelius 1967), and predation by humans (Graham 1987).

Calcium carbonate lacustrine and calcic soil profiles in north-central Texas were sampled by Humphrey and Ferring (1994) for stable carbon and oxygen isotopes in order to detect changes in meteoric waters derived from the Gulf of Mexico during the Late Pleistocene and Holocene. Their data suggest that the Younger Dryas is not recognizable or is masked by complex meltwater rates to the Gulf of Mexico and that pond sediments suggest a cool and dry climate. Musgrove et al. (2001) detect a warming and drying trend at the end of the Pleistocene, as evidenced by rapid decrease in growth rates of stalagmites (Figure 3.6).

3.4.3 Early- to Middle-Holocene Environmental Conditions (about 10,500 to 5,000 years B.P.)

Incision into bedrock valleys ended around 11,000 years B.P. and was followed by an episode of valley widening and slow aggradation, creating a thick fill deposit (Blum, Toomey, and Valastro 1994; Blum and Valastro 1994; Mear 1995) (Figure 3.2). Early-Holocene valley fill deposits of the Pedernales River valley consist of interbedded sand and mud, which indicates upland soil erosion and entrainment of clasts from the exposed Hensell Sands, and deposition in low-relief channel margins. In contrast, gravel deposits reworked from older alluvium dominate the early-Holocene valley fill of the Colorado River. Baker and Penteado-Orellana (1977) report aggradation of coarse sediment followed by finer sediment accumulation in the lower Colorado River valley during the early Holocene. These fluvial deposits reflect a continued warming and drying trend, strongly monsoonal circulation, and intense, localized convectional storms during the summer (Blum, Toomey, and Valastro 1994). Strong localized storms contributed to the loss of the upland soil mantle, but did not produce frequent flood events in the larger rivers. These floodplains were abandoned around 5,000 years B.P. and soil formation began on their upper surface. Waters and Nordt (1995) infer a shift in the hydrologic regime of the Brazos River around 8,500 years B.P., such that the river became an underfit meandering stream in a floodplain formed by vertical accretion of sediments during floods. Streams north of the Edwards Plateau began to downcut because of a flashy, erosive hydrologic regime (Caran and Baumgardner 1990).

Additionally, coarse slack-water-flood deposits of the Pecos River indicate some flood activity west of the Edwards Plateau (Patton and Dibble 1982).

Perennial lakes were mostly eliminated from northern and West Texas, accentuated by the resultant lowering of ground-water levels (Caran and Baumgardner 1990; Holliday 2000). Some aeolian sand units were deposited by westerly winds in the floodplain of the Colorado River and the Rolling Plains during the early Holocene (Caran and Baumgardner 1990; Blum and Valastro 1992). Aeolian deflation of the Southern High Plains occurred between 8,000 to 5,000 years B.P. (Holliday 1997), indicating persistent drought. Aeolian sedimentation in Texas may be related to strengthened zonal flow and enhanced drought conditions caused by a global climatic event around 8,200 years B.P. (Hu et al. 1999). The episodic, but steady, shift led to the warm, dry Altithermal beginning about 7,000 years B.P. and peaking about 5,500 years B.P., when the most widespread aeolian sedimentation occurred (Holliday 1989).

The vegetation record of Central Texas reinforces the gradual warming and drying conditions during the early Holocene. Low pollen counts for trees and grasses occur at 9,000 years B.P. in Boriack Bog in Lee County, which suggests an open community (Bousman 1998). Woodlands again emerged between 9,000 and 8,000 years B.P., followed by a rapid change back to grassland associated with the Altithermal. The driest conditions occurred around 5,000 years B.P., when open plant communities and limited canopy cover were dominant (Bousman 1998). Only oak and hickory trees were able to maintain a steady arboreal population in the uplands, and combined with

grasses, created a stable vegetative landscape adapted to xeric conditions (Bryant 1977; Bryant and Holloway 1985). Overall, the vegetation of the early to middle Holocene is reminiscent of modern conditions, although it was probably more open. Nordt et al. (1994) show that slight increases in C_4 plant abundance from the period 11,000 to 8,000 years B.P. and dominance of C_4 plants between 6,000 and 5,000 years B.P. (Figure 3.4). A decrease in C_4 abundance between 8,000 and 7,000 years B.P., however, may explain a widespread cold period (Hu et al. 1999; Nordt et al. 2002).

A switch to relatively xeric conditions in the early to middle Holocene also affected faunal distributions in central Texas. Bison were absent from the region between 7,500 and 4,500 years B.P., as dry conditions did not support enough grass for feeding (Graham 1987). Mesic species, including the mole and short-tailed shrew, left the area whereas arid-tolerant species, such as the desert shrew, increased in abundance (Toomey, Blum, and Valastro 1993).

As aridity increased, soil erosion of the uplands continued throughout the early Holocene and probably ended around 5,000 years B.P. (Cooke et al. 2003), depleting most of the mantle in many locations throughout the Edwards Plateau. The stable-carbon isotopic record in north-central Texas identifies a moist period during the early Holocene followed by an arid period representing the middle Holocene (Humphrey and Ferring 1994). Relatively low growth rates of stalagmites in caves remain consistent throughout the early to middle Holocene (Musgrove et al. 2001) (Figure 3.6).

3.4.4 Late-Holocene I Environmental Conditions (about 5,000 to 2,500 years B.P.)

Abandonment of the early- to middle-Holocene floodplain and terrace formation occurred around 5,000 years B.P. in fluvial systems of the Edwards Plateau (Figure 3.2). The supply of coarse bed material exceeded the hydraulic capabilities of the rivers, and laterally migrating channels deposited gravel and sand (Blum, Toomey, and Valastro 1994). Waters and Nordt (1995) attribute this large supply of sediment to reduced vegetation and stabilization of hillslopes. Floodplain abandonment along the Pedernales and Colorado Rivers resulted from decreased flood magnitudes during a shift to very dry conditions. Waters and Nordt (1995) interpret humid conditions beginning around 4,000 B.P. based on soil development along Brazos River terraces, but do not consider abandonment as a possible reason for these edaphic processes.

Pollen records indicate the driest conditions present on the plateau occurred between 5,500 and 4,500 years B.P. (Bousman 1998) and are attributed to the Altithermal. An increase in mesquite and cactus accompanied by a decrease in pine is reported by Patton and Dibble (1982), and the central Edwards Plateau appeared to be dominated by short grasses or semi-desert scrub (Toomey, Blum, and Valastro 1993) (Figure 3.5). Following this arid phase, an increase in tree pollen and grasslands were associated with a transition from drought-resistant oaks to oak-hickory woodlands. Some discrepancy among proxy records is evident during this episode. For example, the abundance of C_4 biomass decreased between 4,000 and 3,000 years B.P. (Nordt et al. 1994) (Figure 3.4), and this was attributed to cooler conditions (Nordt et al. 2002).

Additionally, Bousman (1998) detected an increase in tree cover between 5,000 and 3,000 years B.P. One possible explanation for the disagreement among records is a strong east to west climatic gradient during this time (Toomey, Blum, and Valastro 1993).

Some aspects of the faunal record in Central Texas between 5,000 and 2,500 years B.P. reinforce the discrepancies from other records. The presence of bison herds between 4,500 and 1,500 years B.P. suggests that relatively humid conditions fostered the development of lush grasslands (Graham 1987). This might be a mistaken interpretation, however, because healthy grasslands can persist during relatively dry conditions. More compelling is the disappearance of taxa with moisture requirements, including the eastern pipistrelle bat and woodland vole (Toomey, Blum, and Valastro 1993). The replacement of the least shrew by the desert shrew continued through this episode, as well as the importance of the desert cottontail relative to the eastern cottontail (Toomey, Blum, and Valastro 1993).

3.4.5 Late-Holocene II Environmental Conditions (about 2,500 to 1,000 years B.P.)

A return to wetter conditions in the Edwards Plateau occurred around 2,500 years B.P. Rivers deposited thick vertical accretion facies, filled chute channels along the floodplain, and buried soils resting on top of early- to middle-Holocene terraces (Blum, Toomey, and Valastro 1994) (Figure 3.2). This type of fluvial activity suggests frequent moderate- to high-magnitude flood events and a sufficient supply of fine sediment derived from very thin upland soils. The continued supply of coarse bed

material resulted in streams being unable to fully transport the load, and deposition of widespread, thick fill deposits occurred in the valleys creating a cumulic, organic-rich soil (Hall 1990). This accumulation of material created moderately sinuous channels with broad and shallow cross-sections (Blum and Valastro 1989).

The return to mesic conditions between 2,500 and 1,000 years B.P. appear to have increased woodland density in Central Texas. Holloway, Raab, and Stuckenrath (1987), in analyses of pollen from Weakly Bog in Leon County, suggest a relatively dense oak-hickory forest that switched to more open oak woodlands toward the end of this episode. Bryant (1977), however, does not detect any post-Altithermal shift to mesic conditions, essentially stating that present vegetation has not undergone appreciable change for the latter half of the Holocene. Bousman (1998) argues that oak woodlands were replaced by oak-hickory woodlands, suggesting more humid conditions at this time. Hall (1982), in two pollen records from northeastern Oklahoma, shows that a relatively wet climate between 2,000 and 1,000 years B.P. fostered an increase in the abundance in hickory and grasses with water requirements.

The humid climatic regime between 2,500 and 1,000 years B.P. allowed for the return of the woodland vole and eastern pipistrelle bat to the Edwards Plateau, and increased the proportion of least shrews to desert shrews (Toomey, Blum, and Valastro 1993). The presence of the prairie vole in North Texas and northeastern Oklahoma may also testify to mesic conditions in the area (Hall 1982; Graham 1987). Additionally, the

abundance of moist-habitat snails in Oklahoma indicates a pattern of increased precipitation in the region (Hall 1982).

3.4.6 Modern Environmental Conditions (about 1,000 years B.P. to present)

Finally, modern environmental conditions of the last millennium shifted back to drier conditions. Fluvial adjustments to this climatic regime include channel incision and floodplain abandonment, lateral accretion in small point and side bars at bends, and vertical accretion deposits of finer material along straight reaches (Blum and Valastro 1989) (Figure 3.2). Hall (1990) shows a period of channel incision occurring throughout the region around 1,000 years B.P., in both large and small systems, which indicates a common climatic mechanism. The current dominance of fine-grained sediment in floodplains of the Edwards Plateau is a caveat to the rule-of-thumb associating coarse sediment with relatively arid regimes (Blum and Valastro 1989). Most importantly, streams are underfit with respect to their larger channels (Blum and Valastro 1989). Extreme flood events of historic time have overtopped older terraces, but have not left appreciable deposits (Blum, Toomey, and Valastro 1994). The Brazos River has been confined to narrow meander belts with thick natural levees during modern conditions, and instability toward a lower position on the floodplain has resulted in two avulsions during the last 1,000 years (Waters and Nordt 1995).

A decrease in pollen influx rates and arboreal cover, interpreted from Weakly Bog in Leon County, supports the interpretation of drier conditions in the last 1,000 years (Holloway, Raab, and Stuckenrath 1987). Bousman (1998) detected a spike in

grass pollen around 400 to 500 years B.P., which is assumed to correspond with a dry episode. A shift from oak woodlands to the current oak savanna around 1,500 years B.P. also is evidence for more xeric modern conditions (Bryant and Holloway 1985).

Increased aridity over the last 1,000 years resulted in the dominance of the desert shrew over the least shrew in the Edwards Plateau (Toomey, Blum, and Valastro 1993) and the decline of mesic land snails in Oklahoma (Hall 1982). Graham (1987) suggests that the northern range expansions of nine-banded armadillo and collared peccary may have been related to increasing warmth and aridity. Additionally, a dramatic increase of bison in central Texas around 1,000 years B.P. has been attributed to the opening of grassland, thereby accommodating larger herds (Huebner 1991).

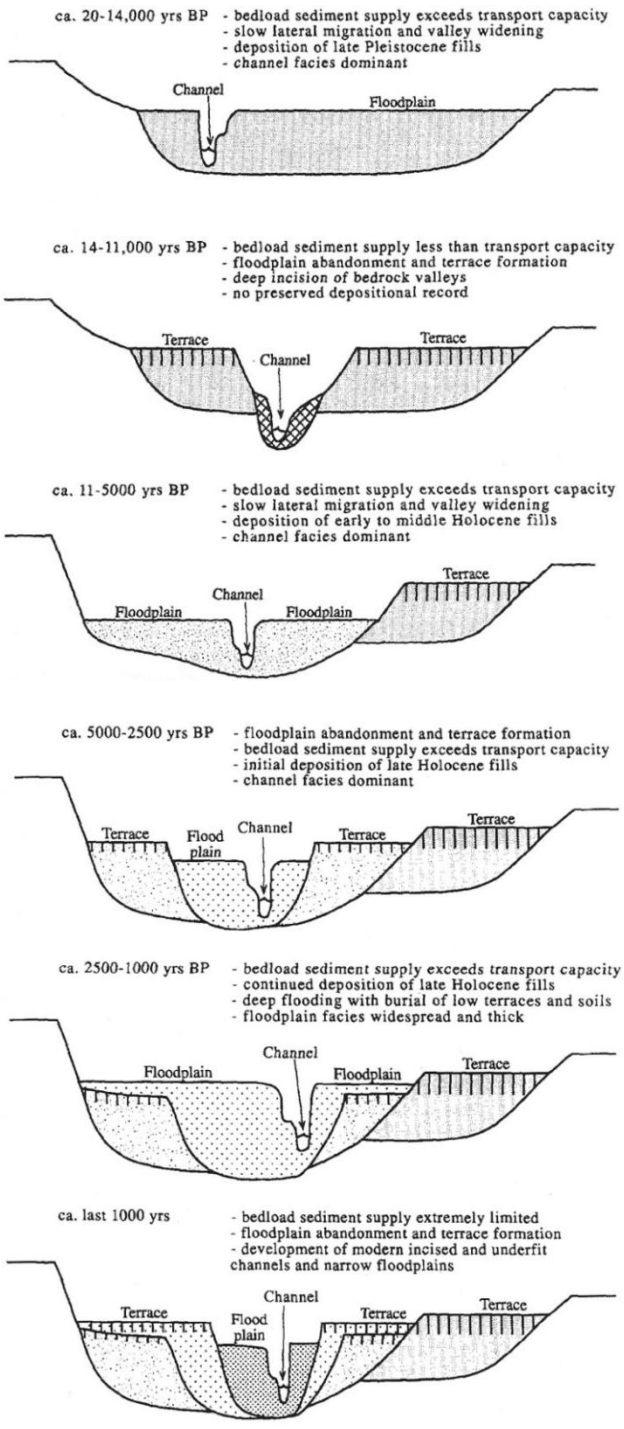

Figure 3.2. Channel, floodplain, and fluvial terrace evolution in the Edwards Plateau, Central Texas, since the Last Glacial Maximum (from Blum, Toomey, and Valastro 1994).

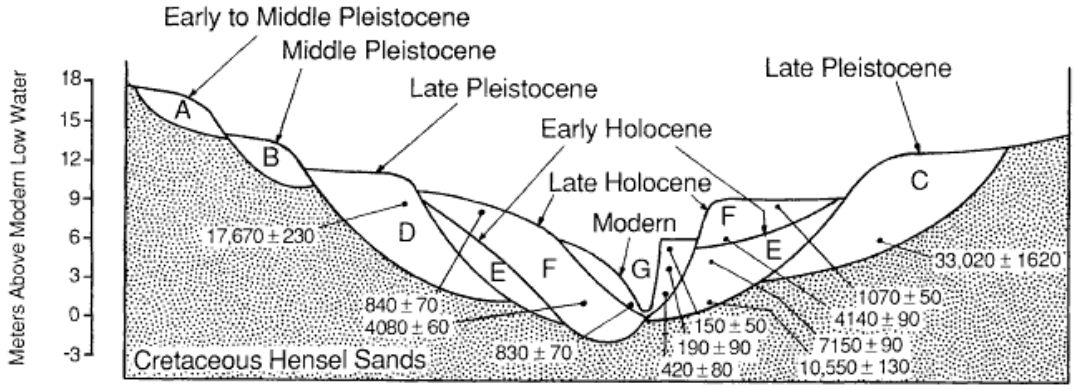

Figure 3.3. Cross-section of depositional units in the Pedernales River valley, Texas, with relative position of radiocarbon ages (from Blum and Valastro 1989).

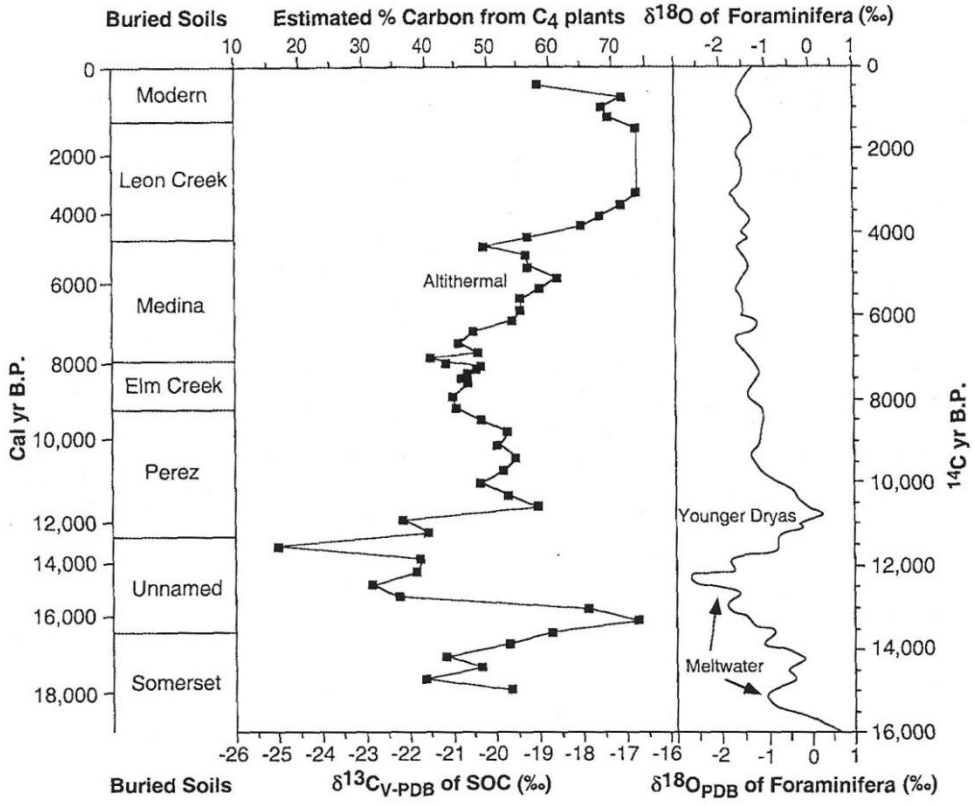

Figure 3.4. Abundance of C_4 plants based on $\delta^{13}C$ signatures extracted from alluvial deposits in the Medina River valley, Texas, and correspondence with $\delta^{18}O$ of foraminifera in the Gulf of Mexico (from Nordt et al. 2002).

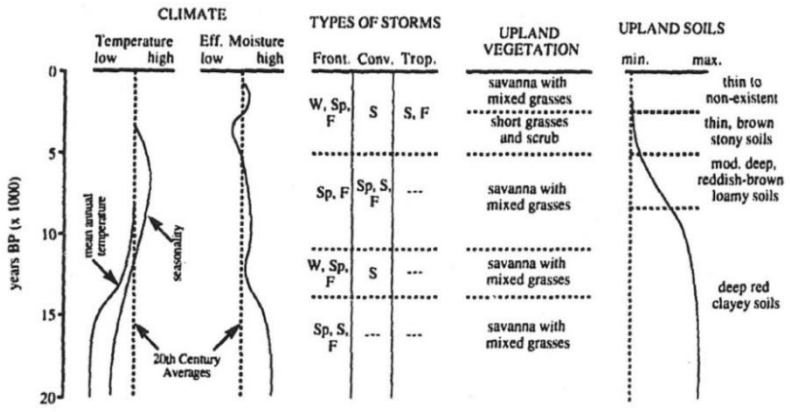

Figure 3.5. Climatic and environmental changes of the Edwards Plateau, Central Texas, since the Last Glacial Maximum based on pollen and faunal records, many of which came from Hall's Cave in the central plateau (from Toomey, Blum, and Valastro 1993). For the types of storms, "W, F, W, and Sp" represent summer, fall, winter, and spring, respectively.

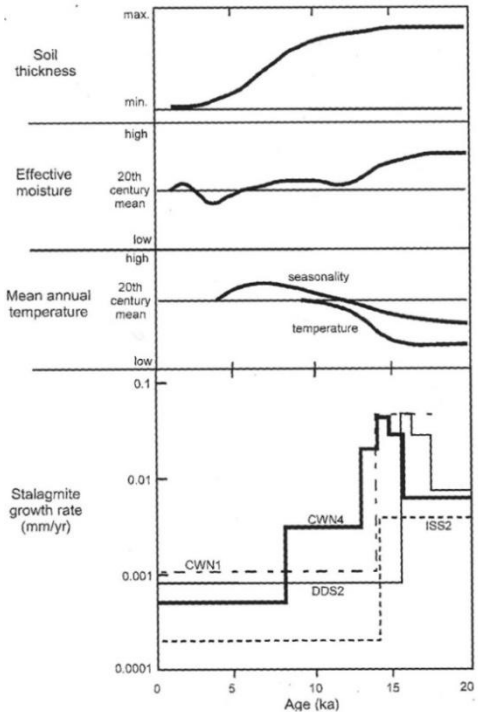

Figure 3.6. Comparison of stalagmite growth rates in Central Texas with independently derived results from Toomey, Blum, and Valastro (1993) (from Musgrove et al. 2001).

3.5 Discussion

The coolest and wettest conditions over the last 20,000 years in the Edwards Plateau occurred during the Last Glacial Maximum (about 20,000 to 14,000 years B.P.) (Table 3.1). River flood regimes were moderate and more frequent, as evidenced by lateral migration of channels, sediment storage in floodplains, and extensive soil development. The persistence of perennial lakes in northern and western Texas was dependent on higher water tables and more abundant precipitation. An open grassland, without a modern analog, was prevalent and accompanied by some boreal tree species. Large mammals grazed on the grasslands and fauna associated with cool, mesic conditions lived sympatrically with species found on the plateau today. Recent chemical and isotopic methods confirm cool, moist full-glacial conditions about 5˚C cooler than today, and highlight the initiation of soil erosion. It is likely that the southern extension of ice sheets in North America strongly affected the routing of mid-latitude low-pressure systems. The major zone of atmospheric divergence associated with stable conditions, currently at about 30˚ latitude, was probably forced to lower latitudes. This would have permitted more frequent rain-producing low-pressure systems to penetrate Central Texas, especially during the summer. Additionally, cooler summer temperatures limited evapotranspiration rates, which also increased available moisture.

A warming and drying trend characterizes the terminus of the Pleistocene (Table 3.1). Fluvial systems remained energetic enough to incise into bedrock, as sediment was totally removed from tributary valleys and upland slopes exhibited relative stability.

Lacustrine environments were still persistent in northern and West Texas. Warmer temperatures and increased seasonality led to the dominance of grasses, increase in C_4 plants, and disappearance of all boreal vegetation. These conditions also forced the removal of certain heat-intolerant and mesic faunal species, and mammalian megafauna became extinct at the end of the late-glacial episode. Isotopic evidence also points toward a warmer and drier climate, and glacial meltwater pulses into the Gulf of Mexico correlate with the coolest, driest conditions. The Younger Dryas cooling episode is not recognized by proxy evidence in the region, and the gradual retreat of continental ice sheets allowed the global belt of relatively high atmospheric pressure to move back towards 30˚ latitude, providing more stable atmospheric conditions and effectively reducing precipitation.

The early- to middle-Holocene in Central Texas is characterized by a continued warming and drying trend (Table 3.1), interrupted by a possible moist period between about 9,000 and 8,500 years B.P. A cool, dry spell around 8,200 years B.P. is detected in increased aeolian activity and a decrease in C_4 plant percentage. Fluvial systems went through a period of gradual floodplain construction. Pluvial lakes were eliminated or diminished in West Texas. A shift to open grassland communities with scattered oak and hickory trees occurred in the uplands, creating an environment similar to today. The progression toward the Altithermal is evidenced in the Edwards Plateau by a marked dominance of grasses in the pollen record. Mesic faunal species were forced to migrate north and east, while xeric species increased in abundance. Upland soil mantles were

reduced to the minimal thicknesses observed today. Increasing aridity in the mid-latitudes has been associated with strong zonal atmospheric circulation (Knox 2000), which limits the collision of cool, dry air masses with warm, moist air masses from the Gulf of Mexico and Pacific Ocean. Such a pattern would lead to relatively arid conditions in the Southern Plains and the Edwards Plateau.

The initial phase of the late Holocene (about 5,000 to 2,500 years B.P.) witnessed the warmest, driest conditions during the last 20,000 years and corresponds with the Altithermal (Table 3.1). Floodplain abandonment associated with a decrease in flood magnitudes occurred throughout river systems in the plateau, and loss of vegetative cover allowed substantial delivery of sediment to the valleys. Although some disagreement appears in reconstructions of vegetative cover, this episode was probably dominated by short grasses and scrub, followed by a gradual shift toward oak woodlands. The strongest records for arid conditions are derived from the faunal assemblage, which indicates the displacement of mesic mammals with arid-tolerant species. Zonal atmospheric circulation probably was the dominant influence for arid conditions associated with the Altithermal in the Edwards Plateau.

The period between 2,500 and 1,000 years B.P. is characterized by increasingly humid conditions (Table 3.1). River systems frequently witnessed moderate- to high-magnitude floods, which led to the development of thick, vertically accreted deposits. Relatively dense oak-hickory woodlands and lush grasses are detected in pollen records at this time. The return of mesic voles, shrews, and snails to previously xeric habitats

also testifies to greater frequencies and rates of precipitation. The mixing of contrasting air masses and resultant increase in the frequency of precipitation events often is linked to meridional atmospheric circulation patterns (Knox 2000).

Finally, the modern episode of the Holocene has shifted toward warmer, drier conditions across the Edwards Plateau (Table 3.1). Rivers and streams have incised into previous floodplains because bedload supply is limited, thereby creating underfit channels with respect to the former floodplain. A decrease in overall pollen accompanied by the conversion of oak-hickory woodlands to oak-dominated savanna reinforces the interpretation of modern xeric conditions. Current faunal assemblages are dominated by drought-tolerant species, and many mesic species formerly inhabiting the Edwards Plateau are no longer present. A relative decrease in tropical activity during the summer and increased zonal flow may be attributed to the modern arid conditions across the Edwards Plateau.

Table 3.1. Summary of paleoenvironmental change in the Edwards Plateau, Central Texas, USA, during the last 20,000 years, organized by an existing scheme (Toomey, Blum, and Valastro 1993).

Episode	Relative conditions	Geomorphic and hydrologic evidence	Pollen evidence	Fauna evidence	Isotopic evidence
Full glacial (about 20,000 to 14,000 years B.P.)	Coolest and wettest	Lateral migration of rivers; sediment storage; soil development; pluvial lakes	Mixed deciduous forest with some boreal trees and grassland	Large mammals; soil-burrowing mammals	Ground-water atmospheric noble gases; rapid stalagmite growth
Late glacial (about 14,000 to 10,500 years B.P.)	Gradual warming and drying trend, but still cool and wet	Deep channel incision; continued presence of pluvial lakes; upland soil erosion	Decline of deciduous trees; replacement with oak savannas; increase in C_4 plants	Extinction of some large mammals; Small, mesic and burrowing mammals gradually decline	Rapid decrease in stalagmite growth; soils indicate no Younger Dryas expression and complex meltwater fluxes
Early to middle Holocene (about 10,500 to 5,000 years B.P.)	Rapid warming and drying trend	Valley widening and slow aggradation; decline of pluvial lakes; aeolian sedimentation; extensive upland soil erosion	Less pollen; open woodlands and grassland; increase in C_4 plants	Periodic decline of bison; abundance of small, xeric mammals	Low stalagmite growth rates; soils show possible brief moist period around 8,500 years B.P.
Late Holocene I (about 5,000 to 2,500 years B.P.)	Warmest and driest	Floodplain abandonment coupled with excessive delivery of coarse gravel to channels	5,000 years B.P. with short grasses and scrub; abundance of C_4 plants; gradual increase of drought-resistant trees	Disappearance of all mesic mammals; gradual increase of bison; xeric mammals	Not available
Late Holocene II (about 2,500 to 1,000 years B.P.)	Slightly cool and wet	Vertical accretion and fill processes;	Possibly denser woodland; increase in trees and grasses with water requirements	Return of some small, mesic species	Not available
Modern (about 1,000 years B.P. to present)	Warm and dry	Channel incision; underfit channels; fine-grained inset deposits; floodplain abandonment	Decreased pollen flux; transition from woodland to open savanna	Dominance of small, xeric mammals; increase in bison about 1,000 years B.P. associated with more open grassland	Not available

3.6 Summary

Insights into changing environmental conditions of the Edwards Plateau provide a long-term context for descriptions and models of regional climate, hydrology, geomorphology, and biogeography. Perhaps most striking are the relatively brief time intervals and large magnitudes of response among geomorphic and biologic systems to changes in climatic regimes. These time intervals could have been on the order of hundreds of years and perhaps decades. With increasing human-related effects on atmospheric composition, water quantity and quality, and land-cover patterns; it is informative to consider the effects of climate change or cycles on spatial and temporal environmental conditions.

The Edwards Plateau presents itself as a complex transition area between temperate, tropical, humid, and arid regimes. Regional impacts of climate change may be difficult to predict, but it can be expected that global warming could lead to increased aridity, such as that experienced during the Altithermal. An increase in sea-surface temperatures could increase tropical system activity during the summer and coupled with reduced vegetative cover, may subject river valleys to incision. The assertion of dominance by drought-tolerant species in the region challenges the practicality of conservation efforts for mesic species. Expected natural consequences are further complicated by human-related phenomena, including land-use patterns, introduction of exotic species, and modification of the fire regime.

Further, investigations of alluvial sediment composition and channel adjustment in the Edwards Plateau initially require a conceptual framework of environmental change through time. Sediment sampling strategies and associations with the present-day hydrologic regime must be considered with respect to the complex suite of sedimentary units and their relative positions shown in Figures 3.2 and 3.3. The channel incision and floodplain abandonment during the last 1,000 years should result in a series of inset floodplains associated with the present-day hydrologic regime, bounded by higher surfaces representative of previous environmental conditions. Additionally, terrace deposits older than the modern alluvium could comprise the bank material where the present-day channels are actively migrating.

Chapter 4. Research Design for Investigation of Downstream Trends in Alluvial Sediment Composition and Channel Adjustment in the Llano River Watershed, Central Texas, USA

The research design to investigate downstream trends in alluvial sediment composition and mutual channel adjustment in the Llano River watershed is split into three general categories: (1) field assessments, (2) laboratory sediment analyses, and (3) data analyses. Project objectives associated with these three categories are briefly described below, and specific methodological details are embedded within result-oriented chapters that follow (Chapters 5 and 6).

4.1 Field Assessment

Field assessments of sediment composition and channel shape were made at nineteen sites along the North Llano, South Llano, and Llano Rivers and selected major tributaries (Figure 4.1). Cross-sections of channel shape were provided by the Lower Colorado River Authority (LCRA) for nine additional sites along tributaries (Figure 4.1). Field sites were chosen to adequately characterize observed downstream changes of channel morphology. For the nineteen sites visited, channel shape was measured and sediment samples were obtained along multiple cross-section transects to ensure that local variability (Phillips 1991; Fonstad and Marcus 2003) was minor relative to general downstream trends (Figure 4.2).

Cross-sectional surveys of channel and floodplain dimensions included subaqueous- and subaerial-instream surfaces (Figure 4.3), banks, floodplain surfaces, fluvial terraces, colluvial wedges, and valley walls. Cross-sectional topographic surveys constitute the majority of morphologic data for this project. For further details on cross-sectional topographic surveys, readers are referred to Section 6.5.1 in Chapter 6.

Sediment samples were obtained for these various geomorphic surfaces along transects identical to the topographic surveys, and field notes coupled with topographic surveys were relied upon later to determine the geomorphic surface that was sampled. Particle size of cobble- to gravel-sized bed-material was sampled at the surface using a modified Wolman pebble count (Wolman 1954) (Figure 4.4), and sand-sized or finer material was scooped and bagged for further laboratory analysis. Sediment samples were obtained to quantify downstream trends in alluvial composition and infer sedimentary controls of channel adjustment. For further details on sediment sampling strategies, readers are referred to Section 5.5 in Chapter 5.

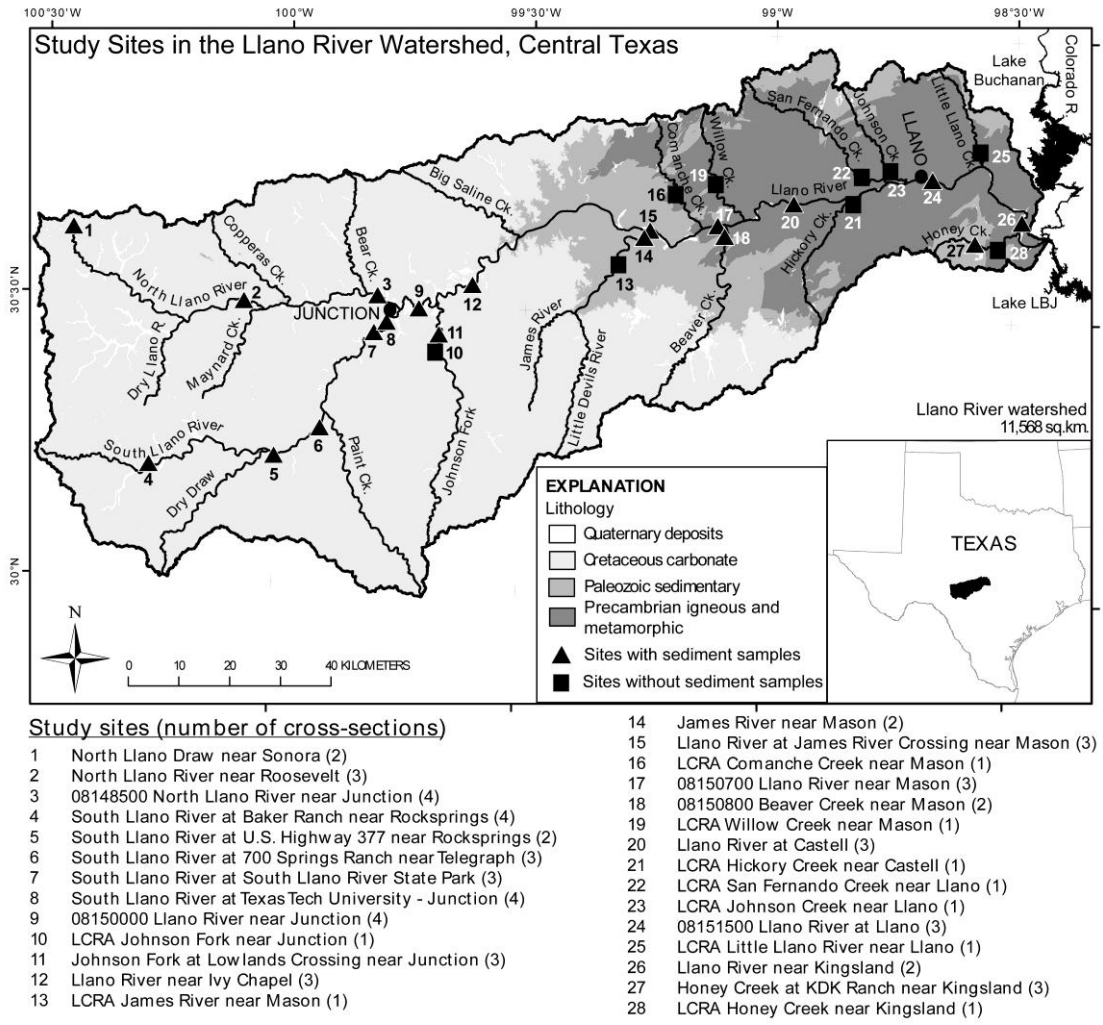

Figure 4.1. Study sites, hydrography, and lithology (Barnes 1981) of the Llano River watershed in Central Texas, USA. Site names preceded with an 8-digit identification number are located at active U.S. Geological Survey streamflow-gaging stations. Site names preceded with "LCRA" are located at active Lower Colorado River Authority streamflow-gaging stations. Sites without a prefix are ungaged.

Figure 4.2. Two cross-section transects (yellow lines) and flow path (blue line) of the James River near Mason, Texas. For scale, yellow lines approximately are 250 meters. Flow direction is toward the north-northeast (upper part of the image). Natural-color imagery from Google Earth, accessed in February 2008.

Figure 4.3. Total-station survey unit and view downstream at the Llano River near Mason, Texas.

Figure 4.4. Equipment used for modified Wolman pebble count procedure on cobble- to gravel-sized bed material.

4.2 Laboratory Sediment Analysis

Sand-sized or finer sediment samples required analysis of particle size, relative carbonate content, and magnetic susceptibility. Particle size analyses are used to determine d_{16}, d_{50}, and d_{84}, descriptors that represent diameters, in millimeters, at which 16, 50, and 84 percent, respectively, of the sample is finer than. Techniques associated with hydrometer and sieve analysis, as outlined in Gee and Bauder (1986), were used for particle-size analyses. Relative carbonate content (Goh, St. Arnaud, and Mermut 1993) and magnetic susceptibility analyses were done to infer the general mineralogy and provenance of alluvial sediment. Samples with relatively high carbonate content and low magnetic susceptibility contain particles likely derived from Cretaceous or Paleozoic carbonate source areas. Relatively low carbonate content and high magnetic susceptibility likely indicates particles from Precambrian igneous or metamorphic source areas, based on lack of calcite and dolomite and presence of metallic elements. For further details on laboratory sediment analyses, readers are referred to Section 5.5 in Chapter 5.

4.3 Data Analysis

Data analyses generally are separated into GIS, hydrologic, and statistical analyses, all done using computer software. GIS analyses of channel planform morphology and alluvial valley width were done using recently acquired orthoimagery. GIS analyses of 10-meter digital elevation models (DEMs) (U.S. Geological Survey

2008a) and the National Hydrography Dataset (U.S. Geological Survey 2008b) were used to delineate watersheds and graph longitudinal profiles. Surface lithology was determined using a digitized version of Barnes (1981) in GIS. A host of other supporting cartographic products also were done using GIS. For further details on laboratory sediment analyses, readers are referred to Section 6.5.3 in Chapter 6.

Hydrologic analyses of U.S. Geological Survey (USGS) and LCRA streamflow data were done using spreadsheets and statistical software. Routine hydrologic analyses, including flow-duration curves of daily mean discharge and summary statistics, were done to characterize the flow regime of the Llano River watershed. Flow resistance and partial-duration flood-frequency analyses were done using spreadsheets and the R environment for statistical computation (R Development Core Team 2004), and the results were used to compute discharge at ungaged locations and associate discharge with average return periods (e.g., 10-year flood). For further details on hydrologic analyses, readers are referred to Sections 6.5.5 and 6.5.6 in Chapter 6.

Finally, other statistics, including correlation coefficients and regression analyses, among others, were computed in R to quantify relations among various sedimentary, hydrologic, and morphologic parameters. For further details on statistical analyses, readers are referred to Section 5.5 in Chapter 5 and Section 6.5.4 in Chapter 6.

Chapter 5. Downstream Trends in Sediment Size and Composition of Channel Bed, Bar, and Bank Deposits Related to Hydrologic and Lithologic Controls in the Llano River Watershed, Central Texas, USA

(accepted pending revisions to *Geomorphology* in March 2009)

5.1 Abstract

The downstream fining of fluvial sediments is considered a fundamental tenet of drainage systems and for decades has been the subject of considerable research within fluvial geomorphology. This topic has been dominated by a legacy of research that has primarily considered downstream variability in channel-bed sediments, which are then considered with respect to several distinctive processes such as abrasion, selective entrainment, and addition or extraction mechanisms. Other sedimentological components of the fluvial system such as bars, bank material, and overbank deposits, however, represent distinctively different processes occurring at various flow magnitudes and durations, and thus provide an opportunity to examine a more comprehensive set of controls on the larger fluvial system. This is particularly important to consider in fluvial systems segmented into sharply different geologic zones, and for systems that exhibit a highly variable flow regime, such as the Llano River watershed (11,568 square kilometers) in Central Texas, USA. The Llano watershed represented an excellent setting to examine topics related to the downstream variability in fluvial

deposits and to shed light on the roles of different processes that control spatial patterns in sediment composition at the watershed scale.

The study design included field, laboratory, and statistical analysis to characterize fluvial deposits and to compute standard sedimentary indices (d_{16}, d_{50}, d_{84}, sorting). Channel bed, bar, bank, and overbank deposits were characterized for nineteen stations along the main-stem channel and at key tributaries, spanning the entire drainage system. Analysis of sedimentological indices revealed contrasting trends in the downstream spatial pattern of fluvial deposits, particularly between bed and bank deposits. In contrast to channel-bar deposits, low-flow-channel (thalweg) deposits are not characterized by a downstream reduction in particle size, a discrepancy attributed to uniformity and continuity of hydraulic sorting mechanisms during both low and high flows. Further, channel-bar deposits reveal an abrupt downstream reduction in gravel size in the upper watershed, attributed to an increase in drainage area, as well as an abrupt gravel-to-sand transition immediately downstream of the Paleozoic-Precambrian contact. The decrease in channel-bar particle size occurs despite an increasingly constricted alluvial valley, commonly associated with greater unit stream power. The gravel-to-sand transition is attributed to an adjustment of sediment source lithology. Weathering mechanisms in the upper Cretaceous carbonate zone of the watershed result in relatively fine-grained (silt, clay, and some fine sand) channel banks along the North, South, and upper Llano Rivers. Weathering mechanisms of Precambrian rocks are weathered to grus in-situ, and considerable quantities of sand-sized material are

delivered to the drainage network. Channel banks of the Llano River are increasingly composed of the sand-sized fraction and less carbonate material. The consideration of distinctive sedimentological components of a dynamic fluvial system represents a more comprehensive and nuanced study of the topic of downstream sediment trends than prior studies, which is important to understanding a range of applied issues in engineering, biology, and planning.

5.2 Introduction

The sedimentary composition of alluvial deposits, including the channel bed, bars, and banks, is one of the most important controls of river morphology (Schumm 1960; Schumm 1977; Ferguson 1987; van den Berg 1995) and determines prevalent mechanisms of sediment transport. As such, downstream analyses of particle size provide information necessary to inform appropriate infrastructure design (e.g., Heitmuller and Asquith 2008), assess aquatic habitat suitability and vulnerability (The Instream Flow Council 2004), rehabilitate degraded channel reaches and riparian corridors, and effectively manage water resources such as reservoirs. Downstream analyses of alluvial sediment characteristics have primarily focused on reductions in bed material size (Bluck 1987; Kodama 1994; Frings 2008), but investigations that include channel bank or floodplain material are notably few (Knighton 1998). The inequality of downstream analyses of bed and bank material possibly results from emphases on bedload-transport processes (e.g, Parker, Klingeman, and McLean 1982;

Andrews and Smith 1992; Kleinhans and van Rijn 2002), the hyporheic zone (e.g., Brunke and Gonser 1997), and fish-spawning and benthic habitat analyses (e.g., Milner et al. 1981; Montgomery et al. 1996). Further, few investigations have compared downstream trends in sedimentary characteristics of various geomorphic surfaces, including channel bars, the thalweg, or bank deposits at given heights above the channel bed; especially for fluvial systems with highly variable flow regimes. The lack of downstream comparisons among different types of alluvial deposits might be attributed to the difficulties associated with access to multiple sampling sites at strategic locations along rivers. Finally, few studies have associated fluvial deposits with lithology to investigate the relative influence of upstream sources, possibly because pragmatic efforts have been directed at quantifying sediment yields and budgets (e.g., Trimble 1983; Phillips, Slattery, and Musselman 2004).

The purpose of this chapter is to compare and interpret downstream characteristics of channel bed, bar, and bank deposits in the rural, unregulated, flood-dominated Llano River watershed in Central Texas, USA (Figure 4.1). Deposits are analyzed for particle size, relative carbonate content, and magnetic susceptibility to determine sediment type and provenance. Controlling for the hydrologic regime, channel slope, and land use, which are similar throughout the watershed, sedimentary characteristics are related to lithology, which is distinctly segregated into Cretaceous carbonate rocks (upper watershed), Paleozoic sedimentary rocks (transition), and Precambrian igneous and metamorphic rocks (lower watershed). Other controls of

downstream sedimentary characteristics, including valley confinement, localized hydraulics, and drainage area, are discussed with respect to observed trends.

5.3 Background

Assessments of sediment transport processes and distribution at the watershed scale are complicated by variations in climate, geologic structure, geologic composition, and land cover. Combinations of these controls determine the hydrologic and sedimentary regimes of stream channels and, therefore, the spatial and temporal potential for erosion, sediment transport, and deposition. In particular, it has been debated that arid, semi-arid, and seasonal fluvial systems with highly variable flow regimes are likely to experience more cumulative sediment transport over time during infrequent, high-magnitude floods than similarly-sized humid systems (Schick 1974; Gupta 1988; Bourke and Pickup 1999). In systems that exhibit a greater dependence on high-magnitude floods, it is likely that sediment transport and depositional mechanisms are not as uniformly distributed through space and time as would be expected in less variable humid environments (Wolman and Gerson 1978). Large, powerful floods commonly are associated with complex overbank patterns of erosion and deposition (Nanson 1986), and can greatly modify the arrangement of instream and overbank landforms conducive to particular sedimentary processes. Further, floods in arid and semi-arid systems usually are not uniformly distributed through time, such that one year might have two or more large floods and the next few years do not have any substantial

flood flows. The timing of infrequent, high-magnitude floods causes irregular pulsing of sediment delivery and transport, in both space and time (Nash 1994; Bourke and Pickup 1999; Heitmuller and Asquith 2008).

The structure and composition of surface geology also exert considerable influence on the spatial arrangement of sedimentary processes in fluvial systems. Geologic structure of a watershed determines the overall valley slope and associated hydraulic forces that promote erosion, sediment transport, and deposition. Abrupt changes in valley slope, at a fault or escarpment for example, can cause shifts in predominant fluvial processes, such as transport-dominated to locally depositional (Schumm 2005). The lithology of the watershed surface, by its mineralogical properties and associated resistance to weathering and erosion, affects the sediment transport regime of a fluvial system in two ways: (1) confinement of the valley and accommodation space for sedimentary processes and (2) type of sediment delivered to stream channels. Relatively resistant rock units reduce valley width and, thereby, confine hydraulic energy, especially during high-magnitude floods (Baker and Costa 1987; Magilligan 1992). Where time-averaged transport processes outpace depositional processes in confined fluvial settings, alluvial deposits are, at best, temporary (e.g., Nanson 1986). Surface lithology also influences the type of sediment found in fluvial systems, most notably characterized by particle size. Differential rates and styles of weathering not only dictate the initial size of detached particles, but also the rate at which size is reduced with downstream distance (Kodama 1994; Morris and Williams

1999; Moussavi-Harami Mahboubi, and Khanehbad 2004) and, therefore, indirectly influences the spatial distribution of sediment in the fluvial system.

The well-documented decrease in bed-material particle size with downstream distance has been attributed to three mechanisms: (1) abrasion (e.g., Kodama 1994), (2) selective transport (e.g., Church and Hassan 1992), and (3) addition and extraction (e.g., Knighton 1980; Bluck 1987; Frings 2008). Abrasion is the process by which sediment particles are reduced in size by instream physical and chemical processes, such as chipping, grinding, and dissolution. Selective transport refers to the preferential entrainment of small particles relative to larger particles. Finally, addition and extraction of particles can occur by tributary inputs, entrainment at local bedrock outcrops, overbank deposition, and distributary bifurcations. In general, the rate of change in bed-material size decreases with downstream distance, especially in sand-bed channels where selective transport processes are weaker (Frings 2008). At gravel-to-sand transitions, however, strong sorting processes exist because of size patchiness and the transition from a clast-supported to a matrix-supported bed (Wilcock 1998). Abrupt gravel-to-sand transitions have mostly been attributed to sharp breaks in channel slope (Howard 1980; Sambrook Smith and Ferguson 1995) or a self-reinforcing non-linear decrease in shear stress (Ferguson 2003) that disproportionally favors sand transport over gravel (Wilcock 1998). Less importance has been placed on lateral inputs of sand (Knighton 1998).

Channel-bank material is representative of floodplain development through time, and consists of both instream and overbank deposits. Basal material of steep, erosional banks commonly reflects channel-lag deposits from hundreds to thousands of years ago, unless mass failure processes have resulted in bank-top material at the base, as would be the case for a rotational slump. Because channel migration and hydraulic sorting mechanisms typically result in coarser basal strata, an anomalous decrease in particle size could either indicate contemporary mass failure processes or buried fine-grained fill deposits. For more gradually-sloping banks, basal deposits might be comparatively recent and comprised of material from the channel bed, as might be expected for high-energy settings where temporary scour-and-fill processes dominate. The uppermost material of most alluvial banks, whether steep or gradual, is expected to reflect contemporary overbank deposition. However, some cases exist in partly-confined systems where alluvial banks seamlessly merge with colluvial or terrace deposits along the valley margin, which could be indicated by an abrupt change in particle size. Few studies have focused on downstream trends in channel bank and overbank material, but it usually is assumed that progressive fining trends (Kolb 1962) are interrupted by additions of material from tributaries or localized outcrops of relatively coarse material (Hudson and Heitmuller 2003).

In summary, research into the downstream fining of fluvial sediment is dominated by a focus on channel-bed material (Knighton 1987), which represents only one component of the overall fluvial system. Other aspects of fluvial systems that are

appropriate to consider for downstream trends include channel bars, banks, and overbank deposits. These geomorphic units are important to consider because they are controlled by processes distinctively different from those at the channel bed, particularly the thalweg. Elucidating the interrelations of channel bed, bar, and bank deposits will provide a more comprehensive assessment of downstream trends in fluvial sediments than which is represented in the literature. Additionally, most studies of downstream trends in bed-material size have not included rivers with highly variable flow regimes, where trends might differ from less variable, humid fluvial systems. Further, examples are few that relate abrupt changes in lithology and associated weathering processes to downstream transitions in fluvial sediment composition. Thus, this study addresses a major gap in the knowledge base concerning the subject of alluvial sedimentology.

5.4 The Llano River Watershed

The Llano River watershed (11,568 square kilometers) (Figure 4.1) is a geologically variable, unregulated, flood prone, rural fluvial system in the Edwards Plateau of Central Texas. The surface geology of the watershed is complex considering its drainage area, and reflects Tertiary tectonic activity of the Llano Uplift. The ground-surface extent of the uplift occurs in a relatively isolated area of Central Texas, centered in the eastern part of the watershed. Expressed at the ground surface, an exhumed outcrop of Precambrian igneous and metamorphic rock is surrounded by an elevated

Cretaceous carbonate rim, with a transitional zone of Paleozoic sedimentary rock occurring between.

The western, upper side of the Llano River watershed occurs in the central Edwards Plateau, an elevated, dissected lower-Cretaceous carbonate tableland with high elevations above 700-meters NAVD88 (North American Vertical Datum of 1988). Formations of the plateau are mostly comprised of horizontally-bedded, fossiliferous limestone and dolomite sequences, with varying amounts of chert. Sand and conglomerate formations, notably the Hensell Sand, are exposed in the valley in the west-central part of the watershed. In total, lower Cretaceous formations comprise 66 percent (7,629 square kilometers) of the total watershed area. Transitioning into the Llano Uplift, Paleozoic sedimentary rocks comprise almost 12 percent (1,369 square kilometers) of the total watershed area. Paleozoic sedimentary units consist of various lithologic types, mostly Ordovician limestone and dolomite and Cambrian sandstone. In the lower, eastern side of the watershed, Precambrian intrusive igneous and metamorphic rocks dominate and comprise 19 percent (2,180 square kilometers) of the total watershed area. Precambrian rocks include granite, gneiss, and schist, and collectively form irregular topography, including large exfoliation domes. The remaining 3 percent (390 square kilometers) are mostly comprised of Quaternary alluvial deposits.

Differential rates and patterns of weathering in the Llano River watershed strongly influence valley confinement, alluvial development, and sedimentary

composition. Relatively high rates of physical and chemical weathering of Cretaceous carbonate rock have widened the Llano River valley to its greatest extent in the vicinity of Junction (Figure 5.1). Fluvial processes and forms associated with unconfined valley settings, including meander cutoffs, alluvial terraces (e.g., Blum, Toomey, and Valastro 1994), and well-defined floodplains, occur in this area. Channel networks of the western and central watershed are dominated by carbonate cobble-, pebble-, and gravel-sized bed material (Figure 5.2). The transition to Paleozoic sedimentary strata is reflected by a marked decrease in valley width, a less sinuous channel, and greater bedrock exposures along the Llano River, indicating a more resistant lithology. Alluvial development is limited to small hydraulically-favorable zones of deposition, including discontinuous floodplains and mid-channel bars. Precambrian granite, gneiss, and schist in the eastern part of the watershed are the most resistant rocks to weathering, containing varying amounts of quartz, microcline, plagioclase feldspar, biotite, and hornblende. Although, by definition, more resistant than carbonates, Precambrian rocks deliver mostly sand-sized sediment to channel networks, implying that most weathering is accomplished in-situ. The Llano River valley also is confined in its lower reaches, and supports limited depositional features.

The plateau-based setting, variable geologic structure of the watershed, and incision history of local rivers has resulted in a remarkably straight longitudinal profile of the Llano River (Figure 5.3). Combining the South Llano River and Llano River, the channel descends from approximately 700- to 250-meters NAVD88 over a distance of

about 300 kilometers, giving an overall dimensionless channel slope of 0.0015. The consistency of the Llano River profile nullifies explanations of downstream sediment variability imposed by abrupt or gradual hydraulic changes related to slope. Therefore, cross-sectional and planform geometry, drainage network characteristics, boundary composition and adjustment, and discharge characteristics are the remaining factors that could explain variation in sediment transport and distribution in the watershed.

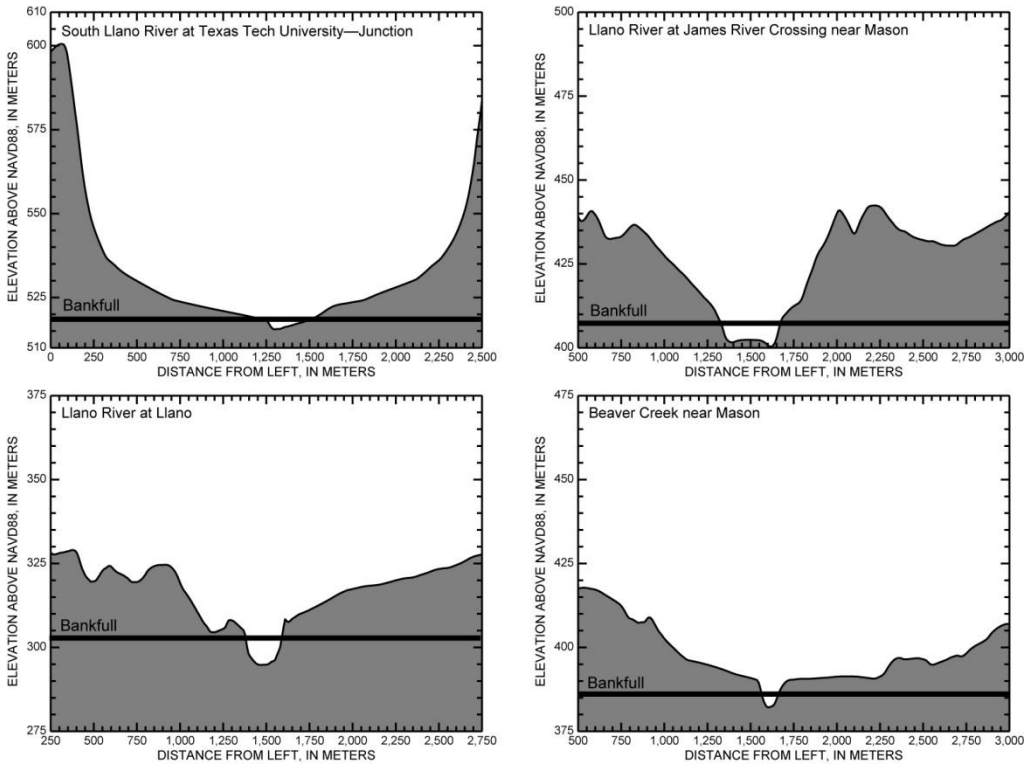

Figure 5.1. Valley cross sections of selected study sites in the Llano River watershed, Central Texas, derived in GIS from a 10-meter digital elevation model. Higher-resolution surveys of channel cross sections are not included. Alluvial bankfull stages, however, are determined from cross-sectional surveys of channel geometry. The alluvial valley in the upper and middle parts of the watershed transitions to a bedrock-controlled valley in the lower watershed.

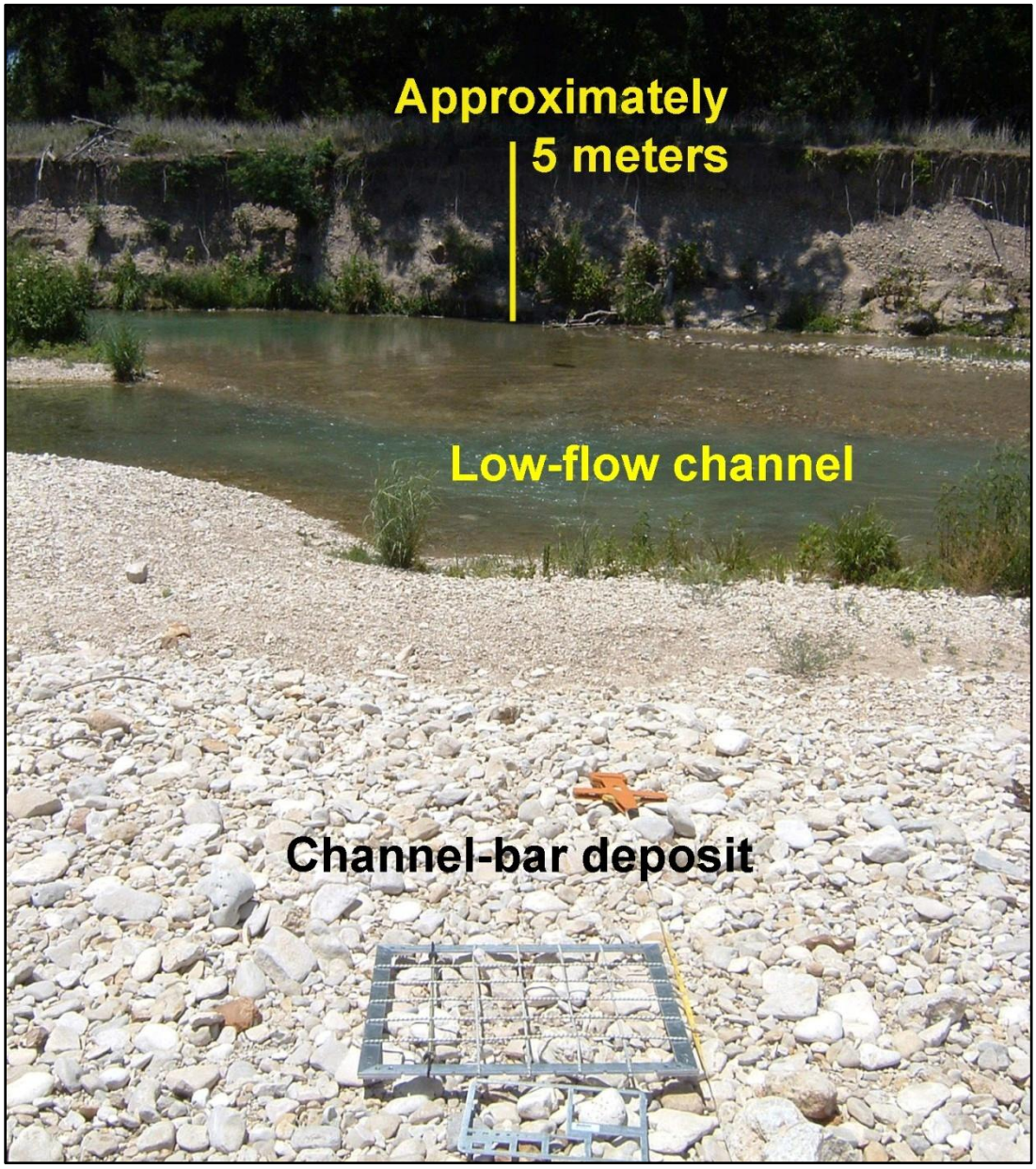

Figure 5.2. Channel bar, low-flow-channel, and left bank (height approximately 5 meters) of the South Llano River at South Llano River State Park near Junction, Texas. The dimensions of the sampling grid on the channel bar are 50 centimeters by 50 centimeters.

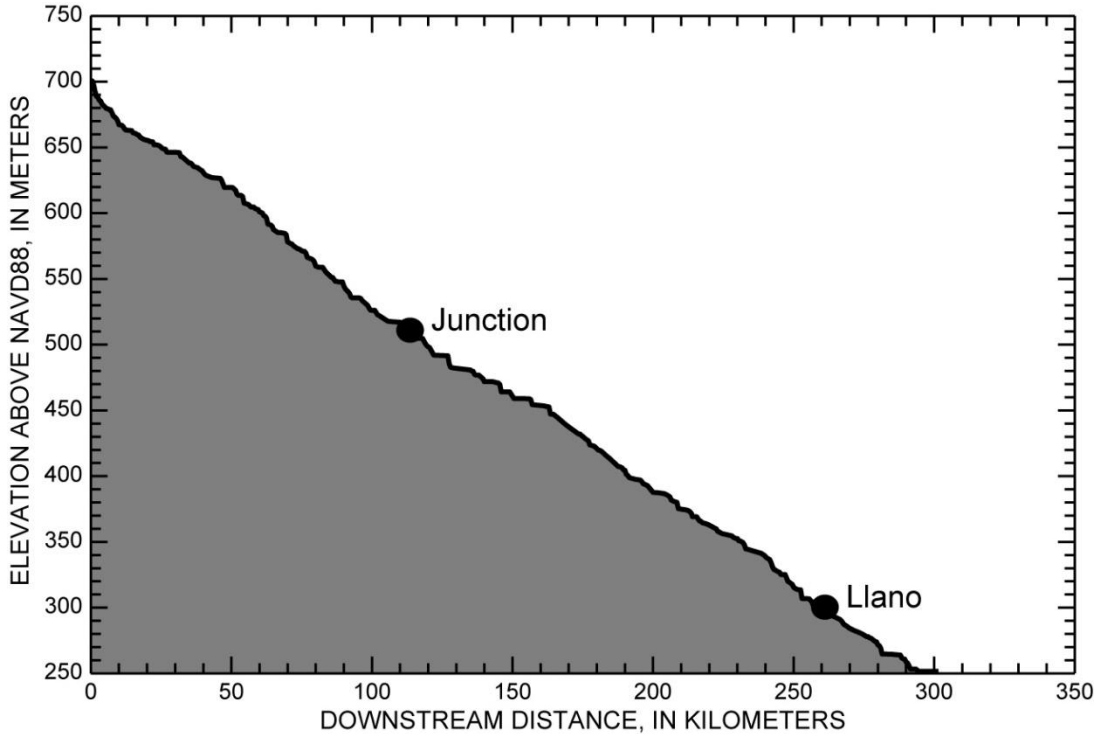

Figure 5.3. Longitudinal profile of the South Llano River and Llano River in Central Texas. Aside from a slight concavity in the uppermost 15 kilometers and subtle downstream irregularities, the rivers have a remarkably linear profile.

The precipitation regime of the Llano River watershed ranges from semi-arid in the west (approximately 580 millimeters of rainfall per year) to sub-humid in the east (approximately 760 millimeters of rainfall per year). Rainfall in Central Texas, however, is highly variable through time, such that episodic periods of drought can transition to repeated flooding conditions within months (Bomar 1983). As a result of locally steep slopes and very thin soils (Cooke et al. 2003), tremendous runoff rates to streams and rivers cause this area to experience extreme flash floods (Beard 1975; Tinkler 2001; Burnett 2008), capable of transporting substantial quantities of fluvial sediment (Heitmuller and Asquith 2008) and greatly modifying channel geometry (Baker 1977).

The hydrology of the Llano River and its tributaries reflects the climatic mechanisms prevalent in Central Texas (Table 5.1, Figure 5.4). Most tributaries to the Llano River exhibit relatively low baseflow conditions for the majority of time, with the lowest flows usually occurring in mid- to late-summer. The South Llano River, however, is fed by karstic springs upstream (south) of Junction, and provides the majority of baseflow to the main-stem Llano River downstream of Junction. Interrupting normal baseflow conditions are extreme floods caused by rainfall associated with stalled low-pressure systems or tropical cyclones (Figure 5.5). Floods along the Llano River at Llano have exceeded 3,000 cubic meters per second ten times since the 1940 hydrologic year, not including the estimated peak instantaneous discharge of 10,760 cubic meters per second in 1935. Suspended-sediment transport

events are dependent on episodic floods (Figure 5.6), and bedload transport in the upper reaches near Junction also has been shown to occur episodically (Heitmuller and Asquith 2008). There are no reservoirs that regulate discharge in the Llano River watershed, although two low-flow-control structures in Junction and Llano allow ponded water to be used for municipal supply.

Table 5.1. Hydrologic data for U.S. Geological Survey streamflow-gaging stations in the Llano River watershed in Central Texas.

[DA, drainage area; km^2, square kilometers; Q_{mn}, mean daily mean discharge; Q_{md}, median daily mean discharge; m^3/s, cubic meters per second; Q_{mnmx}, mean annual maximum discharge; Q_{mdmx}, median annual maximum discharge; Q_{max}, maximum instantaneous discharge; Q_{mnmn}, mean annual minimum discharge; Q_{mdmn}, median annual minimum discharge]

USGS station ID	Station name	DA (km^2)	Period of record used	Q_{mn} and Q_{md} (m^3/s; m^3/s)	Q_{mnmx} and Q_{mdmx} (m^3/s; m^3/s)	Q_{max} (m^3/s) and date	Q_{mnmn} and Q_{mdmn} (m^3/s; m^3/s)[a]
08148500	North Llano River near Junction, Texas	2,335	October 1, 1915 to October 26, 1977; June 13, 2001 to April 5, 2008	1.94; 0.57	595[b]; 173[b]	2,888; September 16, 1936	0.149; 0.050
08150000	Llano River near Junction, Texas	4,815	October 1, 1915 to May 10, 1993; October 1, 1997 to April 5, 2008	5.65; 2.89	982[c]; 374[c]	9,033; June 14, 1935	1.69; 1.44
08150700	Llano River near Mason, Texas	8,418	March 7, 1968 to May 9, 1993; October 1, 1997 to April 5, 2008	9.24; 4.81	1,374[d]; 714[d]	7,447; June 22, 1997	2.59; 2.24
08150800	Beaver Creek near Mason, Texas	558	August 1, 1963 to September 30, 2007	0.55; 0.10	278[e]; 213[e]	1,894; August 3, 1978	0.0092; 0.0011
08151500	Llano River at Llano, Texas	10,885	September 17, 1939 to April 5, 2008	10.9; 4.45	1,458[f]; 796[f]	10,760; June 14, 1935[g]	1.29; 0.934

a From Asquith et al. (2007) using daily mean discharge values from the beginning of the period of record for each gaging station to December 31, 2003.
b Period of record used for annual maximum series from October 1, 1915 to September 30, 1978; June 13, 2001 to September 30, 2006.
c Period of record used for annual maximum series from October 1, 1915 to September 30, 2007.
d Period of record used for annual maximum series from March 7, 1968 to September 30, 2007.
e Period of record used for annual maximum series from October 1, 1963 to September 30, 2007.
f Period of record used for annual maximum series from October 1, 1939 to September 30, 2007.
g Maximum instantaneous discharge value determined from nearby streamflow-gaging station (08151000 Llano River at Castell, Texas) and indirect estimation methods.

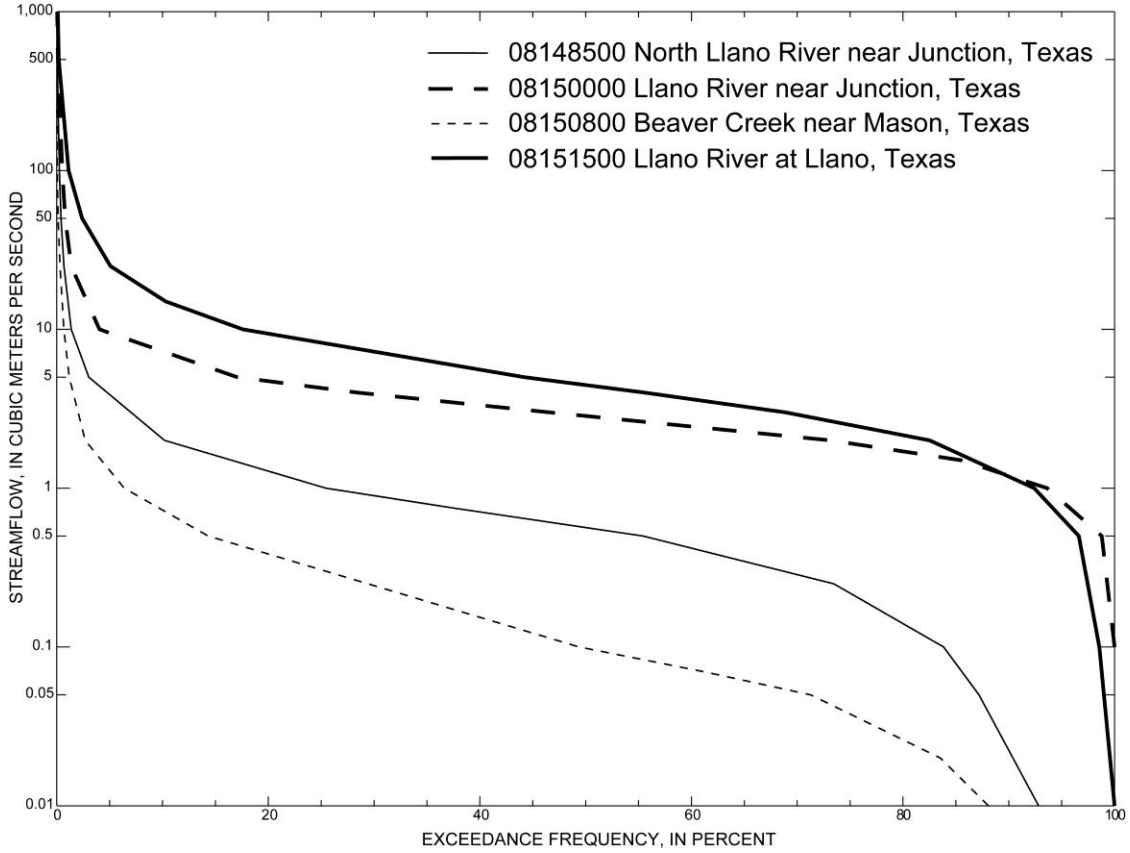

Figure 5.4. Flow-duration curves of daily mean discharge for selected USGS streamflow-gaging stations in the Llano River watershed in Central Texas. The highly variable flow regime is evident from the distribution tails at either end of the exceedance frequency. Zero-flow days are responsible for curves that do not reach 100-percent exceedance frequency.

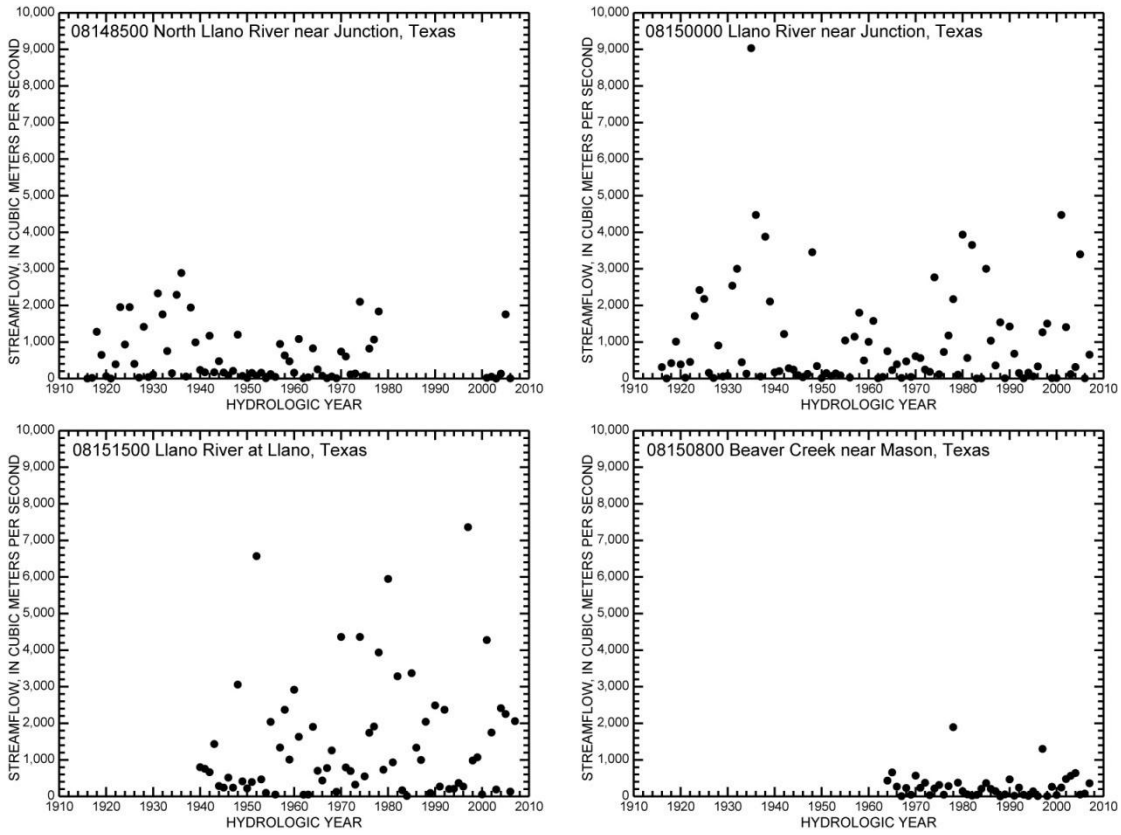

Figure 5.5. Annual maximum instantaneous discharge for selected U.S. Geological Survey streamflow-gaging stations in the Llano River watershed in Central Texas. A peak discharge of 10,760 cubic meters per second in 1935 at 08151500 Llano River at Llano, Texas is not shown.

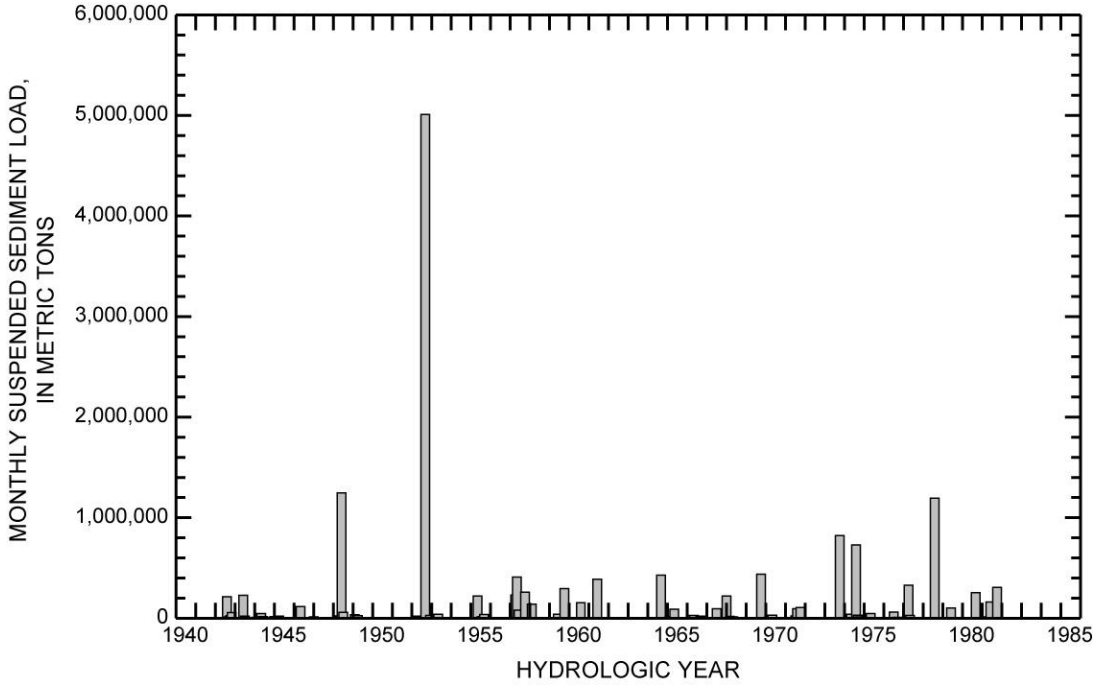

Figure 5.6. Monthly suspended-sediment loads at 08151500 Llano River at Llano, Texas, from August 1942 to September 1982 (data from Stout, Bentz, and Ingram 1961; Adey and Cook 1964; Cook 1967, 1970; Mirabal 1974; Quincy 1988). Suspended sediment transport is episodic with three months of over 1,000,000 metric tons and eighty-five months of less than 100 metric tons.

5.5 Data and Methods

Channel bed (125 samples) and bank (113 samples) sediments were sampled along multiple cross-section transects at nineteen different locations along the Llano River and selected tributaries (Figure 4.1). Sites were selected to represent the progressive increase in drainage area, tributary inputs, and lithologic variability of the watershed (Table 5.2). Multiple bed and bank samples were obtained along each cross-section transect, and were spatially distributed to account for various geomorphic surfaces, including the thalweg, channel bars, banks, and floodplains. Although additional samples of terrace deposits and alluvial-colluvial transitions were obtained, they were not used in analyses for this chapter. Sample locations were geographically referenced using a combination of cross-section survey data, GPS coordinates, and a measuring tape.

Table 5.2. Downstream distance and lithology for study sites in the Llano River watershed in Central Texas. The percentage of area by lithology not accounted for consists of Quaternary deposits.

[km, kilometers; K, Cretaceous; P, Paleozoic; pC, Precambrian; DA, drainage area; km^2, square kilometers; --, not applicable]

Site	Downstream distance (km)	Upstream distance to K-P contact (km)	Upstream distance to P-pC contact (km)	DA (km^2)	% K area	% P area	% pC area
North Llano Draw near Sonora	0.9	--	--	7.8	98.3	0.0	0.0
North Llano River near Roosevelt	56.4	--	--	1,145	94.1	0.0	0.0
North Llano River near Junction	89.2	--	--	2,335	95.2	0.0	0.0
South Llano River at Baker Ranch	29.5	--	--	417	96.8	0.0	0.0
South Llano River at U.S. Highway 377	64.5	--	--	1,134	95.8	0.0	0.0
South Llano River at 700 Springs Ranch	76.3	--	--	1,352	96.2	0.0	0.0
South Llano River State Park	105.2	--	--	2,258	96.9	0.0	0.0
South Llano River at Texas Tech University—Junction	110.1	--	--	2,271	96.7	0.0	0.0
Llano River near Junction	121.4	--	--	4,815	95.7	0.0	0.0
Johnson Fork at Lowlands Crossing	57.5	--	--	778	97.9	0.0	0.0
Llano River near Ivy Chapel	140.2	--	--	5,939	95.7	0.0	0.0
James River near Mason	65.6	32.1	--	877	84.2	13.9	0.0
Llano River at James River Crossing	192.7	40.7	--	8,032	89.2	6.5	0.4
Llano River near Mason	209.5	57.5	6.0	8,418	85.6	8.8	1.9
Beaver Creek near Mason	57.2	31.2	5.7	558	62.0	28.7	3.9
Llano River at Castell	229.7	77.7	26.2	9,429	80.1	10.3	5.9
Llano River at Llano	261.2	109.2	57.7	10,885	70.1	11.3	15.3
Llano River near Kingsland	292.2	140.2	88.7	11,406	66.9	11.4	18.4
Honey Creek at KDK Ranch	11.7	--	--	28.6	0.0	98.2	0.0

Cobble-, pebble-, and gravel-bed material was sampled using a modified Wolman pebble count procedure (Wolman 1954; Elliott 2002; Heitmuller and Asquith 2008). Pebble counts were facilitated by using a sampling grid and particle-size analyzer. The sampling grid measures 50 by 50 centimeters and contains intersections spaced every 10 centimeters, thereby having a total of 25 intersections. The particle directly beneath each intersection was selected and its b-axis, or the short axis along the same dimensional plane as the longest axis, was passed through the smallest possible opening of the particle-size analyzer. The diameter of the analyzer opening was noted for each particle, and cumulative particle-size distribution curves were developed. Subaqueous bed-material samples were obtained using the same modified Wolman method while wading. Additionally, random particles comprising very coarse-grained lenses of bank material were sampled with the size analyzer, but not the sampling grid.

Sand-sized or finer channel-bed and bank sediments were sampled with a scoop and bagged for further analyses. Laboratory analyses of bagged sediment samples included particle size, relative carbonate content, and magnetic susceptibility. Prior to all analyses, samples were dried, pre-weighed, and disaggregated with a pestle and mortar. Pre-treatment for particle-size analyses included further physical disaggregation with a milkshake mixer and chemical disaggregation of the colloidal fraction with a 5-percent concentration of sodium hexametaphosphate ($(NaPO^3)^6$). Particle-size was analyzed by the hydrometer and wet-sieve method (Gee and Bauder 1986; Hudson and

Heitmuller 2003). The analysis data were entered into a pre-formatted spreadsheet and cumulative particle-size distribution curves were developed.

Relative carbonate content (percent) was determined using a modified gravimetric procedure (Goh, St. Arnaud, and Mermut 1993), which involves dissolving a known mass of sediment in a known mass of hydrochloric acid (HCl) (4 mol/liter) - ferrous chloride ($FeCl_2 \cdot 4H_2O$) reagent solution. Two grams of dry, physically disaggregated sediment were gradually added to a pre-weighed beaker containing approximately 20 milliliters of the HCl-ferrous chloride solution. The beakers were weighed after approximately 4 hours, which is a sufficient timespan for the reaction to occur, and the difference in total mass of the combined sediment, solution, and beaker constitutes the mass of dissolved carbonate sediment. Magnetic susceptibility (X) (10^{-8} cubic meters per kilogram) was measured using a Bartington MS-2 instrument. Twenty grams of dry, physically disaggregated sediment were placed in a snap-cap vial and three readings were taken, with the instrument zeroed between each reading. Values were divided by two, as required by the operators' manual, because the instrument is calibrated for 10-gram samples. The average of the three readings was used in the analyses below.

Simple statistical analyses, including particle-size descriptors (e.g., d_{50}, sorting coefficient), were computed in spreadsheets. The sorting coefficient is expressed as $(d_{84}/d_{16})^{1/2}$ for the analyses discussed here and below. More advanced statistical analyses, including correlation coefficients, linear regressions, and LOWESS (LOcally

WEighted Scatterplot Smoothing) trend lines, were done in R (R Development Core Team 2004) (Table 5.3). Linear regression trend lines with very weak statistical relations are only meant to show the general trajectory of the relation, and LOWESS trend lines should be relied upon to explain variability.

Table 5.3. Correlation coefficients for sedimentological relations of composite low-flow-channel, channel-bar, channel-bank, and floodplain deposits in the Llano River watershed in Central Texas. Pearson's r, Spearman's ρ, and Kendall's τ are provided because normality is problematic to determine for the small sample sizes.

[r, Pearson's coefficient; ρ, Spearman's coefficient; τ, Kendall's coefficient; R-squared, R-squared for linear regression; d_{16}, d_{50}, and d_{84}, descriptors that represent diameters at which 16, 50, and 84 percent, respectively, of the sample is finer than; CO^3, carbonate; --, not applicable]

Explanatory variable (x)	Predicted variable (y)	r	ρ	τ	R-squared
Downstream distance	Low-flow-channel d_{16}	-0.124	0.032	0.000	0.015
	Low-flow-channel d_{50}	-0.096	-0.145	-0.091	0.009
	Low-flow-channel d_{84}	-0.040	-0.218	-0.164	0.002
	Channel-bar d_{16}	-0.790**	-0.787**	-0.581**	0.624**
	Channel-bar d_{50}	-0.846**	-0.835**	-0.641**	0.716**
	Channel-bar d_{84}	-0.834**	-0.802**	-0.590**	0.696**
	Basal bank d_{50}	0.657*	0.661*	0.556*	0.432*
	Mid bank d_{50}	0.810**	0.806**	0.689**	0.656**
	Bank top d_{50}	0.823**	0.825**	0.667**	0.677**
	Floodplain d_{50}	0.660	0.571	0.500	0.435
	All bank and floodplain d_{50}	0.790**	0.720**	0.564**	0.624**
Relative CO^3 content (sand)	Magnetic susceptibility (sand)	-0.422**	-0.362**	-0.291**	0.178**
Relative CO^3 content (silt and clay)	Magnetic susceptibility (silt and clay)	-0.547**	-0.496**	-0.366**	0.300**

* Statistically significant at the 95-percent confidence level.
** Statistically significant at the 99-percent confidence level.

5.6 Results

Downstream trends in channel-bed and bank material particle size and sorting are presented for sites along the North Llano River, South Llano River, and Llano River only in order to avoid hydraulic variations and associated sedimentary processes imposed by more steeply-sloping tributary channels. Results of relative carbonate content and magnetic susceptibility analyses, however, are presented for all sites, including tributaries, because sediment composition can be comparatively discussed for all sites in relation to watershed lithology.

5.6.1 Channel-Bed Material

The bed of the Llano River and its tributaries commonly is distinguished by a low-flow channel (thalweg) meandering between various exposed channel bars or bedrock outcrops during normal flow conditions (Figure 5.7). The low-flow channel is usually submerged, except during abnormally protracted dry periods. Longitudinal-bar deposits are usually attached to one of the banks, especially at gradual bends, but also occur as mid-channel bars bounded by two or more low-flow channels at various locations. The results presented for bed material, therefore, are separated into low-flow channels and channel-bars, because constant hydraulic sorting processes in low-flow channels contrast with episodic sorting of bar deposits during high-flow conditions.

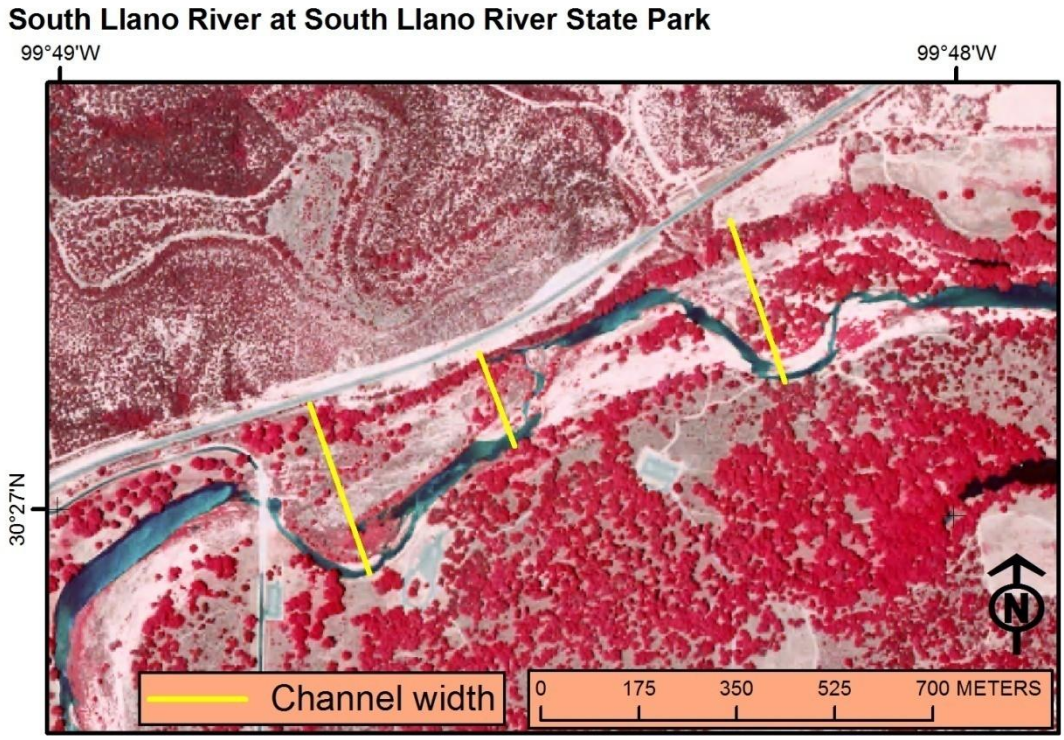

Figure 5.7. 2006 digital orthophoto (2-meter resolution) of the South Llano River at South Llano River State Park near Junction, Texas. Flow direction is from west to east. Note the meandering low-flow-channel and bar deposits set within the larger bankfull channel.

5.6.1.1 Low-Flow Channel (Thalweg)

All low-flow-channel (thalweg) bed material samples are grouped by site, and particle-size descriptors (d_{16}, d_{50}, d_{84}, and sorting coefficient) are computed from the composite distribution. Low-flow-channel (thalweg) deposits of the North Llano, South Llano, and Llano Rivers are characterized by cobbles, pebbles, and gravels (Table 5.4, Figure 5.8), with ranges in median particle size from 25.3 to 60.0 millimeters. Correlation coefficients do not indicate a statistically significant relation between particle size and downstream distance (Table 5.3). Further, a very weak relation (R-squared of 0.01 for d_{50}) of declining particle size with downstream distance is depicted in Figure 5.8. A LOWESS trend line for d_{50} is influenced by relatively small particle sizes (25 to 30 millimeters) between 80 and 150 kilometers downstream, but generally does not support an overall declining or increasing trend in particle size. Sorting coefficients range from 1.39 to 2.50, indicating relatively well-sorted material. One outlier site, Llano River at Castell, was not included in the statistical analyses because it displayed only sand-sized material. Furthermore, the site did not have a distinct low-flow channel (thalweg), but instead was characterized by shallow threads of flow, bedrock outcrops, and limited bar deposits. A low-height road crossing located immediately upstream of this site possibly promotes deposition of coarse bed material upstream of the structure, resulting in minimal cobble-, pebble-, and gravel-sized material downstream.

Table 5.4. Particle-size data for composite samples of low-flow-channel (thalweg) deposits along the North Llano, South Llano, and Llano Rivers in Central Texas.

[km, kilometers; d_{16}, d_{50}, and d_{84}, descriptors that represent diameters at which 16, 50, and 84 percent, respectively, of the sample is finer than; mm, millimeters; Sort, sorting coefficient]

Site	Downstream distance (km)	Number of samples[a]	d_{16} (mm)	d_{50} (mm)	d_{84} (mm)	Sort
North Llano River near Junction	89.2	10	13.4	25.6	46.5	1.86
South Llano River at Baker Ranch	29.5	2	20.0	39.2	74.4	1.93
South Llano River at 700 Springs Ranch	76.3	1	46.6	60.0	90.0	1.39
South Llano River State Park	105.2	8	17.5	34.0	63.5	1.90
South Llano River at Texas Tech University—Junction	110.1	7	10.1	25.9	55.7	2.34
Llano River near Junction	121.4	3	11.0	27.0	68.7	2.50
Llano River near Ivy Chapel	140.2	2	11.0	25.3	41.1	1.93
Llano River at James River Crossing	192.7	6	22.6	35.3	63.9	1.68
Llano River near Mason	209.5	5	25.4	52.8	112.4	2.10
Llano River at Llano	261.2	2	20.7	32.0	61.9	1.73
Llano River near Kingsland	292.2	2	14.1	30.8	52.1	1.92

a Number of samples for cobble- and gravel-sized material is equated to an individual placement of the sampling grid (or approximately 25 individual clasts).

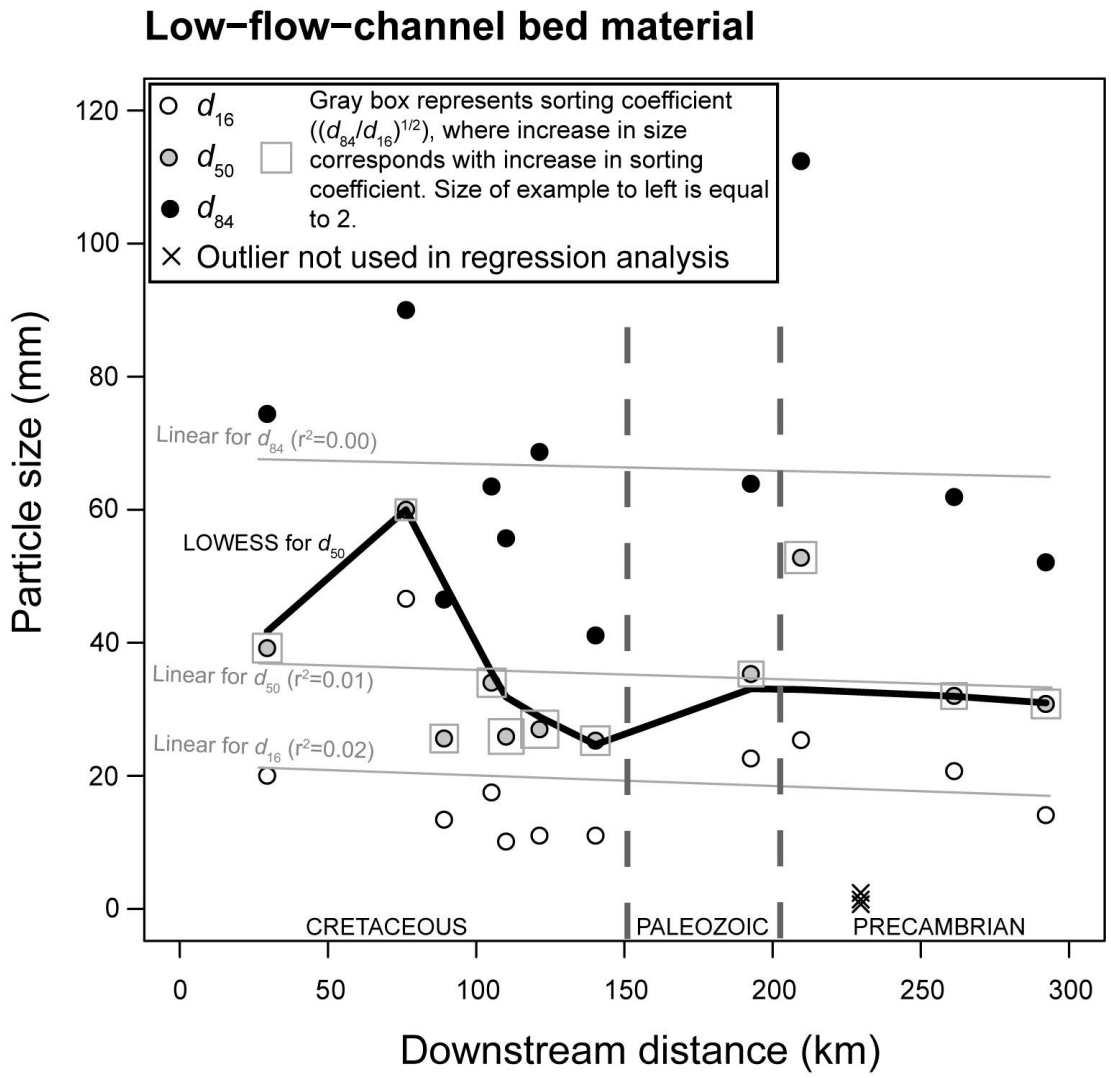

Figure 5.8. Linear regression and LOWESS trend line (smoothing factor of 0.6) of particle size (d_{16}, d_{50}, and d_{84}) with downstream distance for low-flow-channel bed material of the South Llano, North Llano, and Llano Rivers in Central Texas. One outlier at Llano River at Castell is not included in the statistical analyses.

5.6.1.2 Channel Bars

All channel-bar samples are grouped by site and particle-size descriptors are computed from the composite distribution. Channel-bar deposits are characterized by cobble-, pebble-, and gravel-sized material upstream of an abrupt gravel-to-sand transition zone between Mason and Castell, which is 6 to 26 kilometers downstream of the Paleozoic-Precambrian contact (Table 5.5, Figure 5.9). Correlation coefficients indicate a statistically significant (99-percent confidence level) negative relation between particle size and downstream distance (Table 5.3). Further, a similarly significant trend (R-squared of 0.72 for d_{50}) of declining particle size with downstream distance is depicted in Figure 4.10. A LOWESS trend line for d_{50} closely follows the linear regression, but is influenced by an abrupt transition from medium-sized pebbles (d_{50} greater than 35 millimeters) in the uppermost reaches of the North and South Llano Rivers to smaller pebbles and gravels near Junction (d_{50} approximately 15 to 25 millimeters). Sorting coefficients range from 1.53 to 2.40, indicating relatively well-sorted material. One outlier site, South Llano River at Baker Ranch near Rocksprings, was not included in the statistical analyses. Unlike all other locations sampled, the channel at Baker Ranch was filled with fine-grained (d_{50} of 0.039 millimeters) sediment, which could be interpreted as a filling phase of a cyclical cut-and-fill type of channel near the top of the Edwards Plateau.

Table 5.5. Particle-size data for composite samples of channel-bar deposits along the North Llano, South Llano, and Llano Rivers in Central Texas.

[km, kilometers; d_{16}, d_{50}, and d_{84}, descriptors that represent diameters at which 16, 50, and 84 percent, respectively, of the sample is finer than; mm, millimeters; Sort, sorting coefficient]

Site	Downstream distance (km)	Number of samples[a]	d_{16} (mm)	d_{50} (mm)	d_{84} (mm)	Sort
North Llano River near Roosevelt	56.4	8	21.2	36.6	60.5	1.69
North Llano River near Junction	89.2	6	7.4	18.0	42.4	2.40
South Llano River at Baker Ranch	29.5	2	0.0	0.0	1.8	53.2
South Llano River at U.S. Highway 377	64.5	1	27.3	42.2	64.0	1.53
South Llano River at 700 Springs Ranch	76.3	7	24.2	44.9	75.7	1.77
South Llano River State Park	105.2	11	10.1	25.5	52.4	2.27
South Llano River at Texas Tech University—Junction	110.1	5	10.6	21.8	47.7	2.12
Llano River near Junction	121.4	11	7.8	16.3	39.4	2.25
Llano River near Ivy Chapel	140.2	6	11.5	23.7	53.4	2.16
Llano River at James River Crossing	192.7	6	14.6	28.0	60.2	2.03
Llano River near Mason	209.5	5	7.4	14.2	41.5	2.37
Llano River at Castell	229.7	2	0.9	2.1	3.4	1.93
Llano River at Llano	261.2	3	0.2	0.5	0.8	2.04
Llano River near Kingsland	292.2	4	0.3	0.6	1.7	2.27

a Number of samples for cobble- and gravel-sized material is equated to an individual placement of the sampling grid (or approximately 25 individual clasts).

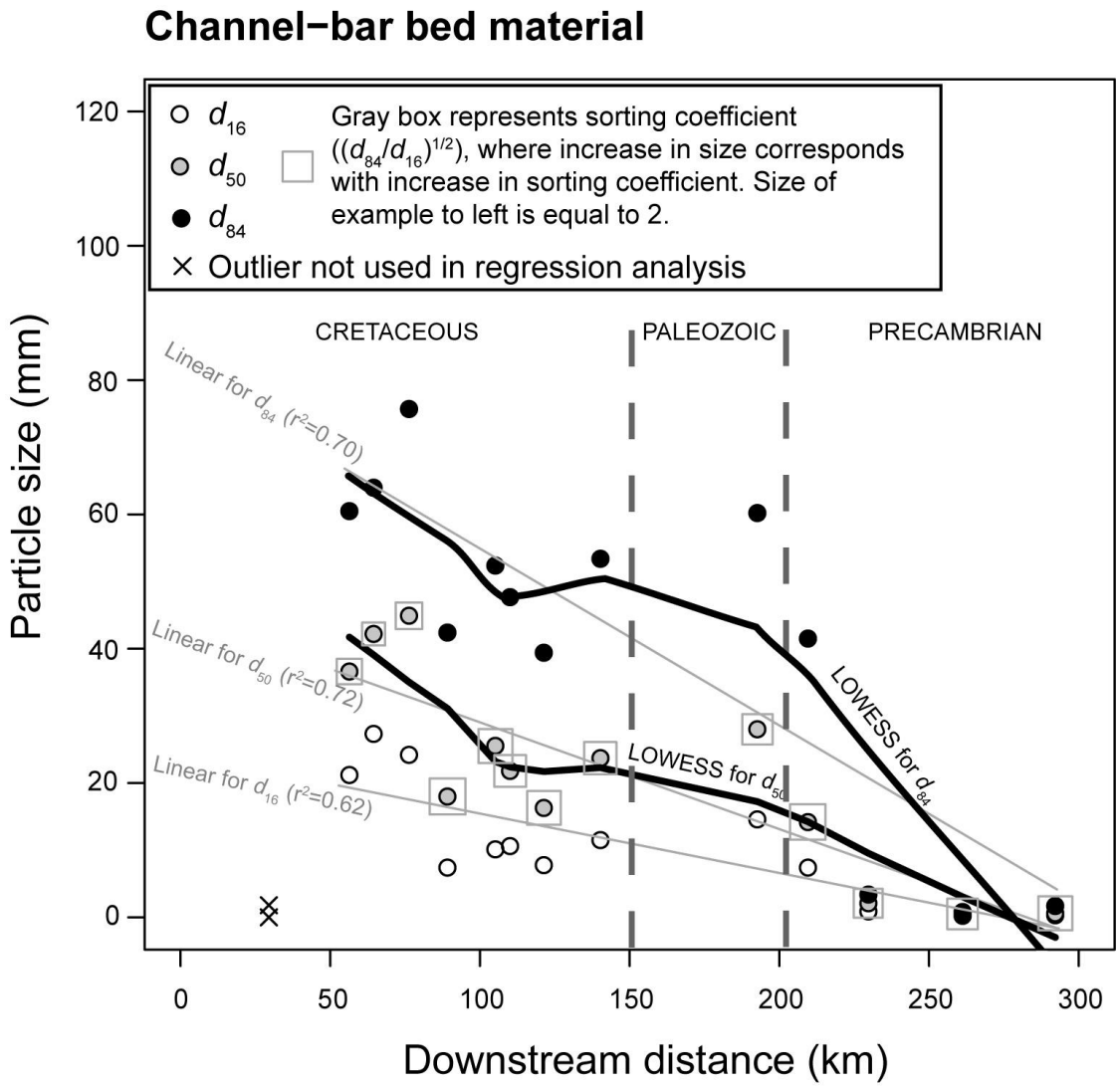

Figure 5.9. Linear regression and LOWESS trend lines (smoothing factor of 0.6) of particle size (d_{16}, d_{50}, and d_{84}) with downstream distance for channel-bar bed material of the South Llano, North Llano, and Llano Rivers in Central Texas. One outlier at South Llano River at Baker Ranch near Rocksprings is not included in the statistical analyses.

5.6.2 Channel-Bank and Floodplain Material

A variety of channel-bank morphologies exist in the Llano River watershed, including erosional and depositional forms. Active floodplain deposits mostly are limited to wider alluvial valleys near Junction, and become progressively limited as valley confinement increases downstream.

For downstream analyses, efforts were made to include only samples that represent fluvial depositional processes, not colluvial or mass wasting processes, and field notes by the author are heavily relied upon for guidance. Further, terrace deposits associated with previous hydrologic and sedimentary regimes, which are identified by their height above the channel and degree of calcite cementation, are not included in downstream analyses. Additionally, localized cobble- to gravel-sized lenses embedded within fine-grained banks (Figure 5.10) are not accounted for in the analyses below, although such bank deposits can account for a considerable proportion of bank material at localities near Junction.

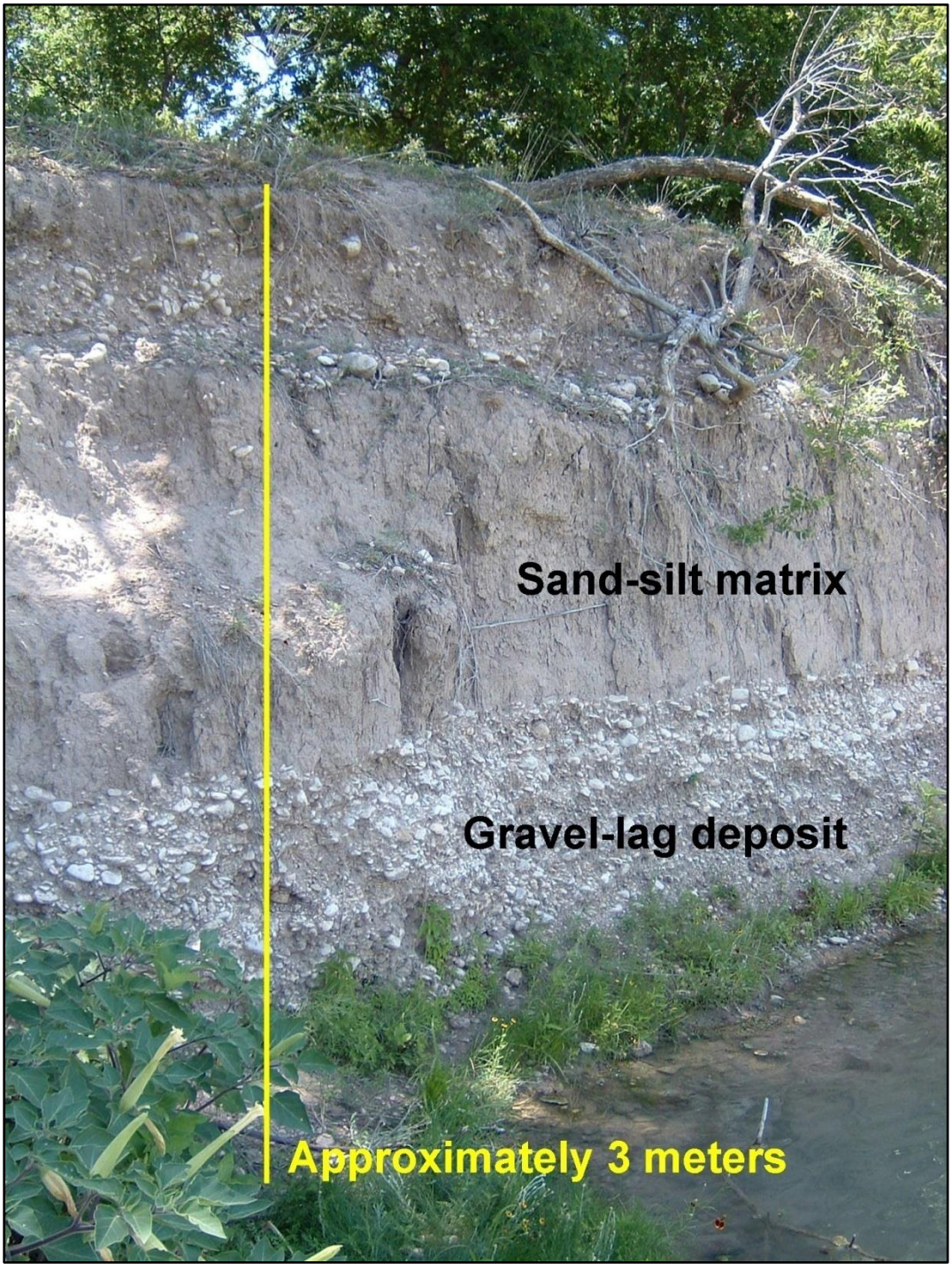

Figure 5.10. Right bank (height approximately 3 meters) of South Llano River at Texas Tech University—Junction, Texas. Note the gravel-lag deposits occurring within a fine-grained matrix at the base.

5.6.2.1 Particle Size

For particle-size analyses, all channel-bank and floodplain samples are grouped by site, and descriptors are computed from the composite distribution. Figure 5.11 shows linear relations of particle size (d_{50}) and downstream distance separately for basal bank, mid-bank, bank-top, and floodplain material. For all types of material, particle size (d_{50}) ranges from about 0.025 to 0.20 millimeters. Correlation coefficients show statistically significant relations (95-percent and 99-percent confidence intervals) of increasing particle size for the three categories of bank deposits, but not for floodplain deposits as a result of a smaller sample size (Table 5.3). Floodplain deposits, however, follow a similarly increasing trend with downstream distance. Although bank-top material generally is slightly finer than lower bank material, the proximity of the linear relations indicates that basal bank, mid-bank, bank-top, and floodplain material could be effectively grouped to investigate downstream trends in particle size. Paired-t tests (assuming normality) and the matched-pairs Wilcoxon signed rank test (distribution free) were used to compare the difference of means among basal bank, mid-bank, bank-top, and floodplain material, and no statistically significant relations were computed. For this reason, composite samples of aggregated bank and floodplain material by site are analyzed for downstream trends below.

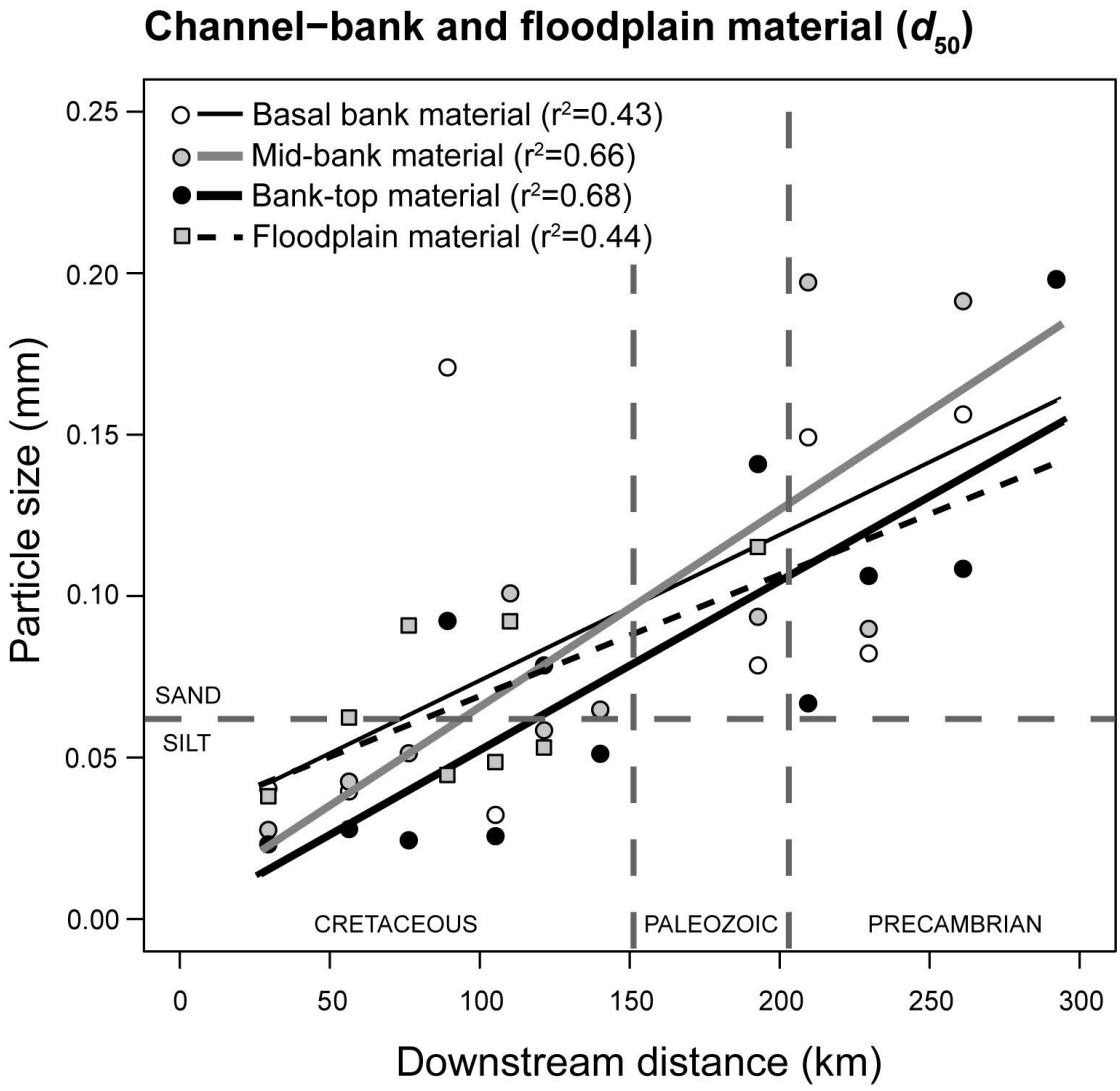

Figure 5.11. Linear regression of median particle size (d_{50}) with downstream distance for basal bank, mid-bank, bank-top, and floodplain deposits of the South Llano, North Llano, and Llano Rivers in Central Texas.

For aggregated bank and floodplain material, particle size (d_{50}) ranges from about 0.03 to 0.20 millimeters (Table 5.6). Correlation coefficients indicate a statistically significant (99-percent confidence level) positive relation between particle-size (d_{50}) of aggregated bank and floodplain material and downstream distance (Table 5.3). A similarly significant trend (R-squared of 0.62 for d_{50}) of increasing particle size with downstream distance is depicted in Figure 5.12. A LOWESS trend line for d_{50} closely follows the linear regression, but is influenced by variability at sites along the North Llano, South Llano, and Llano Rivers near Junction. Sorting coefficients range from 3.62 to 12.67, indicating a wide range of well- to poorly-sorted fine-grained material. The most poorly sorted material generally occurs along reaches near Junction, and sorting coefficients are notably high along the Llano River downstream of Junction and upstream of the Paleozoic-Precambrian contact.

Table 5.6. Particle-size, carbonate content, and magnetic susceptibility data for composite samples of channel-bank and floodplain deposits along the North Llano, South Llano, and Llano Rivers in Central Texas.

[km, kilometers; d_{50}, descriptor that represents diameter at which 50 percent of the sample is finer than; mm, millimeters; Sort, sorting coefficient; CO^3, relative carbonate content; %, percent; X, magnetic susceptibility (10^{-8} cubic meters/kilogram)]

Site	Downstream distance (km)	Number of samples	d_{50} (mm)	Sort	CO^3 (%)	X
North Llano River near Roosevelt	56.4	10	0.044	5.15	39.1	46
North Llano River near Junction	89.2	8	0.110	8.87	53.7	17
South Llano River at Baker Ranch	29.5	5	0.033	4.90	25.2	60
South Llano River at 700 Springs Ranch	76.3	7	0.076	4.84	39.8	44
South Llano River State Park	105.2	18	0.039	9.18	50.9	33
South Llano River at Texas Tech University—Junction	110.1	16	0.127	10.07	54.8	20
Llano River near Junction	121.4	7	0.066	11.40	48.0	22
Llano River near Ivy Chapel	140.2	9	0.062	12.67	48.5	20
Llano River at James River Crossing	192.7	7	0.104	12.16	38.1	19
Llano River near Mason	209.5	7	0.160	3.81	34.3	29
Llano River at Castell	229.7	9	0.090	6.83	30.1	55
Llano River at Llano	261.2	7	0.146	3.62	27.9	54
Llano River near Kingsland	292.2	3	0.198	3.74	23.8	80

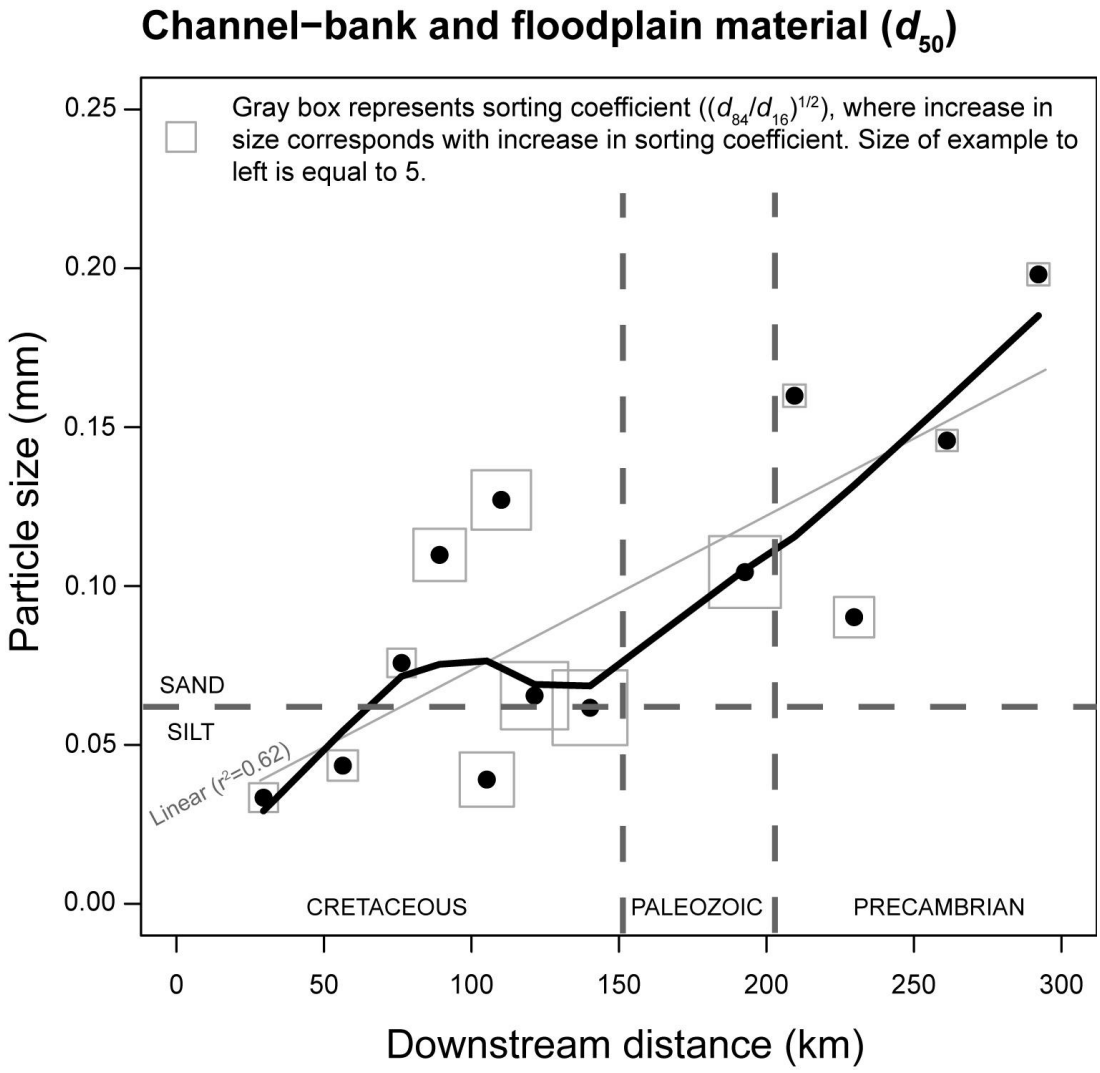

Figure 5.12. Linear regression and LOWESS trend line (smoothing factor of 0.6) of median particle size (d_{50}) with downstream distance for aggregated bank and floodplain material of the South Llano, North Llano, and Llano Rivers in Central Texas.

5.6.2.2 Carbonate Content and Magnetic Susceptibility

For downstream analyses, carbonate (mostly $CaCO_3$) and magnetic susceptibility (X) samples are grouped by site and mean values are computed from the composite distribution. Relative carbonate content ranges from 23.8 to 54.8 percent (Table 5.6), with highest percentages along reaches near Junction. A LOWESS trend line shows an increasing relation of carbonate with downstream distance along reaches in the Cretaceous zone of the watershed, but an initial decrease downstream of Junction is followed by a more pronounced decrease downstream of the Cretaceous-Paleozoic contact (Figure 5.13). A LOWESS trend line of magnetic susceptibility (X) with downstream distance shows a trend opposite of carbonate (Figure 5.14), where values decrease along reaches in the Cretaceous zone of the watershed and increase downstream of the Paleozoic-Precambrian contact. It should be noted that magnetic susceptibility does not initially decrease downstream of Junction or the Cretaceous-Paleozoic contact, which is out-of-phase with the inverse trend of carbonate content.

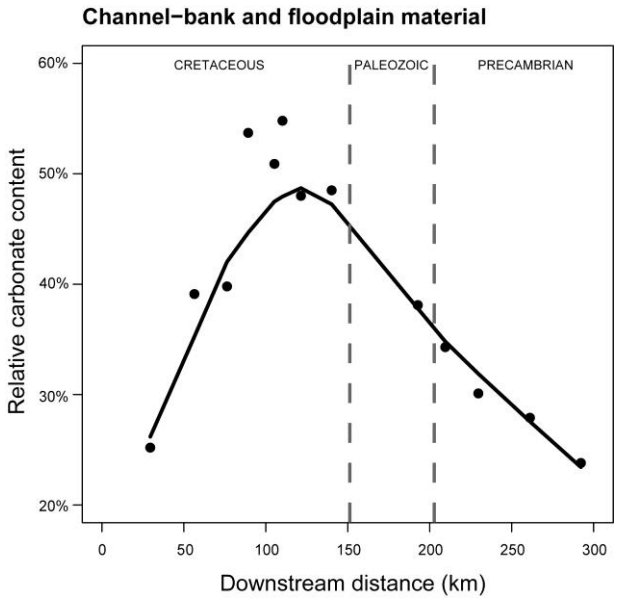

Figure 5.13. LOWESS trend line (smoothing factor of 0.6) of relative carbonate content (percent) with downstream distance for aggregated bank and floodplain material of the South Llano, North Llano, and Llano Rivers in Central Texas.

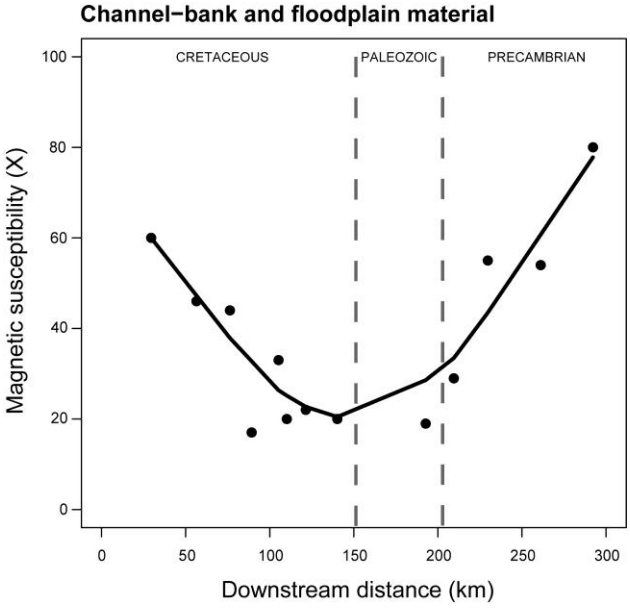

Figure 5.14. LOWESS trend line (smoothing factor of 0.6) of magnetic susceptibility (X) with downstream distance for aggregated bank and floodplain material of the South Llano, North Llano, and Llano Rivers in Central Texas.

Additionally, carbonate content and magnetic susceptibility (X) samples are analyzed individually, as opposed to composite samples by site. Correlation coefficients indicate a statistically significant (99-percent significance level) negative association between carbonate content and magnetic susceptibility (Table 5.3). Further, similarly significant linear trend lines for sand- (R-squared of 0.18) and silt-clay-sized (R-squared of 0.30) sediment show that magnetic susceptibility generally decreases with increasing carbonate content (Figure 5.15). For a given carbonate content, magnetic susceptibility generally is higher for silt-clay-sized sediment than sand. LOWESS trend lines for sand- and silt-clay-sized sediment show a convergence of the trends between a carbonate content range of 35 percent to 40 percent. Additionally, Figure 5.15 shows that samples obtained in the Precambrian zone of the watershed are characterized by the lowest carbonate content and greatest range of magnetic susceptibility. One outlier sample (X = 306) was identified using diagnostic statistics, including Cook's distance (< 1) and a probability plot, and was not included in the statistical analyses.

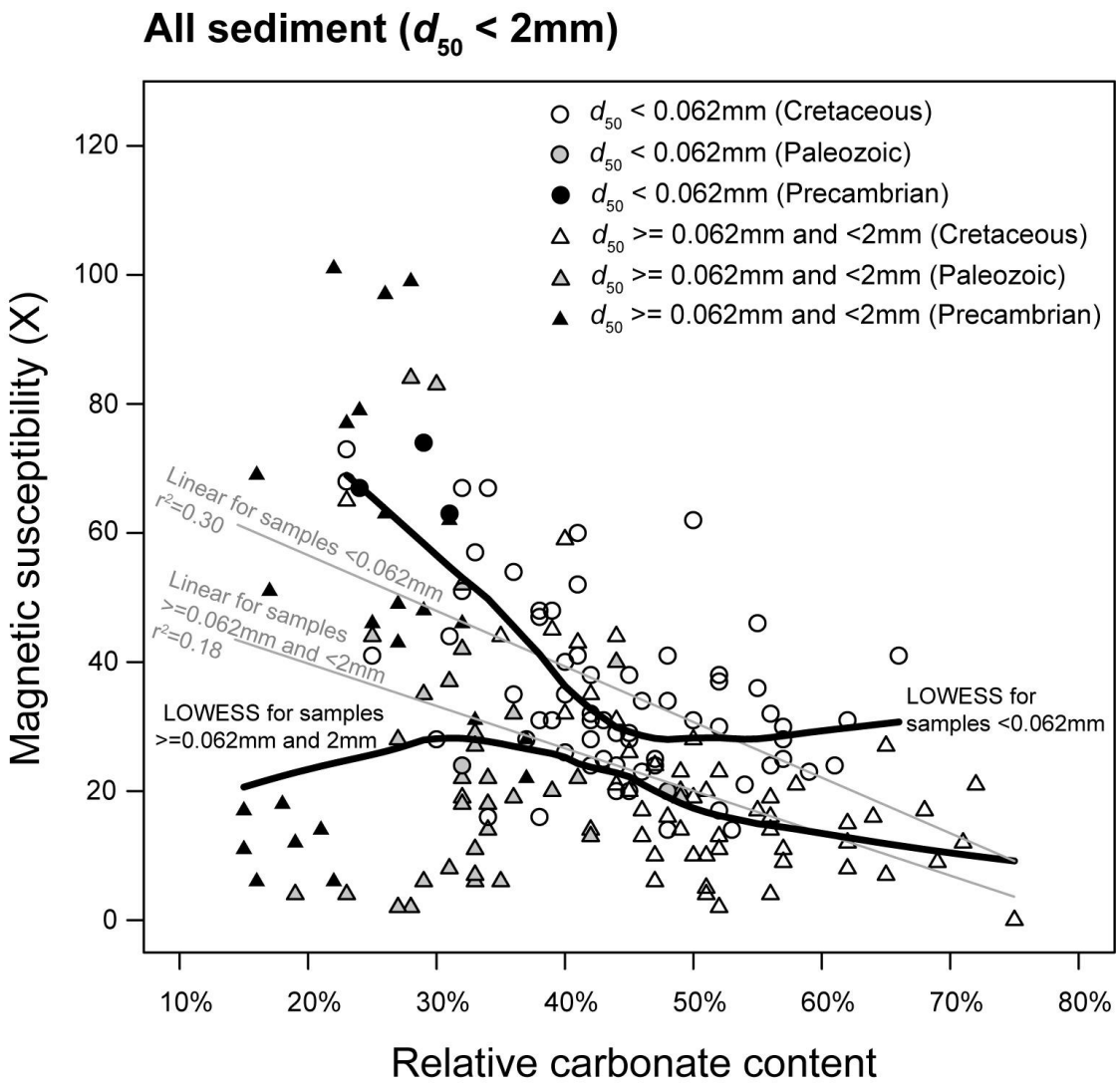

Figure 5.15. Linear regression and LOWESS trend line (smoothing factor of 0.6) of magnetic susceptibility (X) and carbonate content (percent) for individual samples of bank and floodplain material (d_{50} < 2 millimeters) in the Llano River watershed in Central Texas.

5.7 Discussion

The size and composition of channel-bed, bar, and bank deposits in the Llano River watershed are generally determined by abrupt lithologic transitions. Superimposed on those lithologic controls, however, are influential hydrologic and localized hydraulic controls that explain variations in observed downstream trends in particle size. Further, downstream trends of different geomorphic units are unique, and the discussion below is directed at interpreting causes for contrasting observations. A supportive graphical summary of downstream changes in alluvial composition is provided in Figure 5.16.

5.7.1 Channel-Bed Material Particle Size

The Llano River valley becomes increasingly confined by bedrock with distance downstream of the Cretaceous-Paleozoic contact (Figure 5.1). Although it is often assumed that ubiquitous exposures of bedrock to the river channel should result in relatively coarse bed material (Tinkler and Wohl 1998), channel-bar material of the Llano River decreases in size with distance downstream (Table 5.5, Figure 5.9), especially downstream of the Paleozoic-Precambrian contact. This trend is attributed to the different in-situ weathering mechanisms of carbonate and igneous lithologies. A considerable proportion of Cretaceous and Paleozoic carbonate rocks in the upper and middle watershed are removed in large slabs or clasts (Wende 1999) from steep slopes of contributing drainages or valley walls, whereas in-situ weathering of Precambrian granitic material into grus in the lower watershed results in considerable quantities of

sand-sized material that is delivered to contributing drainages. Furthermore, the supply of sand-sized material in the lower watershed is sufficient enough to form channel deposits despite increased flood stream power resulting from valley confinement (Magilligan 1992), which would normally be associated with selective entrainment and relatively coarse material.

Downstream trends of declining bed-material size are much more evident for channel-bar deposits than low-flow-channel (thalweg) deposits (Table 5.4, Figure 5.8) in the Llano River watershed, indicating that stronger hydraulic sorting mechanisms occur along channel bars. Hydraulic forces in the thalweg alternate from uniform during low-flow conditions to highly turbulent during high-flow conditions, and hydraulic irregularity is further promoted by localized configuration of the channel, including meander bends (Clayton and Pitlick 2007). In commenting on observed downstream decreases in particle size of channel bars, Bluck (1987) claims that turbulent conditions selectively entrain particles and promote downstream fining, lending support to observations along the Llano River.

5.7.1.1 Gravel-to-Sand Transition

A gravel-to-sand transition between Mason and Castell is only evident when examining channel-bar deposits (Table 5.5, Figure 5.9). The transition is evident because sand is the final particle size to be deposited on the receding limb of a flow event and, therefore, is represented in surface samples of bed material. It also is possible that perennial flow in the low-flow-channel entrains and transports sand-sized material

to preferential locations, such as relatively deep and slow pools. Sambrook Smith and Ferguson (1995) discuss irregularity in downstream gravel-to-sand transitions related to pool-riffle morphology, but do not specifically distinguish between bars and thalweg deposits. Irrespective of the hydraulic mechanisms responsible for the observed trends, an argument can be made that channel-bar deposits are more representative than thalweg deposits for observing downstream trends in bed-material particle size of perennial rivers with highly variable flow regimes. It is unknown if similar discrepancies in downstream particle-size trends are applicable to intermittent or ephemeral rivers.

The abrupt gravel-to-sand transition between Mason and Castell is explained by two independent factors: (1) distance from upstream sources of gravel-sized material and (2) additions of sand by tributaries draining Precambrian igneous and metamorphic lithologies. First, tributaries that supply gravel to the Llano River are markedly less common downstream of the Cretaceous-Paleozoic contact. A considerable amount of gravel comes from the James River, but its influence rapidly diminishes downstream of the Llano River near Mason. Second, inputs of sand-sized sediment become immediately influential downstream of the Paleozoic-Precambrian contact. The sand-dominated site at Castell occurs only 26.2 kilometers downstream of the contact and the Precambrian part of its drainage area is approximately 680 square kilometers, or 5.9 percent of total watershed area. Sambrook Smith and Ferguson (1995) list lateral inputs of sand as a mechanism for gravel-to-sand transitions, but argue that slope-dependent

hydraulic processes are more common. For the Llano River, however, the straight longitudinal profile nullifies channel slope as an explanation for the gravel-to-sand transition.

5.7.1.2 Coarse-to-Fine Gravel-Bed Transition

Abrupt gravel-to-sand transitions of bed material are observed in many river systems (Sambrook Smith and Ferguson 1995), but few studies have identified abrupt particle-size decreases in gravel-bed channels. Channel-bar deposits of the North and South Llano Rivers abruptly transition from medium-sized pebbles to small pebbles and gravels near Junction (Table 5.5, Figure 5.9). The transition reaches occur between 75 to 90 kilometers downstream of the uppermost draws with a drainage area increase from about 1,350 to 2,250 square kilometers. The decrease in particle size is not explained by an increase in sediment volume (Bluck 1987), because additional sediment from the smaller, steeper adjoining watersheds is presumably coarser. The abrupt particle-size decrease, therefore, is probably explained by increased magnitudes and frequencies of high-flow events capable of transporting and abrading cobble- to gravel-sized material. More frequent opportunities for high flows are expected because of the combined possibilities for both localized rainfall events from various tributaries and widespread regional floods. These findings contrast with many investigations that document a localized increase in bed material size associated with tributary inputs (Knighton 1980; Ichim and Radoane 1990; Rice and Church 1998). This contrast suggests that downstream trends in particle size of gravel-bed rivers with highly variable flow

regimes could be more dependent on the frequency of entrainment and transport rather than distance-dependent abrasion and sorting processes.

5.7.2 Channel-Bed and Bank Particle-Size Comparison

Contrasting downstream trends of simultaneously decreasing bed- and increasing bank-material particle size (Table 5.6; Figures 5.11, 5.12) characterize fluvial deposits of the North Llano, South Llano, and Llano Rivers. Reaches in the upper Cretaceous zone of the watershed have channel beds comprised of cobble- to gravel-sized material and banks comprised of silt, clay, and limited amounts of fine sand. In upland areas, Cretaceous carbonate weathers to a dark, silt- and clay-rich soil, and it is from this material that fine-grained banks and floodplains are derived. Relatively poorly-sorted bank and floodplain material along river reaches near Junction indicate that appreciable quantities of sand are included in the silt-clay matrix. Much of the sand likely is derived from incision into the lowermost Cretaceous unit of the Hensell Sand. Abrasion processes of channel-bed material also contribute to the sand-sized fraction. Relatively coarse bed material in the upper reaches of the watershed originates as plucked (Hancock, Anderson, and Whipple 1998; Wende 1999) or gravity-supplied material from steep slopes and tributaries. As gravel-sized material becomes less available downstream of the James River, the increasing influence of Precambrian-derived sand is detected by the convergence of particle size in both channel-bar and channel-bank deposits.

5.7.3 Carbonate Content and Magnetic Susceptibility

Downstream trends of relative carbonate content (percent) and magnetic susceptibility (X) are inversely related in channel bank and floodplain deposits (Table 5.6; Figures 5.13, 5.14). In the uppermost reaches of the North and South Llano Rivers, the Cretaceous-aged Edwards Limestone contains substantial quantities of siliceous chert, which keeps carbonate content of fluvial deposits below 40 percent. As the river channels incise into the more pure limestone and dolomite of the Glen Rose Formation, carbonate content increases to over 50 percent near Junction. Continuing downstream, inputs from various Paleozoic sedimentary rocks and finally Precambrian igneous and metamorphic rocks reduce carbonate content below 25 percent near watershed outlet. The inverse trend of magnetic susceptibility indicates its association with carbonate content, although it does not display any sensitivity to Paleozoic sedimentary rocks. Further, magnetic susceptibility is largely dependent on particle size (Figure 5.15), such that relatively coarse material will have a higher value than finer material for a given mineralogy. It is therefore noteworthy to mention that magnetic susceptibility peaks near Kingsland (292.2 kilometers downstream), where the particle-size of channel-bank and floodplain material is the coarsest in the watershed. This indicates that Precambrian mineralogy exerts a strong influence on magnetic susceptibility and also illustrates the increasingly dominant supply of Precambrian sands to alluvial deposits in the lower watershed.

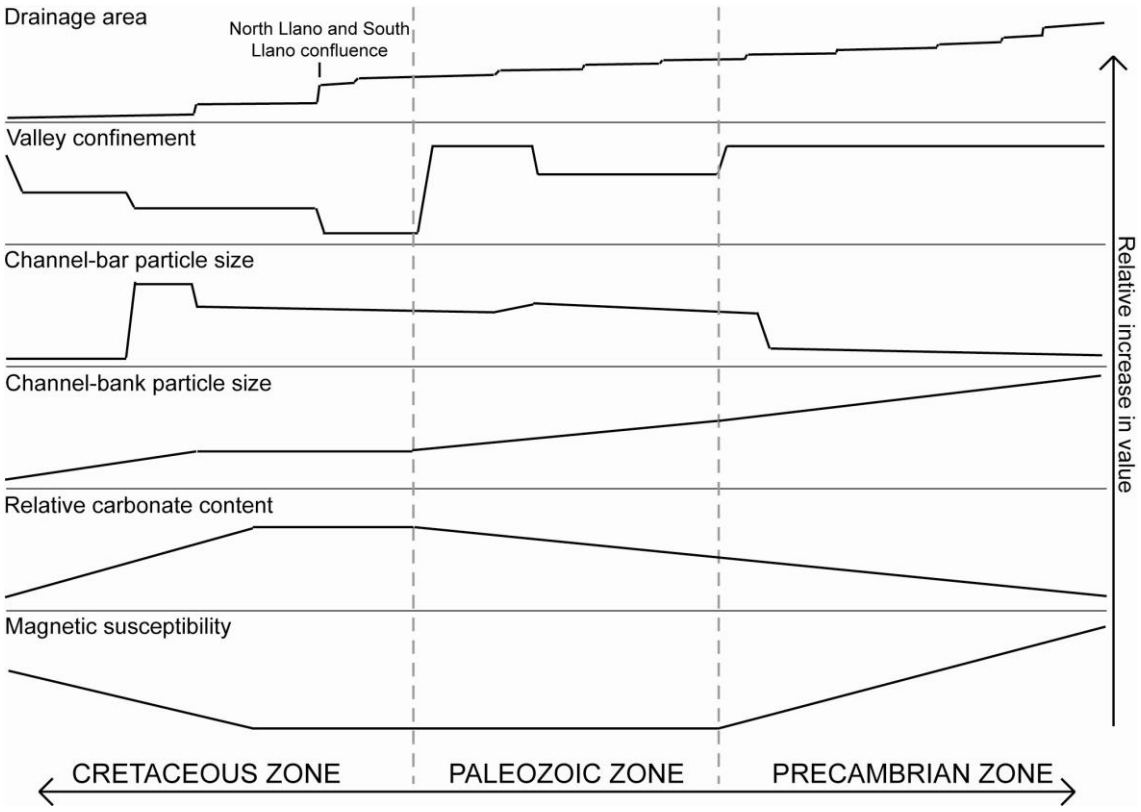

Figure 5.16. A summary of downstream changes in alluvial sediment composition along the North Llano, South Llano, and Llano Rivers in Central Texas. As drainage area and valley confinement generally increase with distance downstream, channel-bed particle size decreases and bank-material particle size increases. Relative carbonate content and magnetic susceptibility are inversely related and are controlled by lithology.

5.8 Conclusions

The Llano River watershed of Central Texas, USA, is characterized by a highly variable flow regime, episodic sediment transport, and abrupt geologic transitions. As a result, downstream characteristics of alluvial deposits in the Llano River watershed differ from fluvial systems in humid environments or with homogeneous lithologies. Hydraulic variations that occur along a continuum ranging from low-flow conditions to severe floods are responsible for abrupt downstream reductions in gravel-bed particle size, and detectable trends of particle-size reduction for channel bars but not for the low-flow-channel (thalweg). Although floods greatly influence fluvial processes and channel geometry in the watershed, surface geology and associated sedimentary composition effectively explain downstream fluvial diversity. Weathering mechanisms in the upper Cretaceous carbonate zone of the watershed result in relatively fine-grained (silt, clay, and some fine sand) channel banks and cobble- to gravel-sized channel beds along the North, South, and upper Llano Rivers. The alluvial valley becomes constricted by resistant bedrock as the river transitions downstream to Paleozoic sedimentary and Precambrian igneous and metamorphic zones. Precambrian rocks are weathered to grus in-situ, and considerable quantities of sand-sized material are delivered to the drainage network. Channel banks of the Llano River are increasingly composed of the sand-sized fraction and less carbonate material in the downstream direction. Further, an abrupt gravel-to-sand transition of the channel bed, not associated

with hydraulic mechanisms, occurs just downstream of the Paleozoic-Precambrian contact and is attributed to a limited gravel supply and increasing supply of sand.

Results of this study are expected to improve the understanding of downstream trends in the composition of alluvial deposits along rivers with highly variable flow regimes. Further, the Llano River watershed provides an example where pronounced geologic and sedimentary controls complement flood hydraulics to explain downstream trends in alluvial composition. Scientists, engineers, and practitioners involved with floodplain and watershed management, aquatic biology, infrastructure development, and riparian restoration efforts along river systems similar to the Llano River should benefit from this investigation.

Chapter 6. Mutual Adjustment of Pattern and Shape of Bankfull- and Macro-Channels in the Llano River Watershed, Central Texas, USA: The Combined Roles of Intense Flooding and Abrupt Transitions in Lithology

6.1 Abstract

Downstream adjustment of river channel geometry is a hallmark of geographically-driven research in fluvial geomorphology. Although numerous investigations focus on adjustment of either pattern (planform), shape (cross section), or profile (slope), few have been designed to address downstream mutual adjustment of those dimensions. Further, systematic investigations are needed along fluvial systems with highly variable flow regimes to clarify the conceptual understanding of dominant (channel-forming) discharge. Other complexities, including abrupt discontinuities in lithology and sedimentology, introduce variability into current models of channel development. The Llano River watershed (11,568 square kilometers) in Central Texas, USA, is a complex fluvial system as a result of its highly variable, flood-prone flow regime and abrupt transitions in surface lithology. The unregulated, rural watershed represents an opportunity to examine downstream channel adjustment of pattern, shape, and profile, in a unique setting.

The study design included field, laboratory, GIS, and statistical analysis to characterize watershed parameters (surface lithology, drainage area), channel geometry, flood hydraulics and hydrology, and sedimentology along the Llano River and key

tributaries. Twenty-one sites, extending across the entire drainage system, were used to quantify these measures, and seven additional sites were added specifically for flow-resistance analyses. Analysis of hydrology, planform morphology, lithology, and alluvial development reveals four general categories of channel classification, listed in order from upstream to downstream: (1) uppermost ephemeral reaches, commonly referred to as "draws" in the study area, (2) Cretaceous straight or sinuous gravel-bed channels, (3) Paleozoic straight or sinuous gravel-bed or bedrock channels, and (4) Precambrian straight, braided, or bedrock-braided sand-bed channels. Based on hydraulic geometry techniques, bankfull channels in the Cretaceous zone compensate for discharge by increasing width at a greater rate than mean depth. Proceeding downstream, mean depth outpaces width in compensating for flows up to bankfull stage despite observed decreases in silt-clay content and lack of cohesion in the channel banks. The increasingly important role of mean depth is attributed to downstream confinement of the alluvial valley, and the reduced potential for channel enlargement by increases in width. Macro-channels, above bankfull stage, form downstream of the confluence of the North Llano and South Llano Rivers. Macro-channels always compensate for discharge by increasing mean depth at a greater rate than width, and the downstream convergence of width-depth relations for bankfull- and macro-channels indicates that the general slope of sub-bankfull, bank-attached deposits in the Precambrian zone closely follows that of higher alluvial deposits and the surrounding bedrock. Finally, bankfull conditions typically have return periods between 1 and 2

years, and macro-channels are maintained by flows with return periods ranging from about 10 to 40 years. Greater macro-channel return periods are associated with sites furthest downstream. Going downstream, the gradual masking of morphologic indicators associated with bankfull stage parallels the reduced frequency of formative flows for macro-channels, indicating that high-magnitude floods play an increasingly important role in channel adjustment.

6.2 Introduction

River channel adjustment to hydraulic and sedimentary controls is a topic that has received considerable attention by fluvial geomorphologists (e.g., Leopold and Wolman 1957; Schumm 1960; Schumm 1985; Ferguson 1987) and is of practical importance to engineers, aquatic biologists, water resource managers, and other riparian specialists. River morphology is expressed in three-dimensional space, including the planform (pattern), cross-sectional (shape), and longitudinal (profile) perspectives. The most relied upon hydraulic index of channel adjustment is bankfull discharge (cubic meters per second) (e.g., Dunne and Leopold 1978; Rosgen 1994; Castro and Jackson 2001), which commonly is related to the scale of size of instream features. Sedimentary indices of channel morphology include bed-material composition (e.g., Osterkamp and Hedman 1982; Howard 1987; van den Berg 1995), bedload transport (e.g., Parker 1979; Bettess and White 1983; Ferguson 1987), and channel-bank composition (e.g., Schumm 1960; Schumm 1963; Simpson and Smith 2001). Much of our knowledge relating these

various indices to channel adjustment are derived from humid settings or for rivers with predictable flow regimes (Doyle et al. 2007). Less is known about the adjustment of rivers with highly variable flow and sediment transport regimes, although evidence indicates that complex arrangements of channel pattern, shape, and profile occur in arid (e.g., Huckleberry 1994; Bourke and Pickup 1999), semi-arid (e.g., García 1995; Heritage, van Niekerk, and Moon 1999), or seasonally active (e.g., Gupta 1995; Kale and Hire 2007) fluvial systems. Additionally, substantial differences in fluvial forms and processes are evident for bedrock-dominated (e.g., Baker and Kale 1998; Erskine and Livingstone 1999) or geologically-complex (Schumm 2005) fluvial systems. Furthermore, few investigations have focused on mutual downstream adjustment of channel pattern and shape imposed by abrupt changes in hydraulic and sedimentary controls.

This chapter investigates the roles of hydrology, lithology, and sedimentary characteristics on mutual downstream adjustment of channel pattern and shape in the Llano River watershed (11,568 square kilometers), Texas, USA (Figure 4.1). The rural, unregulated watershed occurs at a transition between semi-arid conditions in the west and sub-humid conditions in the east and is subject to extreme floods (Beard 1975; Burnett 2008). Further, a lithologic transition from carbonates in the upper watershed to igneous and metamorphic rocks in the lower watershed complicates an assessment of channel adjustment based on hydrology alone. A variety of methods are used to quantify the controls and indices associated with mutual downstream adjustment of

channel pattern and shape in the Llano River watershed, including field surveys of channel geometry and sediment composition, laboratory particle-size analyses, hydraulic and hydrologic analyses, GIS, and statistical analyses.

The research design, methods, and results presented in this chapter constitute an effort dissimilar from other investigations of channel adjustment. First, the distribution of sites along the North Llano, South Llano, and Llano Rivers and selected tributaries adequately characterizes watershed-scale variability, but also encompasses the distribution of hydrologic variables from headwater streams to the main-stem channel. Second, the aforementioned characteristics of the Llano River watershed uniquely qualify it for discerning the relative influence of a highly-variable flow regime and abrupt lithologic transitions on channel morphology. Third, application of refined hydrologic methods, including partial-duration flood frequency analyses, provides more accuracy to interpretations of channel morphology and its relation to the hydrologic regime. Finally, channel-bed and bank particle-size analyses for most sites controls for the influence of alluvial sediment on channel morphology.

6.3 Background

The association of channel geometry to hydraulic and sedimentary controls has been and remains one of the primary emphases of fluvial geomorphology. A discussion of some of the models associated with planform geometry, hydraulic geometry, and dominant discharge is provided below to provide context for this chapter.

6.3.1 Planform Geometry

A variety of efforts have been made to link hydraulic and sedimentary controls to channel pattern. Relying on a purely hydraulic approach, Leopold and Wolman (1957) proposed the following empirical relation of slope and discharge, above which channels are braided and below which channels are meandering (Figure 1.2):

$S = 0.012Q^{-0.44}$, where

S is dimensionless channel slope and Q is bankfull discharge, in cubic meters per second.

The relation indicates that meandering channels transition to braided channels if hydraulic energy increases, but it does not imply that sediment load contributes to channel pattern. Most of the data used to derive this relation were from rivers in the humid eastern and mid-western United States and the northern Rocky Mountains. Few data points were from semi-arid rivers with highly variable flow regimes or rivers in otherwise complex physiographic regions. Further, Ferguson (1987) argues that valley slope, rather than channel slope, better explains transitions between channel patterns. Another hydraulic-based approach by Parker (1976) associates indices of hydraulic energy (slope-to-Froude number ratio) with channel shape (depth-to-width ratio) to explain channel pattern transitions and the intensity of braiding.

Others have advocated for theories that consider sedimentary composition of the channel boundary as an important control of channel pattern. The underlying premise supporting this claim is that relatively fine-grained loads result in a cohesive channel

boundary that promotes meandering and coarse-grained loads result in channel-bar formation and loosely consolidated channel banks. Schumm (1963) shows a relation between silt-clay percentage and sinuosity, and Schumm and Khan (1972) argue that fine sediment is required before meandering develops in laboratory flume experiments. In a variant of the Leopold and Wolman (1957) threshold approach, van den Berg (1995) integrates unit stream power (watts per square meter) with median bed-material size (millimeters) to effectively distinguish between single- and multi-thread channels.

The lack of a consensus among researchers in the geomorphic community to universally predict channel pattern from a particular hydraulic or sedimentary index is not surprising, or even warranted, given the diversity of hydrologic, geologic, and sedimentary regimes on Earth's surface. Ferguson (1987) ultimately resolves that unique combinations of hydraulic and sedimentary controls result in a continuum of channel patterns, a concept summarized in Figure 6.1, which shows a transition from various meandering to braided patterns as sediment supply, particle size, slope, and stream power increase.

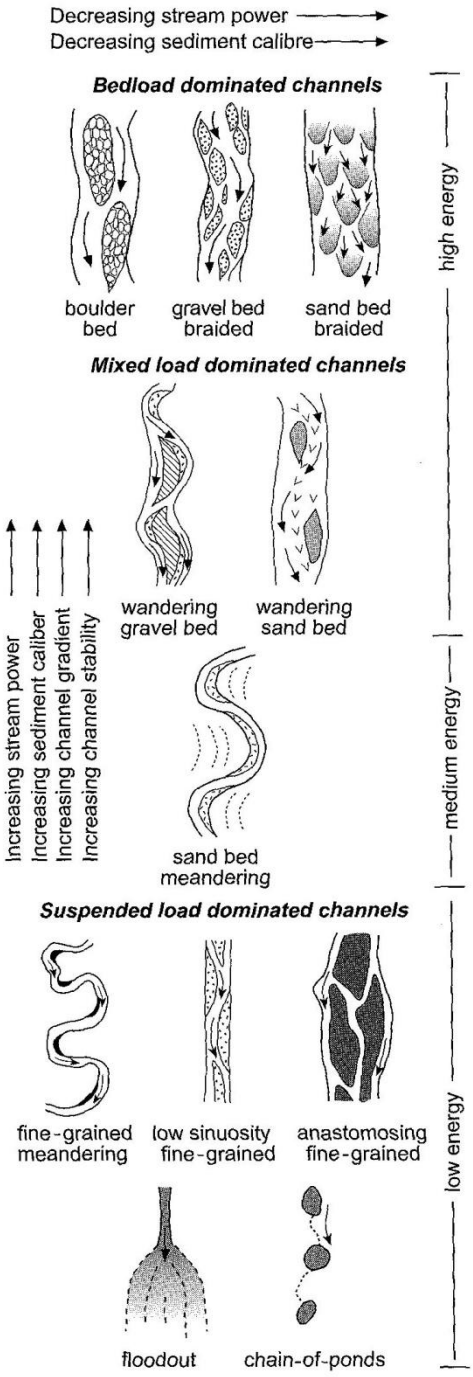

Figure 6.1. The continuum of channel patterns transitions from meandering and anastomosing channels to wandering and braided channels as sediment supply, particle size, and hydraulic energy increase [from Brierley and Fryirs (2005); modified from Church (1992) and Schumm (1977)].

Although it is generally recognized that a continuum of channel patterns results from various combinations of hydraulic and sedimentary controls, it can nonetheless be challenging to categorize patterns within the scheme shown in Figure 6.1, especially for rivers occurring in unique settings. For example, Kale, Baker, and Mishra (1996) and Heritage, van Niekerk, and Moon (1999) identify multi-channel rivers, including anastomosing forms, in bedrock-dominated settings. Others have identified anabranching systems in both high-energy (e.g., Nanson and Knighton 1996) and low-energy settings (e.g., Makaske 2001). Additional variants include discontinuous forms, such as cut-and-fill channels (e.g., Brierley and Fryirs 2005) and arroyos (e.g., Schumm and Hadley 1957). Advances in our understanding of channel pattern are likely to come from rivers where abrupt transitions in either hydraulic or sedimentary controls occur (e.g., Simpson and Smith 2001).

6.3.2 Hydraulic Geometry

Methods to analyze cross-sectional channel adjustment along the Llano River and selected tributaries are founded in the classic work of Leopold and Maddock (1953), which emphasizes the importance of discharge (cubic meters per second) through the concept of hydraulic geometry, or simple power relations associating width (meters), depth (meters), and velocity (meters per second) to discharge (Figure 2.1). The three factors are plotted in log space with discharge on the abscissa axis, such that three slope-dependent exponents (*b*, *f*, and *m*) of the regression-fitted lines satisfy continuity by summing to the value "1". The *b*, *f*, and *m* exponents represent the rate of change of

width, depth, and velocity, respectively, and the fundamental hydraulic geometry equations are:

$w = aQ^b$,

$d = cQ^f$,

$U = kQ^m$, where

w is water-surface width, in meters; d is mean depth, in meters; U is mean velocity, in meters per second; Q is discharge, in cubic meters per second; a, c, and k are empirically-derived coefficients; and b, f, and m are empirically-derived exponents.

Hydraulic geometry is a convenient technique when adequate discharge and cross-sectional geometry data are available, and results are easily interchangeable with common hydrologic analyses, including flood frequency. Hydraulic geometry can be applied to the range of flows at one cross section, termed "at-a-station," or along a channel reach for a user-specified index of discharge at multiple cross sections, termed "downstream." At-a-station hydraulic geometry commonly experiences three phases in most river channels: (1) low-flow conditions that are incapable of entraining bed and bank material, (2) active conditions associated with entrainment and transport of bed (and possibly bank) material, and (3) overbank conditions (Knighton 1998). The diversity of hydraulic processes occurring along a continuum of low- to high-flow conditions complicates geomorphic assessments solely based on at-a-station analyses, and Park (1977) shows that b, f, and m exponents have large variability. Aside from its complications, at-a-station hydraulic geometry can be a very useful technique to

associate the hydrologic regime of a stream to its shape. If applied in conjunction with flood frequency analysis, itself a problematic technique (Kidson and Richards 2005), much can be learned about the relation of various instream geomorphic units to the magnitude and frequency of different flows (Gregory and Madew 1982).

Downstream hydraulic geometry is used to investigate channel adjustment at multiple locations along a river, and requires selection of a common discharge index, such as bankfull, mean annual, or another flow of a given exceedance frequency (e.g., 1.5-year return period). The theory of downstream hydraulic geometry has been criticized in several areas: (1) adherence to log-linear relations and neglect of flow resistance (Richards 1973), (2) interpretive limitations for rivers with relatively low ratios of stream power to particle size (Wohl 2004), (3) interpretive limitations for rivers with diverse sedimentary (e.g., Parker 1979; Knighton 1987; Huang and Warner 1995) and vegetative (e.g., Hey and Thorne 1986) controls, and (4) inherent instability of cross-sectional shape (Phillips 1990; Fonstad and Marcus 2003). Additionally, difficulties in determining bankfull stage (Williams 1978a) complicate many downstream hydraulic geometry assessments. Further, an assumption of progressively increasing discharge with downstream distance is made, although some rivers are not characterized by this trend. Downstream hydraulic geometry, however, has been successfully applied to derive regional regression equations to predict channel morphology (e.g., Betson 1979; Castro and Jackson 2001), infer morphologic changes resulting from a single flood (e.g., Merritt and Wohl 2003), discriminate channel

patterns (e.g., Xu 2004), and determine the relative effects of channel boundary characteristics and hydraulic controls on channel morphology (e.g., Torizzo and Pitlick 2004; Wohl and Wilcox 2005; Arp et al. 2007).

6.3.3 Dominant Discharge

Downstream hydraulic geometry techniques used to assess channel adjustment are applied with the assumption of a dominant, or channel-forming, discharge. Wolman and Miller (1960) concluded that frequent, moderate floods are responsible for the cumulative majority of sediment transport in various alluvial rivers in the United States, occurring with an average return period of 1 to 2 years (Figure 2.4). Others (e.g., Wolman and Leopold 1957; Leopold, Wolman, and Miller 1964) have associated channel geometry with bankfull conditions, and observations over time have concluded that bankfull return periods of many alluvial rivers are between 1 and 2 years (e.g., Dury 1973; Gupta and Fox 1974; Andrews 1980; Biedenharn, Little, and Thorne 1999). Others have shown, however, that channel-forming discharge of rivers with highly variable flow regimes is likely to occur less frequently (e.g., Schick 1974; Pickup and Warner 1976; Baker 1977; López-Bermúdez, Conesa-García, and Alonso-Sarría 2002; Doyle et al. 2007). Further, complex arrangements of alluvial features at various heights above the channel bed along rivers dominated by high-magnitude floods, including seasonal or monsoonal rivers (e.g., Gupta 1995; van Niekerk et al. 1999; Heritage, Broadhurst, and Birkhead 2001), challenge prevailing assumptions of dominant discharge in alluvial systems.

This chapter offers a comprehensive evaluation of dominant discharge from headwater streams to the main-stem channel in a fluvial system characterized by severe flash floods and abrupt discontinuities in lithology and sediment composition. Although a number of investigations have explored these concepts at particular sites or localities, this study was designed to emphasize downstream trends in channel morphology and associated values of dominant discharge. The results should clarify the roles of moderate and severe floods on bankfull and macro-channel development along flood-prone rivers.

6.4 The Llano River Watershed

The Llano River watershed, by nature of its flashy hydrology and diverse lithologic characteristics, is well-situated for at-a-station and downstream assessments of the hydraulic and sedimentary controls that control mutual adjustment of channel planform and shape.

6.4.1 Geology and Lithology

The Llano River watershed (Figure 4.1) is located in the Edwards Plateau of Central Texas, and is part of the larger Colorado River basin. The lithology is complex for its drainage area, and reflects Tertiary tectonic activity associated with the Llano Uplift. Expressed at the surface, the uplift is a basin of exhumed Precambrian intrusive igneous and metamorphic rock, centered in the eastern part of the watershed, surrounded by an elevated Cretaceous carbonate rim. A transitional zone of Paleozoic

sedimentary rock occurs between the Cretaceous rim and the Precambrian basement rock.

The western headwaters of the Llano River watershed have elevations exceeding 700-meters NAVD88. Downstream, the rivers dissect a lower-Cretaceous carbonate tableland comprised of horizontally-bedded, fossiliferous limestone and dolomite sequences, with varying amounts of chert. In total, lower Cretaceous formations comprise 66 percent (7,629 square kilometers) of the total watershed area. Transitioning into the Llano Uplift, Paleozoic sedimentary units consist of a variety of lithologic types, mostly Ordovician limestone and dolomite and Cambrian sandstone, and comprise almost 12 percent (1,369 square kilometers) of the total watershed area. In the lower, eastern side of the watershed, Precambrian granite, gneiss, and schist dominate, and comprise 19 percent (2,180 square kilometers) of the total watershed area. Precambrian rocks in the watershed form irregular topography, including large exfoliation domes. The remaining 3 percent (390 square kilometers) are mostly comprised of Quaternary alluvial deposits.

Differential rates and patterns of bedrock weathering in the Llano River watershed strongly influence valley confinement, alluvial development, and sediment composition. Cretaceous limestone and dolomite in the upper watershed are associated with high rates of physical and chemical weathering, resulting in a relatively wide alluvial valley in the vicinity of Junction (Figure 5.1). Fluvial processes and forms associated with unconfined valley settings, including meander cutoffs, alluvial terraces,

and well-defined floodplains, occur in this area. Despite the susceptibility of carbonate lithology to weathering, channel networks in the upper watershed are characterized by cobble-, pebble-, and gravel-sized bed material. The transition to Paleozoic sedimentary rock is associated with a decrease in valley width and more frequent bedrock exposures along the Llano River, indicating a more resistant lithology. Alluvial development is limited to localized, hydraulically-favorable zones of deposition, including discontinuous floodplains and mid-channel bars. Precambrian granite, gneiss, and schist in the lower watershed are relatively resistant to weathering, and mostly consist of quartz, microcline, plagioclase feldspar, biotite, and hornblende. Although more resistant than carbonates, Precambrian rocks deliver mostly sand-sized sediment to channel networks, implying that most weathering is accomplished in-situ. The Llano River valley is confined in its lower reaches, and supports limited depositional features that thinly overlie bedrock. These deposits, however, provide evidence of bankfull and macro-channel hydraulic conditions based on their vertical extent.

The plateau-based setting, variable geologic structure, and incision history has resulted in remarkably straight longitudinal profiles of the North Llano, South Llano, and Llano Rivers (Figure 6.2). Combining the South Llano and Llano Rivers, the channel descends from approximately 700- to 250-meters NAVD88 over a distance of about 300 kilometers, giving an overall dimensionless channel slope of 0.0015. The North Llano River is slightly steeper (dimensionless channel slope of 0.022) because it descends from roughly a similar elevation to Junction over a shorter channel distance.

Aside from a limited concavity at the uppermost reach and subtle deviations from a generally continuous slope thereafter, the straight profiles of the North Llano, South Llano, and Llano Rivers nullify explanations of downstream channel geometric adjustments based on abrupt discontinuities in hydraulic power related to channel slope.

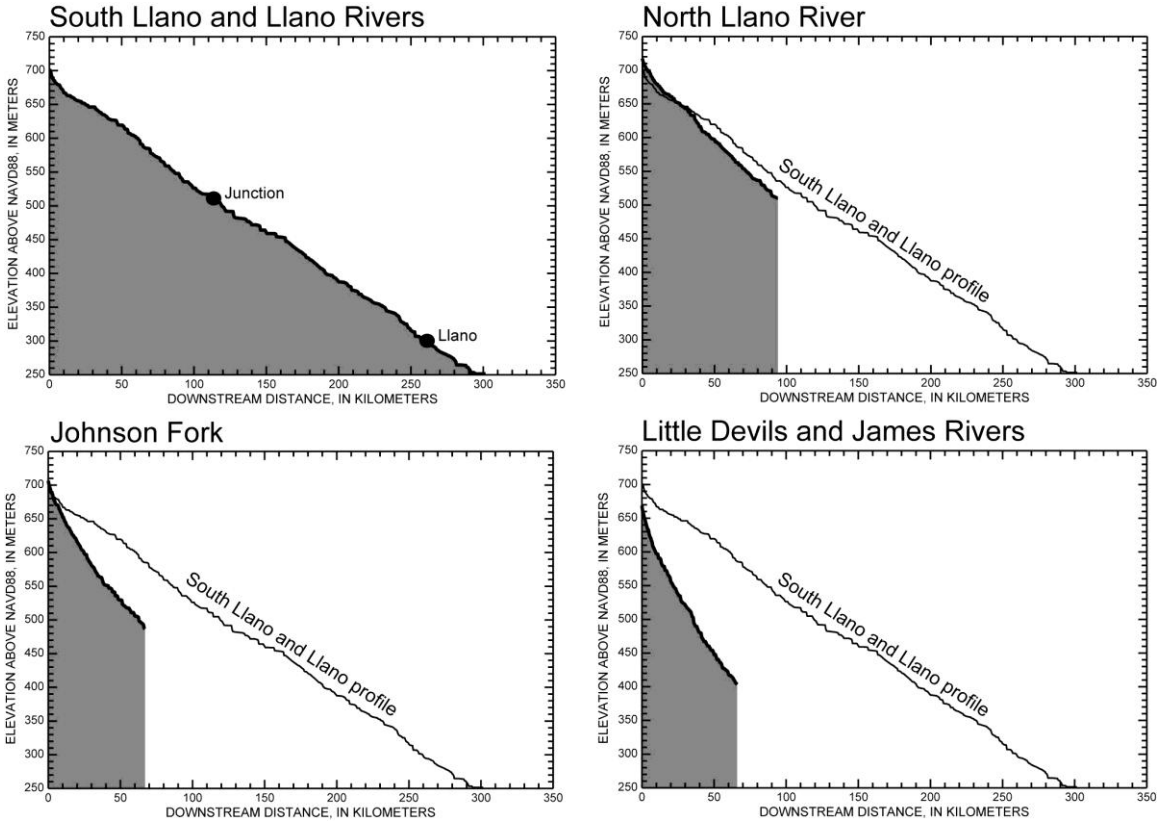

Figure 6.2. Longitudinal profiles of the combined South Llano and Llano Rivers, the North Llano River, Johnson Fork, and the combined Little Devils and James Rivers in Central Texas were rendered from GIS analysis of 10-meter digital elevation models (DEMs). The main-stem South Llano and Llano Rivers, as well as the North Llano River, have a remarkably straight profile, although the overall slope is greater for the North Llano River. Major tributaries of the Llano River show a subtle slope concavity, and are much steeper than main-stem channels.

6.4.2 Precipitation and Hydrology

The precipitation regime of the watershed ranges from semi-arid in the west (approximately 580 millimeters of rainfall per year) to sub-humid in the east (approximately 760 millimeters of rainfall per year). Rainfall in Central Texas, however, is highly variable through time, and droughts can rapidly transition to floods within months (Bomar 1983). As a result of locally steep slopes and very thin soils (Cooke et al. 2003), rapid runoff rates to channel networks cause this area to experience extreme flash floods (Beard 1975; Tinkler 2001; Burnett 2008), capable of transporting substantial quantities of sediment (Heitmuller and Asquith 2008) and greatly modifying channel geometry (Baker 1977).

The hydrology of the Llano River and its tributaries (Table 5.1, Figure 5.4) reflects climatic mechanisms in Central Texas. Tributaries to the Llano River exhibit relatively low baseflow conditions for the majority of time with lowest flows usually occurring in mid- to late-summer. The South Llano River, however, is supplied by karstic springs upstream of Junction and provides the majority of baseflow to the main-stem Llano River. Normal baseflow conditions are interrupted by extreme floods (Figure 5.5) caused by rainfall associated with stalled low-pressure systems or tropical cyclones. Floods along the Llano River at Llano have exceeded 3,000 cubic meters per second ten times since the 1940 hydrologic year, not including the estimated peak instantaneous discharge of 10,760 meters per second in 1935. There are no reservoirs

that regulate discharge in the Llano River watershed, although two low-water control structures in Junction and Llano allow ponded water to be used for municipal supply.

6.5 Data and Methods

The investigation of mutual channel adjustment and the relation to hydraulic, lithologic, and sedimentary controls along the Llano River and selected tributaries required various data sources and methods, including field surveys of channel topography and alluvial sediment, laboratory sediment analyses, flow-resistance analyses, flood-frequency analyses using discharge data, GIS, and statistical analyses.

Field surveys of cross-sectional geometry were used to quantify channel shape and sediment samples of channel-bed and bank material were obtained. Particle size of gravel-sized material was measured in the field. Laboratory analyses were done to quantify particle-size for alluvial deposits composed of sand-sized and finer material. Analyses using present-day (2009) expanded stage-discharge rating tables of U.S. Geological Survey (USGS) and Lower Colorado River Authority (LCRA) streamflow-gaging stations were done to evaluate appropriate flow-resistance coefficients used to compute flow velocity and discharge at gaged and ungaged study sites. Flood-frequency analyses were done to estimate the return periods associated with dominant discharge (channel-forming discharge) at various sites in the watershed. GIS was used to: (1) estimate channel slope at sites without sufficient field-survey data, (2) quantify various planform metrics (e.g., valley width, sinuosity), and (3) classify channel reaches by

morphologic type. Statistical analyses, notably hydraulic geometry, were used to infer site-specific and downstream trends in channel morphology.

6.5.1 Field-Data Collection and Analyses

Multiple surveys of cross-sectional channel topography were made at nineteen sites along the Llano River and selected tributaries (Figure 4.1) using a total-station surveying instrument. Additionally, nine cross-sectional surveys of tributaries in the watershed were provided by the LCRA, two of which (Johnson Fork and James River) did not include any bridge structures. Sites were chosen to represent changes in drainage area, tributary inputs, and lithologic variability of the watershed (Table 6.1). Five sites are located at USGS streamflow-gaging stations and surveyed elevations were associated with the established stage datum at those stations. The remaining sites were assigned an arbitrary elevation datum. GPS coordinates were obtained at total-station setup locations, as well as other surveyed locations at each site. After digitization of survey data in a spreadsheet format, the GPS coordinates were used to overlay survey points on a georeferenced orthophoto in GIS. Lines were digitized to represent flow direction for hydrologic conditions that would span the entire channel width, and angles were measured between the surveyed cross section and the flow direction. Finally, a cosine correction factor was applied to the cross-sectional data to produce a cross-section that is perpendicular to the primary high-flow direction. The correction ensures that cross-sectional dimensions are appropriately scaled to high-flow conditions. Simple hydraulic properties, including hydraulic radius, cross-sectional area, and Froude

number, among others, were computed at 0.25-meter stage increments using WinXSPRO (U.S. Department of Agriculture Forest Service 2008). Channel slopes were mostly derived from site-specific total-station surveys of water-surface elevations, but GIS-based longitudinal profile data were used as needed for sites where measured distances between water-surface elevation points were not sufficient to obtain an accurate measure.

Table 6.1. Selected morphometric and sedimentary characteristics of study sites in the Llano River watershed in Central Texas. Various LCRA sites are not included if cross-sectional geometry measurements contain bridge structures. Particle-size values represent averages of multiple samples collected at each site.

[ED, ephemeral draw; KG, Cretaceous gravel-bed; P, Paleozoic bedrock or gravel-bed; pC, Precambrian straight, braided, or bedrock-braided; DA, drainage area; km^2, square kilometers; DD, downstream distance; km, kilometers; VW, alluvial valley width; m, meters; *S*, dimensionless channel slope; d_{50}, median particle size; mm, millimeters; --, not available]

Site	Category	DA (km^2)	DD (km)	VW (m)	Alluvial sinuosity[a]	*S*	Channel bar d_{50} (mm)	Bank d_{50} (mm)[b]
North Llano Draw near Sonora	ED	7.79	0.90	--[c]	1.00	0.0054[d]	--	0.0042[e]
North Llano River near Roosevelt	KG	1,145	56.4	250-375	1.13	0.0021[f]	36.6	0.044
North Llano River near Junction	KG	2,335	89.2	750-1,000	1.13	0.0029[g]	18.0	0.110
South Llano River at Baker Ranch near Rocksprings	ED	417	29.5	400-415	1.19	0.0015[g]	0.039	0.033
South Llano River at U.S. Highway 377 near Rocksprings	ED	1,134	64.5	100-250	1.06	0.0036[d]	42.2	--
South Llano River at 700 Springs Ranch near Telegraph	KG	1,352	76.3	225-350	1.01	0.0030[d]	44.9	0.076
South Llano River at South Llano River State Park	KG	2,256	105	1,000-1,150	1.31	0.0012[d]	25.5	0.039
South Llano River at Texas Tech University—Junction	KG	2,271	110	1,250-1,600	1.31	0.0014[d]	21.8	0.127
Llano River near Junction	KG	4,815	121	700-1,000[h]	1.38	0.0071[f]	16.3	0.066
LCRA Johnson Fork near Junction	KG	758	52.7	650-850	1.33	0.0026[d]	--	--
Johnson Fork at Lowlands Crossing near Junction	KG	778	57.5	850-950	1.33	0.0053[f]	23.8	0.353
Llano River near Ivy Chapel	KG	5,939	140	300-650	1.24	0.0015[d]	23.7	0.062
LCRA James River near Mason	P	845	53.7	--[c]	1.00	0.0034[d]	--	--
James River near Mason	P	877	65.6	--[c]	1.00	0.0059[f]	46.0	0.228
Llano River at James River Crossing near Mason	P	8,032	193	400-500	1.08	0.0025[f]	28.0	0.104
Llano River near Mason	pC	8,418	210	--[c]	1.00	0.0025[f]	14.2	0.160
Beaver Creek near Mason	pC	558	57.2	--[c]	1.00	0.0031[d]	0.884[i]	0.264
Llano River at Castell	pC	9,429	230	--[c]	1.00	0.0013[d]	2.09	0.090
Llano River at Llano	pC	10,885	261	--[c]	1.00	0.0014[f]	0.457	0.146
Llano River near Kingsland	pC	11,406	292	--[c]	1.00	0.0027[f]	0.629	0.198
Honey Creek at KDK Ranch near Kingsland	P	28.6	11.7	--[c]	1.00	0.022[f]	39.6	0.464

[a] Alluvial sinuosity was measured by dividing the channel length by the valley-axis length. In some cases, alluvial sinousity is approximately 1.0 because of confined valley settings, even though the valley meanders across the land surface.
[b] Composite of channel bank and floodplain surface deposits.
[c] Valley confined by bedrock. Alluvial deposits thinly overlie bedrock, but alluvial floodplains are absent.
[d] Channel slope derived from GIS analysis of 10-m DEMs.
[e] Particle-size for material collected from the base of the draw, which adequately represents all nearby deposits.
[f] Channel slope derived from total-station survey of water-surface elevations at low-flow conditions.
[g] Channel slope derived from total-station survey of thalweg elevations, which were at similar depths below the water surface at the upper and lower ends of the reach.
[h] Valley width is associated with abandoned valley segment, not with present-day channel avulsion through bedrock exposure.
[i] Median particle size only for sand-sized fraction, although material is bimodal with some proportion of gravel-sized material.

Channel bed and bank sediments were sampled along the same cross sections that were used for the topographical surveys. Multiple bed and bank samples were obtained along each cross-section transect, and were spatially distributed to account for various geomorphic surfaces, including the low-flow channel, channel bars, banks, and inset floodplains. Sample locations were referenced using a combination of cross-section survey data, GPS coordinates, and a measuring tape. Cobble-, pebble-, and gravel-bed material was sampled using a modified Wolman (1954) pebble count procedure (e.g., Heitmuller and Asquith 2008). Pebble counts were facilitated by using a sampling grid and particle-size analyzer. The sampling grid measures 50-by-50 centimeters and contains intersections spaced every 10 centimeters for a total of 25 intersections. The particle directly beneath each intersection was selected and the b-axis, or the short axis along the same dimensional plane as the longest axis, was passed through the smallest possible opening in the particle-size analyzer. The diameter of the opening was noted for each particle, and cumulative particle-size distribution curves were developed. Subaqueous bed-material samples were obtained by wading using the same method. Sand-sized or finer channel-bed and bank sediments were sampled with a scoop and bagged for further analyses.

6.5.2 Laboratory Sediment Analyses

Bagged sediment samples were analyzed for particle size in the Applied Geomorphology and Geo-Archaeology Laboratory in the Department of Geography and the Environment at The University of Texas at Austin. Samples were dried and

weighed, and pre-treatment included further physical disaggregation with a milkshake mixer and chemical disaggregation of the colloidal fraction with a 5-percent concentration of sodium hexametaphosphate [$(NaPO^3)^6$]. Particle-size was analyzed by the hydrometer and wet-sieve method described in Gee and Bauder (1986) (e.g., Hudson and Heitmuller 2003). The analysis data were entered into a pre-formatted spreadsheet and cumulative particle-size distribution curves were developed.

6.5.3 GIS Analyses

A variety of morphologic evaluations and products were made using GIS, including longitudinal profiles, valley cross sections, a channel classification scheme, and various planform statistics. GIS analyses of 10-meter digital elevation models (DEMs) and the high-resolution National Hydrography Dataset (NHD) (U.S. Geological Survey 2008a, 2008b) were done to generate longitudinal profiles and valley cross sections. Further, channel slopes for sites with insufficient or indeterminate total-station survey data were computed using 10-meter DEMs and NHD data in GIS by including a reach sufficiently long enough to capture DEM irregularities. The North Llano, South Llano, and Llano Rivers were classified through a combination of field observations and GIS analyses of digital orthophotography (2-meter horizontal resolution) and a geodatabase of surface geology based on Barnes (1981). Orthophotography and surface geology also were used to quantify alluvial sinuosity and valley width at study sites in the watershed.

6.5.4 Statistical Analyses

Simple statistical analyses, including particle-size descriptors (e.g., d_{50}) and various hydraulic values (e.g., stream power), were computed in spreadsheets. Statistical analyses, including hydraulic geometry, trend lines, and flood-frequency, were done in R (R Development Core Team 2004).

6.5.5 Flow Resistance Analyses

Analyses of at-a-station and downstream hydraulic geometry for ungaged sites in the Llano River watershed require an appropriate flow-resistance coefficient to compute mean flow velocity and discharge. Flow-resistance coefficients increase as flow uniformity becomes more disrupted, either by grain, form, or boundary roughness. Coefficients are often selected in the field through observations of bed-material particle size, the presence of bedforms, and vegetation along the banks and floodplains. Two commonly used flow-resistance coefficients are Manning's n and Darcy-Weisbach f. Manning's n is the most commonly utilized flow-resistance coefficient for open-channel flow and is associated with mean flow velocity (U) by the following empirical relation known as Manning's equation:

$$U = \frac{R^{2/3} S^{1/2}}{n},$$

where U is mean flow velocity, in meters per second; R is the hydraulic radius, in meters (often equated to mean flow depth); and S is the energy grade line, which is assumed to be equal with dimensionless channel slope.

Alternatively, the dimensionless Darcy-Weisbach f friction factor, also used for evaluation of flow velocity in open channels, is derived from a more theoretical basis (Robert 2003), and is computed from the following equation:

$$f = \frac{8gdS}{U^2},$$

where g is the acceleration of gravity (9.81 meters per square second) and d is mean flow depth, in meters.

Solving for flow velocity, discharge (Q) (cubic meters per second) can be computed from the following:

$$Q = AU,$$

where A is the cross-sectional area of the flow, in square meters.

Manning's n and Darcy-Weisbach f flow-resistance coefficients were quantitatively solved using surveyed cross-sections and expanded stage-discharge rating curve tables at USGS and LCRA streamflow-gaging stations (Table 6.2, Figure 6.3). Expanded stage-discharge rating curve tables give incremental stage and discharge relations for every 0.003 meters (0.01 feet) of stage. Cross-sectional data, including area and hydraulic radius, were computed at 0.01-meter stage-increments using WinXSPRO (U.S. Department of Agriculture Forest Service 2008). Mean flow velocity was solved for at 0.3048-meter (1-foot) increments by dividing the discharge by the cross-sectional area, and flow-resistance coefficients were solved. The hydraulic values and flow-resistance coefficients reported in Table 6.2 correspond with the stage at observed breaks in slope along alluvial banks or bridge-apron tops of the cross section at the gage

location. Values either correspond with bankfull or macro-channel conditions, depending on the channel morphology at the study site. It is the author's judgment that appropriate comparisons of flow hydraulics are drawn by the choice of bankfull or macro-channel conditions shown in Table 6.2. Flow-resistance computations were not made for at 08150000 Llano River near Junction because a surveyed cross section was not made at the station.

Table 6.2. Manning's n and Darcy-Weisbach f flow-resistance coefficients. The coefficients were solved for using surveyed cross-sections and expanded stage-discharge rating curve tables at selected USGS and LCRA gaging stations in the study area. Values at or near bankfull or macro-channel stage are shown below.

[m, meters; Q, discharge; m^3/s, cubic meters per second; S, dimensionless channel slope; A, cross-sectional area; m^2, square meters; w, water-surface width; R, hydraulic radius; d, mean depth; U, mean flow velocity; m/s, meters per second; n, Manning's n flow-resistance coefficient; f, Darcy-Weisbach friction factor; Fr, Froude number]

Site	Bed-material	Stage (m)	Q (m^3/s)	S	A (m^2)	w (m)	R (m)	d (m)	U (m/s)	n	f	Fr
08148500 North Llano River near Junction	Cobbles, gravel	5.49[a]	462	0.0029	232	88.6	2.59	2.62	1.99	0.051	0.149	0.39
LCRA Johnson Fork near Junction	Cobbles, gravel	6.10[a]	501	0.0026[b]	267	92.1	2.85	2.90	1.87	0.055	0.165	0.35
LCRA James River near Mason	Cobbles, gravel	5.49[c]	1,250	0.0034[b]	318	117	2.71	2.73	3.94	0.029	0.047	0.76
LCRA Comanche Creek near Mason	Sand	3.96[a]	207	0.0048[b]	105	66.8	1.56	1.58	1.97	0.047	0.152	0.50
08150700 Llano River near Mason	Cobbles, gravel	6.71[c]	2,470	0.0025	736	124	5.74	5.92	3.36	0.048	0.099	0.44
LCRA Willow Creek near Mason[d]	Sand	4.57[a]	456	0.0030[b]	190	80.7	2.32	2.35	2.40	0.040	0.095	0.50
LCRA Hickory Creek near Castell[d]	Sand, bedrock	5.79[a]	708	0.0051[b]	318	90.4	3.45	3.52	2.23	0.073	0.279	0.38
LCRA San Fernanado Creek near Llano[d]	Sand, bedrock	5.49[a]	651	0.0025[b]	283	94.7	2.94	2.99	2.30	0.045	0.109	0.42
LCRA Johnson Creek near Llano[d]	Sand	4.88[a]	510	0.0029[b]	142	57.6	2.41	2.46	3.60	0.027	0.042	0.73
08151500 Llano River at Llano	Sand, bedrock	7.62[c]	3,060	0.0014	1,080	198	5.48	5.55	2.82	0.041	0.076	0.38
LCRA Honey Creek near Kingsland[d]	Cobbles, gravel	5.49[a]	756	0.0067[b]	169	58.6	2.83	2.89	4.47	0.037	0.074	0.84

[a] Stage and hydraulic values for bankfull conditions.
[b] Dimensionless channel slope values computed by using 10-meter DEMs and high-resolution NHD in GIS.
[c] Stage and hydraulic values for macro-channel conditions.
[d] Values given for top of concrete bridge apron and not for morphologic bankfull stage. The top of the apron, however, is used to approximate bankfull stage.

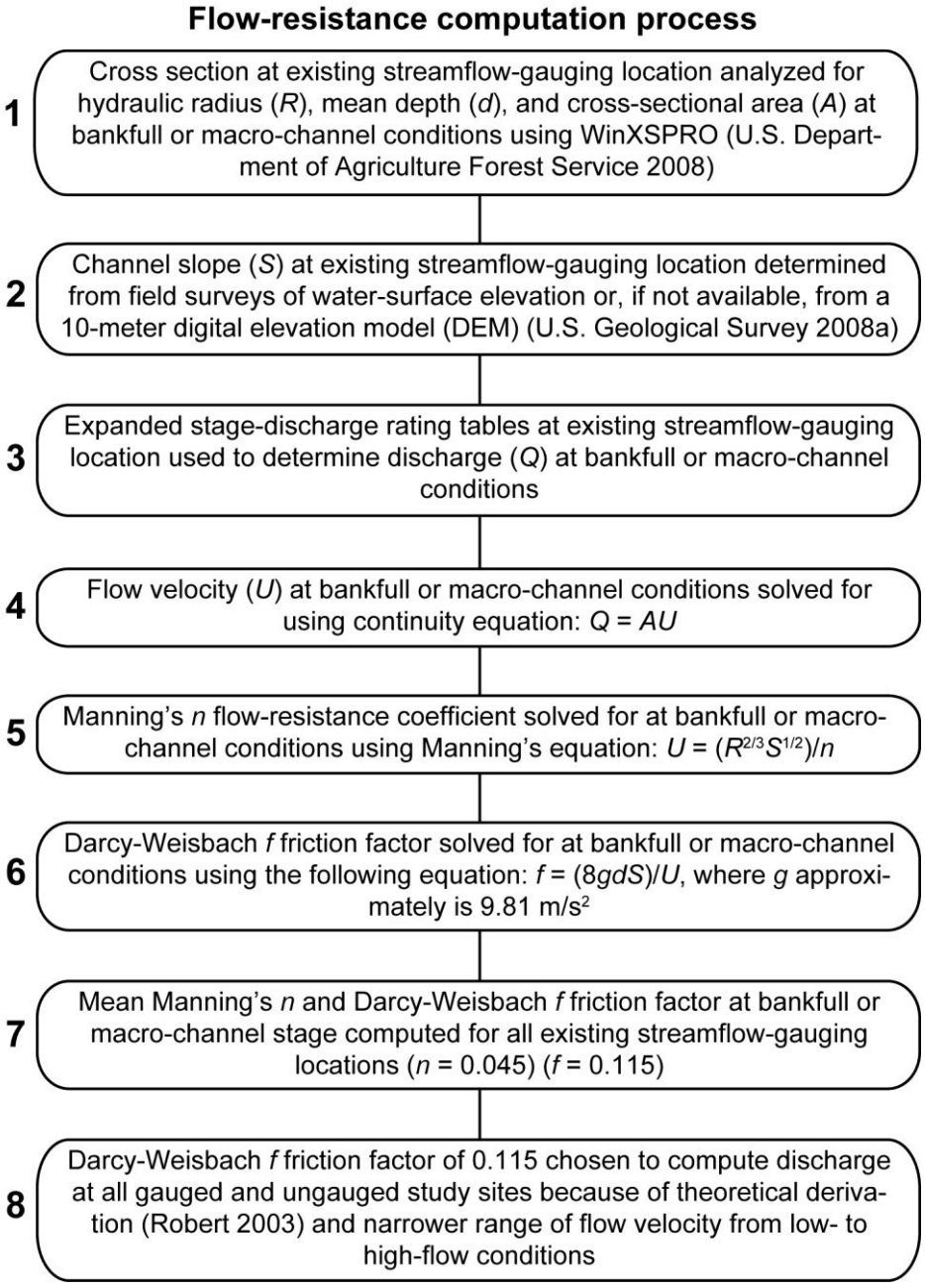

Figure 6.3. Computational process to determine an appropriate flow-resistance coefficient for use in analyses of flow velocity and discharge at study sites in the Llano River watershed in Central Texas.

Manning's n values at or near bankfull stage range from 0.027 to 0.073, and Darcy-Weisbach f friction factors range from 0.042 to 0.279. Although much variability is evident, similarities of mean flow-resistance coefficients for various bed-material conditions emerge. For channels with cobble- to gravel-sized bed material, mean n is 0.044 and mean f is 0.107. For channels with sand-sized bed material, mean n is 0.046 and mean f is 0.126. For channels with bedrock outcrops, mean n is 0.053 and mean f is 0.155. Although sand-bed channels are usually associated with lower flow-resistance coefficients than gravel-bed channels, the ubiquitous presence of irregular bedrock outcrops in sand-bed channels in the Llano River watershed result in comparable values. For hydraulic geometry computations at ungaged sites, an n value of 0.045 and an f value of 0.115 are used at bankfull stage unless otherwise noted, slightly higher than the n value of 0.035 used for bed-material entrainment computations in Heitmuller and Asquith (2008), but within the range suggested by Conyers and Fonstad (2005).

For all study sites in the Llano River watershed, flow velocity was computed using the f value of 0.115 instead of the n value of 0.045 because the Darcy-Weisbach friction factor (f) is derived from a more theoretical basis (Robert 2003) and a narrower range of flow velocity is computed from low to high stages for each cross section (Table 6.3). The discharge values associated with the flood-frequency analyses discussed below ultimately are derived from the f value of 0.115 for all study sites.

Table 6.3. Comparison of flow velocity computed from a Manning's n value of 0.045 and a Darcy-Weisbach f value of 0.115 at minimum low and maximum high stages of surveyed cross sections at selected sites without a cross section at the gage location in the Llano River watershed in Central Texas.

[U, mean flow velocity; n, Manning's n flow-resistance coefficient; m/s, meters per second; f, Darcy-Weisbach friction factor]

Site	Cross-section	Minimum U from n (m/s)	Maximum U from n (m/s)	Minimum U from f (m/s)	Maximum U from f (m/s)
North Llano River near Roosevelt	1	0.23	3.73	0.41	3.21
	2	0.27	3.50	0.46	3.08
	3	0.19	3.87	0.34	3.33
South Llano River at Baker Ranch near Rocksprings	1	0.23	0.47	0.38	0.64
	2	0.12	0.74	0.23	0.90
	3	0.08	0.83	0.18	0.98
	P	0.24	0.88	0.39	1.03
South Llano River at U.S. Highway 377 near Rocksprings	1	0.39	3.00	0.63	2.91
	2	0.56	3.38	0.81	3.20
South Llano River at 700 Springs Ranch near Telegraph	1	0.30	4.42	0.50	3.79
	2	0.42	4.78	0.64	4.04
	3	0.33	4.13	0.55	3.63
South Llano River at South Llano River State Park	1	0.24	1.50	0.37	1.51
	2	0.09	1.36	0.20	1.39
	3	0.25	1.63	0.39	1.62
South Llano River at Texas Tech University—Junction	1	0.18	1.94	0.32	1.86
	2	0.10	1.99	0.20	1.89
	3	0.28	1.52	0.44	1.55
	4	0.25	1.66	0.39	1.65
Llano River near Junction	1	0.25	5.01	0.66	4.73
	2	0.32	4.81	0.62	4.53
	3	0.64	4.81	0.98	4.54
	4	0.46	3.16	0.79	3.30
Llano River near Ivy Chapel	1	0.16	2.60	0.29	2.36
	2	0.08	2.68	0.18	2.39
	3	0.22	2.72	0.38	2.42
Llano River at James River Crossing near Mason	1	0.22	3.44	0.39	3.06
	2	0.29	3.90	0.47	3.38
	3	0.26	3.33	0.43	3.02
Llano River at Castell	1	0.04	2.87	0.09	2.46
	2	0.08	2.70	0.16	2.35
	3	0.22	2.35	0.35	2.12
Llano River near Kingsland	1	0.42	2.48	0.64	2.41
	2	0.05	3.08	0.14	2.84

6.5.6 Flood Frequency Analyses

Flood-frequency analyses include various statistical methods designed to compute site-specific discharges associated with given return periods (e.g., 100-year flood), and are necessary to determine the frequency at which bankfull or macro-channel flow events occur. Two different flood-frequency methods were used in this investigation: (1) partial-duration analyses at sites with USGS stations and (2) a regionally-tuned regression analysis at ungaged sites (Figure 6.4).

Partial-duration analysis uses period-of-record discharges of measured flood peaks above a designated threshold that is referred to as the base discharge. The partial-duration series is preferred over the annual-maximum series to estimate the frequency of relatively small or moderate events (1- to 10-year return period) or for stations with a short period of record (Soong et al. 2004). This is advantageous for investigations of bankfull discharge, which commonly is associated with the 1- to 2-year return period for the majority of rivers (e.g., Dury 1973; Andrews 1980). Further, the episodic flood regime in the study area commonly has 1 year with numerous peaks above the base discharge and numerous years with no peaks above base discharge, a problem circumvented through use of the partial-duration series.

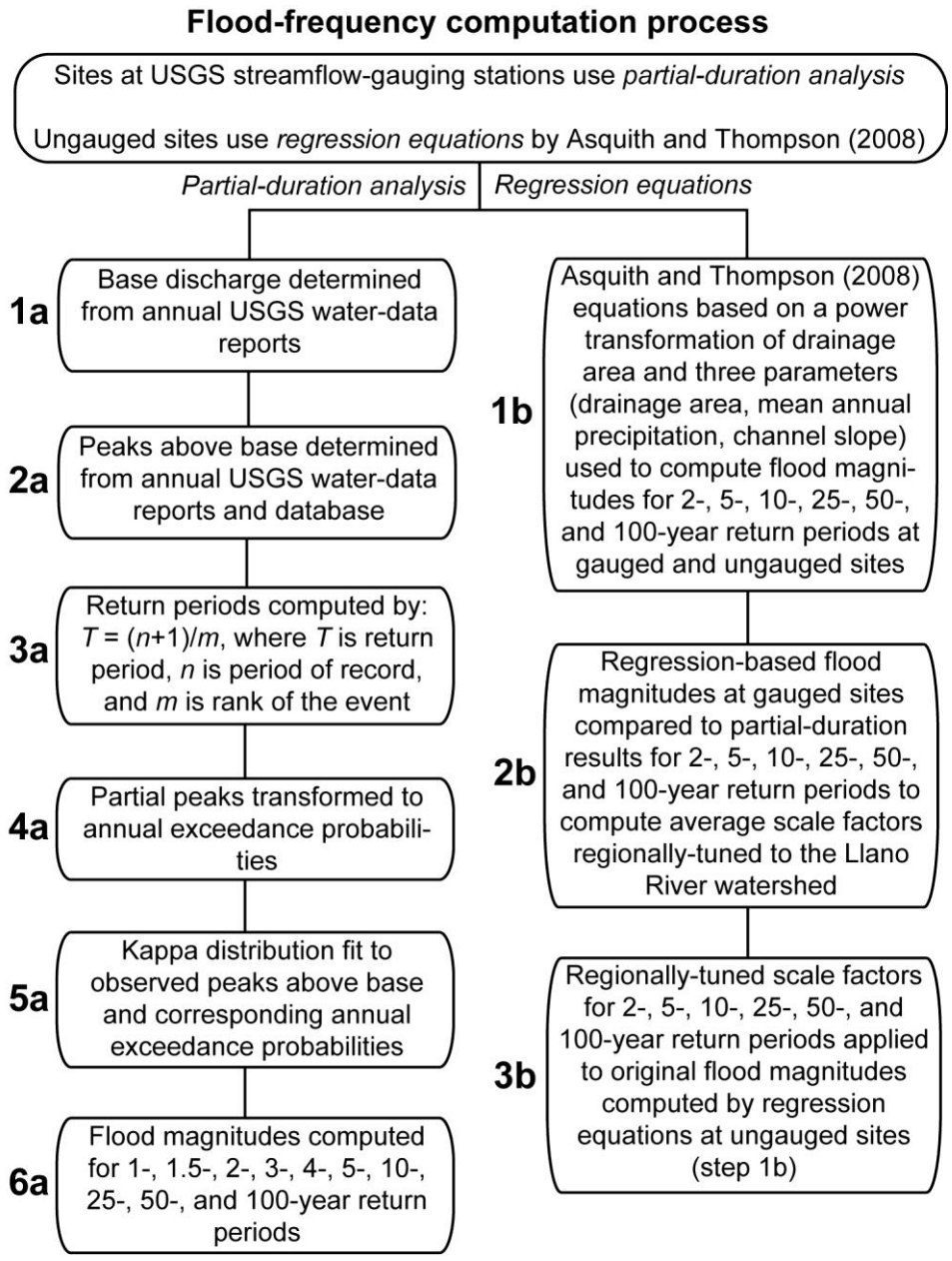

Figure 6.4. Computational process of flood frequency at gaged and ungaged study sites in the Llano River watershed in Central Texas.

Base discharges and peaks above base for USGS stations in the Llano River watershed are published in annual water-data reports (e.g., U.S. Geological Survey 2007). A few published base discharges have either increased or decreased over time, and some early peaks above base are missing for stations with a recent shift to a lower base discharge. Further, USGS water-data reports for Texas since 2001 only have the annual peak discharge, and USGS instantaneous data were used to fill the recent gap.

Peaks above base discharge were digitized and return periods were computed using the following equation:

$T = (n + 1)/m$, where

T is the return period, in years; n is the period of record, in years; and m is the rank of the discharge, in order from largest to smallest.

The peaks above base discharge and associated return periods were read into the `lmomco` package (Asquith 2009) of R (R Development Core Team 2004) and the four-parameter kappa distribution curve fit the L-moments (Hosking and Wallis 1997) of observed data (Figures 6.5). Because partial-duration series include a greater number of peaks than years in the period of record, the lambda technique described on page 18.38 of Stedinger, Vogel, and Foufoula-Georgiou (1993) was used to transform average arrival rates into annual exceedance probabilities, and flood magnitudes for various return periods were calculated from the kappa distribution (Table 6.4, Figure 6.5). For gaged locations, flood magnitudes reported in Table 6.4 do not exactly match discharges of bankfull and macro-channel conditions reported in Table 6.2 because the

mean f value of 0.115 was applied to compute discharge and a mean discharge value of multiple cross sections at each site was used to associate with flood-frequency analyses.

```
library(lmomco)
Tp <- c(1,1.5,2,3,4,5,10,25,50,100)
myfile <- file.choose()
Q   <-   read.table(file=myfile,   header=TRUE,   sep="\t",
fill=TRUE)
names(Q)
attach(Q)
lmr <- lmoms(Qcms)
Qsort <- sort(Qcms)
PP <- pp(Qsort)
plot(PP, log10(Qsort))
lmrdia <- lmrdia()
plotlmrdia(lmrdia, xlim=c(-0.1, 0.6), ylim=c(-0.1, 0.6))
points(lmr$ratios[3], lmr$ratios[4])
ls()
length(Qsort)
para <- parkap(lmr)
plot(PP, log10(Qsort))
lines(PP, log10(quakap(PP, para)), lwd=2)
lambda <- length(Qsort)/52.5
qe <- 1/(Tp*lambda)
G <- 1-qe
SOLUTION <- quakap(G,para)
detach(Q)
H <- list(event=SOLUTION,Tp=Tp,G=G,file=myfile)
points(H$G,log10(H$event),pch=16,col=2,cex=3)
return(H)

event     Tp   G
6025.81224708294         1    0.514018691588785
12536.0335299932         1.5  0.67601246105919
18331.9111174108         2    0.757009345794392
27550.0714136785         3    0.838006230529595
34571.9980314332         4    0.878504672897196
40194.9175827853         5    0.902803738317757
58182.7790138734         10   0.951401869158878
82244.0527803254         25   0.980560747663551
100209.861194574         50   0.990280373831776
117807.815453841         100  0.995140186915888
```

Figure 6.5. Example of R-code and output for partial-duration flood-frequency analyses of USGS streamflow-gaging stations in the Llano River watershed in Central Texas.

For ungaged sites and two LCRA sites with very short periods of record, a regionally-tuned regression analysis specific to undeveloped Texas watersheds was used. Six equations given in Asquith and Thompson (2008) to estimate the 2-, 5-, 10-, 25-, 50-, and 100-year flood magnitudes based on a power transformation of drainage area and three predictors (drainage area, channel slope, and mean annual precipitation) were applied to all study sites. Channel slope for these computations was selected for each site based on longitudinal profile data, not local survey data, because regression equations are designed to capture watershed-scale influences on peak discharge (Asquith and Slade 1997). The channel slope values selected for regression-based analysis at USGS streamflow-gaging stations closely correspond with values in Asquith and Slade (1997) (Table 6.5). Discharge values were compared to corresponding flow magnitudes computed by partial-duration analyses at gaged locations, and the regression-based results were less than the partial-duration analyses (Figure 6.6). Based on a $\log_{10}$-transformation of the partial-duration and regression-derived discharge values, the average residual standard error ($\log_{10}$) for each return period was computed (0.3706, 0.3444, 0.3221, 0.2974, 0.2782, and 0.2595 for the 2-, 5-, 10-, 25-, 50-, and 100-year return periods, respectively) and these scale factors were applied to regression-based results (Asquith and Thompson 2008) at ungaged sites in the Llano River watershed (Table 6.4).

Table 6.4. Flood magnitudes at various return periods for gaged and ungaged sites in the Llano River watershed, Central Texas, based on partial-duration and regionally-tuned regression analyses.

[m^3/s, cubic meters per second; --, not available]

Site	Return period									
	1-year (m^3/s)	1.5-year (m^3/s)	2-year (m^3/s)	3-year (m^3/s)	4-year (m^3/s)	5-year (m^3/s)	10-year (m^3/s)	25-year (m^3/s)	50-year (m^3/s)	100-year (m^3/s)
North Llano Draw near Sonora[a]	--	--	14	--	--	30	45	66	84	103
North Llano River near Roosevelt[a]	--	--	283	--	--	638	970	1,484	1,929	2,426
North Llano River near Junction[b]	171	355	519	780	979	1,138	1,648	2,329	2,838	3,336
South Llano River at Baker Ranch near Rocksprings[a]	--	--	134	--	--	290	433	651	838	1,045
South Llano River at U.S. Highway 377 near Rocksprings[a]	--	--	272	--	--	589	879	1,321	1,698	2,115
South Llano River at 700 Springs Ranch near Telegraph[a]	--	--	305	--	--	660	984	1,478	1,900	2,367
South Llano River at South Llano River State Park[a]	--	--	424	--	--	915	1,363	2,042	2,623	3,265
South Llano River at Texas Tech University—Junction[a]	--	--	426	--	--	919	1,369	2,051	2,634	3,278
Llano River near Junction[b]	242	488	710	1,076	1,369	1,613	2,459	3,772	4,914	6,193
LCRA Johnson Fork near Junction[a]	--	--	251	--	--	563	854	1,302	1,689	2,120
Johnson Fork at Lowlands Crossing near Junction[a]	--	--	255	--	--	572	867	1,322	1,715	2,153
Llano River near Ivy Chapel[a]	--	--	734	--	--	1,481	2,137	3,105	3,914	4,796
LCRA James River near Mason[a]	--	--	312	--	--	717	1,099	1,694	2,212	2,793
James River near Mason[a]	--	--	320	--	--	736	1,127	1,738	2,269	2,865
Llano River at James River Crossing near Mason[a]	--	--	1,047	--	--	2,160	3,145	4,613	5,850	7,204
Llano River near Mason[b]	428	793	1,111	1,635	2,057	2,412	3,675	5,738	7,638	9,879
Beaver Creek near Mason[b]	107	173	227	314	383	440	645	984	1,302	1,686
Llano River at Castell[a]	--	--	1,221	--	--	2,492	3,609	5,264	6,654	8,171
Llano River at Llano[b]	503	928	1,302	1,895	2,345	2,707	3,871	5,456	6,664	7,871
Llano River near Kingsland[a]	--	--	1,450	--	--	2,925	4,211	6,106	7,693	9,418
Honey Creek at KDK Ranch near Kingsland[a]	--	--	75	--	--	194	315	514	694	902

[a] Flood magnitudes computed by regionally-tuned regression analysis.
[b] Flood magnitudes computed by partial-duration analysis.

Table 6.5. Values used in regression-based flood-frequency equations (Asquith and Thompson 2008) based on a power transformation of drainage area and three predictors (drainage area, channel slope, and mean annual precipitation). Channel slope values are compared to published values in Asquith and Slade (1997) to ensure correct application.

[km^2, square kilometers; mm, millimeters]

Site	Drainage area (km^2)	Mean annual precipitation (mm)	Channel slope	Asquith and Slade (1997) channel slope
08148500 North Llano River near Junction, Texas	2,335	635	0.0021	0.0022
08150000 Llano River near Junction, Texas	4,815	635	0.0011	0.0019
08150700 Llano River near Mason, Texas	8,418	711	0.0015	0.0017
08150800 Beaver Creek near Mason, Texas	558	711	0.0034	0.0049
08151500 Llano River at Llano, Texas	10,885	737	0.0015	0.0016

a Number of samples for cobble- and gravel-sized material is equated to an individual placement of the sampling grid (or approximately 25 individual clasts).

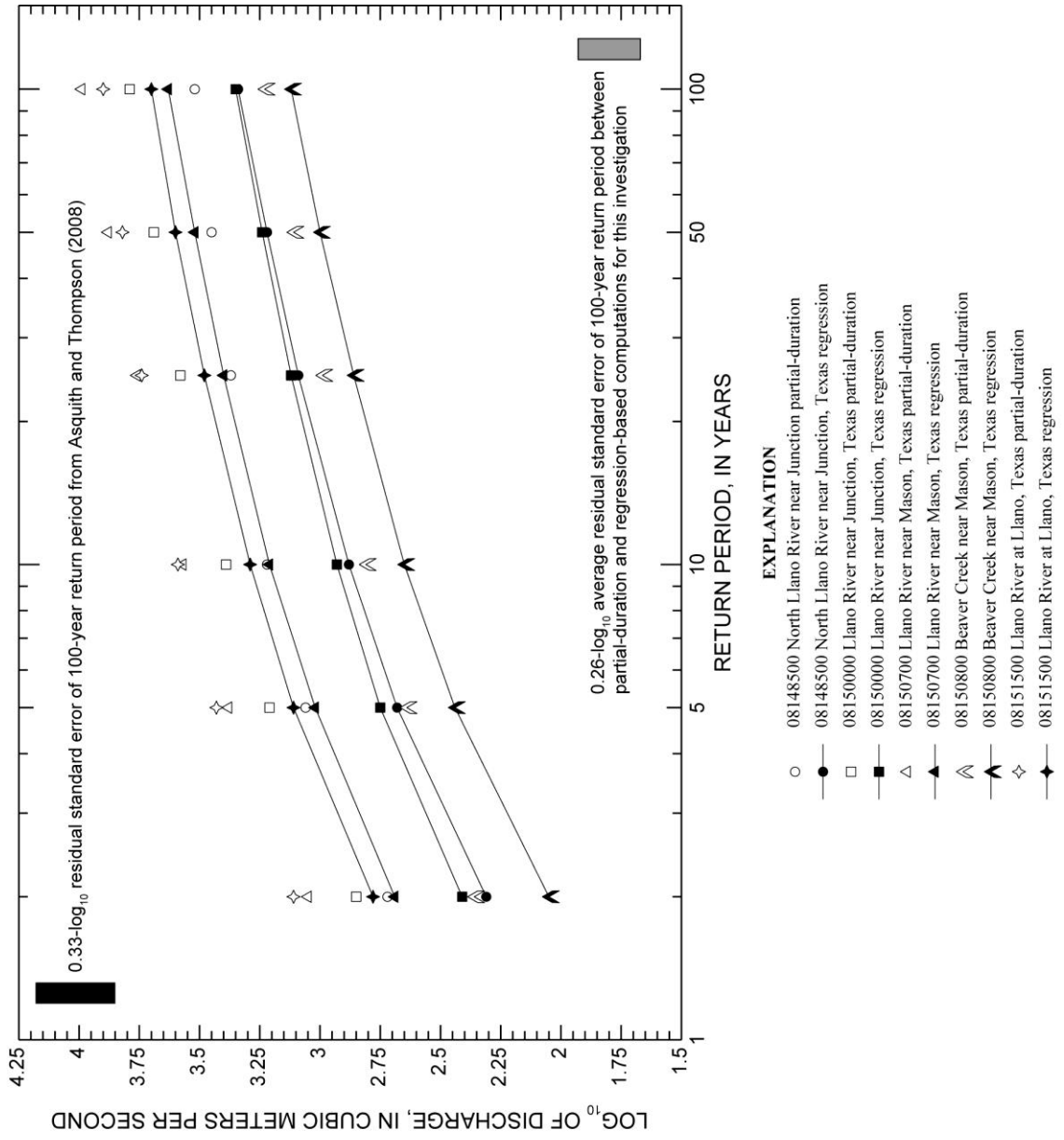

Figure 6.6. Comparison of discharge values computed by partial-duration flood-frequency and Asquith and Thompson (2008) regression-based flood-frequency analyses for selected USGS streamflow-gaging stations in the Llano River watershed in Central Texas.

6.6 Results

Observations and quantification of channel geometry, boundary composition, and hydraulic variables at sites in the Llano River watershed are provided as follows in general order from upstream to downstream. Using GIS and field observations, channels are classified into four general categories based on hydrology, planform morphology, lithology, and alluvial development: (1) uppermost ephemeral reaches, commonly referred to as “draws” in the study area, (2) Cretaceous straight or sinuous gravel-bed channels, (3) Paleozoic straight or sinuous gravel-bed or bedrock channels, and (4) Precambrian straight, braided, or bedrock-braided sand-bed channels (Table 6.6, Figure 6.7). Various morphometric and sedimentary characteristics for individual study sites are provided in Table 6.1. Values of selected hydraulic parameters and at-a-station hydraulic geometry exponents are provided in Tables 6.7 and 6.8.

Table 6.6. Percentage of channel length classified into various geomorphic categories, based on hydrology, planform morphology, lithology, and alluvial development.

[km, kilometers; %, percent]

River	Channel length (km)	Classification and percentage of length	Sum of channel segment lengths (km)
North Llano River	95.6	29.6% ephemeral aggraded	28.3
		14.4% ephemeral bedrock incised	13.8
		44.0% partly-confined Cretaceous sinuous	42.0
		12.0% partly-confined Cretaceous straight	11.5
South Llano River	115	45.6% ephemeral aggraded	52.4
		14.6% ephemeral bedrock incised	16.8
		25.7% partly-confined Cretaceous sinuous	29.6
		14.1% partly-confined Cretaceous straight	16.2
Llano River	187	2.1% confined Cretaceous	3.9
		18.3% partly-confined Cretaceous sinuous	34.2
		12.7% confined Paleozoic bedrock	23.8
		4.4% partly-confined Paleozoic sinuous	8.2
		10.1% confined Paleozoic straight	18.9
		10.9% Precambrian braided	20.4
		13.3% Precambrian bedrock-braided	24.9
		24.6% Precambrian straight	46.0
		3.6% Lake LBJ	6.7

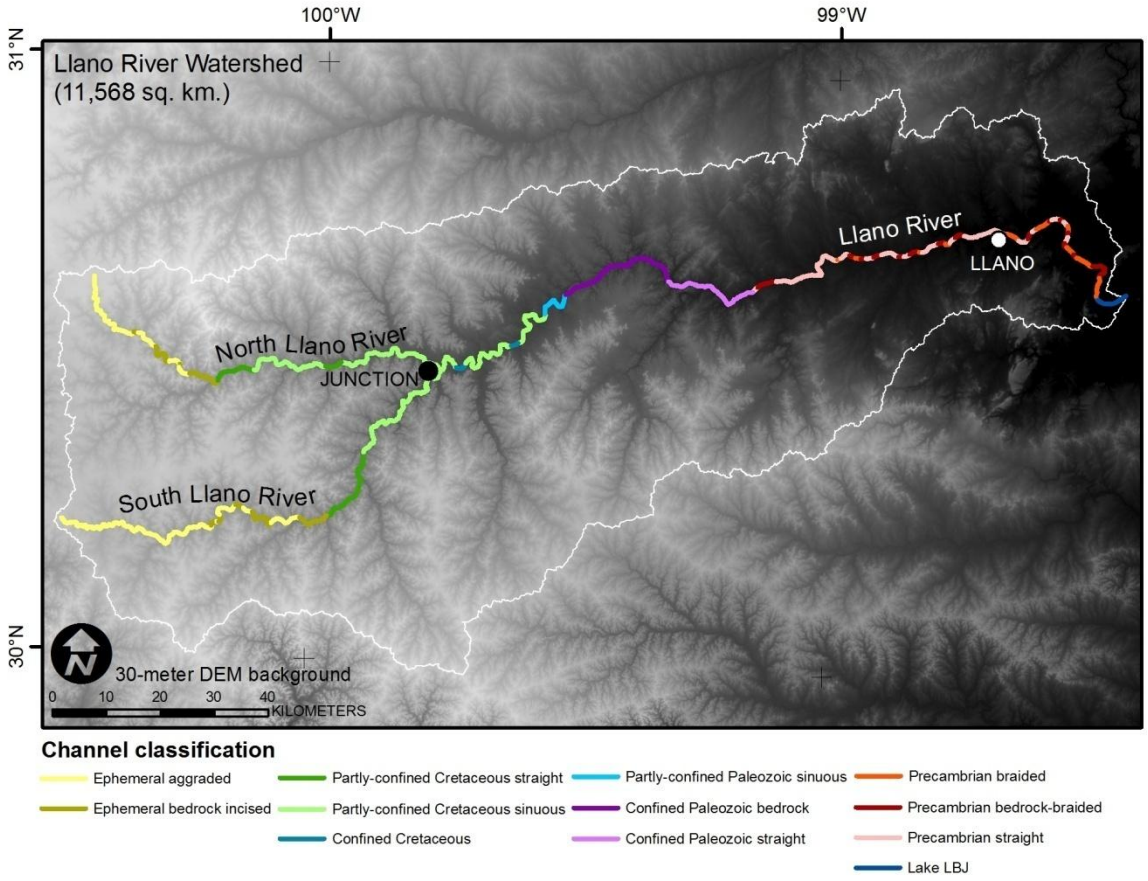

Figure 6.7. The Llano River in Central Texas is classified into four general geomorphic categories: (1) uppermost ephemeral reaches, commonly referred to as "draws" in the study area, (2) Cretaceous straight or sinuous gravel-bed channels, (3) Paleozoic straight or sinuous gravel-bed or bedrock channels, and (4) Precambrian straight, braided, or bedrock-braided sand-bed channels. Straight or sinuous channels are determined by an alluvial sinuosity threshold of 1.1 irrespective of bends in the valley.

Table 6.7. Selected hydraulic characteristics for bankfull stage at study sites in the Llano River watershed in Central Texas. Various LCRA sites are not included if cross-sectional geometry measurements contain bridge-construction features, including concrete aprons and artificial embankments. Values represent averages of multiple cross sections.

[BF Q, bankfull discharge; m^3/s, cubic meters per second; BF Ω, bankfull stream power; W/m, watts per meter; BF ω, bankfull unit stream power; W/m^2, watts per square meter; BF w, bankfull width; m, meters; BF d, bankfull mean depth; BF U, bankfull mean velocity; m/s, meters per second; b, at-a-station hydraulic geometry exponent for bankfull width; f, at-a-station hydraulic geometry exponent for bankfull mean depth; m, at-a-station hydraulic geometry exponent for bankfull mean velocity; --, not available]

Site	BF Q (m^3/s)	BF Ω (W/m)	BF ω (W/m^2)	BF w (m)	BF d (m)	BF U (m/s)	b	f	m
North Llano Draw near Sonora[a]	--	--		--	--	--	--	--	--
North Llano River near Roosevelt[b]	494	10,200	142	71.8	3.05	2.06	0.42	0.39	0.19
North Llano River near Junction[b]	536	15,200	142	107	2.44	2.19	0.47	0.36	0.18
South Llano River at Baker Ranch near Rocksprings[b]	37.1	545	6.47	84.2	0.62	0.78	0.48	0.34	0.18
South Llano River at U.S. Highway 377 near Rocksprings[b]	157	5,520	175	31.6	2.01	2.20	0.22	0.52	0.26
South Llano River at 700 Springs Ranch near Telegraph[b]	556	16,300	139	117	2.21	2.12	0.34	0.44	0.22
South Llano River at South Llano River State Park[b]	382	4,490	25.7	175	1.99	1.25	0.47	0.35	0.21
South Llano River at Texas Tech University—Junction[b]	351	4,820	31.5	153	1.79	1.31	0.38	0.41	0.21
LCRA Johnson Fork near Junction[b]	606	15,400	167	92.1	2.90	2.27	0.34	0.44	0.22
Johnson Fork at Lowlands Crossing near Junction[b]	350	18,200	180	101	1.49	2.32	0.46	0.36	0.18
LCRA James River near Mason[b]	371	12,300	119	103	1.78	2.03	0.30	0.47	0.23
Llano River at James River Crossing near Mason[b]	1,180	28,900	191	151	3.22	2.33	0.32	0.45	0.23
Llano River near Mason[b]	594	14,600	127	115	2.50	2.05	0.27	0.48	0.24
Beaver Creek near Mason[b]	193	5,850	89.6	65.3	1.57	1.82	0.38	0.41	0.21
Llano River at Castell[b]	906	11,500	82.1	140	3.57	1.78	0.20	0.53	0.27
Llano River at Llano[b]	970	13,300	80.6	165	3.31	1.78	0.36	0.43	0.21
Llano River near Kingsland[b]	778	20,600	89.6	230	1.83	1.84	0.46	0.36	0.18
Honey Creek at KDK Ranch near Kingsland[c]	25.3	5,530	205	27.0	0.73	1.30	0.27	0.49	0.24

[a] No data provided for North Llano Draw near Sonora because a definable channel is not present.
[b] Bankfull discharge, stream power, mean velocity, and hydraulic geometry exponents computed from hydraulic analyses using a Darcy-Weisbach f factor of 0.115.
[c] Bankfull discharge, stream power, mean velocity, and hydraulic geometry exponents computed from hydraulic analyses using a Darcy-Weisbach f factor of 0.750.

Table 6.8. Selected hydraulic characteristics for macro-channels at study sites in the Llano River watershed in Central Texas. Values represent averages of multiple cross sections, if more than one cross section was available for the macro-channel. Values are not comparable with one another because they represent individual heights above bankfull stage, and do not necessarily extend to the top of the macro-channel.

[BF, bankfull stage; m, meters; Q, discharge; m^3/s, cubic meters per second; Ω, stream power; W/m, watts per meter; ω, bankfull unit stream power; W/m^2, watts per square meter; w, width; d, mean depth; U, mean velocity; m/s, meters per second; b, at-a-station hydraulic geometry exponent for width above bankfull stage; f, at-a-station hydraulic geometry exponent for mean depth above bankfull stage; m, at-a-station hydraulic geometry exponent for mean velocity above bankfull stage; --, no morphologic indicators of bankfull stage]

Site	Height above BF (m)	Q (m^3/s)	Ω (W/m)	ω (W/m^2)	w (m)	d (m)	U (m/s)	b	f	m
Llano River near Junction[a]	--[b]	2,400	167,000	1,800	93.0	5.33	5.07	0.23	0.51	0.26
Llano River near Ivy Chapel[a]	--[b]	2,360	34,700	208	167	5.75	2.43	0.35	0.43	0.22
LCRA James River near Mason[a]	2.7[b]	1,520	50,600	386	131	3.88	3.00	0.16	0.56	0.28
James River near Mason[a]	--[b]	5,410	313,000	1,750	179	6.04	4.92	0.18	0.55	0.27
Llano River at James River Crossing near Mason[a]	3.9[b]	4,130	101,000	409	247	5.48	3.06	0.24	0.50	0.25
Llano River near Mason[a]	7.1[b]	4,570	112,000	463	242	5.91	3.17	0.40	0.40	0.20
Beaver Creek near Mason[a]	3.4[c]	947	28,700	293	97.9	3.54	2.74	0.26	0.49	0.25
Llano River at Castell[a]	5.0[c]	3,720	47,300	190	249	6.31	2.37	0.43	0.38	0.19
Llano River at Llano[a]	4.9[b]	6,040	82,900	287	289	7.70	2.71	0.32	0.45	0.23
Llano River near Kingsland[a]	3.6[c]	3,690	97,600	330	296	4.39	2.84	0.20	0.53	0.27
Honey Creek at KDK Ranch near Kingsland[d]	2.5[b]	286	62,500	1,280	48.9	2.47	2.40	0.21	0.53	0.26

[a] Discharge, stream power, mean velocity, and hydraulic geometry exponents computed from hydraulic analyses using a Darcy-Weisbach f factor of 0.115.
[b] Top of macro-channel.
[c] Below top of macro-channel.
[d] Discharge, stream power, mean velocity, and hydraulic geometry exponents computed from hydraulic analyses using a Darcy-Weisbach f factor of 0.750.

6.6.1 Ephemeral Draws

The uppermost ephemeral draws of the North and South Llano Rivers occur near the top of the Edwards Plateau. Three study sites are considered representative of this category: (1) North Llano Draw near Sonora, (2) South Llano River at Baker Ranch near Rocksprings, and (3) South Llano River at U.S. Highway 377 near Rocksprings. Although all three are characterized by flow occurring only during storm-driven runoff events, considerable morphologic differences between them can be attributed to increasing hydraulic energy associated with drainage area. Therefore, two sub-categories of ephemeral draws are defined by the author: (1) ephemeral aggraded and (2) ephemeral bedrock incised (Table 6.6, Figure 6.7).

Ephemeral aggraded channels are characterized by fine-grained (silt and clay) bed and bank deposits that have subtle topographic transitions to surrounding valley fill deposits. Discontinuous pools, often containing ponded water and varying proportions of angular cobbles in the bed, interrupt dry channel reaches and are readily distinguished from the surrounding valley fill. After approximately 20 kilometers of downstream distance, the North and South Llano Rivers develop alluvial valleys ranging from about 250 to 750 meters wide, and a sinuous channel ranges from approximately 75 to 100 meters wide. Fine-grained valley fill deposits along ephemeral aggraded reaches are attributed to extensive upland soil erosion during the early and middle Holocene (Cooke et al. 2003) that filled valleys incised at the terminus of the Pleistocene epoch (Blum, Toomey, and Valastro 1994; Mear 1995). As drainage area

and downstream distance increase, the ephemeral draws have enough stream power during runoff events to remove fine-grained sediment and incise the carbonate plateau, and bedrock exposures are numerous.

Ephemeral bedrock incised draws have relatively narrow valleys, ranging between 50 and 250 meters, and narrow straight channels, ranging from about 25 to 75 meters wide. They are characterized by step-like bedrock banks that descend to a bedrock bed with limited cobble- and gravel-sized deposits, and form a transition from channels along the top of the plateau to those with incised valleys.

EXAMPLE LOCALITY: The South Llano River at Baker Ranch near Rocksprings is a good example of an ephemeral aggraded channel in the Llano River watershed (Figure 6.8). The site occurs 29.5 kilometers downstream of the uppermost South Llano River headcut, and has a drainage area of 417 square kilometers. A sinuous, fine-grained channel with discontinuous pools and isolated deposits of angular cobbles occurs in a valley ranging between 400 and 415 meters wide. The bankfull stage of the channel is identified by a gentle break in slope and an abrupt transition to open woodland. Based on hydraulic analyses of four cross sections at the site, including one with a pool, bankfull discharge is 37.1 cubic meters per second. According to regionally-tuned regression analyses, bankfull discharge has a return period much less than 2 years (Tables 6.4, 6.7). At-a-station hydraulic geometry analyses for bankfull stage indicate that channel width (b = 0.48) compensates for increasing discharge at a greater rate than mean channel depth (f = 0.34) because b is greater than f.

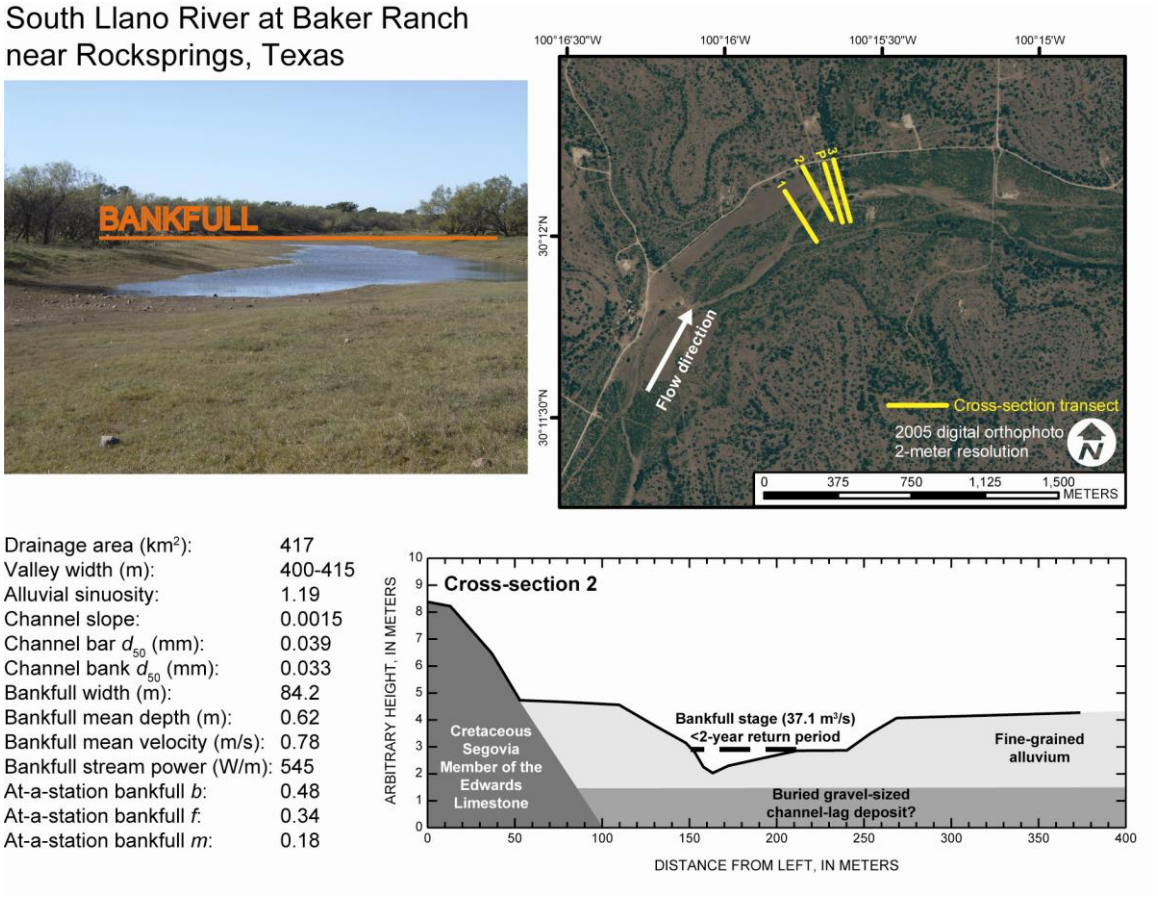

Figure 6.8. The South Llano River at Baker Ranch near Rocksprings, Texas, is representative of ephemeral aggraded channels in the uppermost Llano River watershed. The fine-grained (silt and clay), sinuous channel gently transitions into surrounding valley-fill deposits. The top-left picture is looking upstream from cross-section 2. At-a-station hydraulic geometry analyses at bankfull stage indicate that the rate of change of channel width (b = 0.48) is greater than that of mean depth (f = 0.34). Based on hydraulic analyses of all cross sections, bankfull discharge is 37.1 cubic meters per second and has a return period less than 2 years.

6.6.2 Cretaceous Gravel-Bed Channels

Incised bedrock ephemeral draws transition to perennial, partly-confined straight or sinuous channels at karstic springs along the North Llano and South Llano Rivers. Near the confluence of the North Llano and Dry Llano Rivers, springs contribute perennial flow and drainage area increases, which forms a wider alluvial valley. Upstream of the confluence of Paint Creek and the South Llano River, springs contribute perennial flow and drainage area increases, and the alluvial valley continues to widen. In addition to Paint Creek, Bear Creek and Johnson Fork are considered major tributaries in this zone of the watershed. Bankfull channel widths range from about 75 to 175 meters with channel widths generally increasing downstream. Eight study sites are considered representative of this category: (1) North Llano River near Roosevelt, (2) North Llano River near Junction, (3) South Llano River at 700 Springs Ranch near Telegraph, (4) South Llano River at South Llano River State Park, (5) South Llano River at Texas Tech University—Junction, (6) Llano River near Junction, (7) Johnson Fork at Lowlands Crossing near Junction, and (8) Llano River near Ivy Chapel. Although the eight sites are characterized by mostly perennial flow and cobble- to gravel-sized bed material, morphologic differences between them can be attributed to alluvial sinuosity and relative confinement by bedrock valley walls. Therefore, three sub-categories of Cretaceous gravel-bed channels are defined by the author: (1) partly-confined straight, (2) partly-confined sinuous, and (3) confined (Table 6.6, Figure 6.7).

Partly-confined straight channels are characterized by an alluvial sinuosity less than 1.1 and have beds comprised of cobble- to gravel-sized bed material or bedrock. Banks are either gradually sloping where coarse channel-lag deposits are dominant or steep where overbank fine-grained material is dominant. At some sites, steep bedrock valley walls occur along one side of the channel. Alluvial valleys of straight channels are relatively narrow (200 to 400 meters) and are comprised of cobble- to gravel-sized lag deposits capped with fine-grained overbank sediment. As the North and South Llano Rivers approach Junction, drainage area exceeds 2,000 square kilometers and the alluvial valley widens at some locations to greater than 1.5 kilometers. Sinuous cobble- to gravel-bed channels occur within a Holocene floodplain surrounded by earlier terrace deposits, and frequently occurring longitudinal channel bars occur alongside the low-flow (thalweg) channel.

Partly-confined sinuous channels are characterized by an alluvial sinuosity greater than 1.1 and banks are comprised of various combinations of coarse channel lag deposits, fine-grained overbank deposits, or sand contributed from exposures of the Hensell Sands. Channel banks gently slope on the convex side of gradual meander bends or where the sand percentage is high, or steeply slope on the concave side of gradual meander bends or where the sand percentage is low. Downstream of Junction, the Llano River exhibits enlarged meander bends, similar to those documented in a neighboring watershed by Blum and Valastro (1989). These bends are attributed to relatively humid conditions between 4,500 and 1,000 years B.P.

Confined cobble- to gravel-bed channels in the Cretaceous zone of the watershed occur along two reaches of the Llano River and correspond with the study sites near Junction and Ivy Chapel. The alluvial valley narrows at these two locations to less than 500 meters and bedrock valley walls are comprised of the Hensell Sand unit. At the site near Junction, avulsion through the bedrock exposure results in a completely confined channel less than 100 meters wide. Bedrock also is exposed along the channel bed and banks, and alluvial banks are associated with narrow inset floodplains.

EXAMPLE LOCALITY: The North Llano River near Junction is an example of a partly-confined sinuous channel (Figure 6.9) and is located at a USGS streamflow-gaging station. The site occurs 89.2 kilometers downstream of the uppermost North Llano River headcut, and has a drainage area of 2,335 square kilometers. A sinuous, cobble- to gravel-bed channel can be separated into a low-flow channel (thalweg) and longitudinal bars. The channel banks are comprised of fine-grained sandy alluvium, which thinly separates the channel from older terrace deposits and the Hensell Sand. Including the older fluvial terrace deposit, the valley ranges between 750 and 1,000 meters wide. The bankfull stage of the channel is identified by a break in slope and conspicuous inset floodplains along the right bank at cross-sections 1, 2, and 3, and fine-grained deposits on top of a mid-channel island at cross-section 0. Based on hydraulic analyses of four cross sections at the site, bankfull discharge is 536 cubic meters per second. According to partial-duration flood-frequency analyses, bankfull discharge has a return period of about 2 years (Tables 6.4, 6.7). At-a-station hydraulic

geometry analyses for bankfull stage indicate that channel width (b = 0.47) compensates for increasing discharge at a greater rate than mean channel depth (f = 0.36).

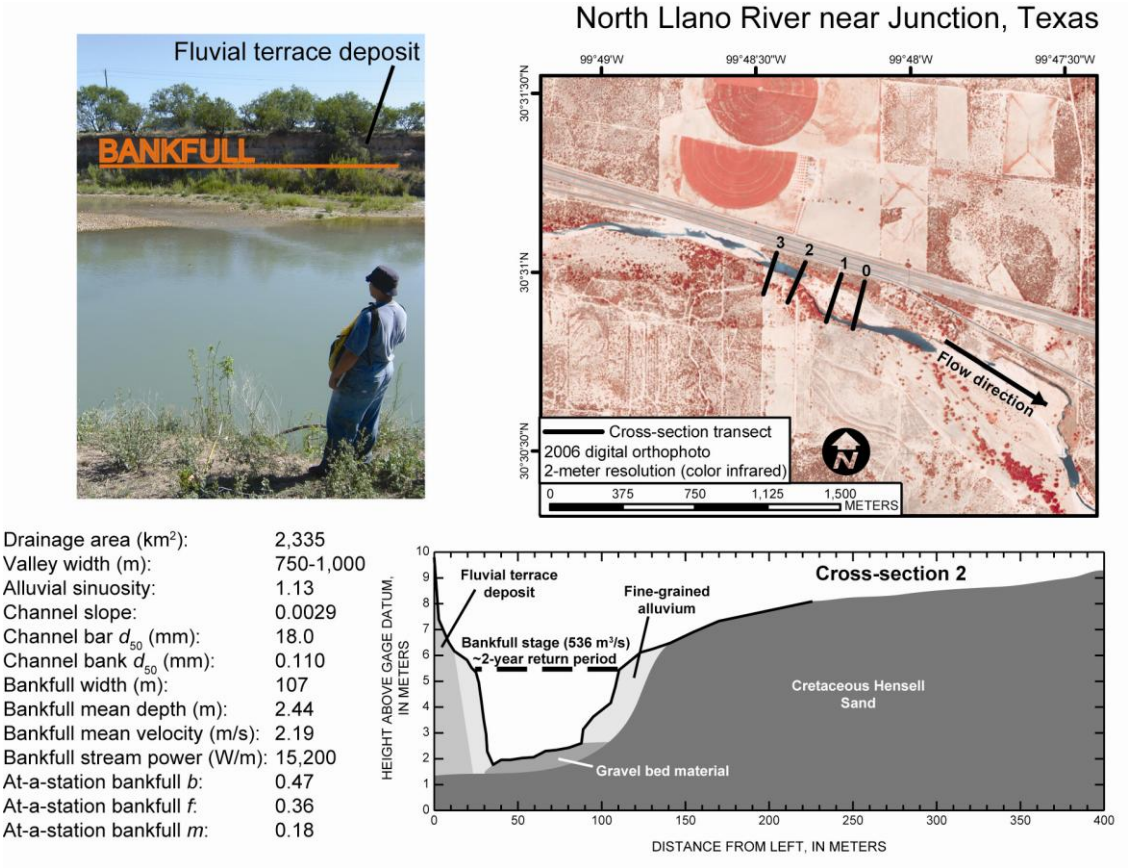

Figure 6.9. The North Llano River near Junction, Texas, is representative of partly-confined sinuous channels in the Cretaceous zone of the Llano River watershed. The cobble- to gravel-bed channel has fine-grained sandy banks that thinly separate it from older terrace deposits and bedrock. The top-left picture is looking from the right bank toward the left bank at cross-section 3. At-a-station hydraulic geometry analyses at bankfull stage indicate that the rate of change of channel width (b = 0.47) is greater than that of mean depth (f = 0.36). Based on hydraulic analyses of all cross sections, bankfull discharge is 536 cubic meters per second and has a return period of about 2 years.

EXAMPLE LOCALITY: The South Llano River at Texas Tech University—Junction is another example of a partly-confined sinuous channel (Figure 6.10), but occurs in a wider alluvial valley than the North Llano River near Junction. The site occurs 110 kilometers downstream of the uppermost South Llano River headcut, and has a drainage area of 2,271 square kilometers. A sinuous, cobble- to gravel-bed channel can be separated into a low-flow channel (thalweg) and longitudinal bars. The channel banks are mostly comprised of fine-grained sandy alluvium, and channel-lag deposits of cobble- to gravel-sized material are prominent near the base. Including fluvial terrace deposits, the valley ranges from 1.3 to 1.6 kilometers wide. The bankfull stage of the channel is identified by breaks in slope on both banks, which separate the channel from horizontally-level, fine-grained floodplains. Hydraulic analyses of four cross sections at the site indicate that bankfull discharge is 351 cubic meters per second. According to regionally-tuned regression analyses, bankfull discharge has a return period less than 2 years (Tables 6.4, 6.7). At-a-station hydraulic geometry analyses for bankfull stage indicate that mean channel depth (f = 0.41) compensates for increasing discharge at a slightly greater rate than channel width (b = 0.38).

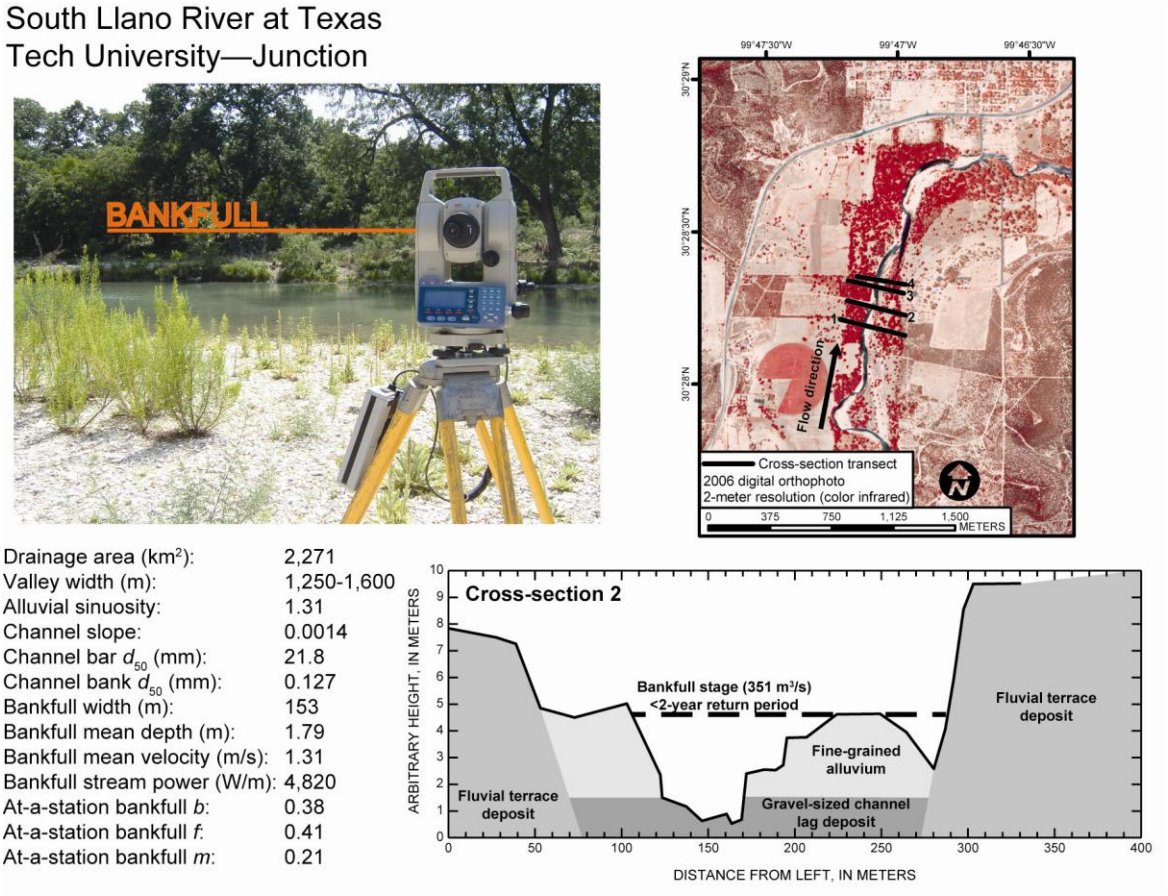

Figure 6.10. The South Llano River at Texas Tech University—Junction, Texas, is representative of partly-confined sinuous channels in the Cretaceous zone of the Llano River watershed. The cobble- to gravel-bed channel has fine-grained sandy banks with cobble- to gravel-sized channel lag deposits at the base. The top-left picture is looking toward the left bank at cross-section 4. At-a-station hydraulic geometry analyses at bankfull stage indicate that the rate of change of mean depth (f = 0.41) is slightly greater than that of channel width (b = 0.38). Based on hydraulic analyses of all cross sections, bankfull discharge is 351 cubic meters per second and has a return period of less than 2 years.

EXAMPLE LOCALITY: The Llano River near Ivy Chapel is an example of a confined channel in the Cretaceous zone of the watershed (Figure 6.11). The site occurs 25 kilometers downstream of the confluence of the North Llano and South Llano Rivers, and has a drainage area of 5,939 square kilometers. The cobble- to gravel-bed and bedrock channel is confined to an alluvial valley less than 500 meters wide for a distance of about 1.5 kilometers, but the channel is sinuous just upstream and downstream of this constriction. The channel can be separated into a low-flow channel (thalweg) and longitudinal bars, and the right bedrock bank juxtaposes with a left bank comprised of mostly silt- and sand-sized material. The distinct break in slope at the top of the left bank is about 10 meters above the channel bed, which is approximately twice the height of alluvial banks along the North and South Llano Rivers. At this stage, discharge is 2,360 cubic meters per second based on hydraulic analyses of three cross sections. According to regionally-tuned regression analyses, this discharge has a return period of about 12 years (Tables 6.4, 6.8). The Llano River near Ivy Chapel is considered an example of a macro-channel, and little to no evidence indicates that channel shape adjusts to flows with return periods less than 5 years. Other hydraulic computations, however, indicate that the channel bed adjusts during more frequent flows with return periods between 1 and 2 years (Heitmuller and Asquith 2008). At-a-station hydraulic geometry analyses for macro-channel stage indicate that mean channel depth (f = 0.43) compensates for increasing discharge at a greater rate than channel width (b = 0.35).

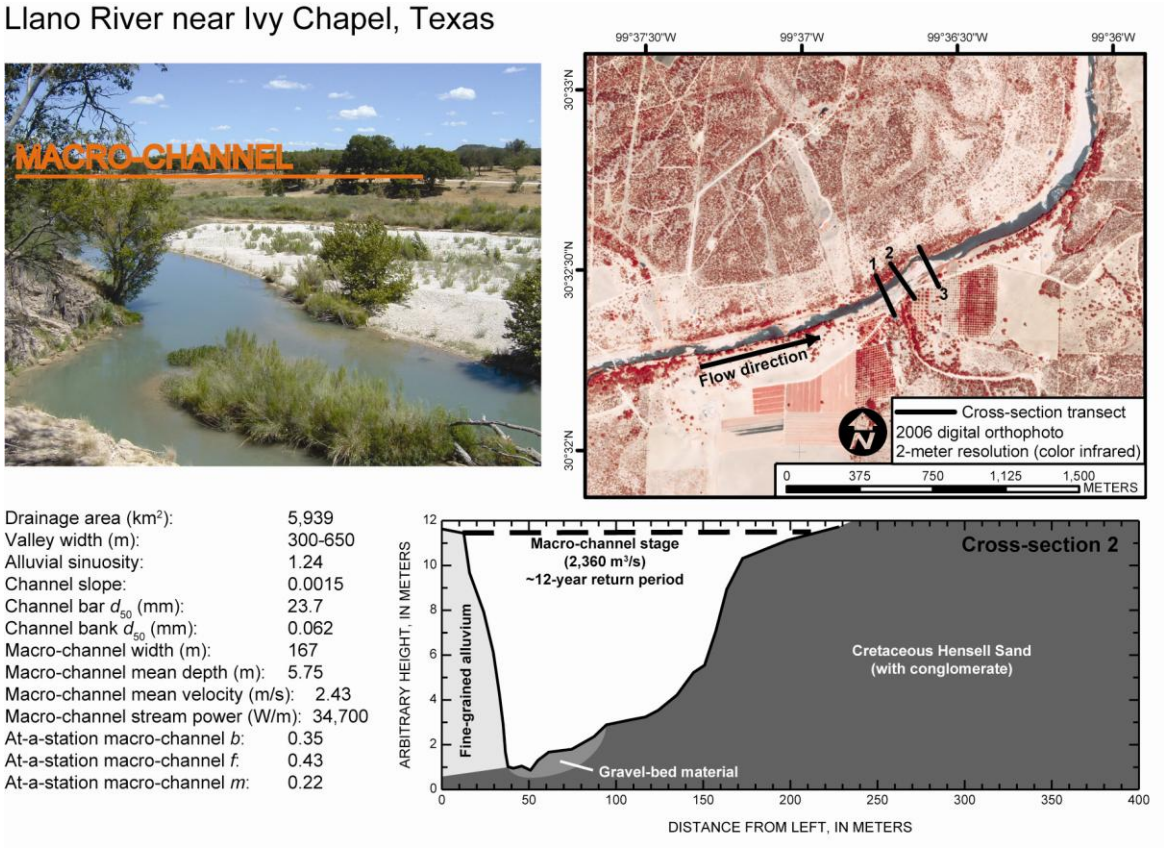

Figure 6.11. The Llano River near Ivy Chapel, Texas, is representative of confined channels in the Cretaceous zone of the Llano River watershed. The cobble- to gravel-bed channel has a fine-grained left bank comprised mostly of silt and sand and a right bank comprised of bedrock. The top-left picture is looking downstream from the left bank at cross-section 3. At-a-station hydraulic geometry analyses at macro-channel stage indicate that the rate of change of mean depth (f = 0.43) is greater than that of channel width (b = 0.35). Based on hydraulic analyses of all cross sections, macro-channel discharge is 2,360 cubic meters per second and has a return period of about 12 years.

6.6.3 Paleozoic Channels (Bedrock and Gravel-Bed)

As the Llano River enters the Paleozoic sedimentary zone the valley becomes more confined, and following a brief sinuous phase the channel becomes remarkably straight. The alluvial sinuosity effectively is reduced to 1.00 because the channel boundary consists entirely of bedrock. Observed bends in the channel pattern are attributed to preferentially weathered joints or fractures in the bedrock. Cobble- to gravel-sized bar deposits are less frequent and occur in hydraulically favorable areas, including the convex side of very gradual bends or at tributary confluences. Bankfull width is about 150 meters, and macro-channel width is about 250 meters along the main-stem Llano River. The James River is a major tributary in the Paleozoic sedimentary zone of the watershed. Three study sites are considered representative of this category: (1) James River near Mason, (2) Llano River at James River Crossing near Mason, and (3) Honey Creek at KDK Ranch near Kingsland. Although most channel reaches are characterized by confined bedrock valleys and varying amounts of cobble- to gravel-sized bed material in this zone of the watershed, morphologic differences can be attributed to alluvial sinuosity and abundance of observed alluvial deposits. Therefore, three sub-categories of Paleozoic channels are defined by the author: (1) partly-confined sinuous, (2) confined bedrock, and (3) confined straight (Table 6.6, Figure 6.7).

Partly-confined sinuous reaches are characterized by an alluvial sinuosity greater than 1.1, and are associated with about 8 kilometers of the Llano River

downstream of the Cretaceous-Paleozoic contact. The valley width gradually reduces along this reach, and Pennsylvanian limestone and shale units are exposed at the surface. The sinuous reaches in this sub-category mark the downstream extent of enlarged meander bends (Blum and Valastro 1989) observed along the Llano River in the Cretaceous zone.

Confined bedrock reaches in the Paleozoic zone are remarkably straight and channel boundaries are comprised of Ordovician-aged carbonate sequences. A few limited inset floodplains and channel-bar deposits are observed along bedrock reaches, but overall the channel is hydraulically efficient and transports sediment to downstream reaches.

Confined straight reaches begin at the location where the Llano River exits the Ordovician-aged bedrock and enters a zone of Cambrian siltstone, carbonate, and sandstone. Downstream of this contact, the alluvial valley widens to about 300 to 500 meters. Cobble- to gravel-sized channel-bar deposits and fine-grained inset floodplains become more numerous, and alluvial sinuosity slightly increases but remains less than 1.1.

EXAMPLE LOCALITY: The Llano River at James River Crossing near Mason is an example of a confined straight channel in the Paleozoic zone of the watershed (Figure 6.12). The site occurs 78 kilometers downstream of the confluence of the North Llano and South Llano Rivers, and has a drainage area of 8,032 square kilometers. The cobble- to gravel-bed and bedrock channel is confined to an alluvial valley less than 500

meters wide, and valley walls are comprised of Cambrian sandstone. The channel can be separated into two low-flow channels (thalwegs) around a large mid-channel bar comprised of cobble- to gravel-sized material with considerable quantities of sand. The large channel bar, about 500 meters long, 250 meters wide, and 5 meters above the thalweg, nearly constitutes an island by virtue of its vertical extent and is associated with considerable quantities of sediment delivered by the James River. Permanent vegetation, however, is not established on the bar surface and, therefore, should not be considered an island. At the top of the mid-channel bar, discharge is 1,180 cubic meters per second based on hydraulic analyses of three cross sections. According to regionally-tuned regression analyses, this discharge has a return period of about 2.5 years (Tables 6.4, 6.7) and is considered synonymous with bankfull conditions along the sinuous reaches in the Cretaceous zone of the watershed.

To confirm hydraulic and flood-frequency regression analyses at this site, high-water marks associated with a March 2007 flow were simultaneously surveyed with cross-section topography. The computed discharge of 325 cubic meters per second for this event has an estimated return period much less than 2 years (Table 6.4), and is comparable to the peak discharge (396 cubic meters per second) and return period of about 1 year computed by partial-duration analyses of USGS streamflow data for the same event downstream at the Llano River near Mason. For the stage associated with the top of the mid-channel bar, at-a-station hydraulic geometry analyses indicate that

mean channel depth (f = 0.45) compensates for increasing discharge at a greater rate than channel width (b = 0.32).

Well-defined inset floodplains along the left and right sides of the Llano River at James River Crossing near Mason are readily distinguished from the channel by breaks in slope along the sandy banks and are about 10 meters above the channel bed (Figure 6.12). At the 10-meter stage, discharge is 4,130 cubic meters per second based on hydraulic analyses of three cross sections. According to regionally-tuned regression analyses, this discharge has a return period of about 20 years (Tables 6.4, 6.8), therefore the height of the inset floodplain demarcates the extent of a macro-channel. At-a-station hydraulic geometry analyses between bankfull and macro-channel stages indicate that mean channel depth (f = 0.50) compensates for increasing discharge at a greater rate than channel width (b = 0.24).

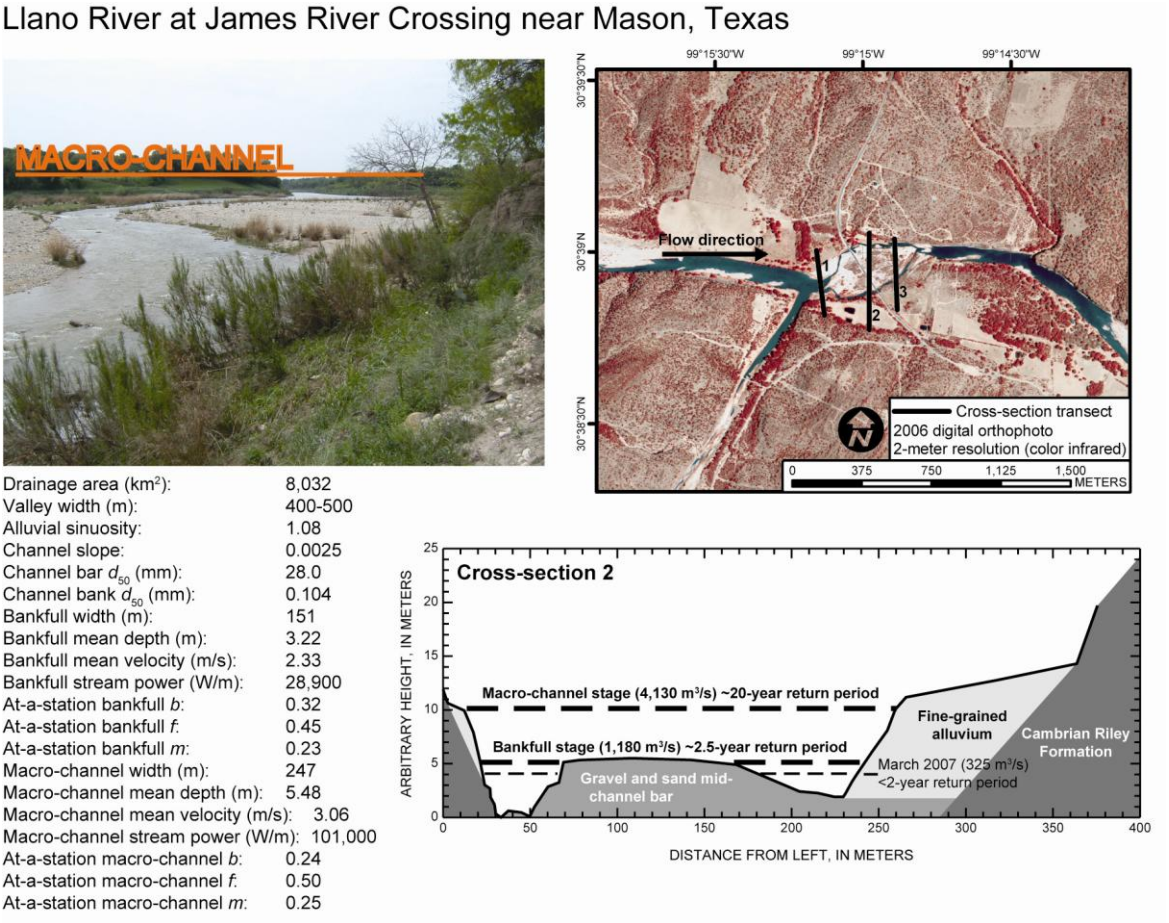

Figure 6.12. The Llano River at James River Crossing near Mason, Texas, is representative of straight channels in the Paleozoic zone of the Llano River watershed. The cobble- to gravel-bed and bedrock channel has a mid-channel bar comprised of cobble- to gravel-sized and sandy material, and the top of the bar is synonymous with bankfull conditions along sinuous reaches in the Cretaceous zone of the watershed. At-a-station hydraulic geometry analyses at bankfull stage indicate that the rate of change of mean depth (f = 0.45) is greater than that of channel width (b = 0.32). Based on hydraulic analyses of all cross sections, bankfull discharge is 1,180 cubic meters per second and has a return period of about 2.5 years. Fine-grained inset floodplains demarcate the extent of a macro-channel. At-a-station hydraulic geometry analyses at macro-channel stage indicate that the rate of change of mean depth (f = 0.50) is greater than that of channel width (b = 0.24). Based on hydraulic analyses of all cross sections, macro-channel discharge is 4,130 cubic meters per second and has a return period of about 20 years. The top-left picture is looking upstream from the left bank at cross-section 2.

6.6.4 Precambrian Channels (Bedrock or Sand-Bed)

Planform morphology of the Llano River becomes more complex upon entering the Precambrian igneous and metamorphic zone of the watershed. Similar to reaches in the Paleozoic sedimentary zone, the valley is largely confined and alluvial sinuosity is 1.00 at most locations. Relatively weak joints or mineralogical seams in the surface bedrock are responsible for observed bends in the river. Increasing additions of sand to the channel result in braided reaches, and numerous irregular outcrops along the bed result in bedrock-braided reaches. Bankfull width ranges from 125 to 250 meters, and macro-channel width ranges from 250 to 450 meters along the main-stem Llano River. Beaver, Hickory, and San Fernando Creeks are major tributaries. Five study sites are considered representative of this category: (1) Llano River near Mason, (2) Beaver Creek near Mason, (3) Llano River at Castell, (4) Llano River at Llano, and (5) Llano River near Kingsland. Although most channel reaches are characterized by confined bedrock valleys and very low alluvial sinuosity in this zone of the watershed, morphologic differences can be attributed to channel-bed composition and the presence or absence of multi-thread low-flow channels. Therefore, three sub-categories of Precambrian channels are defined by the author: (1) braided, (2) bedrock-braided, and (3) straight (Table 6.6, Figure 6.7). A fourth sub-category, which is not discussed, is associated with the Llano arm of Lake LBJ, which is a reservoir along the Colorado River and coincides with the terminus of the Llano River.

Braided reaches are characterized by a sand-bed, multi-thread low-flow channel absent of Precambrian bedrock exposures along the channel bed. In total, braided reaches constitute 20.4 kilometers of the Llano River, and mostly occur downstream of Llano because of relatively voluminous amounts of sand in the channel.

Bedrock-braided reaches are characterized by a multi-thread low-flow channel with exposed, irregular outcrops of Precambrian bedrock along the channel bed. In total, bedrock-braided reaches constitute 24.9 kilometers of the Llano River, and are uniformly distributed along the channel in the Precambrian zone of the watershed.

Straight reaches are characterized by a sand-bed, single-thread channel with limited exposures of Precambrian bedrock along the channel bed. In total, straight reaches constitute 46.0 kilometers of the Llano River in the Precambrian zone of the watershed, and mostly occur upstream of Llano because the quantity of sand is insufficient to form exposed channel-bar deposits. All three types of reaches have limited inset floodplains comprised of sand, and channel banks commonly are exposed bedrock.

EXAMPLE LOCALITY: The Llano River at Llano is an example of a braided channel (Figure 6.13) and occurs at a USGS streamflow-gaging station (08151500). The site occurs 146 kilometers downstream of the confluence of the North Llano and South Llano Rivers and has a drainage area of 10,885 square kilometers. A low-flow control structure just upstream of the site creates a small water-supply reservoir for Llano, but does not regulate flow or sand transport during high-flow conditions. The structure,

however, might interrupt the continuous supply of sand-sized sediment to the reaches immediately downstream. The sand-bed channel has limited bedrock exposures along the bed, and valley walls are comprised of Precambrian Packsaddle Schist. Relatively subtle breaks in slope along the sandy left bank of cross-section 3 and right bank of cross-section 2 identify the conditions considered synonymous with bankfull stage observed at other sites along the river. At this stage, discharge is 970 cubic meters per second based on hydraulic analyses of three cross sections. According to partial-duration flood-frequency analyses, this discharge has a return period of about 1.5 years (Tables 6.4, 6.7). For the stage associated with bankfull conditions, at-a-station hydraulic geometry analyses indicate that mean channel depth (f = 0.43) compensates for increasing discharge at a greater rate than channel width (b = 0.36). Well-defined breaks in slope at the top of sandy inset floodplains along the left and right sides of the channel are about 12 meters above the bed. At this stage, discharge is 6,040 cubic meters per second based on hydraulic analyses of three cross sections. According to partial-duration flood-frequency analyses, this discharge has a return period of about 40 years (Table 6.4, 6.8). Based on these computations, the height of the inset floodplain demarcates the extent of a macro-channel. At-a-station hydraulic geometry analyses between bankfull and macro-channel stages indicate that mean channel depth (f = 0.45) compensates for increasing discharge at a greater rate than channel width (b = 0.32).

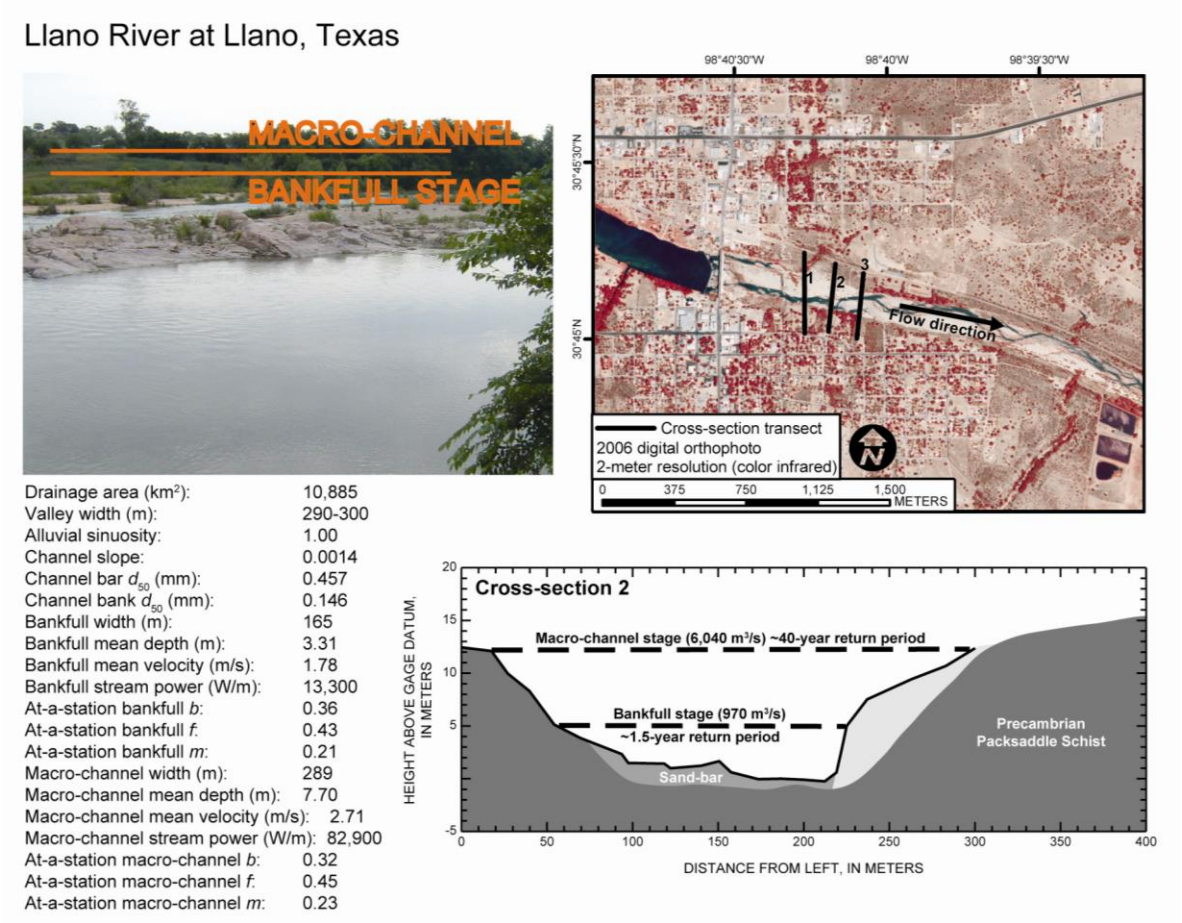

Figure 6.13. The Llano River at Llano, Texas, is representative of braided channels in the Precambrian zone of the Llano River watershed. The sand-bed channel has limited bedrock exposures along the bed, and a subtle break in slope along the channel bank is synonymous with bankfull conditions observed at other sites along the river. At-a-station hydraulic geometry analyses at bankfull stage indicate that the rate of change of mean depth (f = 0.43) is greater than that of channel width (b = 0.36). Based on hydraulic analyses of all cross sections, bankfull discharge is 970 cubic meters per second and has a return period of about 1.5 years. Distinct breaks in slope at the top of sandy inset floodplains demarcate the extent of a macro-channel. At-a-station hydraulic geometry analyses at macro-channel stage indicate that the rate of change of mean depth (f = 0.45) is greater than that of channel width (b = 0.32). Based on hydraulic analyses of all cross sections, macro-channel discharge is 6,040 meters per second and has a return period of about 40 years. The top-left picture is looking downstream from the right bank at cross-section 2.

EXAMPLE LOCALITY: The Llano River near Kingsland occurs at a transition from bedrock-braided to braided conditions (Figure 6.14). The site occurs 177 kilometers downstream of the confluence of the North Llano and South Llano Rivers and has a drainage area of 11,406 square kilometers. The sand-bed and bedrock channel occurs just upstream of Lake LBJ, and valley walls are comprised of Precambrian Town Mountain Granite. Breaks in slope along the sandy left bank of cross-section 2 and right bank of cross-section 1 identify the conditions considered synonymous with bankfull stage of 3.4 meters observed at other sites along the river. At the 3.4-meter stage, discharge is 778 cubic meters per second based on hydraulic analyses of two cross sections. According to regionally-tuned regression analyses, this discharge has a return period much less than 2 years (Tables 6.4, 6.7).

To confirm hydraulic and flood-frequency regression analyses for bankfull stage at this site, high-water marks associated with a March 2007 flow were simultaneously surveyed with cross-section topography. The computed discharge of 502 cubic meters per second has an estimated return period much less than 2 years (Table 6.4) and is comparable to the peak discharge (365 cubic meters per second) and return period (less than 1 year) computed by partial-duration analyses of USGS streamflow data for the same event upstream at the Llano River at Llano. For the stage associated with bankfull conditions, at-a-station hydraulic geometry analyses indicate that channel width (b = 0.46) compensates for increasing discharge at a greater rate than mean channel depth (f = 0.36). Although the measured survey did not reach the top of the macro-channel,

vertical extent of the survey at cross-section 2 is about 6 meters above the bed. At the 6-meter stage, discharge is 3,690 cubic meters per second based on hydraulic analyses of cross-section 2. According to regionally-tuned regression analyses, this discharge has a return period of about 8 years (Tables 6.4, 6.8).

To confirm hydraulic and flood-frequency regression analyses for the macro-channel at this site, high-water marks associated with a June 2007 flow were simultaneously surveyed with cross-section topography. The computed discharge of 3,350 cubic meters per second has an estimated return period of about 6 years (Table 6.4), and is substantially greater than the peak discharge (2,060 cubic meters per second) and return period (about 3.5 years) computed by partial-duration analyses of USGS streamflow data for the same event upstream at the Llano River at Llano (08151500). For the June 2007 high-flow event, however, much of the stormflow was derived from the drainage area downstream from Llano. For example, the LCRA streamflow-gaging station along Honey Creek near Kingsland, Texas, recorded a peak discharge of 504 cubic meters per second, associated with a return period of about 20 years based on partial-duration flood-frequency analyses. It, therefore, is plausible to assume the Llano River near Kingsland had a considerably larger peak discharge than upstream at Llano. At-a-station hydraulic geometry analyses between bankfull and the surveyed macro-channel stage at cross-section 2 indicate that mean channel depth (f = 0.53) compensates for increasing discharge at a greater rate than channel width (b = 0.20).

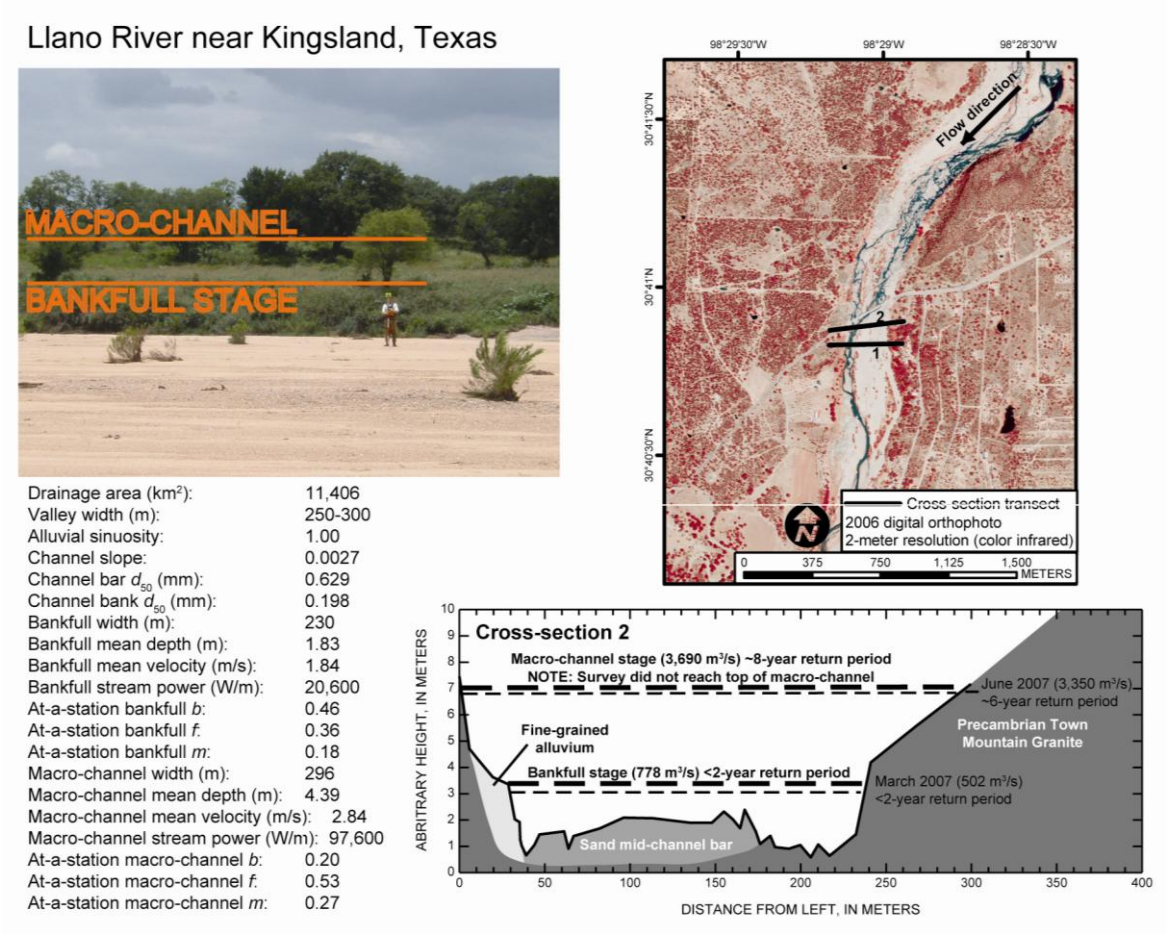

Figure 6.14. The Llano River near Kingsland, Texas, occurs at a transition between bedrock-braided and braided conditions in the Precambrian zone of the Llano River watershed. The sand-bed and bedrock channel can be separated into a low-flow channel (thalweg) and a mid-channel bar, and a break in slope along the channel bank is synonymous with bankfull conditions observed at other sites along the river. At-a-station hydraulic geometry analyses at bankfull stage indicate that the rate of change of channel width (b = 0.46) is greater than that of mean depth (f = 0.36). Based on hydraulic analyses of two cross sections, bankfull discharge is 778 cubic meters per second and has a return period much less than 2 years. The vertical extent of channel surveys went beyond bankfull stage, but did not reach the top of a macro-channel. Nonetheless, at-a-station hydraulic geometry analyses of the macro-channel above bankfull stage at cross-section 2 indicate that the rate of change of mean depth (f = 0.53) is greater than that of channel width (b = 0.20). Based on hydraulic analyses of cross-section 2, macro-channel discharge is 3,690 cubic meters per second and has a return period of about 8 years. The top-left picture is looking toward the right bank at cross-section 1.

6.7 Discussion

Main-stem river channels in the Llano River watershed, including the North Llano, South Llano, and Llano Rivers, undergo a downstream sequence of channel adjustments in association with changes in hydrology, lithology, and sedimentary composition of alluvial deposits. The following adjustments are discussed in further detail below: (1) channel pattern related to abrupt transitions in lithology and associated composition of alluvial deposits, (2) bankfull channel to macro-channel morphology related to a downstream increase in flood power, and (3) divergence in width-depth relations of bankfull and macro-channel shape associated with abrupt transitions in lithology and associated composition of alluvial deposits. A supportive graphical summary of downstream adjustments of channel morphology is provided in Figure 6.15.

6.7.1 Channel Pattern

Downstream adjustments of channel pattern in the Llano River watershed are strongly associated with lithologic transitions and associated sedimentary composition of alluvial deposits. The initial headwater draws of the North Llano and South Llano Rivers take a sinuous path across the higher elevations of the Edwards Plateau before incising into the Cretaceous carbonate bedrock. The incision results in confined channels with low sinuosity. As drainage area and alluvial valley width gradually increase, the cobble- to gravel-bed channels become laterally active (see Figure 6.10) within fine-grained banks comprised mostly of silt and sand, and alluvial sinuosity

peaks for the watershed. Along most reaches, a low-flow channel (thalweg) can be distinguished from longitudinal channel-bar deposits. Downstream of the confluence of the North Llano and South Llano Rivers, the Llano River is characterized by enlarged meander bends, which are likely associated with wetter conditions during the period between 4,500 and 1,000 years B.P. (Blum and Valastro 1989). Relatively wide alluvial valleys become confined along two short reaches (3.9 kilometers total) of the Llano River in the Cretaceous zone of the watershed.

Although a short reach of the Llano River (8.2 kilometers) retains a sinuous course in the uppermost Paleozoic zone, the channel immediately straightens in a confined valley comprised of Ordovician carbonate rock. Observed bends in the channel are not associated with present-day lateral migration processes, but probably are attributed to preferential paths of weathering along joints or fractures in the bedrock. A narrow alluvial valley forms downstream of the Ordovician-Cambrian contact, but confinement between the siltstone, carbonate, and sandstone valley walls maintains an alluvial sinuosity less than 1.1. Cobble- and gravel-sized channel bars are more frequent and contribute to slight variations in the straight channel, such as the large mid-channel bar at the Llano River at James River Crossing near Mason.

Channel pattern is complex in the Precambrian zone of the watershed, but all reaches are confined within the exhumed igneous and metamorphic bedrock. Similar to the Paleozoic sedimentary zone, observed bends in the channel are associated with preferential paths of weathering along mineralogical seams, joints, or fractures in the

bedrock. Straight channel reaches mostly devoid of exposed mid-channel bars and bedrock outcrops characterize most of the Llano River upstream of Llano. As introductions of sand-sized sediment increase downstream, straight channels transition to braided channels downstream of Llano. Along some reaches both upstream and downstream of Llano, irregular outcrops of granite, schist, and gneiss force a bedrock-braided channel pattern characterized by a network of multi-thread, low-flow channels. These bedrock-braided reaches are similar to, but less extensive than, bedrock-anastomosing reaches described in Heritage, van Niekerk, and Moon (1999) and van Niekerk et al. (1999) along the Sabie River in South Africa. The term bedrock-braided is used for the Llano River because individual channels are usually separated by less than 25 meters of cross-section distance and usually rejoin after 10 to 100 meters of downstream length.

6.7.2 Bankfull and Macro-Channel Shape

Reaches along the North Llano and South Llano Rivers generally have a distinct break in slope that identifies bankfull conditions. As an example of an ephemeral draw, the South Llano River at Baker Ranch compensates for increasing discharge by increasing its width (b = 0.48) at a greater rate than mean depth (f = 0.34) (Table 6.9). Proceeding downstream and contrasting with aggraded draws, the South Llano River at U.S. Highway 377 near Rocksprings compensates for increasing discharge by increasing mean depth (f = 0.52) at a greater rate than width (b = 0.22). This is characteristic of channels associated with bedrock incision. Partly-confined, gravel-bed

channels in the Cretaceous zone of the watershed have variable relations of bankfull width to depth, but mean at-a-station hydraulic geometry exponents show that channel width (b = 0.42) slightly outpaces mean depth (f = 0.39) to compensate for increasing discharge. As an example of a major tributary in the Cretaceous zone, at-a-station bankfull width and mean depth exponents along Johnson Fork are equal (0.40) and similar to main-stem channels. Bankfull flows along ephemeral draws have return periods less than 2 years, but occur less frequently (approximately 4-year return periods) for partly-confined channels just downstream of bedrock incised reaches (e.g., North Llano River near Roosevelt, South Llano River at 700 Springs Ranch near Telegraph) (Tables 6.4, 6.7). The abrupt increase in bankfull capacity along these uppermost partly-confined reaches possibly is related to a combination of relatively steep channel slope and accommodation space for channel enlargement. Proceeding downstream, bankfull conditions of sinuous gravel-bed channels near Junction have return periods of about 2 years, and Johnson Fork has bankfull conditions every 3 to 5 years, on average (Tables 6.4, 6.7).

Downstream of the confluence of the North Llano and South Llano Rivers, the Llano River exhibits macro-channel geometry along confined reaches, which demonstrates the sensitivity of channel form to valley confinement (Magilligan 1992; Fuller 2007). The macro-channel extent is identified by distinct breaks in slope along the channel banks, whether comprised of bedrock or alluvium. Evidence of a lower bankfull stage along these reaches is absent. The formation of macro-channel geometry

likely is attributed to infrequent high-magnitude flows greater than 2,000 cubic meters per second (Figure 6.16), total stream power exceeding about 30,000 watts per meter (Figure 6.17), and unit stream power exceeding 200 watts per square meter (Table 6.8). Macro-channel unit stream power for the Llano River in the Cretaceous zone of the watershed is comparable to values reported for the Auranga River (a smaller seasonal fluvial system in eastern India), but is considerably less than reported for the larger Narmada River in western India (Gupta 1995). Finally, confined macro-channels in the Cretaceous zone of the watershed compensate for increasing discharge by increasing mean depth (f = 0.47) at a greater rate than width (b = 0.29) (Table 6.9), a notable shift from bankfull reaches located upstream. Macro-channel flows along confined reaches in the Cretaceous zone have return periods between 10 and 12 years (Tables 6.4, 6.8), alluding to the importance of high-magnitude flows in shaping channel morphology along the Llano River.

Downstream of the Ordovician bedrock-lined reaches of the Llano River, the channel emerges to a narrow alluvial valley with distinctive inset floodplains abutting against Cambrian sedimentary strata. Although distinct breaks in slope along banks identify macro-channel conditions, subtle forms of morphologic evidence can be used to infer the aforementioned “bankfull” conditions associated with reaches along the North and South Llano Rivers. For the Llano River at James River Crossing, bankfull conditions are associated with the top of a large mid-channel bar and macro-channel conditions are associated with the height of inset floodplains at the top of the bank. For

bankfull conditions, the Llano River at James River Crossing compensates for increasing discharge by increasing its mean depth (f = 0.45) at a greater rate than width (b = 0.32) (Table 6.9). For macro-channel conditions above bankfull stage, mean depth (f = 0.50) increases at an even faster rate than width (b = 0.24) in compensating for flow. Three sites along the James River and Honey Creek, tributaries in the Paleozoic zone, also are characterized by increasing mean depth (f = 0.48) at a greater rate than width (b = 0.28) up to the bankfull stage. Similar to the main-stem Llano River, mean depth (f = 0.55) increases at an even faster rate than width (b = 0.18) in compensating for macro-channel flows above bankfull stage. In comparison to upstream reaches along the North Llano and South Llano Rivers, the more prominent increase of mean depth for both bankfull and macro-channel conditions along Paleozoic reaches is explained by increasingly confined valleys and associated limitations for lateral channel adjustment. Bankfull flows at the Llano River at James River Crossing have a return period of about 2.5 years (Tables 6.4, 6.7) and macro-channel conditions occur with a return period of about 20 years (Tables 6.4, 6.8), introducing a dichotomy of relatively frequent flows that maintain alluvial deposits near the channel bed and less frequent flows that maintain overall channel geometry.

Further downstream, the variously classified channel reaches in the Precambrian zone of the watershed are confined by relatively resistant granite, gneiss, and schist. Similar to reaches in the Paleozoic zone, bankfull conditions are identified by subtle breaks in the slope along sandy alluvial banks, occurring no higher than about 5 meters

above the thalweg. At bankfull conditions, sand-bed and bedrock channels of the Llano River in the Precambrian zone compensate for discharge by increasing mean depth (f = 0.45) at a greater rate than width (b = 0.32) (Table 6.9). For macro-channel conditions above bankfull stage, mean depth (f = 0.44) also increases at a greater rate than width (b = 0.34). The minimal difference between at-a-station exponents of bankfull channels and macro-channels in the Precambrian zone of the watershed indicates that macro-channel adjustment is different than observed for Cretaceous and Paleozoic reaches. The highly resistant lithology of the igneous and metamorphic rock in this zone limits lateral development of inset floodplains. The bank-attached alluvial deposits observed at study sites along Precambrian reaches do not have any sharp demarcation identifying an inset floodplain surface, possibly resulting from little cohesion associated with sand-sized material. Therefore, the general slope of sub-bankfull bank-attached deposits closely follows that of higher alluvial deposits and the surrounding bedrock. Bankfull flows along Precambrian reaches have a return period between 1 and 1.5 years (Tables 6.4, 6.7) and macro-channel conditions have return periods between about 20 and 40 years (Tables 6.4, 6.8), reinforcing the dichotomy of relatively frequent flows that maintain alluvial deposits near the channel bed and less frequent flows that maintain overall channel geometry.

A graphical depiction of downstream variability and trends in at-a-station hydraulic geometry exponents for bankfull and macro-channel conditions is shown in Figure 6.18. For bankfull conditions, a gradual increase in *f* and decrease in *b* indicates

that mean depth increasingly compensates for discharge as opposed to width. For macro-channel conditions, mean depth compensates for discharge more than width and width-depth relations are similar from the upper to lower watershed. The similarity of bankfull width-depth and macro-channel width-depth relations in the Precambrian zone of the watershed reiterates that breaks in slope at the bankfull stage are subtle.

Downstream hydraulic geometry plots (Figure 6.19) of bankfull and macro-channel conditions do not provide a complete explanation for downstream patterns of channel adjustment because bankfull discharge did not necessarily increase in a downstream direction. Aside from this caveat, bankfull channel geometry of the North Llano, South Llano, and Llano Rivers compensates for discharge by increasing mean depth (f = 0.44) at a greater rate than width (b = 0.31). Macro-channel geometry, however, compensates for discharge by increasing width (b = 0.58) at a greater rate than mean depth (f = 0.26). To summarize, channel dimensions that convey flows with return periods typically less than 2 years in the Llano River watershed become relatively narrow and deep in a downstream direction. Macro-channel dimensions above the bankfull stage, however, adjust downstream largely through increases in width.

Table 6.9. Mean values of at-a-station hydraulic geometry for sites representative of the four categories of channel classification along the North Llano, South Llano, and Llano Rivers in Central Texas. Mean values of tributaries also are provided for comparison.

[b, at-a-station hydraulic geometry exponent for width; f, at-a-station hydraulic geometry exponent for mean depth; m, at-a-station hydraulic geometry exponent for mean velocity]

Channel classification category	b	f	m
Main-stem channels			
Ephemeral aggraded (bankfull)[a]	0.48	0.34	0.18
Ephemeral bedrock incised (bankfull)[b]	0.22	0.52	0.26
Cretaceous gravel-bed (bankfull)	0.42	0.39	0.20
Cretaceous gravel-bed (macro-channel)	0.29	0.47	0.24
Paleozoic bedrock or gravel-bed (bankfull)	0.32	0.45	0.23
Paleozoic bedrock or gravel-bed (macro-channel)	0.24	0.50	0.25
Precambrian straight, braided, or bedrock-braided (bankfull)	0.32	0.45	0.23
Precambrian straight, braided, or bedrock-braided (macro-channel)	0.34	0.44	0.22
Tributaries			
Cretaceous gravel-bed tributary (bankfull)	0.40	0.40	0.20
Paleozoic bedrock or gravel-bed tributary (bankfull)	0.28	0.48	0.24
Paleozoic bedrock or gravel-bed tributary (macro-channel)	0.18	0.55	0.27
Precambrian straight, braided, or bedrock-braided tributary (bankfull)	0.38	0.41	0.21
Precambrian straight, braided, or bedrock-braided tributary (macro-channel)	0.26	0.49	0.25

[a] Values only for South Llano River at Baker Ranch near Rocksprings. A bankfull channel condition could not be established at North Llano Draw near Sonora.
[b] The South Llano River at U.S. Highway 377 near Rocksprings is considered separately from ephemeral aggraded channels because of the disparity of bankfull hydraulic geometry exponents.

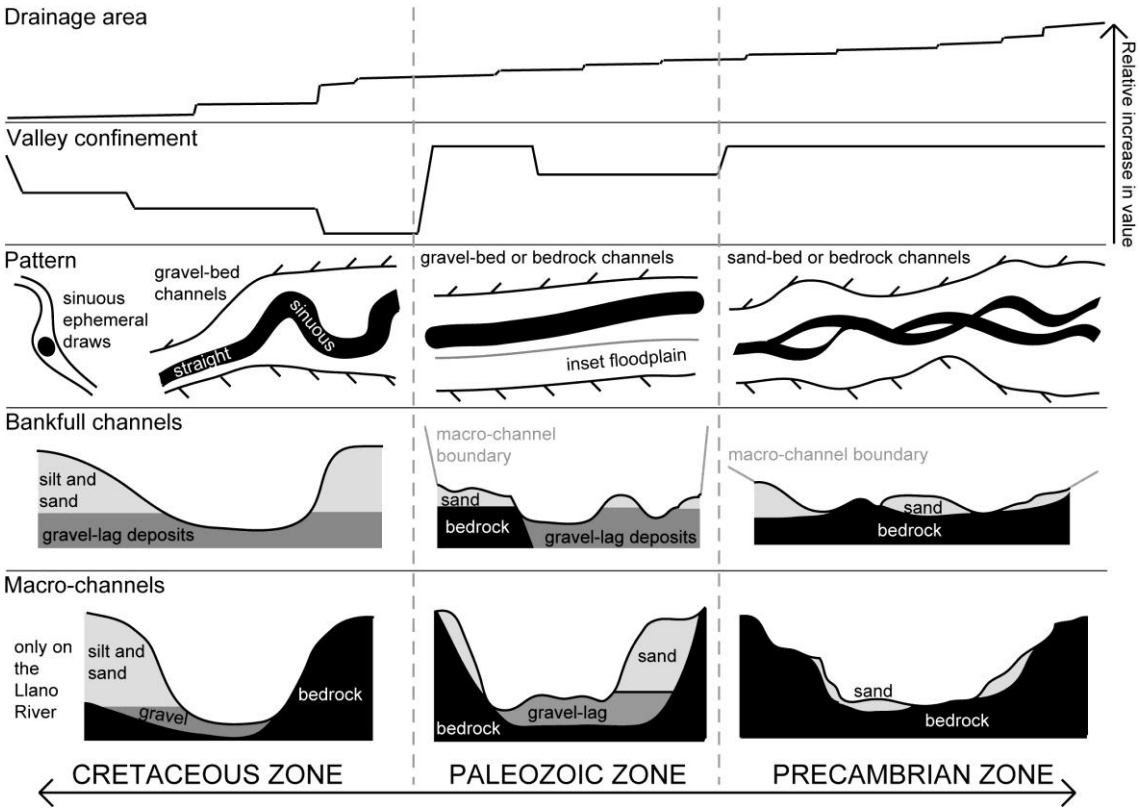

Figure 6.15. A summary of downstream adjustments of channel pattern and shape along the North Llano, South Llano, and Llano Rivers in Central Texas. As drainage area and valley confinement generally increase with distance downstream, channel pattern transitions from sinuous to straight to various braided forms. The morphologic evidence of bankfull stage gradually is obscured by macro-channel development.

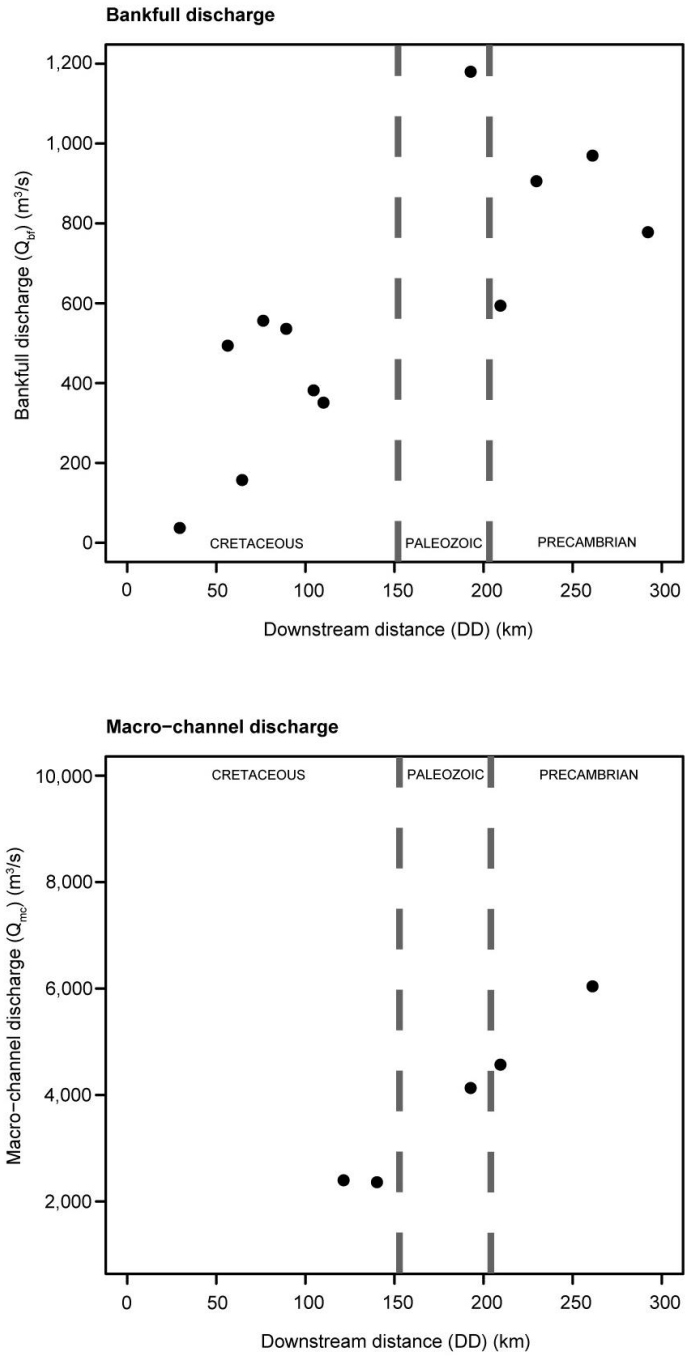

Figure 6.16. Bankfull and macro-channel discharge with downstream distance along the North Llano, South Llano, and Llano Rivers in Central Texas. Bankfull and macro-channel discharge increase downstream. For macro-channel discharge, sites were excluded if the topographic survey did not reach the top of the macro-channel.

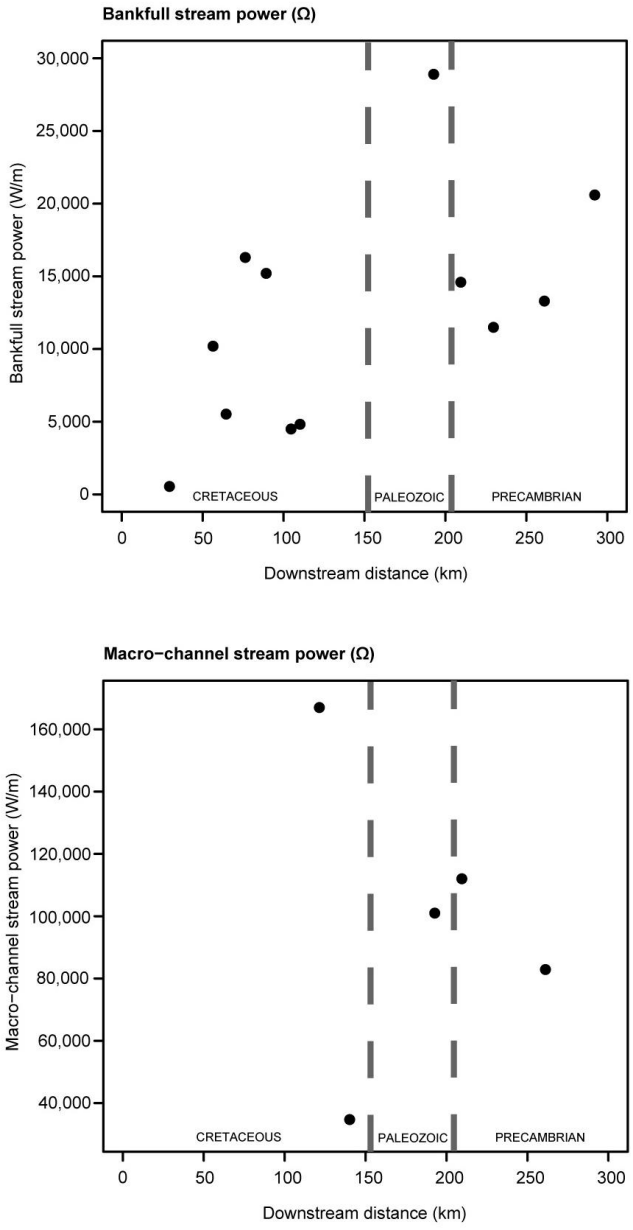

Figure 6.17. Bankfull and macro-channel stream power with downstream distance along the North Llano, South Llano, and Llano Rivers in Central Texas. Bankfull stream power generally increases downstream and is less than 30,000 watts per meter. Macro-channel stream power is highly variable, but ranges from about 35,000 to 165,000 watts per meter. Considerable variability is attributed to local differences in channel slope, which is an influential variable in computation of stream power. For macro-channel stream power, sites were excluded if the topographic survey did not reach the top of the macro-channel.

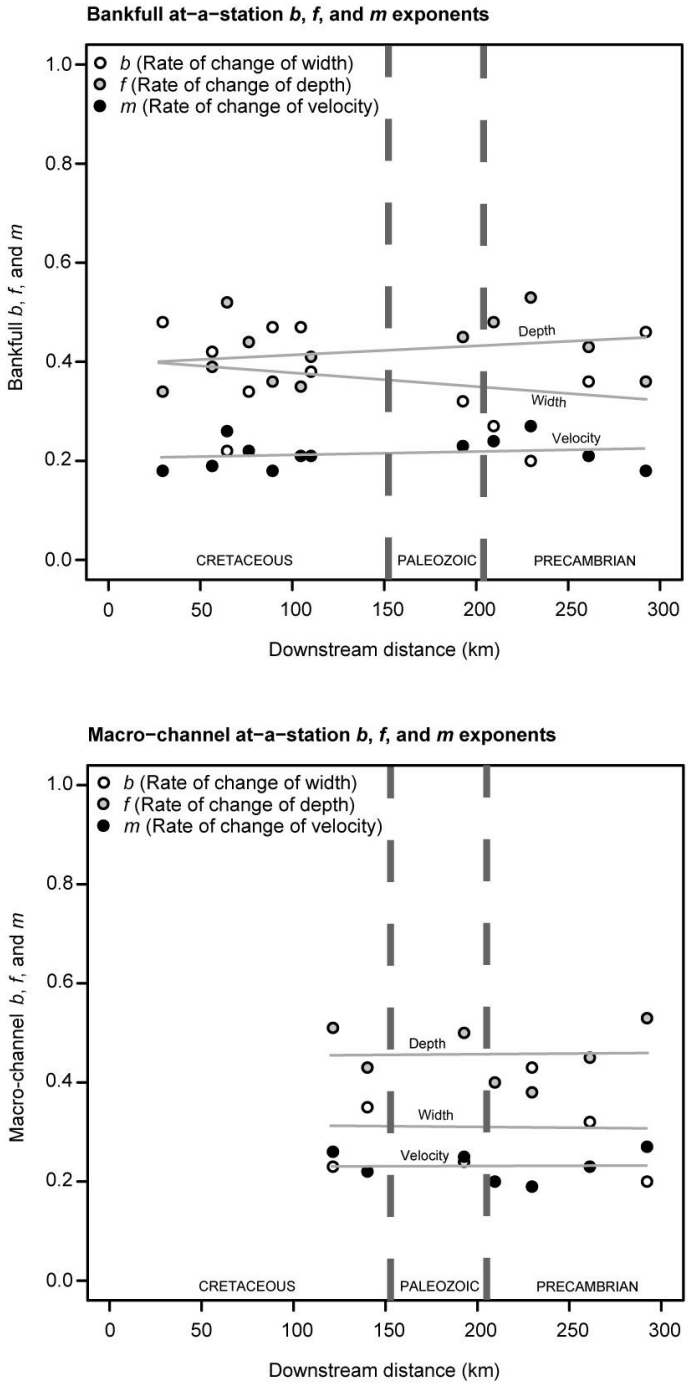

Figure 6.18. Downstream trends and variability in at-a-station hydraulic geometry exponents for bankfull and macro-channel conditions of the North Llano, South Llano, and Llano Rivers in Central Texas.

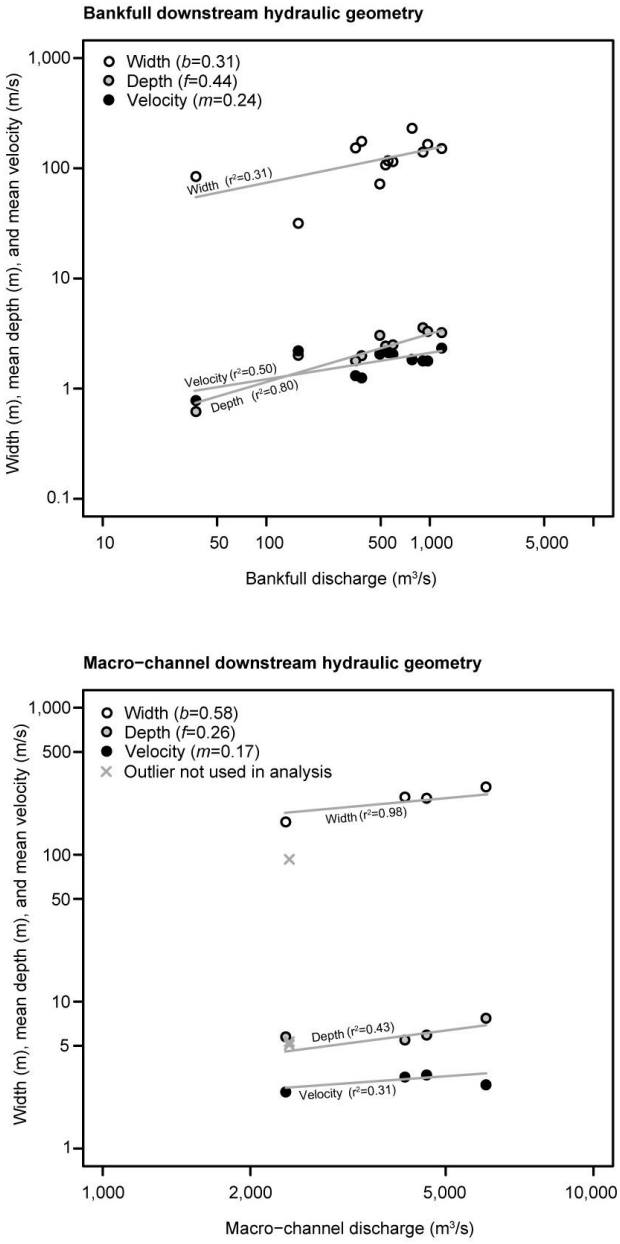

Figure 6.19. Downstream hydraulic geometry for bankfull and macro-channel conditions along the North Llano, South Llano, and Llano Rivers in Central Texas. One outlier, Llano River near Junction, was not included in macro-channel analyses because the locally steep slope associated with a cascade at the site resulted in an anonymously high mean velocity. Further, it should not be assumed that the left-to-right progression of points represents sites in order from upstream to downstream because bankfull and macro-channel discharge did not always increase in a downstream direction.

6.8 Conclusions

Downstream adjustments of channel pattern and shape in the Llano River watershed are complex as a result of abrupt lithologic transitions, the degree of valley confinement, and a highly variable and powerful flow regime. Specifically, four different categories of channels are classified based on hydrology, planform morphology, lithology, and alluvial development: (1) uppermost ephemeral reaches, commonly referred to as "draws" in the study area, (2) Cretaceous straight or sinuous gravel-bed channels, (3) Paleozoic straight or sinuous gravel-bed or bedrock channels, and (4) Precambrian straight, braided, or bedrock-braided sand-bed channels. Sub-categories of these four general channel types can be distinguished based on degree of valley confinement, planform characteristics, and boundary composition.

Bankfull conditions of ephemeral draws and partly-confined, sinuous, gravel-bed reaches in the Cretaceous zone of the watershed are achieved by increasing width at a greater rate than mean depth, although mean depth becomes increasingly important in a downstream direction. The ability of the Cretaceous reaches to adjust in large measure by width is counter-intuitive to the assumption that more silt and clay in the channel boundary results in relatively narrow and deep channels. Channel banks along the North Llano, South Llano, and Llano Rivers are characterized by a decrease in silt-clay content with distance downstream. The characteristic that best explains the increasingly important role of mean depth in downstream adjustments of channel shape is valley confinement. Relatively wide alluvial valleys in the Cretaceous zone of the watershed

allow lateral channel processes, including bank erosion and migration, to enlarge the channel width. In the Paleozoic and Precambrian zones of the watershed, bankfull conditions of bedrock-, gravel-, or sand-bed channels are achieved by increasing mean depth at a greater rate than width. Increasingly confined valley settings in the Paleozoic and Precambrian zones, combined with greater bankfull discharges and stream power, result in channel incision, often into bedrock, and morphologic-bankfull indicators well above the channel bed.

Macro-channel conditions emerge downstream of the confluence of the North Llano and South Llano Rivers, and are associated with relatively high inset floodplains or definitive breaks in slope to the upland landscape. At-a-station hydraulic geometry of macro-channels show that mean depth compensates for discharge at a greater rate than width. A comparison with channel adjustments at the lower bankfull stage shows a downstream convergence of width-depth hydraulic geometry relations, which indicate that the general slope of bank-attached deposits below bankfull stage, especially in the Precambrian zone, closely follows that of higher alluvial deposits and the surrounding bedrock. Again, valley confinement is important because inset floodplain development is limited in the Precambrian zone, and combined with minimal cohesion of sand-sized material, breaks in slope at the bankfull stage are subtle in the lowermost watershed.

The degree of valley confinement in being a primary control of cross-sectional bankfull and macro-channel morphology in the Llano River watershed is likely applicable to other mixed bedrock-alluvial river systems. Investigations of downstream

variations in channel morphology would benefit from a consideration of lithology and its role in constraining or focusing hydraulic energy and the associated flux of alluvial sediment.

Finally, alluvial features and morphologic indicators of bankfull stage, including channel bars and many banks, are associated with relatively frequent flows in the Llano River watershed, mostly with return periods between 1 and 2 years. Macro-channel dimensions, however, are maintained by less frequent, high-magnitude flows. Return periods of macro-channel flows generally increase going downstream the Llano River, from about 10 to 40 years. Proceeding downstream, the gradual masking of morphologic indicators associated with bankfull stage, as indicated by at-a-station hydraulic geometry, parallels less-frequent formative flows for macro-channels, indicating that high-magnitude floods play an increasingly important role in channel adjustment. Independent observations made along the river, including the height of inset floodplains and distinct breaks in slope along banks, also suggest that macro-channel dimensions best describe the overall shape of the Llano River. However, various practitioners, including aquatic biologists and managers interested in sediment-transport dynamics, are likely to have considerable interest in the more frequent bankfull flow events.

The dichotomy of bankfull channels and macro-channels in the Llano River watershed underscores the difficulties in associating channel geometry with one dominant discharge, especially in fluvial systems with highly variable flow regimes.

Although the oft-cited 1- to 2-year return period is supported for bankfull channels, many representative reaches are best described as macro-channels with less frequent formative flows. For much of the Llano River, the work accomplished by severe flash floods in association with valley confinement obscures the cumulative imprint of frequent, moderate floods on observed channel morphology. Moderate floods, however, are important to re-distribute sediment from low-lying alluvial benches, channel bars, and the channel bed.

Chapter 7. Summary and Conclusions

Fluvial geomorphic forms and processes along the Llano River and its tributaries in Central Texas, USA, are complex as a result of the highly variable flow regime and abrupt transitions in surface lithology in the watershed. Although classified as semi-arid and sub-humid at the western and eastern ends of the watershed, respectively, rainfall events are not uniformly distributed through time. Storm events of severe intensity deliver tremendous quantities of runoff to the stream-channel network in relatively short timespans, which results in high-magnitude flash floods that mobilize sediment and modify channel geometry. Unlike neighboring systems in the Cretaceous carbonate Edwards Plateau, the Llano River watershed includes a large Paleozoic sedimentary rock zone and Precambrian igneous and metamorphic rock zone. The distinctive lithology of the watershed imposes strong controls on sedimentology and valley confinement, which, in turn, affects downstream channel adjustment along the Llano River and its tributaries.

7.1 Summary

A summary of findings associated with this investigation are separated below into background information, alluvial sedimentology, and channel adjustment. Further, some suggestions for future research are outlined at the end of the chapter.

7.1.1 Background Information

1. As a tool to infer at-a-station and downstream adjustments of channel shape, hydraulic geometry has been criticized in the literature for various reasons, including variability of b, f, and m exponents, adherence to log-linear relations, neglect of flow resistance, and inherent instability of cross-sectional shape, among others. Aside from its complications, at-a-station and downstream hydraulic geometry can be a very useful technique to associate the hydrologic regime of a stream to its shape. If applied in conjunction with flood-frequency analysis, much can be learned about the relation of various instream geomorphic units to the magnitude and frequency of different flows.

2. The concept of dominant (channel-forming) discharge exerts a considerable influence in investigations of channel adjustment. Dominant discharge usually is associated with bankfull conditions and is further assumed to have a return period of 1 to 2 years. Out of 36 publications reviewed since 1994 that specifically deal with dominant or effective discharge, 8 support and 12 refute the 1- to 2-year association. The other 16 are mostly neutral. The bankfull-stage, 1- to 2-year association is most valid in humid or snowmelt-driven fluvial systems, has mixed results in seasonally-driven systems, and becomes less predictive for small watersheds, incised channels, or in systems with highly variable flow regimes. A variety of recent publications contend that a range of

flows contribute to the maintenance of various fluvial processes and forms in most natural channels.

3. A literature review was done to synthesize the paleoenvironmental record of the Edwards Plateau, Texas for the last 20,000 years. Based on an existing scheme, six distinct episodes can be constructed to conceptualize prevailing environmental conditions: (1) full glacial (about 20,000 to 14,000 years B.P.), (2) late glacial (about 14,000 to 10,500 years B.P.), (3) early to middle Holocene (about 10,500 to 5,000 years B.P.), (4) late Holocene I (about 5,000 to 2,500 years B.P.), (5) late Holocene II (about 2,500 to 1,000 years B.P.), and (6) modern (about 1,000 years B.P. to present). The full-glacial episode is characterized by the coolest, most humid climatic regime for the past 20,000 years. A gradual increase in temperature and decrease in precipitation occurred during the late-glacial episode, as evidenced by channel incision, the disappearance of spruce and fir trees, increase in C_4 plant species, replacement of mesic microfauna with xeric forms, and reduced rates of speleothem growth. Evidence for the Younger Dryas cooling episode (about 10,750 years B.P.) is absent in the region. Desiccation and warming continued through the early to middle Holocene, culminating with the Altithermal (about 5,500 years B.P.). Fluvial systems slowly aggraded during the early to middle Holocene, but later incised deeply after 5,000 years B.P. Grasslands steadily replaced woodlands, C_4

abundance increased, and xeric species dominated the faunal assemblage. By about 5,000 to 2,500 years B.P., the landscape consisted mostly of short grasses and desert scrub. A relatively wet cycle occurred between roughly 2,500 to 1,000 years B.P. as fluvial systems again aggraded to levels above former terraces, and hickory trees and mesic faunal species increased in abundance. Finally, increasing warmth and aridity during the last 1,000 years have resulted in stream incision, open oak woodlands, and domination of xeric species. Superimposed, however, on increasingly dry conditions are extreme floods responsible for many characteristics of present-day channel morphology.

7.1.2 Alluvial Sedimentology

4. The Llano River valley becomes increasingly confined by bedrock with distance downstream of the Cretaceous-Paleozoic contact. Although it often is assumed that ubiquitous exposures of bedrock to the river channel results in relatively coarse bed material, channel-bar material of the Llano River decreases in size with distance downstream, especially downstream of the Paleozoic-Precambrian contact. This trend is attributed to the different in-situ weathering mechanisms of carbonate and igneous lithologies. A considerable proportion of Cretaceous and Paleozoic carbonate rocks in the upper and middle watershed are removed in large slabs or clasts from steep slopes of contributing drainages or valley walls, whereas in-situ weathering of Precambrian granitic material into grus in the lower watershed results in considerable quantities of sand-sized material that

is delivered to contributing drainages. Furthermore, the supply of sand-sized material in the lower watershed exceeds the influence of increased flood stream power as the result of valley confinement, which would normally be associated with selective entrainment and relatively coarse material.

5. Downstream trends of declining bed-material size are much more evident for channel-bar deposits than low-flow-channel (thalweg) deposits in the Llano River watershed, which indicates that stronger hydraulic sorting mechanisms occur along channel bars during high-flow events. Hydraulic forces in the thalweg alternate from uniform during low-flow conditions to highly turbulent during high-flow conditions, and hydraulic irregularity is further promoted by localized configuration of the channel inclusive of meander bends.

6. The abrupt gravel-to-sand transition between Mason and Castell is explained by two independent factors: (1) distance from upstream sources of gravel-sized material and (2) additions of sand by tributaries draining Precambrian igneous and metamorphic lithologies. First, tributaries that supply gravel to the Llano River are less numerous downstream of the Cretaceous-Paleozoic contact. Second, inputs of sand-sized sediment become immediately influential downstream of the Paleozoic-Precambrian contact. The straight longitudinal

profile nullifies channel slope in the Llano River watershed as an explanation for the gravel-to-sand transition.

7. Channel-bar deposits of the North Llano and South Llano Rivers abruptly transition from medium-sized pebbles to small pebbles and gravels near Junction. The transition reaches occur between 75 to 90 kilometers downstream, but drainage areas increase from about 1,350 to 2,250 square kilometers because of tributary inputs to those reaches. The decrease in particle size is not explained by an increase in sediment volume because additional sediment from the smaller, steeper adjoining watersheds is presumably coarser. The abrupt particle-size decrease, therefore, is probably explained by increased magnitudes and frequencies of high-flow events capable of transporting and abrading cobble- to gravel-sized material. These findings contrast with many investigations that document a localized increase in bed material size associated with tributary inputs, which suggests that downstream trends in particle size of gravel-bed rivers with highly variable flow regimes could be more dependent on the frequency of entrainment and transport rather than distance-dependent abrasion and sorting processes.

8. Contrasting downstream trends of simultaneously decreasing bed- and increasing bank-material particle size characterize fluvial deposits of the North

Llano, South Llano, and Llano Rivers. Reaches in the upper Cretaceous zone of the watershed have channel beds comprised of cobble- to gravel-sized material and banks comprised of silt, clay, and limited amounts of fine sand. In upland areas, Cretaceous carbonate weathers to a dark, silt- and clay-rich soil, and it is from this material that fine-grained banks and floodplains are derived. Relatively poorly-sorted bank and floodplain material along river reaches near Junction indicate that appreciable quantities of sand are included in the silt-clay matrix. Much of the sand likely is derived from incision into the Hensell Sand. Abrasion processes of channel-bed material also contribute to the sand-sized fraction. Relatively coarse bed material in the upper reaches of the watershed originates as plucked or gravity-supplied material from steep slopes and tributaries. As gravel-sized material becomes less available downstream of the James River, the increasing influence of Precambrian-derived sand is detected by the convergence of particle size in both channel-bar and channel-bank deposits.

9. Downstream trends of relative carbonate content (percent) and magnetic susceptibility (X) are inversely related in channel bank and floodplain deposits. In the uppermost reaches of the North and South Llano Rivers, the Cretaceous-aged Edwards Limestone contains substantial quantities of siliceous chert, which keeps carbonate content of fluvial deposits below 40 percent. As the river

channels incise into the more pure limestone and dolomite of the Glen Rose Formation, carbonate content increases to over 50 percent near Junction. Continuing downstream, inputs from various Paleozoic sedimentary rocks and finally Precambrian igneous and metamorphic rocks reduce carbonate content below 25 percent near watershed outlet. The inverse trend of magnetic susceptibility indicates its association with carbonate content, although it does not display measurable sensitivity to Paleozoic sedimentary rocks. Further, magnetic susceptibility is largely dependent on particle size, such that relatively coarse material will have a higher value than finer material for a given mineralogy. Notably, magnetic susceptibility peaks near Kingsland, where channel-bank and floodplain particle size are the coarsest in the watershed. The peak indicates that Precambrian mineralogy exerts a strong influence on magnetic susceptibility and also illustrates the increasingly dominant supply of Precambrian sands to alluvial deposits in the lower watershed.

7.1.3 Channel Adjustment

10. Four different categories of channels along the North Llano, South Llano, and Llano Rivers are classified based on hydrology, planform morphology, lithology, and alluvial development: (1) uppermost ephemeral reaches, commonly referred to as “draws” in the study area, (2) Cretaceous straight or sinuous gravel-bed channels, (3) Paleozoic straight or sinuous gravel-bed or bedrock channels, and (4) Precambrian straight, braided, or bedrock-braided

sand-bed channels. Various sub-categories of these four general channel types can be distinguished based on degree of valley confinement, planform characteristics, and boundary composition.

11. Bankfull conditions of ephemeral draws and partly-confined, sinuous, gravel-bed reaches in the Cretaceous zone of the watershed are characterized by increasing width at a greater rate than mean depth, although mean depth becomes increasingly important in a downstream direction. In the Paleozoic and Precambrian zones of the watershed, bankfull conditions of bedrock-, gravel-, or sand-bed channels are characterized by increasing mean depth at a greater rate than width. The ability of the Cretaceous reaches to adjust in large measure by width is counter-intuitive to the assumption that more silt and clay in the channel boundary results in relatively narrow and deep channels. Channel banks along the North Llano, South Llano, and Llano Rivers are characterized by a decrease in silt-clay content with distance downstream. The characteristic that best explains the increasingly important role of mean depth in downstream adjustments of channel shape is valley confinement. Relatively wide alluvial valleys in the Cretaceous zone of the watershed allow lateral channel processes, including bank erosion and migration, to enlarge the channel width. Increasingly confined valley settings in the Paleozoic and Precambrian zones, combined with greater bankfull discharges and stream power, result in deeper channel incision,

often into bedrock and the stranding of morphologic-bankfull indicators well above the channel bed.

12. Macro-channel conditions emerge downstream of the confluence of the North Llano and South Llano Rivers and are associated with relatively high inset floodplains or definitive breaks in slope to the upland landscape. At-a-station hydraulic geometry of macro-channels shows that mean depth compensates for discharge at a greater rate than width. A comparison with channel adjustments at the lower bankfull stage shows a downstream convergence of width-depth hydraulic geometry relations, indicating that the general slope of bank-attached deposits below bankfull stage, especially in the Precambrian zone, closely follows that of higher alluvial deposits and the surrounding bedrock. Valley confinement is important because inset floodplain development is limited in the Precambrian zone, and combined with minimal cohesion of sand-sized material, breaks in slope at the bankfull stage are subtle in the lowermost watershed.

13. Alluvial features and morphologic indicators of bankfull stage, including channel bars and many banks, are associated with relatively frequent flows in the Llano River watershed, mostly with return periods between 1 and 2 years. Macro-channel dimensions, however, are maintained by less frequent, high-magnitude flows. Return periods of macro-channel flows generally increase

going downstream the Llano River, from about 10 to 40 years. Proceeding downstream, the gradual masking of morphologic indicators associated with bankfull stage, as indicated by at-a-station hydraulic geometry, parallels less-frequent formative flows for macro-channels, which indicates that high-magnitude floods play an increasingly important role in channel adjustment.

7.2 Synthesis

The incipient channels of the North Llano and South Llano Rivers near the top of the Edwards Plateau alternate from fine-grained infilled reaches to bedrock-incised, with the bedrock-type becoming dominant as drainage area and, therefore, flood energy increase. The presence of infilled reaches near the top of the plateau leads to questions about the sequence of upland soil erosion and subsequent cut-and-fill activity associated with late Pleistocene and Holocene climatic and environmental change. The fine-grained alluvial deposits along these reaches present a future opportunity to reconstruct chronologies of upland soil erosion and its relation to periods of intense storm activity coupled with prevalent vegetation assemblages.

The wide alluvial valleys near Junction result from weathering and erosion of relatively weak Cretaceous carbonate rocks and the Hensell Sands over geologic timescales. Active floodplains and inactive fluvial terrace deposits accommodate sinuous, gravel-bed reaches of the North Llano, South Llano, and Llano Rivers. As a result of a steeper overall channel slope, the North Llano River does not exhibit full-

scale meandering tendencies (sinuosity < 1.3), which characterizes the lower South Llano and upper Llano Rivers. Conspicuous breaks in slope along well-defined banks delimit bankfull stage, which encapsulates frequently occurring moderate flow events.

Upstream of the North Llano and South Llano confluence, stream power during floods does not exceed a threshold necessary to generate macro-channel morphology. Downstream of the confluence, however, macro-channel morphology develops that contains high-magnitude floods with return periods greater than 10 years. Macro-channel morphology is better developed along reaches that have a greater degree of valley confinement. The original hypothesized model presented in Table 1.1 and shown in Figure 1.4 predicted that return periods of bankfull flows would exceed 2 years, which is not consistent for rivers in the Cretaceous zone, and did not recognize the role of valley confinement in macro-channel development.

The downstream transition to the Paleozoic sedimentary zone is characterized by an abrupt confinement of the valley and the river channel exhibits a straight planform morphology, similar to that shown in Figure 1.4, with bends in its course related to preferential weathering and erosion of bedrock joints over geologic timescales. The relatively resistant Paleozoic lithology might constitute an effective "base level" for lowering of the valley upstream, such that the expected, but not observed, concavity of the longitudinal profile of slope upstream of the Cretaceous-Paleozoic contact is partly filled with alluvium and the gently-sloping (dimensionless slope approximately equal to or less than 0.0015) river meanders to effectively distribute flow energy.

At the Ordovician-Cambrian contact, a narrow alluvial valley forms with well-defined inset-floodplain surfaces delimiting macro-channel dimensions, with return periods approaching 20 years, generally confiming the hypothesis presented in Table 1.1. Set within the macro-channel are various alluvial features, including mid-channel bars and low-lying bank-attached units that define what practitioners refer to as the "bankfull" condition, occurring with a return period between 1 and 2 years. Although the channel-in-channel morphology was originally hypothesized (Table 1.1), the consistency of the 1- to 2-year bankfull return period for the inner channel was not originally anticipated by the author. The alluvial deposits along the Paleozoic reaches consist of greater amounts of sand-sized material when compared to those near Junction, likely resulting from downstream transport of material from the Cretaceous Hensell Sand as well as locally-derived material from Cambrian sandstones.

Finally, the Llano River enters the Precambrian igneous and metamorphic zone, and is characterized by various straight, braided, and bedrock-braided channel patterns occurring within a resistant, confined valley, similar to that shown in Figure 1.4. An abrupt gravel-to-sand transition in bed material occurs, resulting from in-situ weathering processes of granite and metamorphic rocks and the associated delivery of sand-sized material by tributaries. Instream and bank-attached sandy alluvial deposits thinly overlie bedrock, and "bankfull" conditions become increasingly difficult to identify because of subtle breaks in slope. The similarity of at-a-station hydraulic geometry width and depth exponents for bankfull and macro-channel dimensions

indicates that overall channel morphology is adjusted to high-magnitude floods with return periods greater than 10 years, but approaching 40 years at some localities.

A notable implication of this study concerns the role of bankfull discharge. The oft-cited bankfull return period of 1 to 2 years still applies to processes associated with bed-material mobility and adjustment of low-lying alluvial features in river systems with highly variable flow regimes. These short-term adjustments can be very important to practitioners concerned with instream structures (e.g., bridge piers, low-water crossings), reservoir sedimentation, and habitat-suitability indices for aquatic organisms (e.g., macroinvertebrates, fish). Overall channel dimensions, however, are better described by less frequent, high-magnitude floods, especially within confined valley settings. These relatively long-term adjustments probably are more applicable when investigating channel adjustment, flood hazards (e.g., bridge design, floodplain delineation), and disturbance regimes of aquatic organisms.

The research design and methodological approach used for this investigation were successful in indentifying downstream trends in alluvial sediment composition and channel adjustment in the Llano River watershed. The empirical evidence collected to test fluvial geomorphic theories proved invaluable in developing conceptual models that are likely applicable to other fluvial systems with highly variable flow regimes and abrupt discontinuities in lithology. Further, a number of surprising findings were made possible by evaluation of empirical data. Accurate results would not have been possible without other techniques, including flow-resistance tests, partial-duration flood-

frequency analyses, GIS analyses of hydrography and digital elevation models, and statistical analyses. One drawback of the research design is the limited ability to interpolate between sites and definitively associate observations and analyses along all channel reaches. Further, no attempt was made to evaluate the duration of floods, which has been shown to be very important in controlling channel morphology and sediment transport.

7.3 Conclusions

The highly variable, flood-prone flow regime and abrupt lithologic transitions in the Llano River watershed are exhibited in the alluvial sediment composition and channel morphology of the North Llano, South Llano, and Llano Rivers. Major conclusions include:

- Channel-bed and bank sediment are characterized by contrasting downstream trends in particle size. The size decrease of channel-bed material and size increase of bank material are foremost controlled by watershed lithology, notably by inputs of sand in the Precambrian zone of the watershed. Although relatively subtle in their influence of declining bed-material size, instream abrasion and selective entrainment during high flows are responsible for an abrupt coarse-to-fine-gravel transition in the upper watershed. Generally, however, the highly variable flow regime and

increasing valley confinement do not effectively explain downstream trends in particle size of alluvial deposits.

- Planform morphology of the North Llano, South Llano, and Llano Rivers is primarily controlled by lithology, with associated secondary controls being valley confinement and alluvial sediment composition. Sinuous to meandering gravel-bed reaches in the Cretaceous zone of the watershed occur as a result of relatively fine-grained, erodible banks occurring in a wide alluvial valley. As valley confinement increases downstream, the channel becomes straight and bends result from joints or relatively weak seams in the bedrock. Alternating braided and bedrock-braided conditions along the lower Llano River are associated with sand- and bedrock-dominated reaches, respectively.
- For the Llano River downstream of the confluence of the North Llano and South Llano Rivers, "bankfull" channel characteristics become less distinguished and "macro-channel" dimensions become dominant. This observed dichotomy of channel shape is congruent with downstream increases in stream power during high-magnitude flows and valley confinement. "Bankfull" return periods correspond with the oft-cited 1- to 2-year return period, but "macro-channel" conditions are associated with return periods greater than 10 years.

- A number of findings associated with this dissertation research project were unexpected, including: (1) the contrast of low-flow-channel (thalweg) and channel-bar particle size, where the latter better defines downstream trends in alluvial sediment composition; (2) coarse- to fine-gravel transitions upstream of Junction and their relation to an abrupt increase in drainage area; (3) the rapid transition from gravel to sand downstream of the Paleozoic-Precambrian contact; (4) the downstream increase of particle size in channel bank deposits and its contrast with bed material; (5) poorly-sorted bank material near Junction and its relation to contributions from the Hensell Sand; (6) the relatively low carbonate content and high magnetic susceptibility of alluvial deposits in the uppermost reaches of the North Llano and South Llano Rivers, explained by greater amounts of chert; (7) comparable flow-resistance coefficients for upper cobble- to gravel-bed reaches and lower bedrock and sand-bed reaches; (8) the close association of channel planform characteristics and surface lithology; (9) the validity of the oft-cited 1- to 2-year return period flow in maintaining bankfull channel morphology; (10) the dichotomy of bankfull channels and macro-channels with the latter having return periods of flows exceeding 10 years; and (11) the considerable influence of valley confinement on hydraulic geometry of bankfull and macro-channels.

- Finally, the research completed for this dissertation project indicates that relatively abrupt downstream changes in alluvial sedimentology and channel morphology complement abrupt changes in watershed hydrology and lithology. For fluvial systems with highly-variable flow regimes, there is relatively little downstream translation of observed sedimentary and morphologic characteristics once a hydrologic (e.g., drainage area) or lithologic boundary is crossed.

7.4 Recommendations for Future Research

The list of conclusions and synthesis presented above are based on a watershed-scale approach to understanding downstream variability in alluvial sedimentology and channel morphology. The scope, therefore, is limited, and provides limited insight about fluvial processes operating at smaller spatial and temporal scales. Further, observed trends from this study are not fully elaborated because the data required to fully address them are insufficient. Listed below are some research questions posed as a result of shortcomings associated with this investigation.

1. What is (are) the hydraulic mechanism(s) responsible for contrasting downstream trends in particle size for low-flow channels and channel bars? This study concludes that hydraulic conditions during high flows are more uniform over longitudinal channel bars than at the low-flow channel (thalweg), implying

that greater turbulence in the deeper part of the channel results in a more heterogeneous mixture of particle sizes and a decreased possibility for sand deposition in downstream reaches.

2. What is the explanatory control for the coarse- to fine-gravel transition along the North Llano and South Llano Rivers upstream of Junction? This study concludes that an abrupt increase in drainage area is associated with an increased probability for moderate- to high-magnitude flows that abrade and entrain gravel-sized bed material, resulting in the rapid decrease in particle size. A key, missing piece of evidence is a sampling of particle size along tributaries adjacent to and upstream of the particle-size transition.

3. What explains the relatively low carbonate content and high magnetic susceptibility of alluvial sediment along the uppermost reaches of the North Llano and South Llano Rivers? This study concludes that considerable quantities of siliceous chert embedded in the Cretaceous Edwards Limestone decreases carbonate content and increases magnetic susceptibility.

4. Do abrupt additions of sand-sized bed material contribute to abrasion processes of gravel-sized bed material? This study locates an abrupt gravel-to-sand transition along the Llano River between Mason and Castell. Further, tributaries

of the Llano River, notably Beaver Creek, have bimodal distributions of Cretaceous- or Paleozoic-derived gravel and Paleozoic or Precambrian-derived sand. Basically, does "sandblasting" of gravel-sized material occur downstream of the sand introductions?

5. What are the watershed-scale characteristics that contribute to remarkably straight longitudinal profiles of slope? This study finds that main-stem channels of the Llano River have straight profiles, but only proposes a few possible reasons for this. Does relatively resistant downstream lithology (Paleozoic and Precambrian) act as a "base-level" control of channel incision? If it does, does this explain the wider, more developed alluvial valley in the upstream, Cretaceous zone of the watershed, basically acting as a "fill" within the expected concavity?

6. Is there a threshold-value of stream power associated with the development of macro-channels? Macro-channels are observed along both small and large channels in the Llano River watershed, similar to observations from other regions of the world. This study provides values for discharge and stream power associated with macro-channels, but the sample size is not enough to reliably determine a threshold hydraulic value.

7. How do bed-material entrainment frequency and the effective discharge of bedload transport relate to flow magnitudes and return periods computed for bankfull and macro-channel morphology? This study quantifies dominant discharge of river channels, but does not relate channel geometry to sediment transport processes, which are important controls of channel morphology.

8. Is flow duration an important control of channel morphology along rivers with highly variable flow regimes? This study specifically addresses flow magnitude and frequency, but does not associate flow duration with channel adjustment processes, which has been shown to be an influential control of channel morphology.

Bibliography

Ackers, P. 1982. Meandering channels and the influence of bed material. In *Gravel-bed rivers*, ed. R. D. Hey, J. C. Bathurst, and C. R. Thorne, 389–414. Chichester, U.K.: Wiley.

Ackers, P., and F. G. Charlton. 1970. Meander geometry arising from varying flows. *Journal of Hydrology* 11:230–52.

Adey, E. A., and H. M. Cook. 1964. *Suspended-sediment load of Texas streams: Compilation report: October 1959–September 1961*. Texas Water Commission Bulletin 6410.

Allen, B. D., and R. Y. Anderson. 1993. Evidence from western North America for rapid shifts in climate during the last glacial maximum. *Science* 260:1920–23.

Amos, B. B., and C. M. Rowell. 1988. Floristic geography of woody and endemic plants. In *Edwards Plateau vegetation*, ed. B. B. Amos and F. R. Gehlbach, 25–42. Waco, TX: Baylor University Press.

Andrews, E. D. 1980. Effective and bankfull discharges of streams in the Yampa River basin, Colorado and Wyoming. *Journal of Hydrology* 46:311–30.

Andrews, E. D., and J. M. Nankervis. 1995. Effective discharge and the design of channel maintenance flows for gravel-bed rivers. In *Natural and anthropogenic influences in fluvial geomorphology*, ed. J. E. Costa, A. J. Miller, K. W. Potter, and P. R. Wilcock, 151–64. Washington, DC: American Geophysical Union.

Andrews, E. D., and J. D. Smith. 1992. A theoretical model for calculating marginal bed load transport rates of gravel. In *Dynamics of gravel bed rivers*, ed. P. Billi, R. D. Hey, C. R. Thorne, and P. Tacconi, 41–52. Chichester, U.K.: Wiley.

Arp, C. D., J. C. Schmidt, M. A. Baker, and A. K. Myers. 2007. Stream geomorphology in a mountain lake district: Hydraulic geometry, sediment sources and sinks, and downstream lake effects. *Earth Surface Processes and Landforms* 32:525–43.

Ashmore, P. E., and T. J. Day. 1988. Effective discharge for suspended sediment transport in streams of the Saskatchewan River basin. *Water Resources Research* 24:864–70.

Asquith, W. H. 2009. *The lmomco package*. http://cran.r-project.org/web/packages/lmomco/lmomco.pdf (last accessed 15 March 2009).

Asquith, W. H., and R. M. Slade. 1997. *Regional equations for estimation of peak-streamflow frequency for natural basins in Texas*. U.S. Geological Survey Water-Resources Investigations Report 96–4307.

Asquith, W. H., and D. B. Thompson. 2008. *Alternative regression equations for estimation of annual-peak streamflow frequency for undeveloped watersheds in Texas using PRESS minimization*. U.S. Geological Survey Scientific Investigations Report 2008–5084.

Asquith, W. H., J. Vrabel, and M. C. Roussel. 2007. *Summary of annual mean, maximum, minimum, and L-scale statistics of daily mean streamflow for 712 U.S. Geological Survey streamflow-gaging stations in Texas through 2003*. U.S. Geological Survey Data Series 248.

Baker, V. R. 1977. Stream-channel response to floods, with examples from central Texas. *Geological Society of America Bulletin* 88:1057–71.

Baker, V. R. 1988. Flood erosion. In *Flood geomorphology*, ed. V. R. Baker, R. C. Kochel, and P. C. Patton, 81–95. Chichester, U.K.: Wiley.

Baker, V. R., and J. E. Costa. 1987. Flood power. In *Catastrophic flooding*, ed. L. Mayer and D. Nash, 1–24. London: Allen and Unwin.

Baker, V. R., and V. S. Kale. 1998. The role of extreme floods in shaping bedrock channels. In *Rivers over rock: Fluvial processes in bedrock channels*, ed. K. J. Tinkler and E. E. Wohl, 153–65. Washington, DC: American Geophysical Union.

Baker, V. R., and M. M. Penteado-Orellana. 1977. Adjustment to Quaternary climatic change by the Colorado River in central Texas. *Journal of Geology* 85:395–422.

Barnes, H. H. 1967. *Roughness characteristics of natural channels*. U.S. Geological Survey Water-Supply Paper 1849.

Barnes, V. E. 1981. *Geologic atlas of Texas: Llano sheet*. Austin, TX: The University of Texas at Austin Bureau of Economic Geology. Map scale 1:250,000.

Batalla, R. J., and M. Sala. 1995. Effective discharge for bedload transport in a subhumid Mediterranean sandy gravel-bed river (Arbúcies, north-east Spain). In *River geomorphology*, ed. E. J. Hickin, 93–103. Chichester, U.K.: Wiley.

Bates, B. C. 1990. A statistical log piecewise linear model of at-a-station hydraulic geometry. *Water Resources Research* 26:109–18.

Beard, L. R., 1975. *Generalized evaluation of flash-flood potential*. The University of Texas at Austin Center for Research in Water Resources Report CRWR–124.

Betson, R. P. 1979. A geomorphic model for use in streamflow routing. *Water Resources Research* 15:95–101.

Bettess, R., and W. R. White. 1983. Meandering and braiding of alluvial channels. *Proceedings of the Institution of Civil Engineers* 75:525–38.

Biedenharn, D. S., R. R. Copeland, C. R. Thorne, P. J. Soar, R. D. Hey, and C. C. Watson. 2000. *Effective discharge calculation: A practical guide*. U.S. Army Corps of Engineers ERDC/CHL TR–00–15.

Biedenharn, D. S., C. D. Little, and C. R. Thorne. 1999. *Magnitude-frequency analysis of sediment transport in the Lower Mississippi River*. U.S. Army Corps of Engineers Miscellaneous Paper CHL–99–2.

Biedenharn, D. S., and C. R. Thorne. 1994. Magnitude-frequency analysis of sediment transport in the lower Mississippi River. *Regulated Rivers: Research and Management* 9:237–51.

Blair, W. F. 1950. The biotic provinces of Texas. *Texas Journal of Science* 2:93–117.

Bluck, B. J. 1987. Bed forms and clast size changes in gravel-bed rivers. In *River channels: Environment and process*, ed. K. S. Richards, 159–78. Oxford, U.K.: Blackwell.

Blum, M. D, R. S. Toomey, and S. Valastro. 1994. Fluvial response to Late Quaternary climatic and environmental change, Edwards Plateau, Texas. *Palaeogeography, Palaeoclimatology, Palaeoecology* 108:1–21.

Blum, M. D., and S. Valastro. 1989. Response of the Pedernales River of central Texas to Late Holocene climatic change. *Annals of the Association of American Geographers* 79:435–56.

Blum, M. D., and S. Valastro. 1992. Quaternary stratigraphy and geoarchaeology of the Colorado and Concho Rivers, West Texas. *Geoarchaeology* 7:419–48.

Blum, M. D., and S. Valastro. 1994. Late Quaternary sedimentation, lower Colorado River, Gulf Coastal Plain of Texas. *Geological Society of America Bulletin* 106:1002–16.

Bomar, G. W. 1983. *Texas weather*. Austin, TX: University of Texas Press.

Bourke, M. C., and G. Pickup. 1999. Fluvial form variability in arid central Australia. In *Varieties of fluvial form*, ed. A. J. Miller and A. Gupta, A., 249–71. Chichester, U.K.: Wiley.

Bousman, C. B. 1998. Paleoenvironmental change in central Texas: The palynological evidence. *Plains Anthropologist* 43:201–19.

Bretz, J. H. 1923. The Channeled Scabland of the Columbia Plateau. *Journal of Geology* 31:617–49.

Brierley, G. J., and K. A. Fryirs. 2005. *Geomorphology and river management: Applications of the River Styles Framework*. Oxford, U.K.: Blackwell.

Brunke, M., and T. Gonser. 1997. The ecological significance of exchange processes between rivers and groundwater. *Freshwater Biology* 37:1–33.

Bryant, V. M. 1977. A 16,000 year pollen record of vegetational change in central Texas. *Palynology* 1:143–56.

Bryant, V. M., and R. G. Holloway. 1985. A Late-Quaternary paleoenvironmental record of Texas: An overview of the pollen evidence. In *Pollen records of Late-Quaternary North American sediments*, ed. V. M. Bryant and R. G. Holloway, 39–70. Dallas, TX: American Association of Stratigraphic Palynologists Foundation.

Burge, L. M. 2004. Testing links between river patterns and in-channel characteristics using MRPP and ANOVA. *Geomorphology* 63:115–30.

Burnett, J. 2008. *Flash floods in Texas*. College Station, TX: Texas A&M University Press.

Butzer, K. W. 1974. *Environment and archaeology: An ecological approach to prehistory*. 3rd ed. Chicago, IL: Aldine.

Caran, S. C., and R. W. Baumgardner. 1990. Quaternary stratigraphy and paleoenvironments of the Texas Rolling Plains. *Geological Society of America Bulletin* 102:768–85.

Carlston, C. W. 1965. The relation of free meander geometry to stream discharge and its geomorphic implications. *American Journal of Science* 263:864–85.

Castro, J. M., and P. L. Jackson. 2001. Bankfull discharge recurrence intervals and regional hydraulic geometry relationships: Patterns in the Pacific Northwest, USA. *Journal of the American Water Resources Association* 37:1249–62.

Church, M. 1988. Floods in cold climates. In *Flood geomorphology*, ed. V. R. Baker, R. C. Kochel, and P. C. Patton, 205–29. Chichester, U.K.: Wiley.

Church, M. 1992. Channel morphology and typology. In *The river handbook*, ed. P. Calow and G. E. Petts, 126–43: Oxford, U.K.: Blackwell.

Church, M., and M. A. Hassan. 1992. Size and distance of travel of unconstrained clasts on a streambed. *Water Resources Research* 28:299–303.

Clayton, J. A., and J. Pitlick. 2007. Spatial and temporal variations in bed load transport intensity in a gravel bed river bend. *Water Resources Research* 43:W02426.

Conyers, M. M., and M. A. Fonstad. 2005. The unusual channel resistance of the Texas Hill Country and its effect on flood flow predictions. *Physical Geography* 26:379–95.

Cook, H. M. 1967. *Suspended-sediment load of Texas streams: Compilation report: October 1961–September 1963*. Texas Water Development Board Report 45.

Cook, H. M. 1970. *Suspended-sediment load of Texas streams: Compilation report: October 1963–September 1965*. Texas Water Development Board Report 106.

Cooke, M. J., L. A. Stern, J. L. Banner, L. E. Mack, T. W. Stafford, and R. S. Toomey. 2003. Precise timing and rate of massive late Quaternary soil denudation. *Geology* 31:853–56.

Costa, J. E., and J. E. O'Connor. 1995. Geomorphically effective floods. In *Natural and anthropogenic influences in fluvial geomorphology*, ed. J. E. Costa, A. J. Miller, K. W. Potter, and P. R. Wilcock, 45–56. Washington, DC: American Geophysical Union.

Day, T. J., and H. R. Hudson. 2001. River management: The recent New Zealand experience. In *Gravel-bed rivers V*, ed. M. P. Mosley, 555–76. Wellington, N.Z.: New Zealand Hydrological Society.

Deodhar, L. A., and V. S. Kale. 1999. Downstream adjustments in allochthonous rivers: Western Deccan Trap upland region, India. In *Varieties of fluvial form*, ed. A. J. Miller and A. Gupta, 295–315. Chichester, U.K.: Wiley.

Doyle, M. W., D. Shields, K. F. Boyd, P. B. Skidmore, and D. Dominick. 2007. Channel-forming discharge selection in river restoration design. *Journal of Hydraulic Engineering* 133:831–37.

Doyle, M. W., E. H. Stanley, D. L. Strayer, R. B. Jacobson, and J. C. Schmidt. 2005. Effective discharge analysis of ecological processes in streams. *Water Resources Research* 41:W1141.

Dunne, T., and L. B. Leopold. 1978. *Water in environmental planning*. New York: W.H. Freeman.

Dury, G. H. 1973. Magnitude-frequency analysis and channel morphometry. In *Fluvial geomorphology*, ed. M. Morisawa, 91–121. Binghampton, NY: State University of New York, Binghampton.

Dury, G. H. 1980. Neocatastrophism?: A further look. *Progress in Physical Geography* 4:391–413.

Elliott, J. G. 2002. *Bed-material entrainment potential, Roaring Fork River at Basalt, Colorado*. U.S. Geological Survey Water-Resources Investigations Report 02–4223.

Elsner, J. B., K. Liu, and B. Kocher. 2000. Spatial variations in major U.S. hurricane activity: Statistics and a physical mechanism. *Journal of Climate* 13:2293–305.

Emmett, W. W., and M. G. Wolman. 2001. Effective discharge and gravel-bed rivers. *Earth Surface Processes and Landforms* 26:1369–80.

Erskine, W. D., and E. A. Livingstone. 1999. In-channel benches: The role of floods in their formation and destruction on bedrock-confined rivers. In *Varieties of fluvial form*, ed. A. J. Miller and A. Gupta, 445–75. Chichester, U.K.: Wiley.

Ferguson, R. I. 1986. Hydraulics and hydraulic geometry. *Progress in Physical Geography* 10:1–31.

Ferguson, R. I. 1987. Hydraulic and sedimentary controls of channel pattern. In *River channels: Environment and process*, ed. K. S. Richards, 129–58. Oxford, U.K.: Blackwell.

Ferguson, R. I. 2003. Emergence of abrupt gravel to sand transitions along rivers through sorting processes. *Geology* 31:159–62.

Fonstad, M., and W. A. Marcus. 2003. Self-organized criticality in riverbank systems. *Annals of the Association of American Geographers* 93:281–96.

Frings, R. M. 2008. Downstream fining in large sand-bed rivers. *Earth-Science Reviews* 87:39–60.

Frye, R. G., K. L. Brown, and C. A. McMahan. 1984. *The vegetation types of Texas*. Austin, TX: Texas Parks and Wildlife Department.

Fuller, I. C. 2007. Geomorphic work during a "150-year" storm: Contrasting behaviors of river channels in a New Zealand catchment. *Annals of the Association of American Geographers* 97:665–76.

García, C. C. 1995. Torrential flow frequency and morphological adjustments of ephemeral channels in south-east Spain. In *River geomorphology*, ed. E. J. Hickin, 169–92. Chichester, U.K.: Wiley.

Gee, G. W., and J. W. Bauder. 1986. Particle-size analysis. In *Methods of soil analysis: Part 1: Physical and mineralogical methods*. 3rd ed., ed. A. Klute. *Agronomy* 9:383–411.

Goh, T. B., R. J. St. Arnaud, A. R. Mermut. 1993. Carbonates. In *Soil sampling and methods of analysis*, ed. M. R. Carter, 177–85. Boca Raton, FL: Lewis.

Graf, W. L. 1988. Definition of flood plains along arid-region rivers. In *Flood geomorphology*, ed. V. R. Baker, R. C. Kochel, and P. C. Patton, 231–42. Chichester, U.K.: Wiley.

Graham, R. W. 1987. Late Quaternary mammalian faunas and paleoenvironments of the southwestern plains of the United States. In *Late Quaternary mammalian biogeography and environments of the Great Plains and Prairies*, ed. R. W. Graham, H. A. Semken, and M. A. Graham, 24–45. Springfield, IL: Illinois State Museum.

Grams, P. E., and J. C. Schmidt. 1999. Geomorphology of the Green River in the eastern Uinta Mountains, Dinosaur National Monument, Colorado and Utah. In *Varieties of fluvial form*, ed. A. J. Miller and A. Gupta, A., 81–111. Chichester, U.K.: Wiley.

Gregory, K. J., and J. R. Madew. 1982. Land use change, flood frequency and channel adjustments. In *Gravel-bed rivers*, ed. R. D. Hey, J. C. Bathurst, and C. R. Thorne, 757–80. Chichester, U.K.: Wiley.

Griffith, G. E., S. A. Bryce, J. M. Omernik, J. A. Comstock, A. C. Rogers, B. Harrison, S. L. Hatch, and D. Bezanson. 2004. *Ecoregions of Texas*. Reston, VA., U.S. Geological Survey. Map scale 1:2,500,000.

Gupta, A. 1988. Large floods as geomorphic events in the humid tropics. In *Flood geomorphology*, ed. V. R. Baker, R. C. Kochel, and P. C. Patton, 301–15. Chichester, U.K.: Wiley.

Gupta, A. 1995. Magnitude, frequency, and special factors affecting channel form and processes in the seasonal tropics. In *Natural and anthropogenic influences in fluvial geomorphology*, ed. J. E. Costa, A. J. Miller, K. W. Potter, and P. R. Wilcock, 125–36. Washington, DC: American Geophysical Union.

Gupta, A. 1999. The Narmada River, India, through space and time. In *Varieties of fluvial form*, ed. A. J. Miller and A. Gupta, 113–43. Chichester, U.K.: Wiley.

Gupta, A., and H. Fox. 1974. Effects of high-magnitude floods on channel form: A case study in Maryland Piedmont. *Water Resources Research* 10:499–509.

Hall, S. A. 1982. Late Holocene paleoecology of the Southern Plains. *Quaternary Research* 17:391–407.

Hall, S. A. 1990. Channel trenching and climatic change in the southern U.S. Great Plains. *Geology* 18:342–45.

Hall, S. A., and S. Valastro. 1995. Grassland vegetation in the Southern Great Plains during the last glacial maximum. *Quaternary Research* 44:237–45.

Hancock, G. S., R. S. Anderson, and K. X. Whipple. 1998. Beyond power: Bedrock river incision process and form. In *Rivers over rock: Fluvial processes in bedrock channels*, ed. K. J. Tinkler and E. E. Wohl, 35–60. Washington, DC: American Geophysical Union.

Harvey, A. M. 1987. Sediment supply to upland streams: Influence on channel adjustment. In *Sediment transport in gravel-bed rivers*, ed. C. R. Thorne, J. C. Bathurst, and R. D. Hey, 121–46. Chichester, U.K.: Wiley.

Heitmuller, F. T., and W. H. Asquith. 2008. *Potential for bed-material entrainment in selected streams of the Edwards Plateau: Edwards, Kimble, and Real Counties, Texas, and vicinity*. U.S. Geological Survey Scientific Investigations Report 2008–5017.

Heritage, G. L., L. J. Broadhurst, and A. L. Birkhead. 2001. The influence of contemporary flow regime on the geomorphology of the Sabie River, South Africa. *Geomorphology* 38:197–211.

Heritage, G. L. and D. J. Milan. 2004. A conceptual model of the role of excess energy in the maintenance of a riffle-pool sequence. *Catena* 58:235–57.

Heritage, G. L., A. W. van Niekerk, and B. P. Moon. 1999. Geomorphology of the Sabie River, South Africa: An incised bedrock-influenced channel. In *Varieties of fluvial form*, ed. A. J. Miller and A. Gupta, 53–79. Chichester, U.K.: Wiley.

Hey, R. D. 1998. Management and restoration of gravel-bed rivers. In *Gravel-bed rivers in the environment*, ed. P. C. Klingeman, R. L. Beschta, P. D. Komar, and J. B. Bradley, 435–54. Highlands Ranch, CO: Water Resources Publications.

Hey, R. D., and C. R. Thorne. 1986. Stable channels with mobile gravel beds. *Journal of Hydraulic Engineering* 112:671–89.

Hickin, E. J. 1995. Hydraulic geometry and channel scour, Fraser River, British Columbia, Canada. In *River geomorphology*, ed. E. J. Hickin, 155–67. Chichester, U.K.: Wiley.

Holliday, V. T. 1987. A reexamination of Late-Pleistocene boreal forest reconstructions for the Southern High Plains. *Quaternary Research* 28:238–44.

Holliday, V. T. 1989. Middle Holocene drought on the Southern High Plains. *Quaternary Research* 31:74–82.

Holliday, V. T. 1997. Origin and evolution of lunettes on the High Plains of Texas and New Mexico. *Quaternary Research* 47:54–69.

Holliday, V. T. 2000. Folsom drought and episodic drying on the Southern High Plains from 10,900–10,200 ^{14}C yr B.P. *Quaternary Research* 53:1–12.

Holloway, R. G., L.M. Raab, and R. Stuckenrath. 1987. Pollen analysis of late-Holocene sediments from a central Texas bog. *Texas Journal of Science* 39:71–79.

Hosking, J. R. M., and J. R. Wallis. 1997. *Regional frequency analysis*: Cambridge, U.K.: Cambridge University Press.

Howard, A. D. 1980. Thresholds in river regimes. In *Thresholds in geomorphology*, ed. D. R. Coates and J. D. Vitek, 227–58. Boston, MA: Allen and Unwin.

Howard, A. D. 1987. Modelling fluvial systems: Rock-, gravel-, and sand-bed channels. In *River channels: Environment and process*, ed. K. S. Richards, 69–94. Oxford, U.K.: Blackwell.

Hu, F. S., D. Slawinski, H. E. Wright, E. Ito, R. G. Johnson, K. R. Kelts, R. F. McEwan, and A. Boedigheimer. 1999. Abrupt changes in North American climate during early Holocene times. *Nature* 400:437–40.

Huang, H. Q., and R. F. Warner. 1995. The multivariate controls of hydraulic geometry: A causal investigation in terms of boundary shear distribution. *Earth Surface Processes and Landforms* 20:115–30.

Huckleberry, G. 1994. Contrasting channel response to floods on the middle Gila River, Arizona. *Geology* 22:1083–86.

Hudson, P. F., and F. T. Heitmuller. 2003. Local- and watershed-scale controls on the spatial variability of natural levee deposits in a large fine-grained floodplain: Lower Pánuco basin, Mexico. *Geomorphology* 56:255–69.

Hudson, P. F., and J. Mossa. 1997. Suspended sediment transport effectiveness of three, large impounded rivers, U.S. Gulf Coastal Plain. *Environmental Geology* 32:263–73.

Huebner, J. A. 1991. Late Prehistoric bison populations in central and southern Texas. *Plains Anthropologist* 36:343–58.

Humphrey, J. D., and C. R. Ferring. 1994. Stable isotopic evidence for latest Pleistocene and Holocene climatic change in north-central Texas. *Quaternary Research* 41:200–13.

Ichim, I., and M. Radoane. 1990. Channel sediment variability along a river: A case study of the Siret River (Romania). *Earth Surface Processes and Landforms* 15:211–25.

Inglis, C. C. 1941. *Meandering of rivers*. Central Board of Irrigation (India) Publication 24:98–99.

Intergovernmental Panel on Climate Change. 1990. *Climate change: The IPCC scientific assessment*. Cambridge, U.K.: Cambridge University Press.

Kale, V. S., V. R. Baker, and S. Mishra. 1996. Multi-channel patterns of bedrock rivers. *Catena* 26:85–98.

Kale, V. S., and P. S. Hire. 2007. Temporal variations in the specific stream power and total energy expenditure of a monsoonal river: The Tapi River, India. *Geomorphology* 92:134–46.

Kemp, J. 2004. Flood channel morphology of a quiet river, the Lachlan downstream from Cowra, southeastern Australia. *Geomorphology* 60:171–90.

Kennedy, B. A. 1999. Flow and sedimentation at tributary river mouths: A comparison with mesotidal estuaries. In *Varieties of fluvial form*, ed. A. J. Miller and A. Gupta, 409–26. Chichester, U.K.: Wiley.

Kidson, R., and K. S. Richards. 2005. Flood frequency analysis: Assumptions and alternatives. *Progress in Physical Geography* 29:392–410.

Kleinhans, M. G., and L. C. van Rijn. 2002. Stochastic prediction of sediment transport in sand-gravel bed rivers. *Journal of Hydraulic Engineering* 128:412–425.

Knighton, A. D. 1974. Variation in width-discharge relation and some implications for hydraulic geometry. *Geological Society of America Bulletin* 85:1069–76.

Knighton, A. D. 1975. Variations in at-a-station hydraulic geometry. *American Journal of Science* 275:186–218.

Knighton, A. D. 1977. Short-term changes in hydraulic geometry. In *River channel changes*, ed. K. J. Gregory, 101–19. Chichester, U.K.: Wiley.

Knighton, A. D. 1980. Longitudinal changes in size and sorting of stream-bed material in four English rivers. *Geological Society of America Bulletin* 91:55–62.

Knighton, A. D. 1982. Asymmetry of river channel cross-sections: Part II: Mode of development and local variation. *Earth Surface Processes and Landforms* 7:117–31.

Knighton, A. D. 1987. River channel adjustment: The downstream dimension. In *River channels: environment and process*, ed. K. S. Richards, 95–128. Oxford, U.K.: Blackwell.

Knighton, A. D. 1998. *Fluvial forms and processes: A new perspective*. London: Arnold.

Knox, J. C. 1995. Fluvial systems since 20,000 years B.P. In *Global continental palaeohydrology*, ed. K. J. Gregory, L. Starkel, and V. R. Baker, 87–108. Chichester, U.K.: Wiley.

Knox, J. C. 2000. Sensitivity of modern and Holocene floods to climate change. *Quaternary Science Reviews* 19:439–57.

Kochel, R. C. 1988. Geomorphic impact of large floods: Review and new perspectives on magnitude and frequency. In *Flood geomorphology*, ed. V. R. Baker, R. C. Kochel, and P. C. Patton, 169–87. Chichester, U.K.: Wiley.

Kodama, Y. 1994. Downstream changes in the lithology and grain size of fluvial gravels, the Watarase River, Japan: Evidence of the role of abrasion in downstream fining. *Journal of Sedimentary Research* A64:68–75.

Kolb, C. R. 1962. *Distribution of soils bordering the Mississippi River from Donaldsonville to Head of Passes*. U.S. Army Corps of Engineers Waterways Experiment Station Technical Report 3–601.

Komar, P. D. 1988. Sediment transport by floods. In *Flood geomorphology*, ed. V. R. Baker, R. C. Kochel, and P. C. Patton, 97–111. Chichester, U.K.: Wiley.

Langbein, W. B. 1964. Geometry of river channels. *Journal of the Hydraulics Division, American Society of Civil Engineers* 90(HY2):301–12.

Langbein, W. B., and L. B. Leopold. 1964. Quasi-equilibrium states in channel morphology. *American Journal of Science* 262:782–94.

Latrubesse, E. M. 2008. Patterns of anabranching channels: The ultimate end-member adjustment of mega rivers. *Geomorphology* 101:130–45.

Leopold, L. B. 1992. Sediment size that determines channel morphology. In *Dynamics of gravel-bed rivers*, ed. P. Billi, R. D. Hey, C. R. Thorne, and P. Tacconi, 297–307. Chichester, U.K.: Wiley.

Leopold, L. B., and T. Maddock. 1953. *The hydraulic geometry of stream channels and some physiographic implications*. U.S. Geological Survey Professional Paper 252.

Leopold, L. B., and M. G. Wolman. 1957. *River channel patterns: Braided, meandering, and straight*. U.S. Geological Survey Professional Paper 282–B:39–85.

Leopold, L. B., M. G. Wolman, and J. P. Miller. 1964. *Fluvial processes in geomorphology*. San Francisco: W.H. Freeman.

Lewin, J. 1989. Floods in fluvial geomorphology. In *Floods: Hydrological, sedimentological, and geomorphological implications*, ed. K. J. Beven and P. A. Carling, 265–84. Chichester, U.K.: Wiley.

López-Bermúdez, F., C. Conesa-García, and F. Alonso-Sarría. 2002. Floods: Magnitude and frequency in ephemeral streams of the Spanish Mediterranean region. In *Dryland rivers: Hydrology and geomorphology of semi-arid channels*, ed. L. J. Bull and M. J. Kirkby, 329–50. Chichester, U.K.: Wiley.

Lundelius, E. L. 1967. Late-Pleistocene and Holocene faunal history of central Texas. In *Pleistocene extinctions*, ed. P. S. Martin and H. E. Wright, 287–319. New Haven, CT: Yale University Press.

Lyndon B. Johnson School of Public Affairs. 1978. *Preserving Texas' natural heritage*. LBJ Policy Research Report 31.

Magilligan, F. J. 1992. Thresholds and spatial variability of flood power during extreme floods. *Geomorphology* 5:373–90.

Makaske, B. 2001. Anastomosing rivers—A review of their classification, origin, and sedimentary products. *Earth-Science Reviews* 53:149–96.

Mear, C.E. 1995. Quaternary geology of the upper Sabinal River valley, Uvalde and Bandera Counties, Texas. *Geoarchaeology* 10:457–80.

Merigliano, M. F. 1997. Hydraulic geometry and stream channel behavior: An uncertain link. *Journal of the American Water Resources Association* 33:1327–36.

Merritt, D. M., and E. E. Wohl. 2003. Downstream hydraulic geometry and channel adjustment during a flood along an ephemeral, arid-region drainage. *Geomorphology* 52:165–80.

Millar, R. G. 2005. Theoretical regime equations for mobile gravel-bed rivers with stable banks. *Geomorphology* 64:207–20.

Milner, N. J., J. Scullion, P. A. Carling, and D. T. Crisp. 1981. The effects of discharge on sediment dynamics and consequent effects on invertebrates and salmonids in upland rivers. *Advances in Applied Biology* 6:153–220.

Mirabal, J. 1974. *Suspended-sediment load of Texas streams: Compilation report: October 1965–September 1971*. Texas Water Development Board Report 184.

Montgomery, D. R., J. M. Buffington, N. P. Peterson, D. Schuett-Hames, and T. P. Quinn. 1996. Stream-bed scour, egg burial depths, and the influence of salmonid spawning on bed surface mobility and embryo survival. *Canadian Journal of Fisheries and Aquatic Sciences* 53:1061–70.

Morris, P. H., and D. J. Williams. 1999. A world-wide correlation for exponential bed particle size variation in subaerial aqueous flows. *Earth Surface Processes and Landforms* 24:835–47.

Moussavi-Harami, R., A. Mahboubi, and M. Khanehbad. 2004. Analysis of controls on downstream fining along three gravel-bed rivers in the Band-e-Golestan drainage basin NE Iran. *Geomorphology* 61:143–53.

Musgrove, M., J. L. Banner, L. E. Mack, D. M. Combs, E. W. James, H. Cheng, and R. L. Edwards. 2001. Geochronology of late Pleistocene to Holocene speleothems from central Texas: Implications for regional paleoclimate. *Geological Society of America Bulletin* 113:1532–43.

Nanson, G. C. 1986. Episodes of vertical accretion and catastrophic stripping: A model of disequilibrium floodplain development. *Geological Society of America Bulletin* 97:1467–75.

Nanson, G. C., and A. D. Knighton. 1996. Anabranching rivers: Their cause, character, and classification. *Earth Surface Processes and Landforms* 21:217–39.

Nash, D. B. 1994. Effective sediment-transporting discharge from magnitude-frequency analysis. *Journal of Geology* 102:79–95.

National Research Council of the National Academies. 2005. *The science of instream flows: A review of the Texas Instream Flow Program*. Washington, DC: The National Academies Press.

Neilson, R. P., and D. Marks. 1994. A global perspective of regional vegetation and hydrologic sensitivities from climatic change. *Journal of Vegetation Science* 5:715–30.

Nordt, L. C., T. W. Boutton, C. T. Hallmark, and M. R. Waters. 1994. Late Quaternary vegetation and climate changes in central Texas based on the isotopic composition of organic carbon. *Quaternary Research* 41:109–20.

Nordt, L. C., T. W. Boutton, J. S. Jacob, and R. D. Mandel. 2002. C_4 plant productivity and climate-CO_2 variations in south-central Texas during the Late Quaternary. *Quaternary Research* 58:182–88.

Osterkamp, W. R., M. M. Fenton, T. C. Gustavson, R. F. Hadley, V. T. Holliday, R. B. Morrison, and T. J. Toy. 1987. Great Plains. In *Geomorphic systems of North America*, ed. W. L. Graf, 163–210. Boulder, CO: Geological Society of America.

Osterkamp, W. R., and E. R. Hedman. 1982. *Perennial-streamflow characteristics related to channel geometry and sediment in Missouri River basin*. U.S. Geological Survey Professional Paper 1242.

Park, C. C. 1977. World-wide variations in hydraulic geometry exponents of stream channels: An analysis and some observations. *Journal of Hydrology* 33:133–46.

Parker, G. 1976. On the cause and characteristic scales of meandering and braiding in rivers. *Journal of Fluid Mechanics* 76:457–80.

Parker, G. 1979. Hydraulic geometry of active gravel rivers. *Journal of the Hydraulics Division, American Society of Civil Engineers* 105(HY9):1185–201.

Parker, G., P. C. Klingeman, and D. G. McLean. 1982. Bedload and size distribution in paved gravel-bed streams. *Journal of the Hydraulics Division, American Society of Civil Engineers* 108:544–71.

Patton, P. C. 1988a. Drainage basin morphometry and floods. In *Flood geomorphology*, ed. V. R. Baker, R. C. Kochel, and P. C. Patton, 51–64. Chichester, U.K.: Wiley.

Patton, P. C. 1988b. Geomorphic response of streams to floods in the glaciated terrain of southern New England. In *Flood geomorphology*, ed. V. R. Baker, R. C. Kochel, and P. C. Patton, 261–77. Chichester, U.K.: Wiley.

Patton, P. C., and D. S. Dibble. 1982. Archaeologic and geomorphic evidence for the paleohydrologic record of the Pecos River in West Texas. *American Journal of Science* 282:97–121.

Phillips, J. D. 1990. The instability of hydraulic geometry. *Water Resources Research* 26:739–44.

Phillips, J. D. 1991. Multiple modes of adjustment in unstable river channel cross-sections. *Journal of Hydrology* 123:39–49.

Phillips, J. D., M. C. Slattery, and Z. A. Musselman. 2004. Dam-to-delta sediment inputs and storage in the lower Trinity River, Texas. *Geomorphology* 62:17–34.

Pickup, G. 1976. Adjustment of stream-channel shape to hydrologic regime. *Journal of Hydrology* 30:365–73.

Pickup, G., and W. A. Rieger. 1979. A conceptual model of the relationship between channel characteristics and discharge. *Earth Surface Processes* 4:37–42.

Pickup, G., and R. F. Warner. 1976. Effects of hydrologic regime on magnitude and frequency of dominant discharge. *Journal of Hydrology* 29:51–75.

Pitlick, J. C., and C. R. Thorne. 1987. Sediment supply, movement and storage in an unstable gravel-bed river. In *Sediment transport in gravel-bed rivers*, ed. C. R. Thorne, J. C. Bathurst, and R. D. Hey, 151–78. Chichester, U.K.: Wiley.

Pitlick, J., and M. M. Van Steeter. 1998. Geomorphology and endangered fish habitats of the upper Colorado River 2: Linking sediment transport to habitat maintenance. *Water Resources Research* 34:303–16.

Poff, N. L., J. D. Olden, D. M. Pepin, and B. P. Bledsoe. 2006. Placing global stream flow variability in geographic and geomorphic contexts. *River Research and Applications* 22:149–66.

Potzger, J. E., and B. C. Tharp. 1947. Pollen profile from a Texas bog. *Ecology* 28:274–80.

Potzger, J. E., and B. C. Tharp. 1954. Pollen study of two bogs in Texas. *Ecology* 35:462–66.

Quincy, R. M. 1988. *Suspended-sediment load of Texas streams: Compilation report: October 1975–September 1982*. Texas Water Development Board Report 306.

R Development Core Team. 2004. *R: A language and environment for statistical computing*. Vienna, Austria: R Foundation for Statistical Computing. http://www.r-project.org/ (last accessed for version 2.6.2 on 17 December 2008).

Reeves, C. C. 1973. The full-glacial climate of the Southern High Plains, West Texas. *Journal of Geology* 81:693–704.

Rhoads, B. L. 1992. Statistical models of fluvial systems. *Geomorphology* 5:433–55.

Rhodes, D. D. 1977. The b-f-m diagram: Graphical representation and interpretation of at-a-station hydraulic geometry. *American Journal of Science* 277:73–96.

Rhodes, D. D. 1987. The b-f-m diagram for downstream hydraulic geometry. *Geografiska Annaler* 69A:147–61.

Rice, S. P., and M. Church. 1998. Grain size along two gravel-bed rivers: Statistical variation, spatial pattern and sedimentary links. *Earth Surface Processes and Landforms* 23:345–63.

Richards, K. S. 1973. Hydraulic geometry and channel roughness: A non-linear system. *American Journal of Science* 273:877–96.

Richards, K. S. 1976. Channel width and the riffle-pool sequence. *Bulletin of the Geological Society of America* 87:883–90.

Richards, K. S. 1977. Channel and flow geometry: A geomorphological perspective. *Progress in Physical Geography* 1:65–102.

Richards, K. S. 1982. *Rivers: Form and process in alluvial channels*. London: Methuen.

Ridenour, G. S., and J. R. Giardino. 1991. The statistical study of hydraulic geometry: A new direction for compositional data analysis. *Mathematical Geology* 23:349–66.

Riskind, D. H., and D. D. Diamond. 1988. An introduction to environments and vegetation. In *Edwards Plateau vegetation*, ed. B.B. Amos and F.R. Gehlbach, 1–15. Waco, TX: Baylor University Press.

Robert, A. 2003. *River processes—An introduction to fluvial dynamics*. London, Arnold.

Rosgen, D. L. 1994. A classification of natural rivers. *Catena* 22:169–99.

Sambrook Smith, G. H., and R. I. Ferguson. 1995. The gravel-sand transition along river channels. *Journal of Sedimentary Research* A65:423–30.

Scheepers, A. C. T., and I. C. Rust. 1999. The Uniab River fan: An unusual alluvial fan on the hyper-arid Skeleton Coast, Namibia. In *Varieties of fluvial form*, ed. A. J. Miller and A. Gupta, 273–94. Chichester, U.K.: Wiley.

Schick, A. P. 1974. Formation and obliteration of desert stream terraces: A conceptual analysis. *Zeitschrift für Geomorphologie Supplement* 21:88–105.

Schick, A. P., J. Lekach, and M. A. Hassan. 1987. Bed load transport in desert floods: Observations in the Negev. In *Sediment transport in gravel-bed rivers*, ed. C. R. Thorne, J. C. Bathurst, and R. D. Hey, 617–36. Chichester, U.K.: Wiley.

Schumm, S. A. 1960. *The shape of alluvial channels in relation to sediment type*. U.S. Geological Survey Professional Paper 352–B:17–30.

Schumm, S. A. 1963. Sinuosity of alluvial rivers on the Great Plains. *Geological Society of America Bulletin* 74:1089–100.

Schumm, S. A. 1977. *The fluvial system*. Chichester, U.K.: Wiley.

Schumm, S. A. 1985. Patterns of alluvial rivers. *Annual Review of Earth and Planetary Sciences* 13:5–27.

Schumm, S.A., 2005. River Variability and Complexity. Cambridge University Press, Cambridge, UK. 220 pp.

Schumm, S. A., and R. F. Hadley. 1957. Arroyos and the semi-arid cycle of erosion. *American Journal of Science* 255:161–74.

Schumm, S. A., and H. R. Khan. 1972. Experimental study of channel patterns. *Geological Society of America Bulletin* 83:1755–70.

Simon, A., and S. E. Darby. 1999. The nature and significance of incised river channels. In *Incised river channels: Processes, forms, engineering and management*, ed. S. E. Darby and A. Simon, 3–18. Chichester, U.K.: Wiley.

Simon, A., W. Dickerson, and A. Heins. 2004. Suspended-sediment transport rates at the 1.5-year recurrence interval for ecoregions of the United States: Transport conditions at the bankfull and effective discharge? *Geomorphology* 58:243–62.

Simpson, C. J., and D. G. Smith. 2001. The braided Milk River, northern Montana, fails the Leopold-Wolman, gradient-discharge test. *Geomorphology* 41:337–53.

Singh, V. P., and L. Zhang. 2008a. At-a-station hydraulic geometry relations, 1: Theoretical development. *Hydrological Processes* 22:189–215.

Singh, V. P., and L. Zhang. 2008b. At-a-station hydraulic geometry relations, 2: Calibration and testing. *Hydrological Processes* 22:216–28.

Smakhtin, V. Y. 2001. Low flow hydrology: A review. *Journal of Hydrology* 240:147–86.

Soong, D. T., A. L. Ishii, J. B. Sharpe, and C. F. Avery. 2004. *Estimating flood-peak discharge magnitudes and frequencies for rural streams in Illinois*. U.S. Geological Survey Scientific Investigations Report 2004–5103.

Stedinger, J. R., R. M. Vogel, and E. Foufoula-Georgiou. 1993. Frequency analysis of extreme events. In *Handbook of hydrology*, ed. D. A. Maidment, 18.1–66. New York: McGraw-Hill.

Stewardson, M. 2005. Hydraulic geometry of stream reaches. *Journal of Hydrology* 306:97–111.

Stout, I. M., L. C. Bentz, and H. W. Ingram. 1961. *Silt load of Texas streams: A compilation report: June 1889–September 1959*. Texas Board of Water Engineers Bulletin 6108.

Stute, M., P. Schlosser, J. F. Clark, and W. S. Broecker. 1992. Paleotemperatures in the southwestern United States derived from noble gases in ground water. *Science* 256:1000–03.

The Instream Flow Council. 2004. *Instream Flows for Riverine Resource Stewardship*. Cheyenne, WY: The Instream Flow Council.

Tinkler, K. J. 2001. The case of the missing flood: The unrecorded flood of 1935 on the James River, Mason County, Texas. *Geomorphology* 39:239–50.

Tinkler, K. J., and E. E. Wohl. 1998. A primer on bedrock channels. In *Rivers over rock: Fluvial processes in bedrock channels*, ed. K. J. Tinkler and E. E. Wohl, 1–18. Washington, DC: American Geophysical Union.

Thorne, C. R., A. P. G. Russell, and M. K. Alam. 1993. Planform pattern and channel evolution of the Brahmaputra River, Bangladesh. In *Braided rivers*, ed. J. L. Best and C. S. Bristow, 257–76. London: Geological Society Special Publications 75.

Thornes, J. B. 1977. Hydraulic geometry and channel change. In *River channel changes*, ed. K. J. Gregory, 91–100. Chichester, U.K.: Wiley.

Toomey, R. S., M. D. Blum, and S. Valastro. 1993. Late Quaternary climates and environments of the Edwards Plateau, Texas. *Global and Planetary Change* 7:299–320.

Torizzo, M., and J. Pitlick. 2004. Magnitude-frequency of bed load transport in mountain streams in Colorado. *Journal of Hydrology* 290:137–51.

Trimble, S. W. 1983. A sediment budget for Coon Creek basin in the Driftless Area, Wisconsin, 1853–1977. *American Journal of Science* 283:454–74.

U.S. Department of Agriculture Forest Service. 2008. WinXSPRO version 3.0. http://www.stream.fs.fed.us/publications/winxspro.html (last accessed 18 October 2008).

U.S. Department of Agriculture Natural Resources Conservation Service. 2007. *National engineering handbook, part 654, stream restoration design*. Washington, DC: U.S. Department of Agriculture, Natural Resources Conservation Service.

U.S. Geological Survey. 2007. *Water resources data for the United States, water year 2006*: U.S. Geological Survey Water-Data Report WDR–US–2006. http://wdr.water.usgs.gov/wy2006/search.jsp (last accessed 15 March 2007).

U.S. Geological Survey. 2008a. Earth Resources Observation and Science (EROS): Seamless data distribution system. http://seamless.usgs.gov (last accessed 19 December 2008).

U.S. Geological Survey. 2008b. National Hydrography Dataset. http://nhd.usgs.gov (last accessed 19 December 2008).

van den Berg, J. H. 1995. Prediction of alluvial channel pattern of perennial rivers. *Geomorphology* 12:259–79.

van Niekerk, A. W., G. L. Heritage, L. J. Broadhurst, and B. P. Moon. 1999. Bedrock anastomosing channel systems: Morphology and dynamics in the Sabie River, Mpumalanga Province, South Africa. In *Varieties of fluvial form*, ed. A. J. Miller and A. Gupta, 33–51. Chichester, U.K.: Wiley.

Vogel, R. M., J. R. Stedinger, and R. P. Hooper. 2003. Discharge indices for water quality loads. *Water Resources Research* 39:1273.

Walling, D. E., and B. W. Webb. 1987. Suspended load in gravel-bed rivers: UK experience. In *Sediment transport in gravel-bed rivers*, ed. C. R. Thorne, J. C. Bathurst, and R. D. Hey, 691–723. Chichester, U.K.: Wiley.

Waters, M. R., and L. C. Nordt. 1995. Late Quaternary floodplain history of the Brazos River in east-central Texas. *Quaternary Research* 43:311–19.

Wende, R. 1999. Boulder bedforms in jointed-bedrock channels. In *Varieties of fluvial form*, ed. A. J. Miller and A. Gupta, 189–216. Chichester, U.K.: Wiley.

Wharton, G. 1995. Information from channel geometry-discharge relations. In *Changing river channels*, ed. A. Gurnell and G. Petts, 325–46. Chichester, U.K.: Wiley.

Whiting, P. J., J. F. Samm, D. B. Moog, and R. L. Orndorff. 1999. Sediment-transporting flows in headwater streams. *Geological Society of America Bulletin* 111:450–66.

Wilcock, P. R. 1998. Two-fraction model of initial sediment motion in gravel-bed rivers. *Science* 280:410–12.

Wilkerson, G. V. 2008. Improved bankfull discharge prediction using 2-year recurrence-period discharge. *Journal of the American Water Resources Association* 44:243–58.

Williams, G. P. 1978a. Bank-full discharge of rivers. *Water Resources Research* 14:1141–58.

Williams, G. P. 1978b. *Hydraulic geometry of river cross sections: Theory of minimum variance*. U.S. Geological Survey Professional Paper 1029.

Williams, M., D. Dunkerley, P. De Deckker, P. Kershaw, and J. Chappell. 1998. *Quaternary environments*. 2nd ed. London: Arnold.

Williams, P. B., M. K. Orr, and N. J. Garrity. 2002. Hydraulic geometry: A geomorphic design tool for tidal marsh channel evolution in wetland restoration projects. *Restoration Ecology* 10:577–90.

Wohl, E. E. 2004. Limits of downstream hydraulic geometry. *Geology* 32:897–900.

Wohl, E. E., and A. Wilcox. 2005. Channel geometry of mountain streams in New Zealand. *Journal of Hydrology* 300:252–66.

Wolman, M. G. 1954. A method for sampling coarse bed material. *Transactions of the American Geophysical Union* 35:951–56.

Wolman, M. G., and R. Gerson. 1978. Relative scales of time and effectiveness of climate in watershed geomorphology. *Earth Surface Processes* 3:189–208.

Wolman, M. G., and L. B. Leopold. 1957. *River flood plains: Some observations on their formation*. U.S. Geological Survey Professional Paper 282–C:87–109.

Wolman, M. G., and J. P. Miller. 1960. Magnitude and frequency of forces in geomorphic processes. *Journal of Geology* 68:54–74.

Xu, J. 2004. Comparison of hydraulic geometry between sand- and gravel-bed rivers in relation to channel pattern discrimination. *Earth Surface Processes and Landforms* 29:645–57.

Yu, B., and M. G. Wolman. 1987. Some dynamic aspects of river geometry. *Water Resources Research* 23:501–09.

Vita

Franklin Thomas Heitmuller attended Gulf Breeze High School in Gulf Breeze, Florida. In August, 1995, he entered Florida State University in Tallahassee, Florida. He received the degree of Bachelor of Science from Florida State University in May 1998. During the following year, he was employed at both the U.S. Environmental Protection Agency and Johnson Controls World Services, Inc., in Gulf Breeze, Florida. He also volunteered at the Navarre Beach Volunteer Fire Department. In August, 1999, he entered the Graduate School at The University of Texas at Austin and received the degree of Master of Arts in May 2002. From 2001 to present (2009), he is a full-time employee at the U.S. Geological Survey in Austin, Texas. In August, 2003, he re-entered the Graduate School at The University of Texas at Austin.

Permanent Address: 6902 Duquesne Drive, Austin, Texas 78723

This manuscript was typed by the author.